

CELLULOSE SUPPORTED TRANSITION
METAL (Cu, Pd) CATALYSTS FOR CARBON-
CARBON AND CARBON-NITROGEN BONDS
FORMATION REACTIONS



MD SHAHARUL ISLAM

Doctor of Philosophy

UNIVERSITI MALAYSIA PAHANG

UNIVERSITI MALAYSIA PAHANG

DECLARATION OF THESIS AND COPYRIGHT

Author's Full Name : MD. SHAHARUL ISLAM

Date of Birth : 19 DECEMBER 1978

Title : CELLULOSE SUPPORTED TRANSITION METAL (Cu, Pd) CATALYSTS
FOR CARBON-CARBON AND CARBON-NITROGEN BONDS
FORMATION REACTIONS

Academic Session : 2017/2018

I declare that this thesis is classified as:

- CONFIDENTIAL (Contains confidential information under the Official Secret Act 1997)*
- RESTRICTED (Contains restricted information as specified by the organization where research was done)*
- OPEN ACCESS I agree that my thesis to be published as online open access (Full Text)

I acknowledge that Universiti Malaysia Pahang reserves the following rights:

1. The Thesis is the Property of Universiti Malaysia Pahang
2. The Library of Universiti Malaysia Pahang has the right to make copies of the thesis for the purpose of research only.
3. The Library has the right to make copies of the thesis for academic exchange.

Certified by:

(Student's Signature)

BM0801242

New IC/Passport Number
Date:

(Supervisor's Signature)

Dr. Tan Suat Hian

Name of Supervisor Date:

NOTE : * If the thesis is CONFIDENTIAL or RESTRICTED, please attach a thesis declaration letter.

SUPERVISOR'S DECLARATION

We hereby declare that we have checked this thesis and in our opinion, this thesis is adequate in terms of scope and quality for the award of the degree of Doctor of Philosophy.

(Supervisor's Signature)

Full Name : DR. TAN SUAT HIAN

Position : SENIOR LECTURER

Date :

(Co-supervisor's Signature)

Full Name : DR. MD. SHAHEEN SARKAR

Position : SENIOR LECTURER

Date :

STUDENT'S DECLARATION

I hereby declare that the work in this thesis is based on my original work except for quotations and citations which have been duly acknowledged. I also declare that it has not been previously or concurrently submitted for any other degree at Universiti Malaysia Pahang or any other institutions.

(Student's Signature)

Full Name : MD. SHAHARUL ISLAM

ID Number : PKT 13003

Date



UMP

**CELLULOSE SUPPORTED TRANSITION METAL (Cu, Pd) CATALYSTS
FOR CARBON-CARBON AND CARBON-NITROGEN BONDS FORMATION
REACTIONS**



MD. SHAHARUL ISLAM

Thesis submitted in fulfillment of the requirements
for the award of the degree of
Doctor of Philosophy

UMP

Faculty of Industrial Sciences & Technology
UNIVERSITI MALAYSIA PAHANG

APRIL 2018

ACKNOWLEDGEMENTS

Firstly, I am deeply grateful to almighty Allah, the Most Beneficent, and the Most Merciful who granted me the ability and willing to start and complete PhD study. I would like to express my great debt of gratitude to all, who helped me over this period. I would like to thank my supervisor Dr. Tan Suat Hian supported enormously to my research, during my PhD studies. I also, would like to thank my previous supervisor Prof. Dr. Rezaul Karim for his support and guidance. I wish to give a special thanks to my co-supervisor Dr. Md. Shaheen Sarkar for all of his help during my PhD studies. I also would like to thank to Dr. Shah Samiur Rashid for his valuable advices during my PhD.

I would like to use this opportunity to express my sincere thanks to the Dean of Faculty of Industrial Sciences & Technology (FIST), Assoc. Prof. Dr. Mohd Hasbi Ab. Rahim for support throughout this work. I also extend my sincere thanks to the Director Assoc. Prof. Dr. Gaanty Pragas Maniam and his staff of Central Laboratory for their help with the various instrumental facilities during my PhD study. I would always appreciate the valuable support extended by all the science officer and technical staff in the FIST.

I would like to acknowledge Prof. Dr. Provash Kumar Karmokar, who helped me to start my PhD at UMP. Then, I would like to convey my hearty thanks to the Dean of Institute of Postgraduate Studies, Prof. Dato Dr. Hasnah Binti Haron, and all other staff for their help throughout my course of study. I also owe my sincere appreciation to all the staff in the International Office for their timely help and support. Lastly, I would like to thank my family for giving me support for studies and life: my parents, my sisters and brothers.

The logo of Universiti Malaysia Perlis (UMP) is a large, stylized letter 'V' shape. The left side of the 'V' is light blue, the right side is light green, and the bottom point is a darker blue. The letters 'UMP' are written in white, bold, sans-serif font across the center of the 'V'.

ABSTRAK

Kajian ini terutama berkaitan dengan sintesis, pencirian, dan aplikasi mangkin logam heterogen berasaskan selulosa berfungsi untuk pelbagai jenis tindak balas penggandingan silang. Tindak balas penggandingan silang secara amnya dijalankan dengan kehadiran kompleks logam homogen. Cabaran eksperimen untuk melakukan tindak balas katalitik homogen adalah rumit disebabkan kesukaran pemisahan produk daripada campuran tindak balas, serta ketidakupayaan untuk menggunakan semula mangkin logam. Untuk mengatasi masalah ini, penyelidik-penyelidik telah mengkaji penggunaan pelbagai sokongan pepejal heterogen untuk spesies pemangkin logam seperti nanotub karbon, grafin, silikat, polimer, oksida logam, dan pelbagai bahan bukan organik hibrid. Walaupun banyak protokol yang berekonomi dan mampan telah digunakan oleh para penyelidik yang berdedikasi dalam pengkajian tindak balas penggandingan silang yang mesra alam, tetapi masih terdapat permintaan yang tinggi untuk meneroka pemangkin yang lebih berkesan untuk tindak balas transformasi kimia. Pada masa kini, sains dan teknologi beralih ke arah persekitaran yang mesra alam, dan proses untuk mengkaji pengeluaran bahan kimia halus. Dalam perspektif ini, biopolimer semulajadi (selulosa) boleh dipertimbangkan sebagai bahan sokongan padu yang boleh diterima kerana kelebihan seperti mudah diperolehi, mempunyai ketumpatan yang rendah, boleh diperbaharui, ketersediaan, kos rendah dan sifat kimia dan mekanikal yang menarik. Oleh itu, selulosa semulajadi akan menjadi sokongan padat sempurna sebagai mangkin. Dalam kajian ini, selulosa tongkol buah jagung telah diasingkan dan tulang belakang selulosa diubahsuai secara kimia melalui pempolimeran. Kumpulan polimer berfungsi yang dihasilkan telah ditukar menjadi ligand pengkelat poli(amidoksim) yang sesuai. Selulosa poli(amidoksim) mudah menjalani tindak balas kompleks dengan rawatan garam logam (Pd/Cu) untuk menghasilkan logam poli(amidoksim) heterogen yang berasaskan selulosa. Kompleks palladium yang berasaskan selulosa mempamerkan aktiviti pemangkin tinggi (0.1 hingga 0.05 mol%) terhadap tindak balas penggandingan silang Mizoroki-Heck aril halida dengan pelbagai olefin untuk memberikan produk gandingan sehingga hasil 97%. Pengeluaran elektron aril halida dapat memproses hasil yang lebih tinggi berbanding dengan aril halida yang menderma elektron. Kompleks palladium juga digunakan untuk sintesis Ozagrel, perencat thromboxane A₂-sintetas melalui tindak balas Mizoroki-Heck dengan penghasilan 88%. Kompleks tembaga (amidoksim) yang berasaskan selulosa digunakan untuk tindak balas Klik [Cu (II) 1 hingga 0.05 mol%] daripada azida organik dengan alkil terminal untuk membekalkan triazol sehingga hasil 96%. Selain itu, nanopartikel tembaga telah disediakan dari kompleks tembaga dan distabilkan dengan baiknya oleh ligan poli(amidoksim). Nanopartikel tembaga tersebut mempercepatkan tindak balas amina alifatik chemoselective Aza-Michael [Cu(0), 0.1 hingga 0.005 mol%] dengan α , β -sebatian-sebatian yang tidak tepu dengan cecap untuk memberikan penghasilan sehingga 95%. Tambahan pula, semua pemangkin polimer berasaskan selulosa adalah mudah diperolehi semula daripada campuran tindak balas dan digunakan beberapa kali tanpa kehilangan aktiviti permangkin yang ketara.

ABSTRACT

This research mainly deals with the synthesis, characterization, and applications of functionalized cellulose supported heterogeneous metal catalysts for various types of cross-coupling reactions. Cross-coupling reactions generally proceed in the presence of homogeneous metal complexes. The practical limits to perform homogeneous catalysis reactions are complicated due to the difficulty in the separation of the product from the reaction mixture, as well as the inability to reuse the metal catalysts. To overcome these problems, scientific communities have investigated the use of various heterogeneous solid supports for metal catalyst species such as carbon nanotubes, graphene, silicates, polymers, metal oxides, and various hybrid inorganic materials. Although many economic and sustainable protocols have been employed by researchers dedicated to the development of green processes for cross-coupling reactions, there is still a high demand to explore more efficient catalysts for chemical transformation reactions. Nowadays, science and technology are shifting towards environmentally friendly, sustainable resources, and processes to investigate low-cost production of fine chemicals. In this perspective, natural biopolymers (cellulose) could be considered as acceptable solid support materials because of their promising merits such as being largely abundant in nature, having low density, bio-renewability, universal availability, low-cost and interesting chemical and mechanical properties. Therefore, natural cellulose would be a perfect solid support for catalysts. In this study, corn-cob cellulose was isolated from bio-waste corn-cobs, and the backbone of the cellulose was chemically modified through polymerization. The resulting polymeric functional group was converted into suitable poly(amidoxime) chelating ligand. The cellulose-supported poly(amidoxime) readily underwent a complexation reaction by treatment with metal (Pd/Cu) salts to give the corresponding cellulose-supported heterogeneous poly(amidoxime) metal complexes. The cellulose-supported palladium complex exhibited a high catalytic activity (0.1 to 0.05 mol%) towards Mizoroki-Heck cross-coupling reactions of aryl halides with a variety of olefins to give the corresponding coupling products of up to 97% yield. The electron withdrawing aryl halides processes higher yields compare to electron donating aryl halides. The palladium complex was also applied to the synthesis of Ozagrel, a thromboxane A₂-synthetase inhibitor through Mizoroki-Heck reaction with 88% yield. The cellulose-supported poly(amidoxime) copper complex was applied to the Click reaction [Cu(II) 1 to 0.05 mol%] of organic azide with terminal alkyne to afford triazole in up to 96% yield. Moreover, copper nanoparticles were prepared from the copper complex and well stabilized by the poly(amidoxime) ligands. The copper nanoparticles were efficiently promoted the chemoselective Aza-Michael reaction [Cu(0) 0.1 to 0.005 mol%] of aliphatic amines with α, β -unsaturated compounds to give addition products in up to 95% yield. Additionally, all polymeric cellulose supported catalysts were easy to recover from the reaction mixture and reused several times without significant loss of their catalytic activities.

TABLE OF CONTENT

DECLARATION	
TITLE PAGE	
ACKNOWLEDGEMENTS	ii
ABSTRAK	iii
ABSTRACT	iv
TABLE OF CONTENT	v
LIST OF TABLES	x
LIST OF FIGURES	xi
LIST OF SYMBOLS	xvi
LIST OF ABBREVIATIONS	xvii
CHAPTER 1 INTRODUCTION	1
1.1 Background	1
1.2 Problem Statement	5
1.3 Hypothesis	6
1.4 Objective of Research	6
1.5 Scope of Research	7
1.6 Thesis Outline	7
CHAPTER 2 LITERATURE REVIEW	8
2.1 Catalysts	8
2.2 Different Types of Catalysts	9
2.2.1 Homogeneous Catalysts	9
2.2.2 Heterogeneous Catalysts	10

2.3	Cellulose	11
2.4	Cellulose Supported Catalysts	12
2.5	Transition Metal Catalyzed Reactions	13
2.5.1	Sonogashira Reaction (C≡C)	14
2.5.2	Suzuki Reaction (C-C)	14
2.5.3	Negishi Reaction (C-C)	15
2.5.4	Stille Reaction (C-C)	16
2.5.5	Mizoroki-Heck Reaction (C-C)	16
2.5.6	Buchwald-Hartwig Reaction (C-N)	27
2.5.7	Click Reaction (C-N)	28
2.5.8	Aza-Michael Reaction (C-N)	35
2.6	Importance of Mizoroki-Heck, Click and Aza-Michael Reactions	40
2.7	Summary	41
CHAPTER 3 MATERIALS AND METHODS		42
3.1	Introduction	42
3.2	Chemicals and Instruments used	42
3.3	Research Methodology	43
3.4	Materials Collection	44
3.5	Extraction of Cellulose from Corn-Cobs	44
3.5.1	Graft Copolymerization of Corn-Cob Cellulose [Poly(acrylonitrile) 1]	44
3.5.2	Determination of the Grafting Percentage	45
3.5.3	Synthesis of Poly(amidoxime) Ligand 2	45

3.6	Preparation of the Catalysts	47
3.6.1	Preparation of Poly(amidoxime) Pd(II) Complex 3	47
3.6.2	Preparation of Poly(amidoxime) Cu(II) Complex 4	47
3.6.3	Preparation of Poly (amidoxime) Copper Nanoparticles (CuNP@PA)	48
3.7	Catalytic Activity Test	48
3.7.1	General Procedure for the Mizoroki-Heck Reaction of Aryl Halide and Olefins	49
3.7.2	General Procedure for the Heck-Matsuda Reaction of Arenediazonium Tetrafluoroborate with Olefins	49
3.7.3	General Procedure for Click Reaction	50
3.7.4	General Procedure for Aza-Michael Reaction	51
3.8	Synthesis of Functional Molecules	51
3.8.1	Preparation of (E)-4-(Hydroxymethyl) Cinnamic Acid Butyl Ester 5o	51
3.8.2	Preparation of Ozagrel Butyl Ester 5p	52
3.8.3	Preparation of Ozagrel Hydrochloride 5q	52
CHAPTER 4 RESULTS AND DISCUSSION		54
4.1	Introduction	54
4.2	Preparation and Characterization of Poly(amidoxime) Pd(II) Complex 3	54
4.2.1	Fourier Transform Infrared Spectroscopy (FTIR) Analysis of Cellulose and Modified Celluloses	55
4.2.2	Field Emission Scanning Electron Microscopy (FE-SEM) Images Analysis of Corn-Cob Cellulose, Modified Celluloses and	

	Energy-Dispersive X-Ray Spectroscopy (EDX) of Pd(II) Complex 3	57
4.2.3	High-Resolution Transmission Electron Microscopy (HR-TEM) Images of Fresh and 4 th Reused of Poly(amidoxime) Pd(II) Complex 3	59
4.2.4	X-Ray Powder Diffraction (XRD) of Fresh and Reused Pd(II) Complex 3	60
4.2.5	X-Ray Photoelectron Spectroscopy (XPS) of Fresh and Reused Poly(amidoxime) Pd(II) Complex 3	60
4.2.6	Inductively Coupled Plasma Atomic Emission Spectroscopy (ICP-AES)	62
4.3	Characterization of the Poly(amidoxime) Cu(II) Complex 4	62
4.3.1	Fourier Transform Infrared Spectroscopy (FTIR) of Poly(amidoxime) Cu(II) Complex 4	62
4.3.2	Field Emission Scanning Electron Microscopy (FE-SEM) Images of Ligand 2 , Cu(II) Complex 4 and Energy-Dispersive X-Ray Spectroscopy (EDX) of Cu(II) Complex 4	64
4.3.3	High-Resolution Transmission Electron Microscopy (HR-TEM) Images of Cu(II) Complex 4 and CuNP@PA	65
4.3.4	X-Ray Powder Diffraction (XRD) of Cu(II) Complex 4 , Fresh and Reused CuNP@PA	67
4.3.5	X-Ray Photoelectron Spectroscopy (XPS) of Poly(amidoxime) Cu(II) Complex 4 , Cu(I), Fresh and Reused CuNP@PA	68
4.4	Application of the Catalysts in Cross-Coupling Reaction	71
4.4.1	Poly(amidoxime) Pd(II) Complex Catalyzed Mizoroki-Heck Reaction	71
4.4.2	Synthetic Application of Pd(II) Complex 3 (Synthesis of Ozagrel)	79

4.4.3	Characterization of Mizoroki-Heck Reaction Products	79
4.4.4	Recycling of Pd(II) Complex 3	85
4.4.5	Hot Filtration or Heterogeneity Test of Pd(II) Complex 3	86
4.4.6	Corn-Cob Cellulose Supported Poly(amidoxime) Cu(II) Complex 4 Catalyzed Click Reaction	87
4.4.7	Characterization of Click Reaction Products	91
4.4.8	Recycling Test of Cu(II) Complex 4	94
4.4.9	Hot Filtration or Heterogeneity Test of Cu(II) Complex 4	95
4.4.10	Copper Nanoparticles (CuNP@PA) Catalyzed Aza-Michael Reaction	96
4.4.11	Aza-Michael Reaction of Aliphatic Amines with Olefins	98
4.4.12	Characterization of Aza-Michael Reaction Products	101
4.4.13	Recycling Test of Cellulose Supported CuNP@PA	106
CHAPTER 5 CONCLUSION AND RECOMMENDATION		108
5.1	Conclusion	108
5.2	Recommendation	109
REFERENCES		110
APPENDIX A (¹H NMR)		127
APPENDIX B (¹³C NMR)		149
ACHIEVEMENTS		171

LIST OF TABLES

Table 4.1	List of FTIR data for cellulose, modified cellulose and poly(amidoxime) Pd(II) complex 3 .	57
Table 4.2	List of FTIR data for cellulose, modified cellulose and poly(amidoxime) Cu(II) complex 4 .	63
Table 4.3	Optimization of the Mizoroki-Heck reaction.	72
Table 4.4	Effect of temperature on the Mizoroki-Heck reaction.	73
Table 4.5	Mizoroki-Heck reaction of aryl iodides with olefins.	74
Table 4.6	Mizoroki-Heck reaction of aryl bromides with olefins.	76
Table 4.7	Heck-Matsuda reaction of arenediazonium tetrafluoroborate with olefins.	78
Table 4.8	Optimization of the Click reaction using phenyl acetylene and benzyl azide.	88
Table 4.9	Click reaction of organic azides and alkynes.	90
Table 4.10	Optimization of the Aza-Michael reaction.	97
Table 4.11	Effect of solvent on the Aza-Michael reaction.	98
Table 4.12	Aza-Michael reaction with olefins ^[a] .	99

UMP

LIST OF FIGURES

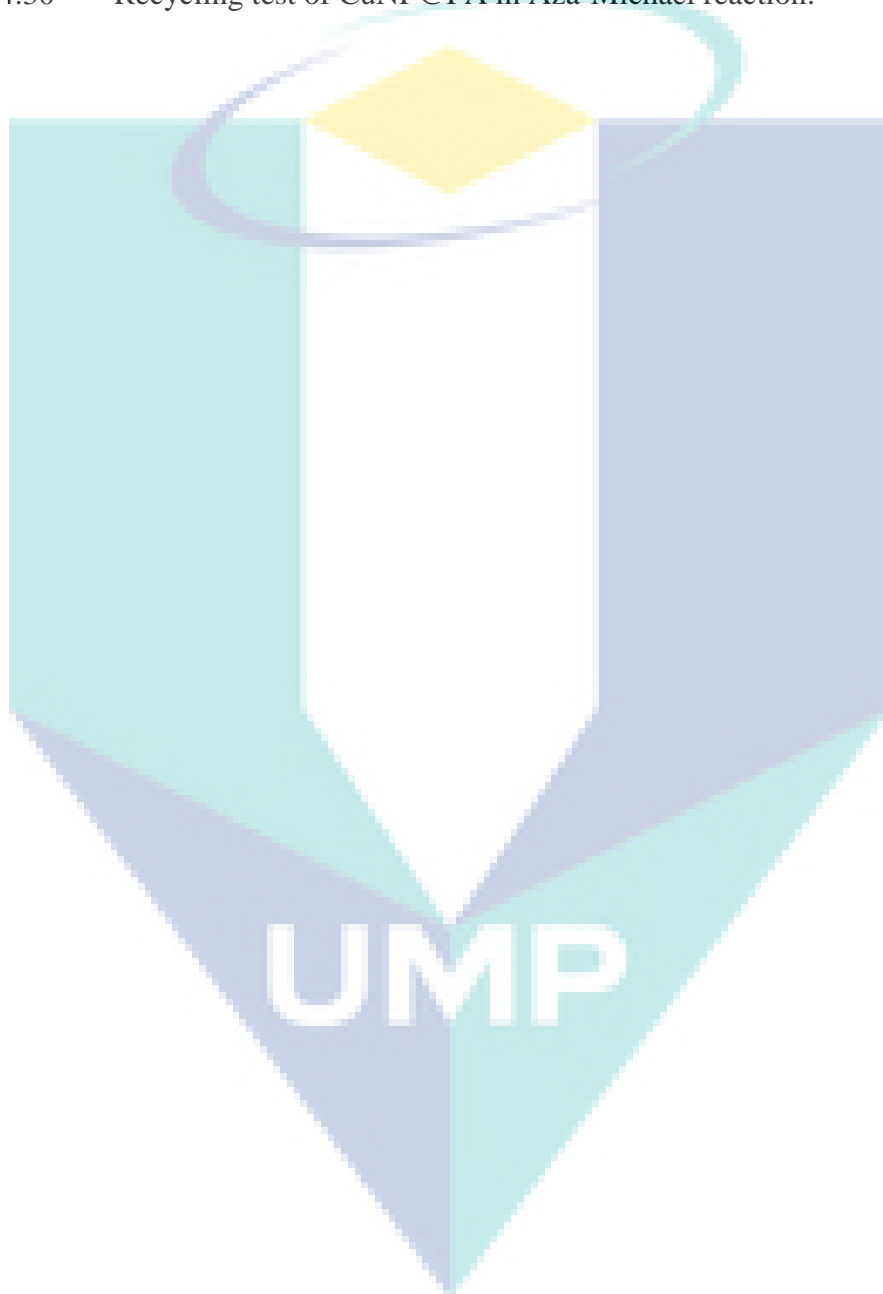
Figure 2.1	Homogeneous ruthenium complex catalyzed reaction.	10
Figure 2.2	Heterogeneous PdNP@NG catalyzed Heck reaction.	11
Figure 2.3	Cellulose structure.	12
Figure 2.4	Suzuki coupling reaction.	15
Figure 2.5	Mechanism of the Negishi coupling.	15
Figure 2.6	Stille coupling reaction.	16
Figure 2.7	Mizoroki coupling reaction.	17
Figure 2.8	Heck coupling reaction.	17
Figure 2.9	(Pd-DABCO- γ -Fe ₂ O ₃) complex supported Mizoroki-Heck cross-coupling reaction.	18
Figure 2.10	4-amino-5-methyl-3-thio-1,2,4-triazole-functionalized polystyrene resin-supported Heck reaction.	19
Figure 2.11	Heck coupling reaction with aryl halide.	19
Figure 2.12	Fe ₃ O ₄ /SiO ₂ /HPGeOPPh ₂ -PNP supported Heck reaction.	20
Figure 2.13	Heck coupling reaction using heterogeneous Pd(0) catalyst.	20
Figure 2.14	Lignin@Pd-NPs catalyzed Heck reaction.	21
Figure 2.15	Gelatin/pectin stabilized palladium nanoparticles catalyzed Heck reaction.	21
Figure 2.16	Heck cross-coupling reaction using Pd complex as a catalyst.	22
Figure 2.17	PS-NHC-Pd(II) catalyzed Heck reaction.	23
Figure 2.18	Pd/MnBDC catalyzed Heck coupling reaction.	23
Figure 2.19	Fe ₃ O ₄ @CS-Schiff base palladium catalyzed reaction.	24
Figure 2.20	MNPs-NHC-Pd(II) catalyzed Heck reaction.	24
Figure 2.21	Poly(vinyl chloride) supported palladium complex catalyzed reaction.	25

Figure 2.22	Palladium-catalyzed Heck cross-coupling reaction.	25
Figure 2.23	Polystyrene-anchored Pd(II) phenyldithiocarbazate complex catalyzed reaction.	26
Figure 2.24	Heterogeneous PNP-SSS catalyzed Heck coupling reaction.	26
Figure 2.25	Heck coupling reaction using a heterogeneous catalyst.	27
Figure 2.26	Buchwald-Hartwig cross-coupling reaction.	28
Figure 2.27	Click coupling reaction.	29
Figure 2.28	Copper(II) complex catalyzed Click reaction.	29
Figure 2.29	Heterogeneous copper-catalyzed Click reaction.	30
Figure 2.30	Poly(hydroxamic acid) Cu(II) complex catalyzed reaction.	30
Figure 2.31	Cu(I) complex catalyzed Click coupling reaction.	31
Figure 2.32	Heterogeneous Cu@PyIm-SBA-15 catalyzed Click reaction.	32
Figure 2.33	Modified silica mesopore CuI/AK catalyzed reaction.	32
Figure 2.34	Cellulose supported Cu(0) catalyzed reaction.	33
Figure 2.35	Cellulose supported cuprous iodide nanoparticles (Cell-CuI NPs) reaction.	33
Figure 2.36	CuNPs@agarose catalyzed Click reaction.	34
Figure 2.37	Heterogeneous Cu(I)-MMT catalyzed Click reaction.	34
Figure 2.38	Heterogeneous imidazole-copper catalyzed Click reaction.	35
Figure 2.39	Aza-Michael reaction.	36
Figure 2.40	CuN@PHA catalyzed reaction.	37
Figure 2.41	Bio-heterogeneous poly(amidoxime) copper nanoparticles catalyzed Aza-Michael reaction.	37
Figure 2.42	Aza-Michael reaction catalyzed by heterogeneous catalyst.	38
Figure 2.43	Aza-Michael reaction using heterogeneous catalyst [bmIm]OH.	38
Figure 2.44	Fe ₃ O ₄ @SiO ₂ @Me&Et- PhSO ₃ H catalyzed reaction.	39
Figure 3.1	Research methodology flow chart.	43


Figure 3.2	Synthesis of poly(acrylonitrile) 1 .	45
Figure 3.3	Synthesis of poly(amidoxime) ligand 2 .	46
Figure 3.4	Photographic images of (a) waste corn-cob (b) corn-cob cellulose (c) poly(acrylonitrile) grafted corn-cob cellulose 1 and (d) poly(amidoxime) ligand 2 .	46
Figure 3.5	Preparation of corn-cob cellulose supported poly(amidoxime) Pd(II) complex 3 .	47
Figure 3.6	Preparation of corn-cob cellulose supported Cu(II) complex 4 .	48
Figure 3.7	Preparation of corn-cob cellulose-supported CuNP@PA.	48
Figure 3.8	General Mizoroki-Heck reaction.	49
Figure 3.9	Heck-Matsuda reaction of arenediazonium tetrafluoroborate with olefins.	50
Figure 3.10	General Click reaction.	50
Figure 3.11	Aza-Michael reaction.	51
Figure 3.12	Preparation of cinnamic acid butyl ester.	52
Figure 3.13	Preparation of Ozagrel butyl ester.	52
Figure 3.14	Preparation of Ozagrel hydrochloride.	53
Figure 4.1	Synthesis of poly(amidoxime) Pd(II) complex 3 .	55
Figure 4.2	FTIR spectra of the (a) corn-cob cellulose, (b) Poly(acrylonitrile) 1 (corn-g-PAN), (c) poly(amidoxime) chelating ligand 2 and (d) poly(amidoxime) Pd(II) complex 3 .	56
Figure 4.3	FE-SEM images of (a) corn-cob cellulose, (b) Poly(acrylonitrile) 1 , (c) poly(amidoxime) chelating ligand 2 , and (d) poly(amidoxime) Pd(II) complex 3 respectively.	58
Figure 4.4	EDX spectrum of Pd(II) complex 3 .	59
Figure 4.5	(a) HR-TEM image of poly(amidoxime) Pd(II) complex 3 and (b) HR-TEM image of 4 th reused poly(amidoxime) Pd(II) complex 3 .	59
Figure 4.6	X-ray powder diffraction (XRD) of (a) fresh and (b) reused Pd(II) complex 3 .	60

Figure 4.7	(a) Full scan XPS spectrum of fresh Pd(II) complex 3 and (b) narrow scan XPS spectrum of fresh Pd(II) complex 3 .	61
Figure 4.8	(a) Full scan XPS spectrum of reused Pd(II) complex 3 and (b) narrow scan XPS spectrum of reused Pd(II) complex 3 .	61
Figure 4.9	Synthesis of poly(amidoxime) Cu(II) complex 4 .	62
Figure 4.10	FTIR spectrum of (a) corn-cob cellulose, (b) (corn-g-PAN), (c) poly(amidoxime) 2 and (d) poly(amidoxime) Cu(II) complex 4 .	63
Figure 4.11	FE-SEM images of (a) poly(amidoxime) chelating ligand 2 , (b) poly(amidoxime) Cu(II) complex 4 .	64
Figure 4.12	EDX spectrum of corn-cob cellulose supported poly(amidoxime) Cu(II) complex 4 .	65
Figure 4.13	HR-TEM image of Cu(II) complex 4 .	65
Figure 4.14	Synthesis of CuNP@PA.	66
Figure 4.15	Size distribution of the CuNP@PA.	66
Figure 4.16	(a) HR-TEM image of CuNP@PA, (b) HR-TEM image of 3 rd reused CuNP@PA.	67
Figure 4.17	XRD pattern of Cu(II) complex 4 .	67
Figure 4.18	XRD pattern of (a) fresh CuNP@PA and (b) reused CuNP@PA.	68
Figure 4.19	(a) Full scan XPS of Cu(II) complex 4 and (b) narrow scan XPS of Cu(II) complex 4 .	69
Figure 4.20	(a) Full scan XPS of Cu(I) and (b) narrow scan XPS of Cu(I).	69
Figure 4.21	(a) Full scan XPS of fresh CuNP@PA and (b) narrow scan XPS of fresh CuNP@PA.	70
Figure 4.22	(a) Full scan XPS of reused CuNP@PA and (b) narrow scan XPS of reused CuNP@PA.	70
Figure 4.23	Synthesis of Ozagrel hydrochloride.	79
Figure 4.24	Mizoroki-Heck reaction using recycled Pd(II) complex 3 .	86
Figure 4.25	Hot filtration or heterogeneity test (according to Table 4.5, entry 3).	87
Figure 4.26	Photo images of (a) Cu(II) complex 4 , (b) after reduction of Cu(II) complex 4 using sodium ascorbate.	89

Figure 4.27	Recycling of the Cu(II) complex 4 .	95
Figure 4.28	Hot filtration of Cu(II) complex 4 .	96
Figure 4.29	Chemoselective Aza-Michael reaction.	101
Figure 4.30	Recycling test of CuNP@PA in Aza-Michael reaction.	106

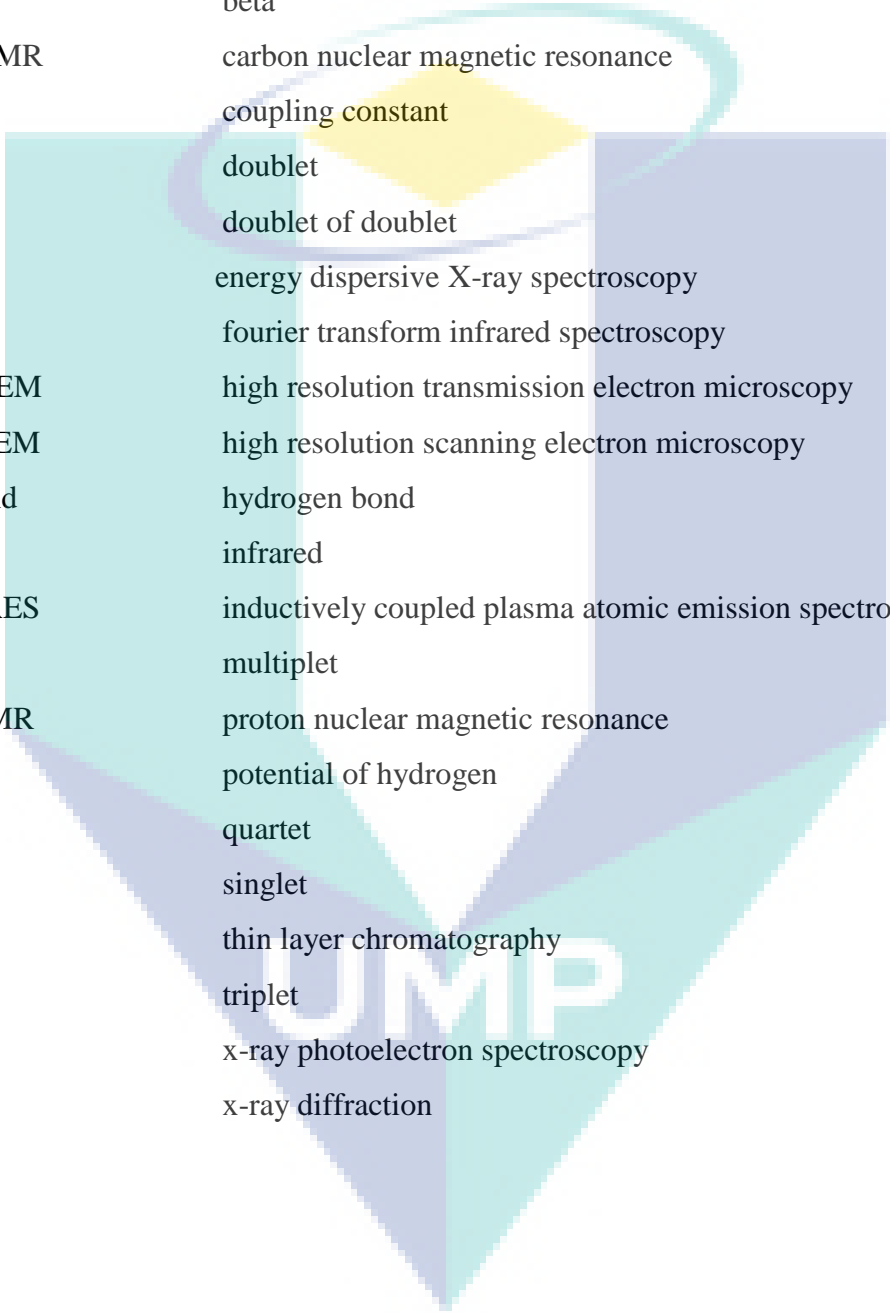


LIST OF SYMBOLS



°C	degree centigrade
g	gram
cm ⁻¹	per centimetre
δ	chemical shift
equiv	equivalence
Hz	hertz
h	hour
L	litre
MHz	mega hertz
µm	micrometre
mg	milligram
ml	millilitre
mmol	millimole
mol	mole
mol L ⁻¹	mole per litre
nm	nanometre
%	percentage
M	molar
N	normality
sec	second
cm ²	square of centimetre
mol%	mole percentage

LIST OF ABBREVIATIONS



α	alpha
Ar	aromatic
β	beta
^{13}C NMR	carbon nuclear magnetic resonance
J	coupling constant
d	doublet
dd	doublet of doublet
EDX	energy dispersive X-ray spectroscopy
FTIR	fourier transform infrared spectroscopy
HR-TEM	high resolution transmission electron microscopy
HR-SEM	high resolution scanning electron microscopy
H-bond	hydrogen bond
IR	infrared
ICP-AES	inductively coupled plasma atomic emission spectroscopy
m	multiplet
^1H NMR	proton nuclear magnetic resonance
pH	potential of hydrogen
q	quartet
s	singlet
TLC	thin layer chromatography
t	triplet
XPS	x-ray photoelectron spectroscopy
XRD	x-ray diffraction

CHAPTER 1

INTRODUCTION

1.1 Background

Carbon-carbon bonds provide the framework on which most organic molecules are formed. Therefore, the development of this method for selective synthesis of carbon-carbon and carbon-nitrogen bonds are very important in the synthetic organic chemistry. Such importance is reflected in the fact that the Nobel Prize in Chemistry was awarded several times in this area (Grignard reaction 1912, Diels-Alder reaction 1950, Wittig reaction 1979, Olefin metathesis 2005 and most recently palladium catalyzed cross-coupling reactions 2010).

Increasing environmental concerns have pushed chemists to turn their attention from the traditional concepts of process efficiency to green and sustainable chemistry that assign minimization of waste generation and avoid the use of toxic and/or hazardous substances (Anastas & Kirchhoff, 2002; Anastas & Eghbali, 2010; Dunn, 2012; Marques & Machado, 2014; Chao-Jun & Anastas, 2012). Specifically, the guiding principle of green chemistry can be paraphrased as: safer products by design, innocuous solvents and auxiliaries, atom efficiency, less hazardous/toxic chemicals, more energy efficient by design, inherently safer processes, preferably renewable raw materials, shorter syntheses, catalytic rather than stoichiometric reagents, design products for degradation, analytical methodologies for pollution prevention and waste prevention instead of remediation (Himaja et al., 2011; Sheldon, 2012).

Green catalysis, a key component of these principles, is extremely important in the modern development of green chemistry (Wenda et al., 2011; Beletskaya & Kustov, 2010; Sheldon, 2014). A good catalyst must possess specific features, including low

preparation cost, high activity, great selectivity, high stability, efficient recovery, and good recyclability (Di Lena & Matyjaszewski, 2010). Nowadays, several effective strategies resulting in green catalysis have been discovered, such as the recovery of catalyst, cascade reaction protocol, the use of green solvents (neat condition, water, ethanol and ionic liquids), flow conditions, photocatalysis, and so on (Kalidindi & Jagirdar, 2012 ; Sheldon, 2014). The design and use of recoverable catalysts are the most promising and straightway to green catalysis because the recovery of the catalyst is not only a task of great economic and environmental importance in catalysis science but also overcome the problem of metal contamination in products.

Catalyst recovery can be done by the experimental manipulations of precipitation, centrifugation, traditional filtration, magnetic separation, and extraction (Su et al., 2010; Corma et al., 2010). To achieve these processes, organic and inorganic supports including metal oxides, dendrimers, alumina, polymers, zeolites, silica, graphene and metal nanoparticles are needed for immobilizing free catalytic species to form heterogeneous catalysts.

The Mizoroki-Heck cross-coupling reaction is very important in the synthesis of natural products and fine chemicals (Torborg & Beller, 2009; Khazaei et al., 2013; Vadaparthi et al., 2015; Gøgsig et al., 2012). It has been widely applied in diverse areas such as pharmaceuticals, biologically-active molecules and material science, where they provide a powerful and straightforward method for C-C bond formation (Favier et al., 2011; Lasch et al., 2016; Mahdavi & Sahraei, 2016; McGlacken & Bateman, 2009). To date, many metallic catalysts have been widely studied for Mizoroki-Heck, Click and Aza-Michael reactions. Among the metal catalysts, palladium-based catalysts have become the main topic because of their outstanding performance in cross-coupling reactions (Molnár, 2011; Amatore & Jutand, 2000; Shang et al., 2014; Leclerc & Fagnou, 2006). The palladium-mediated cross-coupling of an aryl halide with an alkene afforded the corresponding aryl alkene independent reports by Mizoroki (1971), Mori (1973), and Heck (1979).

However, homogeneous palladium-based catalyzed Heck reactions (Pryjomka et al., 2006) have significant drawbacks including the low stability of the catalyst, the toxicity caused by the residual metal species, and the difficulty in recovering the

catalyst which has impeded large-scale production in industries. Moreover, the homogeneous palladium catalysts tend to lose their catalytic activity because of aggregation and precipitation as a palladium metal (Tsuji & Fujihara, 2007). The high cost of metal catalysts, the toxicity of the reaction residues, and the complication of isolating the final product and the catalyst precursors demands the development of easily recoverable palladium catalysts that can be reused without a significant reduction in their catalytic activity (Pagliaro et al., 2011).

To overcome this serious issue, a common strategy has been adopted to prepare heterogeneous metal catalysts by anchoring suitable transition metal salts onto solid supports to provide high catalytic activity and selectivity. In recent years, numerous heterogeneous supported palladium catalysts have successfully been employed in the Mizoroki-Heck reaction, such as mesoporous materials (Echeandia et al., 2014), polymers (Rangel et al., 2015), activated carbons (Yang et al., 2013), graphene (Elazab et al., 2015) and cellulose (Jadhav et al., 2016). However, in these hybrid systems, palladium nanoparticles are usually involved.

On the other hand, the number of covalently anchored palladium-based molecular catalysts with a naturally wide abundance, cost-effective, and chemically and mechanically stabilized heterogeneous solid supports is limited. The scientific community is recently looking for bio-renewable materials and resources to meet green sustainable approaches. In this aspect, bio-cellulose can be the most alternative resources due to its wide natural abundance and low cost, biodegradability, high stability, and insolubility in the common organic solvents. However, cellulose can be modified and suitable chelating group can be introduced. Recently, Rahman et al. (2016) modified the cellulose backbone and introduced poly(amidoxime) and poly(hydroxamic acid) which were efficiently removed the transition metal ions from the waste water. The cellulose backbone or modified cellulose supported metal catalysts have also been used for various chemical transformations (Reddy and Kumar, 2006).

The original reaction conditions that Professor Heck reported are, in some ways, more desirable than those that are commonly used today. In his system, all reactions were carried out on the bench top, essentially under hot condition. When heat was required, a steam bath was used as the heat source (Heck & Nolley, 1972). Over time,

with the development of new ligand systems of the reaction, the conditions have had to evolve as well. It is now very common to see these reactions being carried out in some polar solvents (including but not limited to tetrahydrofuran (THF), dimethylformamide (DMF), dimethylacetamide (DMA), dioxane, and even in water mixtures) at elevated temperatures (Lee et al., 2011). Generally, these solvents must be degassed to protect the integrity of the catalyst or the phosphine ligands as they will oxidize in the presence of oxygen. Pd(OAc)₂ is still commonly used, as well as other palladium sources such as Pd₂(dba)₃CHCl₃ (Kang et al., 1998). The copper-catalyzed alkyne-azide Huisgen-type cycloaddition (Click reaction) yielding 1,4-disubstituted 1,2,3-triazoles has received a lot of attention and has driven various applications in biological science, synthetic organic chemistry and medicinal chemistry (Meldal, 2008; Sharpless & Manetsch, 2006).

In addition, the conjugate reaction of various amines with α , β -unsaturated carbonyl compounds provides β -amino carbonyl ingredients which have received a great attention because of its numerous synthetic applications such as in the synthesis of biologically active molecules, functional materials, and pharmaceutical products (Fustero et al., 2002; Amara et al., 2013; Sanchez-Rosello et al., 2014). Generally, Aza-Michael reactions proceed in the presence of strong acids or bases, and some side products are also formed. Despite the great advances in metal-catalyzed Aza-Michael reactions, there are still shortcomings for their practical utilization, such as the use of expensive precious metals, the use of air and moisture sensitive metal catalysts, etc. Among the numerous protocols involving Aza-Michael reactions, copper-catalyzed processes are particularly attractive due to their ease of handling, the use of environmentally benign and low-cost copper salts, and the mild reaction conditions (Ying et al., 2013; Sunaba et al., 2014).

Raw materials are an important factor for industrial growth. The proper utilization of indigenously available organic resources not only solves the disposal problem and ensures rich dividends to the agro-based community, but can open up a reservoir of natural resources for meeting the various challenges faced during industrial development. The importance of agricultural and forestry waste to the national economy in the production of useful chemicals has been emphasized (Taylor et al., 2010). Several tons of cellulose materials (such as from corn, bagasse) are annually produced globally

and a majority of these materials are considered as wastes after using a small percentage of the production capacity as fuel or for other purposes (García et al., 2016). Thus, these agricultural wastes or natural cellulose could be utilized for the production of useful heterogeneous catalysts.

Scientists are currently searching for cheap and more environmentally-friendly renewable resources and sustainable processes. In this context, bio-cellulose, which is widely abundant in nature, would be a compatible material. The improvement of bio-based materials and composites could be a promising solution in terms of both environmental and application aspects. The structure of biopolymers provide several advantages such as low density and cost, a bio-renewable character, ubiquitous, and interesting mechanical properties compared to glass fibers (Bolton, 1994). Thus, natural celluloses would be desirable and attractive materials to be explored as solid supports for catalysts (Guibal, 2005). Therefore, the development of a promising heterogeneous catalyst in an easy and convenient method which can be applied to a number of substrates of different natures in a catalytic process under mild reaction conditions is highly attractive.

1.2 Problem Statement

Homogeneous metal catalyzed reactions are complicated and difficult to purify the product from the reaction mixture. Homogeneous metal catalyzed reactions have several disadvantages such as highly cost, unstable in the reaction media, not environmental friendly, and cannot be recycled. Therefore, attempts were made to attach catalysts to an insoluble support to improve the handling and separation of the catalysts from the reaction mixture and enhance its recycling capability as well. Due to the change of metal oxidation states and the leaching of metal ion into the reaction media, reclamation and purification have become complicated; the overall efficiency of synthetic processes is significantly reduced. On the other hand, cellulose wastes generation is daily increasing due to underutilization. Thus, it is essential to utilize these cellulose materials to develop heterogeneous metal catalysts with high catalytic activity, selectivity, stability, safe and reusability for green organic synthesis.

1.3 Hypothesis

We have isolated cellulose from waste corn-cob to prepare cellulose support heterogeneous metal complexes and its applications. Cellulose is a biodegradable natural polymer and most abundant renewable organic raw material in the world. The backbone of cellulose could be tailored with the attachments of chelating or metal binding functionalities. Through the grafting polymerization of cellulose with selective chelating group, the strength of the cellulose could be enhanced and metal catalysts could be immobilized. In this present work, cellulose was isolated from the waste corn-cob and it was successfully functionalized to poly(amidoxime) chelating ligand. The chelating ligand was treated with palladium and copper salts to give cellulose supported poly(amidoxime) palladium and copper complexes. The synthesis procedure of cellulose supported poly(amidoxime) metal complexes were easy and both complexes were well stable in an aerobic condition.

The cellulose supported heterogeneous poly(amidoxime) metal complexes were successfully utilized for C-C and C-N bond formation reactions. The complexes were stable in the reaction media and repeatedly used several cycles with significant loss of their catalytic activity. Additionally, poly(amidoxime) palladium complex was used to synthesis of Ozagrel hydrochloride which is an important antiasthmatic agent.

1.4 Objective of Research

The goal of this research is to synthesize and characterize cellulose supported bio-heterogeneous copper and palladium catalysts using cellulosic waste materials such as corn-cobs. The application of these catalysts in different types of cross-coupling reactions in the synthesis of the biologically active molecule has attracted great attention. The main objectives of this study are as follows:

- 1) To synthesize and characterize heterogeneous palladium and copper catalysts using modified cellulose.
- 2) To study the application of the catalysts for C-C and C-N bonds formation reactions namely, Mizoroki-Heck, Click and Aza-Michael.
- 3) To synthesize biologically active molecule Ozagrel hydrochloride.

1.5 Scope of Research

The scope of the study is as follows:

- 1) The corn-cob cellulose was extracted from waste corn-cobs and chemically modified through graft copolymerization and subsequent amidoximation.
- 2) The resulting poly(amidoxime) ligand was treated with palladium and copper salts to give heterogeneous poly(amidoxime) palladium or copper complexes.
- 3) The prepared poly(amidoxime) metal complexes were characterized using several spectroscopic methods such as FTIR, FE-SEM, ICP-AES, HR-TEM, XRD, EDX and XPS.
- 4) Application of the metal complexes for various chemical bonds formation reactions.
- 5) The heterogeneity of the metal complexes was evaluated through hot filtration.
- 6) The poly(amidoxime) palladium complex was applied for the synthesis of biologically active molecules.

1.6 Thesis Outline

The study presented in this thesis aims to understand the catalytic activity of cellulose supported copper and palladium complexes and nanoparticles as catalyst in Mizoroki-Heck, Aza-Michael and Click reactions. It also intended to apply the complexes in the synthesis of biologically important molecules. The outline of this thesis is as follows: Chapter 1: Presented of the research background, problem statement, hypothesis, objectives of the study, scope of the research, and the thesis outline. Chapter 2: Provided the theoretical aspects which are related to the research. Chapter 3: Presented the procedures and the synthetic pathways adopted in the study. Chapter 4: Presented the characterization of the synthesized compounds. Chapter 5: Concluded the study by relating the results with the theoretical and experimental findings.

CHAPTER 2

LITERATURE REVIEW

2.1 Catalysts

A catalyst is a substance which speeds up a chemical reaction but is not consumed in the reaction. Catalysts typically increase the speed of a reaction by reducing the activation energy or changing the reaction mechanism. Enzymes are proteins that act as catalysts in biochemical reactions. Common types of catalysts include enzymes, acid-base, homogeneous and heterogeneous catalysts (Hattori, 2001). Generally, catalysts work by either lowering the energy of the transition state, lowering the activation energy, or changing the mechanism involving the transition state. Any chemical reaction must undergo a rearrangement of their chemical bonds during the reaction. Energy (activation energy) is required to form the transition state of reactions.

Lower energy reactants, compared to the activation energy, cannot pass through the transition state to react and form products. The catalyst can work by providing a different route via lowering the reaction activation energy. At any given time, the presence of a catalyst allows a greater proportion of the reactant species to acquire sufficient energy to pass through the transition state and become products (Gladysz, 2001). Catalysts cannot shift the position of a chemical equilibrium; the forward and backward reactions are both quickly run and as a result, the equilibrium constant is unchanged. However, removing products from the reaction mixture as they form will increase the overall rate of product formation.

2.2 Different Types of Catalysts

The catalyst can be classified in many ways, but they are commonly divided into two types which are homogeneous and heterogeneous catalysts.

2.2.1 Homogeneous Catalysts

A homogeneous catalyst is a type of catalyst which remains in the same phase with the reactants; usually dissolved in a solvent. Homogeneous catalysts have important advantages over their heterogeneous counterparts. For example, all catalytic sites are accessible because the catalyst is usually dissolved into the reaction mixtures (Cole-Hamilton, 2003). However, many homogeneous catalytic systems have not been commercialized because of their major disadvantages compared to the heterogeneous catalysts. Generally, homogeneous catalysts cannot be separated from the reaction mixture; as a result, product is always contaminated by the catalyst. Another drawback of this catalyst is that it cannot be completely recycled or reused in the next run.

Nowadays, the application of membrane technology in homogeneous catalyst recycling has received more attention (Dijkstra et al., 2002; Janssen et al., 2011). This technology offers a solution for the homogeneous catalysis, which is, recycling of the catalyst. On both environmental and industrial points of view, this technology is very interesting as it allows the future application of homogeneous catalysts in the synthesis of commercial products, leading to a faster, cleaner, and highly selective green industrial processes. A great variety of homogeneous catalysts are known, ranging from Brønsted and Lewis acids widely used in organic synthesis to metal complexes, metal ions, organometallic complexes and etc. A reaction between carbon dioxide and hydrogen in the presence of a homogeneous catalyst (ruthenium complex) to form methanol and water is shown in Figure 2.1.

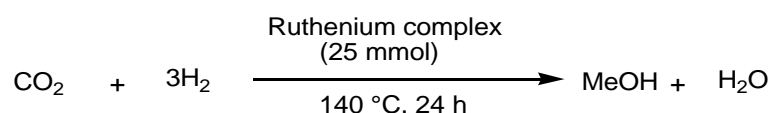


Figure 2.1 Homogeneous ruthenium complex catalyzed reaction. Reaction conditions: ruthenium complex (25 μmol), substrate (2.5 mmol) and THF (2 mL) at 140 $^\circ\text{C}$ for 24 h.

Source: Wesselbaum et al. (2012).

2.2.2 Heterogeneous Catalysts

Heterogeneous catalysts refer to the form of catalysts where the phase of the catalyst differs from that of the reactants and reaction media. Different types of solids are used in the heterogeneous catalysis reactions (Lee et al., 2009). These may be metals, metal oxides, or metal sulfides. These materials may be used in their pure form or in their mixtures (Bauer et al., 1993). Furthermore, they may be crystalline, microcrystalline, and amorphous. These catalysts are used in a very small amount and also as a powder so as to provide a large surface area.

The advantage of the heterogeneous catalyst is that they can be recycled and reused several times. Generally, heterogeneous catalysts are prepared by the dispersion of transition metals onto a good solid surface phenomenon. This offers a greater percentage of metal atoms on the surface of the metal crystallites and also a higher efficiency of the catalyst (Schatz et al., 2010). This also showed that the crystalline-sized metal catalysts are better for a facile reaction (Hosseini et al., 2015; Zhou et al., 2010). Most of the research in the field of heterogeneous catalysts are carried out on producing more finely-dispersed metal particles. An example of a heterogeneously catalyzed reaction is shown in Figure 2.2.

The core-shell nanogels are attractive stabilizers and support for catalytically-active metallic nanoparticles (Pontes da Costa et al., 2017). The synthesis and characterization of a nanostructured well-defined core-shell nanogel which can stabilize palladium nanoparticles requires the utilization of a heterogeneous catalyst. This heterogeneous catalyst hybrid nanogel displays a remarkable stability in both solid states and in solution. These properties allowed its successful application as a

heterogeneous catalyst for the Mizoroki-Heck reaction between *n*-butyl acrylate and a series of bromo and iodoarenes. The yields were excellent, and the catalyst can be reused for several runs without a significant loss in its catalytic activity.

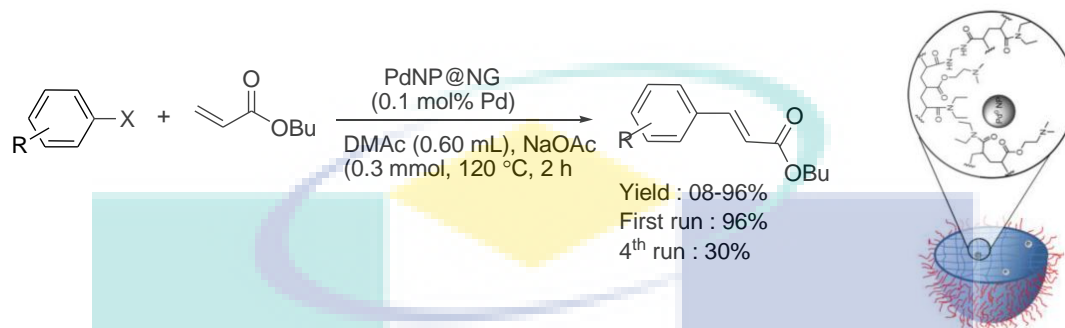


Figure 2.2 Heterogeneous PdNP@NG-catalyzed Heck reaction. Reaction conditions: aryl halide (0.25 mmol), *n*-butyl acrylate (0.425 mmol), NaOAc (0.3 mmol), PdNP@NG (0.1 mol% Pd) and DMAc (0.60 mL) at 120 °C for 2 h.

Source: Pontes da Costa et al. (2017).

2.3 Cellulose

Cellulose is an organic compound with the formula $(C_6H_{10}O_5)_n$ and is found in the cellular structure of all plant matter. Cellulose constitutes the most abundant and renewable polymer resource available worldwide (William et al., 2008). This organic compound, which is considered the most abundant on earth, is even excreted by some bacteria. Cellulose provides structure and strength to the cell walls of plants and provides fiber in our diets. Although some animals, such as ruminants, can digest cellulose, humans cannot.

Cellulose falls into the category of indigestible carbohydrates known as dietary fiber for a human being. In recent years, cellulose has become a popular food additive due to its unique chemical and physical properties when combined with water. Although cellulose can be found in most plant matter, the most economical sources of industrial cellulose are cotton and wood pulp (Morán et al., 2008). Cellulose has a ribbon shape that allows it to twist and bend in the direction out of the plane, as a result, the molecule is moderately flexible (William et al., 2008). A comparatively very strong interaction between neighbouring cellulose molecules in dry fibers due to the presence of the

hydroxyl (-OH) groups which stick out from the chain form intermolecular hydrogen bonds.

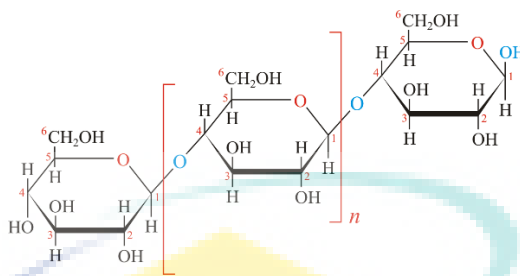


Figure 2.3 Cellulose structure.

Source: Brown (2004).

Cellulose can be extracted from wood pulp or cotton and chemically processed with acids or alkali. Some types of modified cellulose are soluble and some insoluble. It can also be produced from corn-cobs or stalks, soybean hulls, sugar cane stalks, oat hulls, rice hulls, wheat straw, sugar beet pulp, bamboo, jute, and flax. Chemical modification can be used to vary certain properties of cellulose such as its hydrophilic or hydrophobic character, elasticity, water absorbency, adsorptive or ion exchange capability, resistance to microbiological attack, and thermal resistance (McDowall et al., 1984). Modified cellulose is also used as a medium for the preparation of transition metal catalysts like palladium nanoparticles, copper nanoparticles which are used in Mizoroki-Heck, Click and Aza-Michael reactions (Mandal et al., 2016; Sarkar et al., 2017).

2.4 Cellulose Supported Catalysts

Currently, scientists are looking for sustainable, biodegradable and environmental friendly resources. Cellulose is the most common biopolymer which can be obtained a bulk amount from the nature. Cellulose has high chemical and mechanical stability and metal binding capacity. Interestingly, the hydroxyl groups on cellulose easily enable chemical modifications, like carboxymethylation, silylation and periodate oxidation, to improve the physical and chemical properties (Mondal et al., 2015). There are several researchers have been used commercial cellulose as a solid support for a variety of chemicals transformations such as Cell-CuI NPs catalyzed Click reaction (Chavan et al., 2014), PdNPs@TiO₂-Cell catalyzed Heck-Suzuki reactions (Jadhav et

al., 2016), crystalline cellulose supported Cu(I) catalyzed Huisgen reaction (Koga et al., 2012), Fe₃O₄@chitosan-Schiff base Pd-nanoparticle catalyzed Suzuki and Heck reactions (Naghipour & Fakhri, 2016), cellulose-supported Cu(0) catalyzed Aza-Michael reaction (Reddy & Kumar, 2006) and chitosan supported copper catalyzed Click reactions (Anil Kumar et al., 2015). However, there are few examples where cellulose was isolated from the natural sources and it was utilized for various chemical transformation reactions (Mandal et al., 2016; Sultana et al., 2016).

2.5 Transition Metal Catalyzed Reactions

Developing efficient and atom-economic methods for C-C bond formation are always an important concern in synthetic chemistry (Liu et al., 2011; Sheldon, 2012). The cross-dehydrogenative coupling reaction is a desirable synthetic approach toward the carbon-carbon bond formation, as it does not require additional functionalization of subcomponents (Girard et al., 2014). The first period of transition metals is scandium (Sc), titanium (Ti), vanadium (V), chromium (Cr), manganese (Mn), iron (Fe), cobalt (Co), nickel (Ni), copper (Cu), and zinc (Zn). Generally, the common features of these metals are the presences of *d*-electron and their unfilled *d*-orbitals. As a result, transition metals form complexes with variable oxidation states (Rai et al., 2016). Thus, transition metals are electron banks that give up electrons at the appropriate time and store them for chemical species at the other times.

Transition metal-catalyzed cross-coupling reactions of organic electrophiles and organometallic reagents have appeared as tremendously powerful synthetic tools (Liu et al., 2011). The development has reached a level that allows a wide range of coupling partners to be combined efficiently (Smith & Basset, 1977). In the past three decades, this illustration for carbon-carbon bond formation has allowed chemists to gather complex molecular frameworks of diversified interests, surrounding the total synthesis of natural products, medicinal chemistry, and development of industrial processes, as well as chemical biology, materials, and nanotechnology. The rise of transition metal catalyzed cross-coupling reactions as a popular method in the area of synthesis develops from both the diversity of organometallic reagents utilized in these reactions and also the broad range of functional groups that can be incorporated into these reagents (Shi et al., 2011).

Transition metal-catalyzed cross-coupling reactions also have been considered as one of the most powerful and reliable tools for those bond connections, giving complex molecular structures to be prepared in an efficient and economical manner. In particular, coupling reactions, including Sonogashira, Mizoroki-Heck, Kumada, Negishi, Stille, Aza-Michael, Suzuki–Miyaura, Click, and Buchwald–Hartwig reactions have extensively utilized transition metal catalysts such as palladium, copper, nickel, gold, silver, platinum (Aiken & Finke, 1999), and some of them are discussed below:

2.5.1 Sonogashira Reaction (C≡C)

Sonogashira cross-coupling reaction involved C≡C bond formation and mostly used palladium catalyst. The palladium-catalyzed mechanism begins with the oxidative addition of the organohalide to the Pd(0) to form a Pd(II) complex (Mino et al., 2011). This reaction, which provides a powerful tool for the formation of alkynes, has widely contributed to pharmaceutical, agrochemical, and chemical industries. Recently, other transition metals such as platinum, ruthenium, gold, copper, and silver are also used in this cross-coupling reactions (Jun 2004; Molnár, 2011). Palladium-catalyzed reactions, in particular, carbon-carbon bond forming reactions, including Sonogashira reaction either through homogeneous or heterogeneous catalysis have gained prominence in organic chemistry (Sonogashira et al., 1975).

2.5.2 Suzuki Reaction (C-C)

Suzuki reaction is classified as a coupling reaction where the coupling partners are boronic acid and an organohalide catalyzed by Pd(0) complex. It was first published in 1979 by Akira Suzuki, and he shared the 2010 Nobel Prize in Chemistry with Richard F. Heck and Ei-ichi Negishi for their effort in the discovery and development of palladium-catalyzed cross-couplings in organic synthesis. In many publications, this reaction also goes by the name Suzuki–Miyaura reaction and is also referred to as the Suzuki coupling (Paul et al., 2015). It is widely used to synthesize poly-olefins, styrene's, and substituted biphenyls. The general scheme for the Suzuki reaction is shown in Figure 2.4, where a carbon-carbon single bond is formed by coupling an organoboron species with a halide using a palladium catalyst in presence of a base.

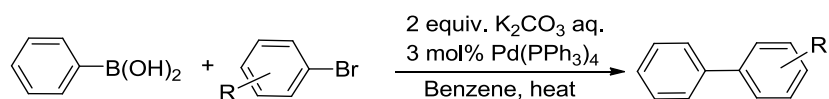


Figure 2.4 Suzuki coupling reaction.

Source: Suzuki et al. (1981).

Figure 2.4 showed the first published Suzuki coupling which is the palladium-catalyzed cross-coupling between organoboronic acid and halides. Recent catalyst and method developments have broadened the possible applications enormously so that the scope of the reaction partners is not restricted to aryls, but includes alkyls and alkynyls (Maluenda & Navarro, 2015). Potassium trifluoroborate and organoboranes may be used in place of boronic acids. Some pseudohalides (for example triflates) may also be used as coupling partners. This reaction is used to create carbon-carbon bonds to produce conjugated systems of alkenes, styrenes, or biaryl compounds.

2.5.3 Negishi Reaction (C-C)

Negishi coupling widely employs palladium and nickel metals which allow the formation of unsymmetrical biaryls with good yields. Negishi cross-coupling is an organic reaction between organohalide and an organozinc compound to give the biaryl product (Negishi et al., 1977; Haas et al., 2016; Phapale & Cárdenas, 2009). The Pd-catalyzed mechanism begins with the oxidative addition of the organohalide to the Pd(0) to form Pd(II) complex (Nicolaou et al., 2005). After transmetalation of organozinc reagent (Figure 2.5), become Zn(II), followed by the reductive elimination which gives the final biaryl coupled product with the regeneration of the catalytic species (Casares et al., 2007).

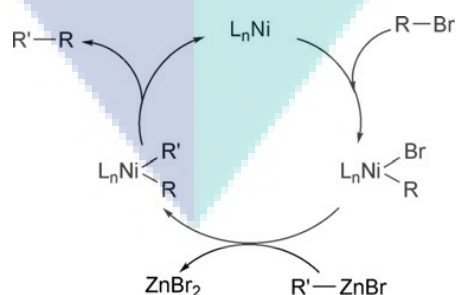


Figure 2.5 Mechanism of the Negishi coupling.

Source: Phapale & Cárdenas (2009).

2.5.4 Stille Reaction (C-C)

Stille reaction, named after the late John Kenneth Stille, is a Pd-catalyzed cross-coupling reaction. It involves the coupling of an organic halide with an organotin compound (Espinet & Echavarren, 2004; Xu et al., 2015). The reaction proceeds according to Figure 2.6. The groundwork for the Stille reaction was laid in 1976 and 1977 by Colin Eaborn, Toshihiko Migita, and Masanori Kosugi, who explored numerous palladium-catalyzed couplings involving organotin reagents. John Stille and David Milstein developed a much milder and more broadly applicable procedure in 1978. Stille's work on this area might have earned him a share of the 2010 Nobel Prize, which was awarded to Richard Heck, Ei-ichi Negishi, and Akira Suzuki for their work on the Heck, Negishi, and Suzuki coupling reactions.



Figure 2.6 Stille coupling reaction.

Source: Espinet & Echavarren (2004).

Stille coupling is a versatile C-C bond forming reaction between stannanes and halides (Cordovilla et al., 2015) or pseudohalides with very few limitations on the R-groups. Well elaborated methods allow the preparation of different products from all the combinations of halides and stannanes.

2.5.5 Mizoroki-Heck Reaction (C-C)

Over the last fifty years, many new C-C bond forming reactions have been discovered. Among them a broad genus lies the art of coupling reactions-reactions that catalytically bring together two neutral organic precursors (Heck and Nolley 1972; Shirakawa et al., 1999; Mizoroki et al., 1971; Suzuki, 1999; Negishi et al., 1977). One important participant in this particular field is the Heck olefination reaction. In its most basic form, the Heck olefination is the palladium-catalyzed coupling of an aryl halide and an olefin to form an aryl alkene. The first example of such reaction was discovered in 1971 by Mizoroki (Figure 2.7).

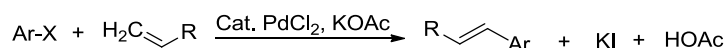


Figure 2.7 Mizoroki coupling reaction.

Source: Mizoroki (1971).

In January 1972, Richard Heck reported an optimized and improved coupling based on the work reported by Mizoroki (Figure 2.8). Heck's experimental procedure calls for 1% catalyst loading of palladium acetate, olefin, aryl halide, and some hindered amine to act as a base to neutralize the HX produced as a byproduct of the catalytic cycle (Heck & Nolley, 1972).

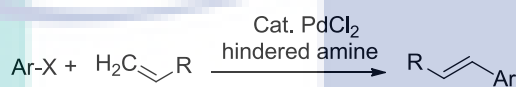


Figure 2.8 Heck coupling reaction.

Source: Heck & Nolley (1972).

In this way, Heck demonstrated that the reaction was practical, useful, and reasonable in general. This must lead to continuing interest over the past forty plus years. Since the discovery of this reaction, chemists have discovered ways to alter the original procedure to bend the outcome towards more favorable results for their individual needs (Hartmann & Kevan, 1999; Ehrentraut et al., 2000). The general reaction procedure has largely remained unchanged from the original except for the use of ligands to promote catalytic turnover rates, as well as to induce stereoselectivity in appropriate substrates (Shibasaki & Vogl, 1999; Ozawa et al., 1993).

Palladium-catalyzed Mizoroki-Heck reaction (Heck & Nolley, 1972) often represents a crucial synthetic reaction step which has received considerable attention due to its functional group tolerance and broad application ranging from synthetic organic chemistry to applied materials science (Heck, 1979). Gong et al. (2016) have reported a palladium-catalyzed Heck reaction of tosylate with electron poor olefin. The nickel-catalyzed Heck reaction of arenetosylate with an aliphatic olefin was also described by Tasker et al. (2014). However, arenediazonium tetrafluoroborate salts can be used instead of aryl halides and tosylates in the Heck-Matsuda coupling reaction (Oger et al., 2014). The practical benefits of using arenediazonium salts over common electrophiles such as aromatic halides and triflates are the economy, environment-

friendly, and synthetic accessibility since these salts can be easily prepared from cheap and commercially available amines (Schmidt & Wolf, 2017). Aryl halides are successfully employed as electrophiles in the Heck reaction due to their high reactivity but it suffers numerous drawbacks such as high temperature and long reaction time. Thus, the development of a new kind of electrophile to replace aryl halide is still in demand. Mizoroki-Heck reactions catalyzed by different heterogeneous catalysts are described below:

The palladium-DABCO complex supported on γ -Fe₂O₃ magnetic nanoparticles (Pd-DABCO- γ -Fe₂O₃) was synthesized and characterized by transmission electron microscopy, scanning electron microscopy, x-ray diffraction, x-ray photoelectron spectroscopy, fourier transform infrared spectroscopy, thermogravimetric analysis, and elemental analysis (Sobhani & Pakdin-Parizi, 2014). The synthesized catalyst was successfully applied as a new magnetically recyclable heterogeneous catalyst in Mizoroki-Heck cross-coupling reaction of aryl halides with alkyl acrylates and styrene under solvent-free conditions shown in Figure 2.9.

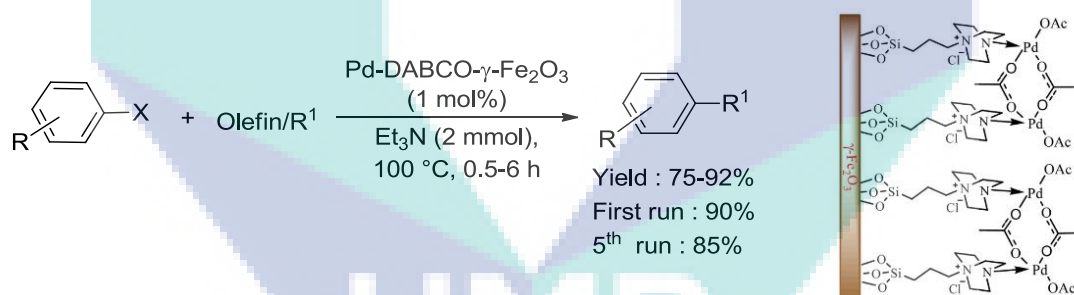


Figure 2.9 Pd-DABCO- γ -Fe₂O₃) complex supported Mizoroki-Heck cross-coupling reaction. Reaction conditions: aryl halide (1 mmol), olefin (1.1 mmol), Et₃N (2 mmol) and Pd-DABCO- γ -Fe₂O₃ catalyst (1 mol%) at 100 °C for 0.5-6 h.

Source: Sobhani & Pakdin-Parizi (2014).

4-amino-5-methyl-3-thio-1,2,4-triazole-functionalized polystyrene resin-supported Pd(II) complex was found to be an efficient catalyst in the palladium-catalyzed Mizoroki-Heck reactions of aryl iodides and bromides in water (Bakherad et al., 2013). Under appropriate conditions, this reaction gives the desired products in moderate to excellent yields. The catalyst is air-stable and easily available. The

palladium catalyst is easily separated and can be reused for several times without a significant loss in its catalytic activity (Figure 2.10).

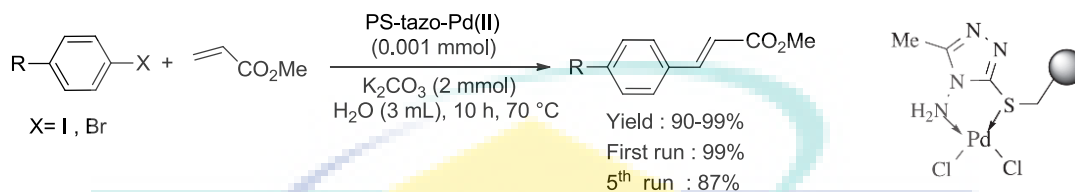


Figure 2.10 4-amino-5-methyl-3-thio-1,2,4-triazole-functionalized polystyrene resin-supported Heck reaction. Reaction conditions: aryl halide (1.0 mmol), methyl acrylate (1.5 mmol), PS-tazo-Pd(II), (0.001 mmol), K₂CO₃ (2.0 mmol) and H₂O (3 mL) at 70 °C for 10 h.

Source: Bakherad et al. (2013).

Aryl bromides could carry out the coupling reaction with a variety of alkenes at 80 °C in aqueous media under atmospheric condition. More importantly, the inexpensive catalyst is stable, which shows negligible metal leaching and retain good activity for at least ten successive runs (Figure 2.11) without any additional activation treatment (Wu et al., 2011).

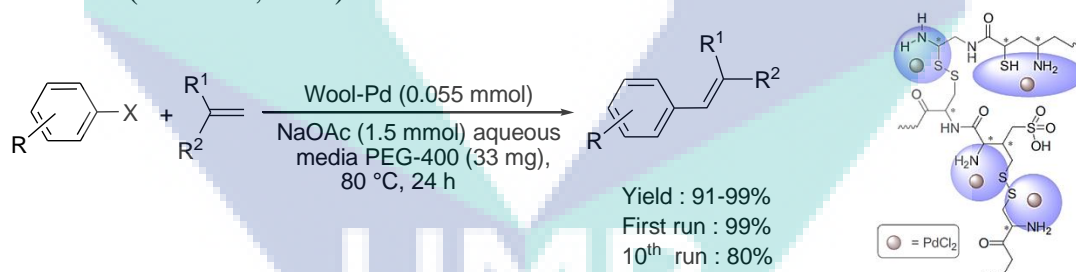


Figure 2.11 Heck coupling reaction with aryl halide. Reaction conditions: aryl halides (1.0 mmol), alkene (1.5 mmol), NaOAc (1.5 mmol), catalyst (50 mg), stirred in 15 mL aqueous media with PEG-400 (33 mg) at 80 °C for 24 h.

Source: Wu et al. (2011).

Fe₃O₄/SiO₂/HPGeOPPh₂-PNP was found as a magnetically separable and highly active catalyst for the Heck reactions of aryl iodides and bromides (Du et al., 2012). Under suitable conditions, all the reactions gave the desired products in moderate to excellent yields (Figure 2.12). Moreover, this catalyst can be easily recovered by using a magnet and directly reused for at least six cycles without significant loss of its catalytic activity.

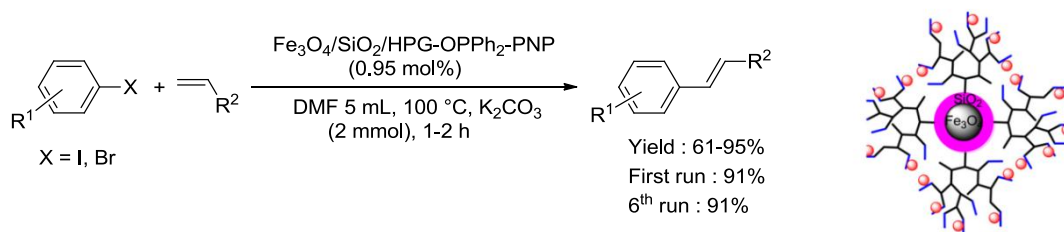


Figure 2.12 $\text{Fe}_3\text{O}_4/\text{SiO}_2/\text{HPGeOPPh}_2\text{-PNP}$ supported Heck reaction. Reaction conditions: aryl halides (1.0 mmol), olefins (1.5 mmol), K_2CO_3 (2.0 mmol), DMF (5.0 mL) and catalyst (0.025 g, 0.95 mol% of Pd) at 100 °C for 1-2 h.

Source: Du et al. (2012).

Silica gel has been directly phosphorylated to form silica diphenyl-phosphinite (SDPP). This new phosphorylated silica contains a higher amount of Pd(II) moiety compared to the method based on the sol-gel technique. The phosphorylated silica reacts with Pd(II) to produce nano Pd(0)/SDPP which was characterized by different techniques (Iranpoor et al., 2012). The obtained nano Pd(0) catalyst exhibited excellent reactivity and stability in the Mizoroki-Heck cross-coupling reaction with different aryl iodides and bromides. This heterogeneous catalyst can be easily recovered and reused in several runs (Figure 2.13).

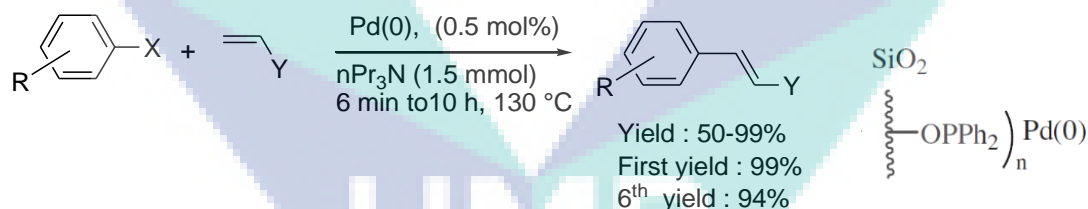


Figure 2.13 Heck coupling reaction using heterogeneous Pd(0) catalyst. Reaction conditions: aryl halide (1.0 mmol), *n*-butyl acrylate or styrene (1.5 mmol), $n\text{Pr}_3\text{N}$ (1.5 mmol) and SDPP/Pd(0), (0.5 mol%, 2 mg) at 130 °C for 6 min-10 h.

Source: Iranpoor et al. (2012).

The performance of lignin@Pd-NPs catalyst has been investigated for the Mizoroki-Heck C-C bond formation reactions. The reaction proceeds between *n*-butyl propene-2-enoate, halobenzenes and substituted halobenzenes in polar to highly polar solvents, as well as under solvent-free environment in the presence of organic or inorganic bases (Marulasiddeshwara & Kumar, 2016). The catalyst was found to be

highly efficient and yielded the desired products of up to 94% under solvent-free conditions in short reaction times (Figure 2.14). The catalyst was heterogeneous and hence, recovered by filtration and reused several times in the subsequent batches of the same reaction.

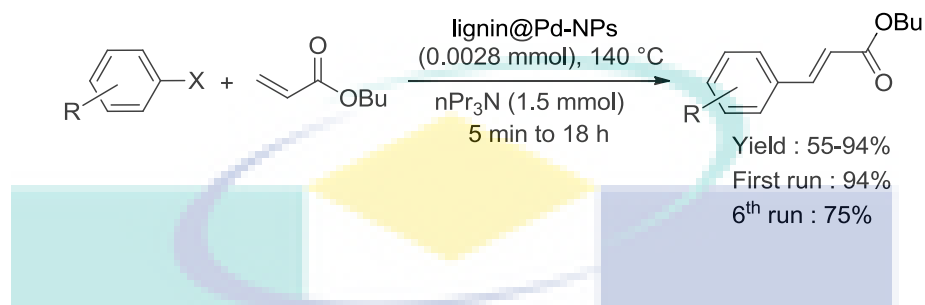


Figure 2.14 Lignin@Pd-NPs catalyzed Heck reaction. Reaction condition: reactions were carried out using (1 mmol) of iodobenzene, (1.5 mmol) of *n*-butyl acrylate and (1.5 mmol) of base in the presence of lignin@Pd-NPs (0.050 g; 0.0028 mmol of Pd) at 140 °C for 5 min-18 h.

Source: Marulasiddeshwara & Kumar (2016).

Gelatin/pectin stabilized palladium nanoparticles were prepared under green conditions without the addition of any external reducing agent and ligand. The synthesized palladium nanoparticles were studied in Mizoroki–Heck reaction between different aryl halides and *n*-butyl acrylate (Khazaei et al., 2015). The reaction was carried out under solvent-free conditions, and no complicated work-up process was needed for the separation of the nanoparticles. Besides, the products were obtained in highly short reaction times with excellent yields of up to 72 - 98%, and also reused up to six times without any significant loss of its catalytic activity (Figure 2.15).

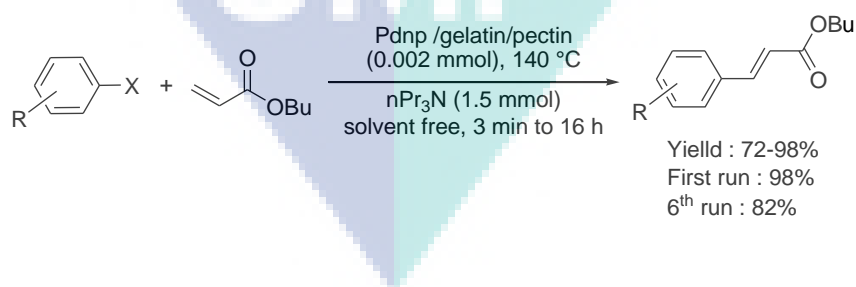


Figure 2.15 Gelatin/pectin stabilized palladium nanoparticles catalyzed Heck reaction. Reaction condition: reactions were carried out in the presence of aryl halide (1 mmol), alkene (1.5 mmol), *n*Pr₃N (1.5 mmol) and Pd-nanoparticles supported on gelatin and pectin (0.05 g, containing 0.002 mmol of Pd) at 140 °C for 3 min-16 h.

Source: Khazaei et al. (2015).

Palladium complexes were synthesized on the aromatic network of a graphenic material employing diazonium chemistry and additional easy modifications to generate a bidentate coordination site for the palladium atoms. The modified palladium-graphene hybrid was found to be active as a catalyst in the cross-coupling Heck reaction between styrene or butyl acrylate with a wide range of aryl bromides substituted with different electron-acceptor and electron-withdrawing groups (Fernández-García et al., 2016). The coupled products were obtained in good to excellent yields (Figure 2.16). In addition, the catalyst showed excellent cyclability and air stability and was reused over eight cycles without any loss of its catalytic activity.

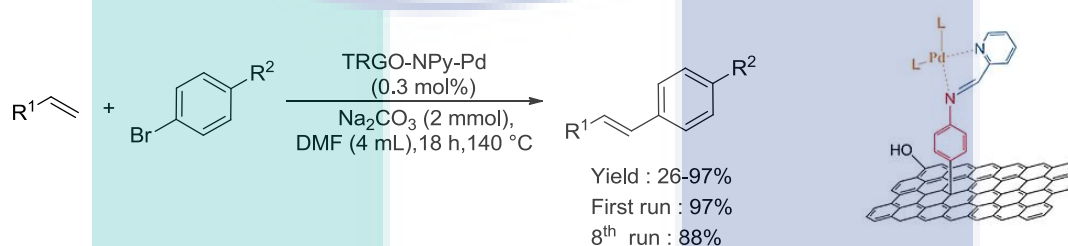


Figure 2.16 Heck cross-coupling reaction using Pd complex as a catalyst. Reaction conditions: vinyl substrate (1 mmol), aryl bromide (1 mmol), Na_2CO_3 (2 mmol), DMF (4 mL) and the catalyst (0.3 mol%) at 140 °C for 18 h.

Source: Fernández-García et al. (2016).

Polystyrene-supported Pd(II)-*N*-heterocyclic carbene complex PS-NHC-Pd(II) was successfully synthesized from theophylline as an environmentally benign NHC precursor using chloromethylated polystyrene resin (Figure 2.17). This catalyst exhibits an excellent catalytic activity and stability for the Heck-Matsuda cross-coupling reaction under mild conditions (Mohammadi & Movassagh, 2016). Different types of arenediazonium tetrafluoroborate salts were coupled with the olefinic substrates in ethanol solvent in the presence of 0.9 mol% of Pd(II)-NHC catalyst to give the corresponding cross-coupling products in high yields under aerial conditions. Moreover, the heterogeneous catalyst can be easily separated by simple filtration and reused for eight cycles without a significant loss in its catalytic activity.

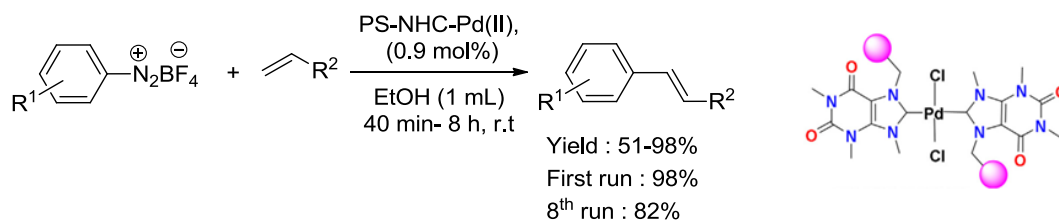


Figure 2.17 PS-NHC-Pd(II) catalyzed Heck reaction. Reaction conditions: arenediazonium tetrafluoroborate salt (0.5 mmol), olefin (0.75 mmol), PS-NHC-Pd(II) catalyst (0.9 mol%) in EtOH (1 mL) at room temperature for 40 min -8 h.

Source: Mohammadi & Movassagh (2016).

Supported palladium nanoparticles on Mn-carboxylate coordination polymer (Pd/MnBDC) were prepared using solution impregnation method (Bagherzadeh et al., 2014). This Pd/MnBDC catalyst exhibited more efficient catalytic activity for the Mizoroki–Heck coupling reaction between iodobenzene and either aromatic or aliphatic terminal alkenes and was reused up to four runs without a significant loss of its catalytic activities (Figure 2.18).

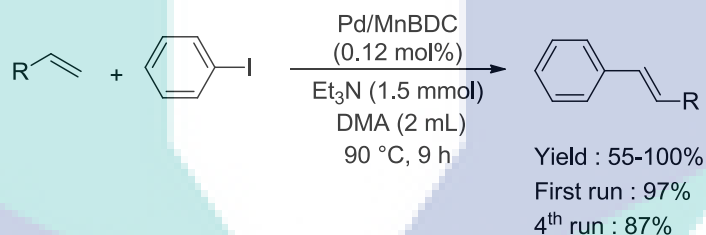


Figure 2.18 Pd/MnBDC catalyzed Heck coupling reaction. Reaction condition: the reactions were run in the presence of 13 mg Pd/MnBDC (0.12 mol% Pd), Et₃N (1.5 mmol), iodobenzene (1 mmol) and olefin (1.1 mmol) in DMA solvent (2 mL) at 90 °C for 9 h.

Source: Bagherzadeh et al. (2014).

Fe₃O₄@CS-Schiff base palladium catalyst showed a high activity for the Mizoroki–Heck reaction of aryl halides and *n*-butyl acrylate (Figure 2.19). Interestingly, the novel catalyst could be recovered in a facile manner from the reaction mixture and recycled for five consecutive runs without any significant loss of its catalytic activity (Naghypour & Fakhri, 2016).

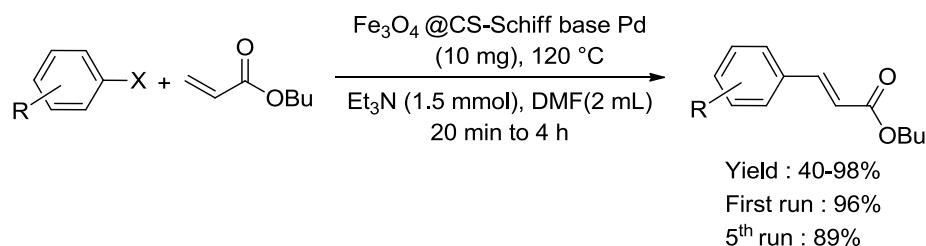


Figure 2.19 Fe_3O_4 @CS-Schiff base palladium catalyzed reaction. Reaction condition: aryl halides (1 mmol), *n*-butyl acrylate (1.2 mmol), Et_3N (1.5 mmol), Fe_3O_4 @CS-Schiff base palladium (10 mg) and DMF (2 mL) at 120 °C for 20 min- 4 h.

Source: Naghipour & Fakhri (2016).

MNPs-NHC-Pd(II) catalyst was found to be a highly active catalyst in the Mizoroki–Heck reactions (Hajipour et al., 2016). These reactions were best performed in dimethylformamide in the presence of only 0.054 mol% of palladium under mild conditions. Moreover, the catalyst could be recovered easily and reused at least five times without any considerable loss of its catalytic activity (Figure 2.20).

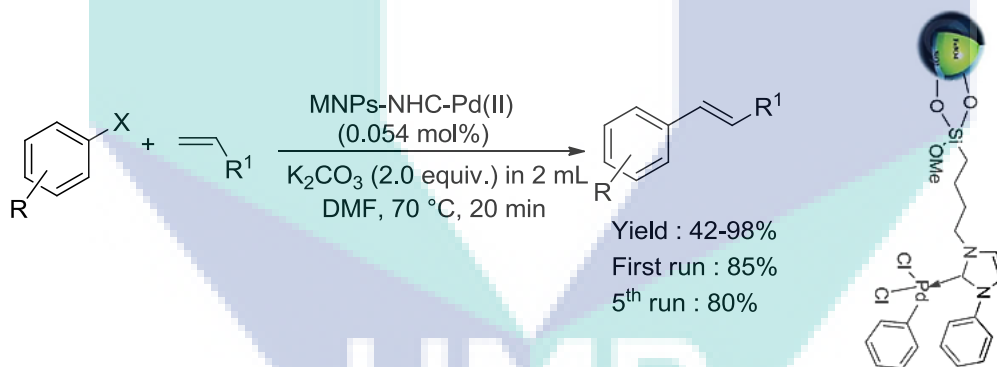


Figure 2.20 MNPs-NHC-Pd(II) catalyzed Heck reaction. Reaction condition: reactions were carried out with aryl halide (1.0 mmol), alkene (1.2 mmol), K_2CO_3 (2.0 equiv.) in 2.0 mL of DMF and 30 mg of catalyst (0.054 mol% of Pd) at 70 °C for 20 min.

Source: Hajipour et al. (2016).

Poly(vinyl chloride) supported palladium complex is thermally stable and can be easily recovered and reused (Figure 2.21). The poly(vinyl chloride) supported palladium catalyst was recycled up to five runs without an appreciable loss of its catalytic activity and with a negligible metal leaching (Bakherad et al., 2014).

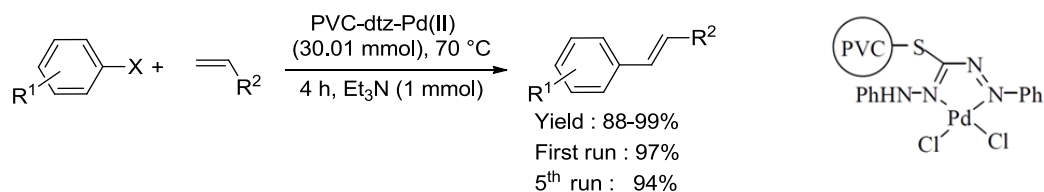


Figure 2.21 Poly(vinyl chloride) supported palladium complex catalyzed reaction. Reaction conditions: aryl halide (1.0 mmol), alkenes (1.2 mmol), Et₃N (1.0 mmol), PVC-dtz-Pd (II), (30.01 mmol) at 70 °C for 4 h.

Source: Bakherad et al. (2014).

MCM-48 supported 2-pyridinylmethanimine palladium catalyst efficiently promoted coupling reactions with ppm level of palladium to give the corresponding coupling products in up to 96% yield (Sarkar et al., 2015). The MCM-48 supported 2-pyridinylmethanimine palladium catalyst was readily recovered and reused several times without a significant loss of its catalytic activity (Figure 2.22).

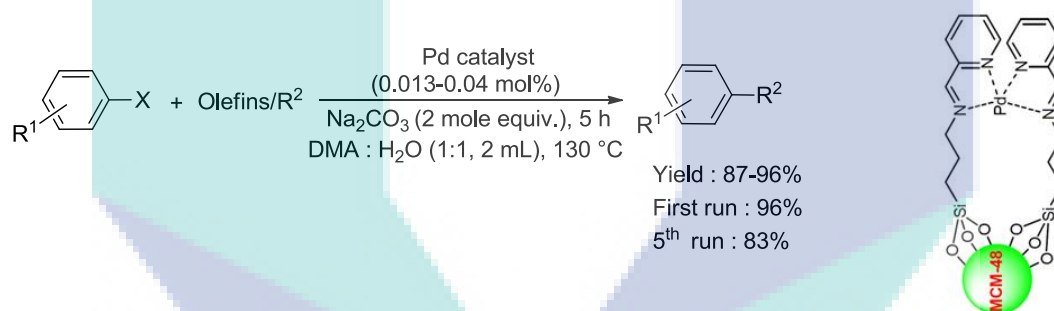


Figure 2.22 Palladium-catalyzed Heck cross-coupling reaction. Reaction conditions: reactions were carried out using (1 mmol) of aryl iodide, (1.2 mol equiv) of olefin, (0.013 mol%) of MCM-48 supported 2-pyridinylmethanimine palladium catalyst, (2 mol equiv) of Na₂CO₃ in 2 mL of DMA/H₂O (1:1) at 130 °C for 5 h.

Source: Sarkar et al. (2015).

A new polystyrene-anchored Pd(II) phenyldithiocarbazate complex was synthesized and characterized by Bakherad et al. (2012), (Figure 2.23). This palladium complex behaved as an efficient heterogeneous catalyst in the Heck reaction under aerobic conditions. Moreover, the catalyst showed a good thermal stability and recyclability.

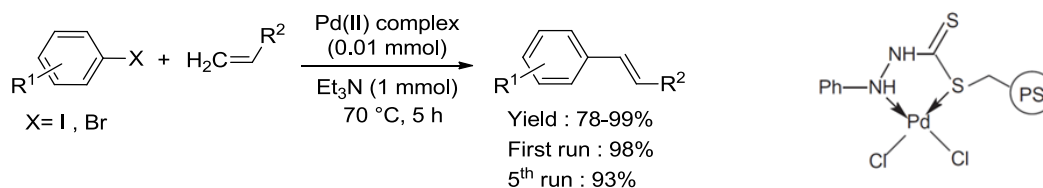


Figure 2.23 Polystyrene-anchored Pd(II) phenyldithiocarbazate complex catalyzed reaction. Reaction conditions: aryl halide (1.0 mmol), alkene (1.2 mmol), palladium catalyst (0.01 mmol) and Et₃N (1.0 mmol) at 70 °C for 5 h.

Source: Bakherad et al. (2012).

Khalafi-Nezhad & Panahi (2014) prepared an efficient heterogeneous catalyst system based on the immobilization of palladium nanoparticles on a silica starch substrate (PNP-SSS). This catalyst was highly effective and recyclable in the Heck reaction. The silica starch substrate (SSS) can stabilize the palladium nanoparticles effectively so that it can provide a platform and prevent the aggregation of nanoparticles and their separation from the substrate surface. It also provides suitable catalytic sites for reactions in aqueous media. The Heck reaction was performed in the presence of a small amount of this catalyst in water as a green solvent (Figure 2.24). The catalyst can be reused more than five times with almost a consistent efficiency and can be recovered by simple filtration.

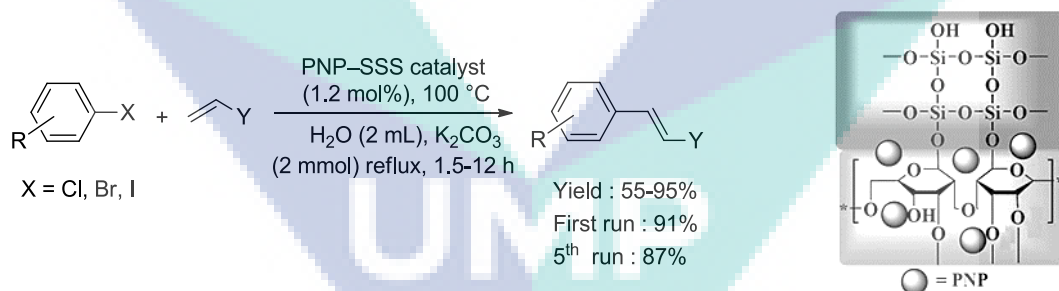


Figure 2.24 Heterogeneous PNP-SSS catalyzed Heck coupling reaction. Reaction conditions: aryl halides (1 mmol), acrylate or styrene (1.2 mmol), base (2 mmol), amount of catalyst (0.05 g, 1.2 mol%) and water (2 mL) at 100 °C for 1.5-12 h.

Source: Khalafi-Nezhad & Panahi (2014).

The novel 1-glycyl-3-methyl imidazolium chloride-Pd(II) complex [Gmim]Cl-Pd(II) was found to be a heterogeneous catalyst for an efficient Heck reaction with good to excellent yield under solvent-free conditions (Karthikeyan et al. 2012). Tetra-coordinated palladium complex was prepared by reacting PdCl₂ with 1-glycyl-3-methyl

imidazolium chloride and its catalytic function invented for the carbon-carbon bond formation. The spectroscopic evidence of the complex has been proved by powder x-ray diffraction (XRD), scanning electron microscopy (SEM), and Fourier transform infrared spectroscopy (FTIR). This protocol provides a simple strategy for the generation of a variety of new carbon-carbon bonds under environmentally benign conditions (Figure 2.25).

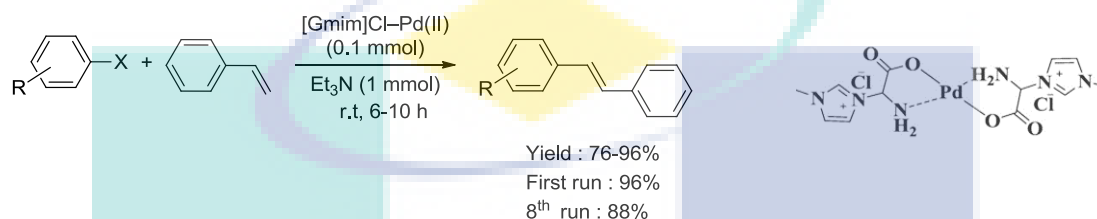


Figure 2.25 Heck coupling reaction using a heterogeneous catalyst. Reaction condition: aryl halide (1 mmol), olefin (1.2 mmol), triethylamine (1 mmol) and [Gmim]Cl-Pd(II), (0.1 mmol) stirring at ambient temperature for 6 to 10 h.

Source: Karthikeyan et al. (2012).

2.5.6 Buchwald-Hartwig Reaction (C-N)

The palladium-catalyzed Buchwald–Hartwig cross-coupling reaction of amines and aryl halides yields carbon-nitrogen bonds which have an extensive application in organic chemistry. Although palladium catalyzed carbon-nitrogen couplings were reported as early as 1983, credit for its development is typically assigned to Stephen L. Buchwald and John F. Hartwig whose publications between 1994 and the late 2000s established the scope of this transformation. The reaction's synthetic utility stems primarily from the shortcomings of typical methods (nucleophilic substitution, reductive amination, etc.) for the synthesis of aromatic carbon-nitrogen bonds. Most of the methods suffer from limited substrate scope and functional group tolerance (Urgaonkar et al., 2003; Dai et al., 2006).

The development of the Buchwald–Hartwig reaction allowed for the facile synthesis of aryl amines (Marion et al., 2006), replacing the harsher methods (Goldberg reaction, nucleophilic aromatic substitution, etc.) to an extent. It significantly expands the type of possible C–N bond formation. A very straightforward synthesis of

(IPr)Pd(acac)Cl from two commercially available starting materials, Pd(acac)₂ and IPr.HCl [acac = acetylacetonate; IPr = *N,N*-bis(2,6-diisopropylphenyl)imidazol-2-ylidene], has been developed. The resulting complex, (IPr)Pd(acac)Cl, has proven to be a highly active Pd(II) precatalyst in the Buchwald-Hartwig reactions. A wide range of substrates has been screened, including inactivated, sterically hindered, and heterocyclic aryl chlorides (Marion et al., 2006). One of the Buchwald-Hartwig cross-coupling reactions is shown in Figure 2.26.

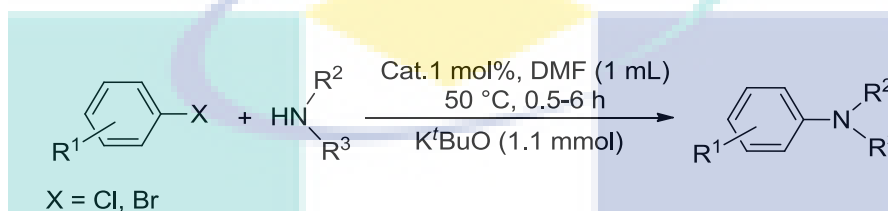


Figure 2.26 Buchwald-Hartwig cross-coupling reaction. Reaction conditions: aryl halide (1 mmol), amine (1.1 mmol), catalyst (IPr)Pd(acac)Cl (1 mol%), K^tBuO (1.1 mmol) and DME (1 mL) at 50 °C for 0.5 to 6 h.

Source: Marion et al. (2006).

2.5.7 Click Reaction (C-N)

The addition reaction is important for carbon-nitrogen bond formation reactions and has a wide range of application in the modern scientific communities (Lv et al., 2006). It is also called Click reaction (Huisgen, 1963). Traditionally, different copper complex sources have been used for these reactions, such as Cu(II)/Cu(0) comproportionation (Appukkuttan et al., 2004), mixed Cu/CuO nanoparticles (Huisgen, 1963), and in-situ reduction of Cu(II) to Cu(I) salts (Aragão-Leoneti et al., 2010).

Click chemistry is a newer approach to the synthesis of drug-like molecules which can increase the drug discovery process by using a few practical and reliable reactions. Sharpless and co-worker's in 2001 defined Click reaction (Huisgen 1,3-dipolar cycloaddition) as one that is wide in scope and easy to perform, uses only readily available reagents, and is insensitive to oxygen and water. This reaction was also described as having a high yield, wide in scope, and remove byproducts without chromatography (Kolb & Sharpless, 2003). In fact, in several instances, water is the ideal reaction solvent, providing the best yields and highest rates. Reaction workup and

purification of products are very simple and sometimes column chromatography can be avoided. The Cu(I) catalyzed Click reaction of organo azides with alkyne smoothly gives 1,4-disubstituted 1,2,3-triazoles with quantitative yield (Figure 2.27).

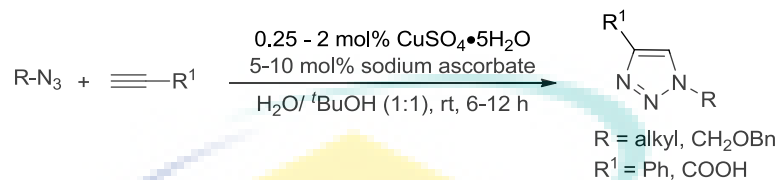


Figure 2.27 Click coupling reaction. Reaction conditions: aryl azides (20 mmol), amine (10 mmol), catalyst (2 mol%), H₂O/ ^tBuOH (50 mL) and sodium ascorbate (10 mol%) at r.t for 6-12 h.

Source: Himo et al. (2005).

The Cu(II) complex of 1,2-bis(4-pyridylthio) ethane immobilized on polystyrene was used as a highly stable, active, reusable and green catalyst for Click synthesis of 1,2,3-triazoles via one-pot three-component reaction of organic halides, sodium azide and alkynes (Tavassoli et al., 2015). High selectivity, broad diversity of organic halides or α -bromoketones, alkyl/aryl terminal alkynes, and excellent yields of the products were obtained using 0.2 mol% of the catalyst (Figure 2.28). Moreover, the catalyst could be recycled and reused for seven cycles without any reduction in its catalytic activity.

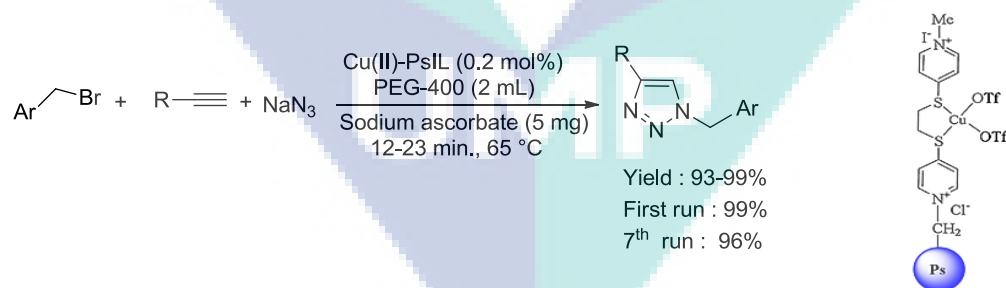


Figure 2.28 Copper(II) complex catalyzed Click reaction. Reaction conditions: benzyl bromide (1 mmol), phenylacetylene (1 mmol) sodium azide (1.2 mmol), Cu(II)-PsIL (0.2 mol%) and sodium ascorbate (5 mg) were added to mixture in PEG-400 (2 mL) at 65 °C for 12-23 min.

Source: Tavassoli et al. (2015).

Facile, efficient, and environmentally friendly one-pot protocol has been developed for the synthesis of 1,4-diaryl-1,2,3-triazoles from boronic acids, sodium

azide, and acetylenes using copper sulfate immobilized on chitosan as a recyclable heterogeneous catalyst (Anil et al., 2015). This green synthetic three-component protocol avoids the handling of hazardous and toxic azides involved in its in-situ generation. The use of aqueous medium at room temperature, ease of recovery of the catalyst, and reuse for six cycles without any decrease in its catalytic activity made the process interesting (Figure 2.29).

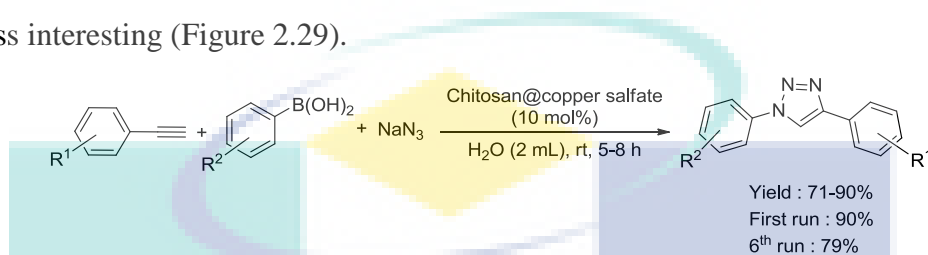


Figure 2.29 Heterogeneous copper-catalyzed Click reaction. Reaction conditions: phenylacetylene (1 mmol), phenylboronic acid (1 mmol), NaN_3 (1.2 mmol) and chitosan@ CuSO_4 (10 mol%) in H_2O (2 mL) at r.t for 5-8 h.

Source: Anil et al. (2015).

Bio-heterogeneous kenaf cellulose supported poly(hydroxamic acid) Cu(II) complex was applied to the Click reactions of organic azides with alkynes in the presence of sodium ascorbate as highly active catalysts under mild reaction conditions (Mandal et al., 2016). The poly(hydroxamic acid) Cu(II) complex (0.25 mol%) efficiently promoted Click reaction to give the corresponding 1,2,3-triazoles in up to 94% yields. Excellent reusability of the supported copper catalysts was found with no significant loss of its catalytic activity for several cycles (Figure 2.30).

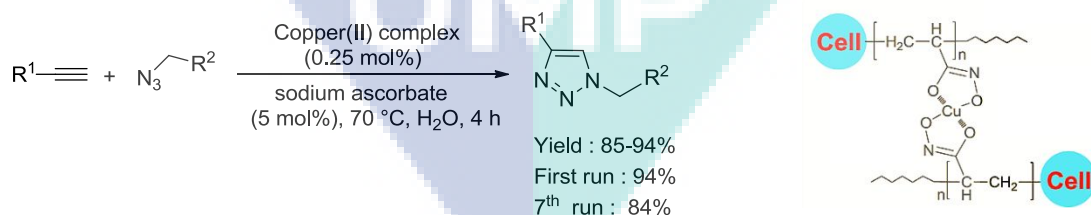


Figure 2.30 Poly(hydroxamic acid) Cu(II) complex catalyzed reaction. Reaction conditions: reactions were carried out using (1 mmol) of azide, (1.1 mmol) of alkyne, (0.25 mol%) of poly(hydroxamic acid) Cu(II) complex, in 5 mol% aqueous solution (2 mL) of sodium ascorbate at 70 °C for 4 h.

Source: Mandal et al. (2016).

Naeimi & Shaabani (2017) described a facile one-pot-three component reaction of alkyl halides. Sodium azide with terminal alkynes can be catalyzed by functionalized graphene oxide copper(I) complex under ultrasonic irradiation at room temperature. In this protocol, the 1,4-disubstituted 1,2,3-triazoles were afforded as target pure products in excellent yields and short reaction times. Besides, the catalyst is chemoselective and stable and can be reused several times without any appreciable loss of its catalytic activity (Figure 2.31).

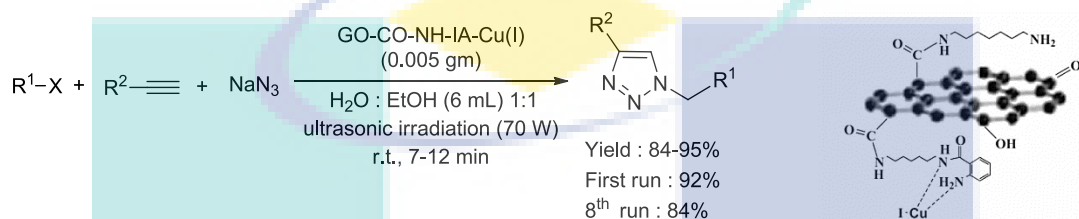


Figure 2.31 Cu(I) complex catalyzed Click coupling reaction. Reaction conditions: (1 mmol) alkyne, (1 mmol) alkyl halide, (1.2 mmol) NaN_3 , catalyst, (0.005 g) were added to the 1:1 mixture solvent of EtOH : H_2O as solvent (6 mL) under ultrasound irradiation (70 W) power at room temperature for 7-12 min.

Source: Naeimi & Shaabani (2017).

New pyridine-imine functionalized mesoporous silica (SBA-15) has been synthesized through the Schiff-base condensation of 3-aminopropyl functionalized SBA-15 with 2-pyridinecarboxaldehyde, followed by the grafting of Cu(II) onto it resulting in a new Cu@PyIm-SBA-15 material (Roy et al., 2014). The Cu(II)-anchored mesoporous material, Cu@PyIm-SBA-15 showed an excellent catalytic activity towards the one-pot Click reaction between azides formed in situ from the corresponding amines and acetylenes in water at 0°C to room temperature, resulting in a wide variety of 1,4-disubstituted 1,2,3-triazoles. The catalyst has been recycled for five cycles without any appreciable loss of catalytic activity and also without any appreciable copper leaching (Figure 2.32).

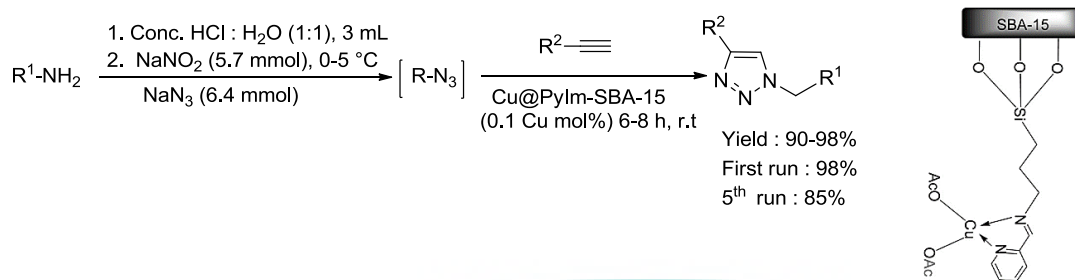


Figure 2.32 Heterogeneous Cu@PyIm-SBA-15 catalyzed Click reaction. Reaction conditions: aniline (5.4 mmol), conc. HCl : H₂O = 1:1, (1.3 mL : 1.3 mL), NaNO₂ (5.7 mmol), NaN₃ (6.4 mmol), alkyne (4.6 mmol) and Cu@PyIm-SBA-15 (0.1 mol%) for 6-8 h.

Source: Roy et al. (2014).

Heterogeneous copper nanocatalyst supported on modified silica mesopore KIT-5 was successfully prepared using the one-pot procedure for the syntheses of 1,4-disubstituted 1,2,3-triazole derivatives via a three-component reaction. This reaction occurred between terminal alkynes, alkyl halides, and sodium azide, namely Click reaction in the presences of 3 mol% nanoparticles. Copper/APTES-KIT-5 (CuI/AK) as a catalyst was developed to give the products in good to excellent yields (Figure 2.33). This catalyst showed high catalytic activity in water as a green solvent. This reaction was performed under open-air conditions and required no special reaction conditions and chromatographic separation for purification (Mirsafaei et al., 2015).

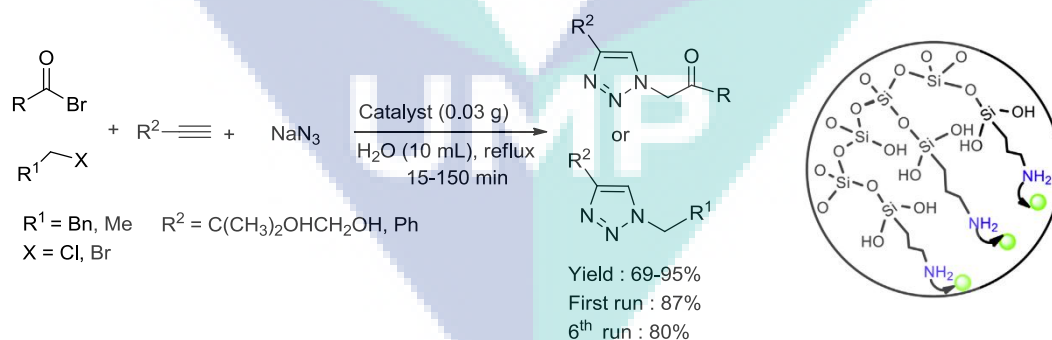


Figure 2.33 Modified silica mesopore CuI/AK catalyzed reaction. Reaction conditions: α -haloketone (1 mmol) or alkyl halide (1 mmol), alkyne (1 mmol), sodium azide (1.1 mmol) were mixed 10 mL water, 0.03 g of prepared CuI/AK as catalyst and reflux for 15-150 min.

Source: Mirsafaei et al. (2015).

Cellulose supported Cu(0) was used as a highly active heterogeneous catalyst to synthesize *N*-glycosyl-1,2,3- triazoles from glycosyl azides and alkynes (Yu et al., 2016). Cellulose-Cu(0) catalyzed the cycloaddition reaction to produce the corresponding products with excellent yields in water (Figure 2.34). This heterogeneous catalyst has the advantages of high catalytic reactivity and low copper leaching. The separation and reuse of the catalyst were easy and efficient.

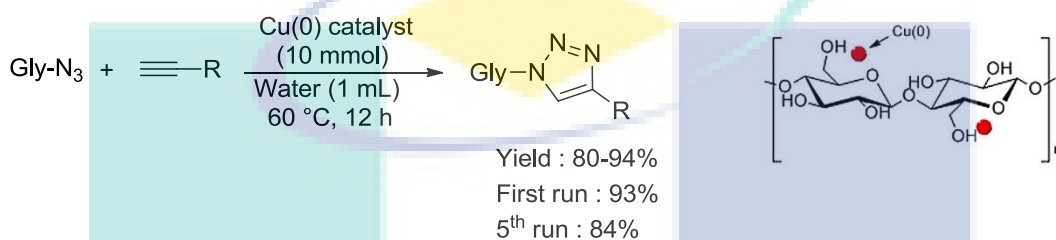


Figure 2.34 Cellulose supported Cu(0) catalyzed reaction. Reaction conditions: O-acetyl- α -L-arabinopyranosyl azide (1 mmol), phenylacetylene (1 mmol), cellulose-Cu(0), (10 mmol) and water (1 mL) at 60 °C for 12 h.

Source: Yu et al. (2016).

The cellulose supported cuprous iodide nanoparticles (Cell-CuI NPs) have been demonstrated for the first time as an efficient heterogeneous catalyst in the Click synthesis of 1,4-disubstituted 1,2,3-triazoles by a one-pot three-component reaction between aryl/alkyl bromides, alkynes, and sodium azide in water (Chavan et al., 2014). It was found to be reusable for five consecutive runs without significant loss of its catalytic activity (Figure 2.35).

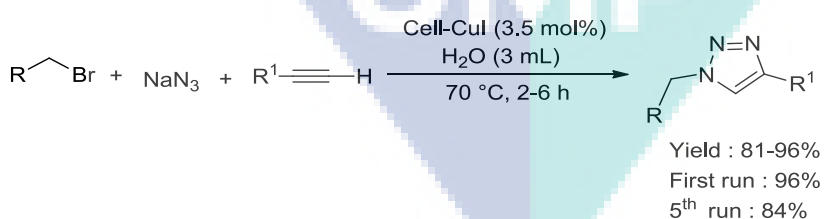


Figure 2.35 Cellulose supported cuprous iodide nanoparticles (Cell-CuI NPs) reaction. Reaction conditions: benzyl bromide (1 mmol), alkyne (1 mmol) and sodium azide (1.1 mmol), Cell-CuI (3.5 mol%) and water (3 mL) at 70 °C for 2-6 h.

Source: Chavan et al. (2014).

The agarose supported copper nanoparticles (CuNPs@agarose) were prepared by immobilization of copper bromide on agarose, followed by in situ chemical reduction (Gholinejad & Jeddi, 2014). The catalytic activity of CuNPs@agarose was assessed in the three-component click synthesis of 1, 2, 3-triazoles in water under low catalyst loading and mild reaction conditions (Figure 2.36). The easy synthesis and air-stable catalyst were recycled for five runs with a small drop in its catalytic activity.

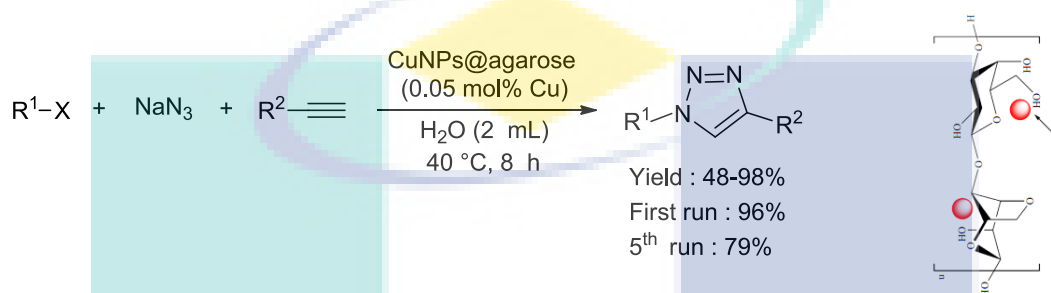


Figure 2.36 CuNPs@agarose catalyzed Click reaction. Reaction condition: (1 mmol) alkyl halides or arenediazonium salt, (1.5 mmol) NaN_3 , (1.5 mmol) alkyne, (0.05 mol%) catalyst and 2 mL H_2O at 40 °C for 8 h.

Source: Gholinejad & Jeddi (2014).

Cu(I)-exchanged solid based on montmorillonite material was investigated as a catalyst in organic synthesis. The catalytic potential of this material was evaluated in the Huisgen 1,3-dipolar cycloaddition. This catalytic system has been examined and proved to be an efficient heterogeneous catalyst for this Click chemistry-type transformation (Mekhzoum et al., 2016). The ensuing catalyst can be recycled and reused five times without a dramatic yield loss (Figure 2.37).

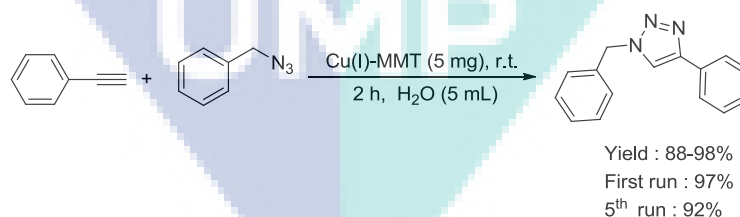


Figure 2.37 Heterogeneous Cu(I)-MMT catalyzed Click reaction. Reaction conditions: (1.2 mmol) of alkyl azide, (1 mmol) of alkyne, Cu(I)-MMT (5 mg) and H_2O (5 mL) at r.t. for 2 h.

Source: Mekhzoum et al. (2016).

Self-assembly of copper sulfate and a poly-(imidazole-acrylamide) amphiphile provided a highly active, reusable, globular, solid-phase catalyst for Click chemistry (Yamada et al., 2012). The self-assembled polymeric Cu-catalyst was readily prepared from poly(*N*-isopropylacrylamide-co-*N*-vinylimidazole) and CuSO₄ via coordinative convolution. Moreover, the imidazole units in the polymeric ligand coordinate to CuSO₄ to give a self-assembled, layered, polymeric copper complex. The insoluble amphiphilic polymeric imidazole copper catalyst with even 4.5–45 mol ppm drove the Huisgen 1,3-dipolar cycloaddition of a variety of alkynes and organic azides, including the three-component cyclization of a variety of alkynes, organic halides, and sodium azide (Figure 2.38). The catalyst was readily reused without a loss of catalytic activity to give the corresponding triazoles quantitatively.

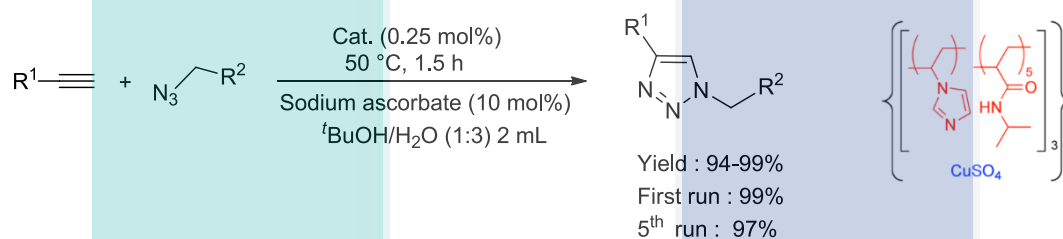


Figure 2.38 Heterogeneous imidazole-copper catalyzed Click reaction. Reaction conditions: alkyne (0.5 mmol), organic azide (0.5 mmol), imidazole-copper catalyst (0.25 mol%), sodium ascorbate (10 mol%), ^tBuOH (0.5 mL) and H₂O (1.5 mL) at 50 °C for 1.5 h.

Source: Yamada et al. (2012).

2.5.8 Aza-Michael Reaction (C-N)

The Aza-Michael reaction has drawn high attention in the synthesis of biologically-active natural products as well as the synthetic precursors of antibiotics and pharmaceutical intermediates. In recent years, some metal complexes are used in Aza-Michael reaction, such as PtCl₄·5H₂O (Kobayashi et al., 2002), InCl₃/chlorotrimethylsilane (Yang et al., 2007), Bi(NO₃)₃ (Srivastava & Banik, 2003), boric acid (Chaudhuri et al., 2005), and bases (Bo et al., 2007). However, these homogeneous metal catalyzed reactions have several limitations like side products, a high cost of metal complexes, harsh conditions, long reaction times, metal leaching out into the reaction mixture, difficult to recover the catalyst and require large excesses of reagents or catalysts.

Therefore, the use of heterogeneous catalysts for organic synthesis is rapidly growing over homogeneous catalytic systems because of their several advantages such as high stability and tolerance to harsh reaction conditions, the reusability of the catalyst, environmental friendliness and ease of purifying the products (Keipour et al., 2012).

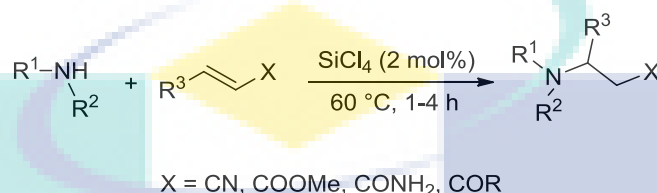


Figure 2.39 Aza-Michael reaction. Reaction conditions: 5 mmol of Michael acceptor, 8 mmol of amine and SnCl₄ (2 mol%) at 60 °C for 1-4 h.

Source: Azizi et al. (2010).

Some heterogeneous catalysts have been used in the Aza-Michael reaction, such as MOF-99 (Nguyen et al., 2012), silica sulphuric acid (Wang et al., 2009), Amberlyst-15 (Das & Chowdhury, 2007), cellulose-Cu(0), (Reddy et al., 2006), polystyrene-AlCl₃ (Dai et al., 2013), KF doped natural zeolite (Keipour et al., 2012), MCM-41 immobilized heteropoly acids (Xie et al., 2013) and amine-functionalized silica supported Co(acac)₂ (Sodhi et al., 2015). They have proved to have good catalytic activities. Some heterogeneous catalyzed Aza-Michael reactions are given below:

Bio-heterogeneous kenaf cellulose supported poly(hydroxamic acid) copper nanoparticles was successfully applied to the Aza-Michael reaction of amines with α , β unsaturated carbonyl/cyano compounds under mild reaction conditions (Mandal et al., 2016). The CuN@PHA (50 mol ppm) selectively boosted Aza-Michael reaction to give the corresponding alkylated products in up to 96% yield. Excellent reusability of the supported copper catalysts was found with no significant loss of its catalytic activity for several cycles (Figure 2.40).

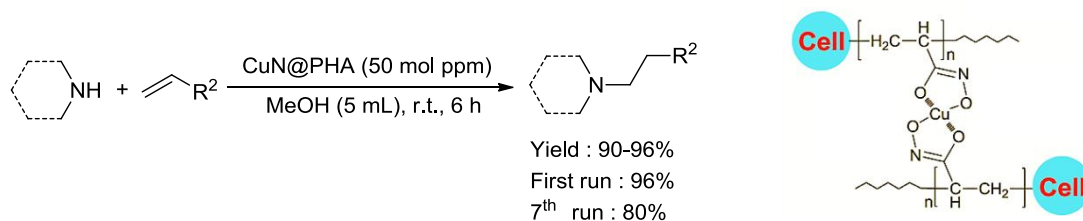


Figure 2.40 **CuN@PHA** catalyzed reaction. Reaction condition: reactions were carried out using (10 mmol) of amine, (11 mmol) of Aza-Michael acceptor, and **CuN@PHA** (1 mg, 50 mol ppm) in 5 mL MeOH at room temperature for 6 h.

Source: Mandal et al. (2016).

Recently, Sarkar (2016) developed waste corn-cob cellulose supported bio-heterogeneous poly(amidoxime) copper nanoparticles which were successfully applied to the Aza-Michael reaction of aliphatic amines with an olefin to give the corresponding alkylated products at room temperature (Figure 2.41). The supported nanoparticles were easy to recover and reused eight times without significant loss of its catalytic activity.

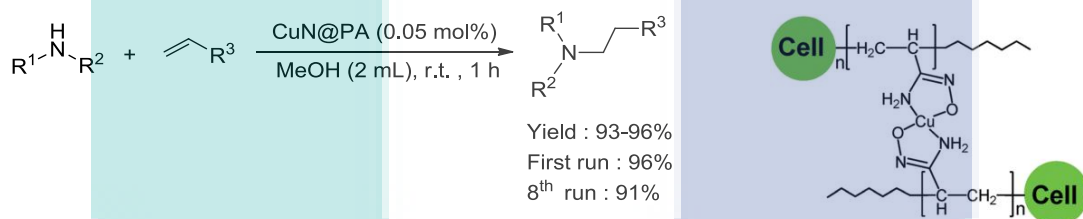


Figure 2.41 Bio-heterogeneous poly(amidoxime) copper nanoparticles catalyzed Aza-Michael reaction. Reaction condition: reactions were carried out using (1 mmol) of amine, (1.1 mol equiv) of Michael acceptor and (0.05 mol%) of **CuN@PA** in 2 mL MeOH at room temperature for 1 h.

Source: Sarkar et al. (2016).

Datta (2016) described the synthesis and characterization of new Cu(II)-L-3,4-dihydroxyphenylalanine-based magnetically separable nanocatalyst, namely $\text{Fe}_3\text{O}_4@\text{L-DOPA}@\text{Cu(II)}$, (L-DOPA = L-3,4-dihydroxyphenylalanine). This catalyst could simply be separated and recovered from the reaction mixture with the assistance of an external magnet and reused several times without the loss of its catalytic activity (Figure 2.42).

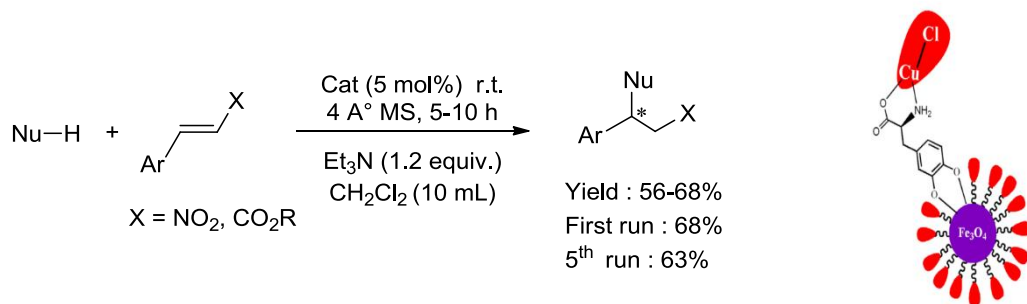


Figure 2.42 Aza-Michael reaction catalyzed by heterogeneous catalyst. Reaction condition: phthalimide or cyclohexanone (1 mmol), $\text{Fe}_3\text{O}_4\text{@L-DOPA@Cu(II)}$ (5 mol%), β -nitrostyrene or α, β -unsaturated ester (1.0 mmol), dichloromethane (10 mL) and 1.2 equivalent of triethyl amine at room temperature for 5-10 h.

Source: Datta et al. (2016).

A fast, mild, and quantitative procedure for Michael reactions between various amines and α, β -unsaturated carbonyl compounds and nitriles in the presence of an easily accessible basic ionic liquid 3-butyl-1-methylimidazolium hydroxide, [bmIm]OH as both catalyst and reaction medium has been developed (Xu et al., 2007). For large-scale reactions, the products could be directly distilled from the ionic liquid, allowing the use of organic solvents to be avoided totally. The ionic liquid could be reused at least eight times with consistent activity and was stable during the reaction process (Figure 2.43).

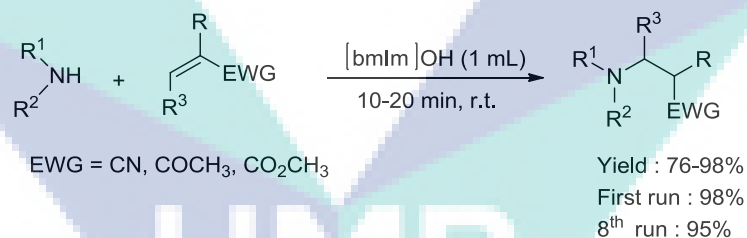


Figure 2.43 Aza-Michael reaction using heterogeneous catalyst [bmIm]OH. Reaction conditions: amine (1 mmol), α, β -unsaturated carbonyl compound (1.2 mmol) and [bmIm]OH (1 mL) at room temperature for 10-20 min.

Source: Xu et al. (2007).

Movassagh et al. (2015) developed two convenient green protocols for the synthesis of β -amino ketones. It involves one-pot Aza-Michael-type and Mannich-type reactions of a series of aldehydes, ketones, and amines in the presence of a catalytic amount of the magnetic solid sulfonic acid catalyst, $\text{Fe}_3\text{O}_4\text{@SiO}_2\text{@Me\&Et-PhSO}_3\text{H}$ at

room temperature. The catalyst can be reused four times without a loss of activity (Figure 2.44).

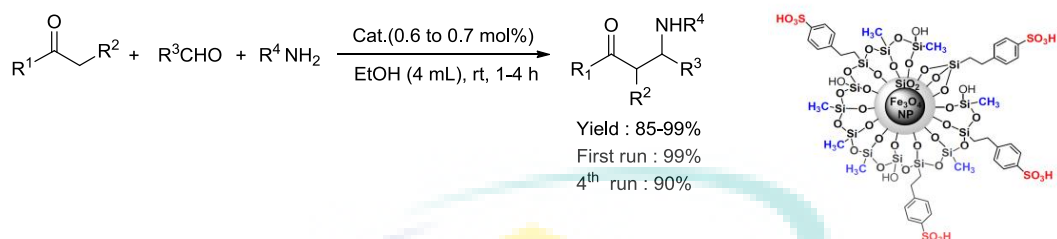


Figure 2.44 $\text{Fe}_3\text{O}_4@\text{SiO}_2@\text{Me}\&\text{Et}-\text{PhSO}_3\text{H}$ catalyzed reaction. Reaction conditions: cyclohexanone (3.0 mmol), benzaldehyde (2.0 mmol), aniline (2.0 mmol), catalyst 0.6 or 0.7 mol% and solvent (4 mL) at room temperature for 1-4 h.

Source: Movassagh et al. (2015).

On the basis of the above information, there is still a high demand to explore more efficient catalyst for chemical transformation reactions with the aspect of green technology. Nowadays, scientists are continuing their effort to investigate low-cost environmental friendly and sustainable processes using renewable resources. In this perspective, natural biopolymers such as cellulose could be considered as a more acceptable material because it has some promising merits like large abundance in nature, low density, bio-renewability, universal availability, low-cost and interesting mechanical properties compared to the glass fibers (William et al., 2008).

Therefore, natural cellulose would be the perfect candidate to be considered as a solid support for catalysts (Dahou et al., 2010). In addition, cellulose backbone can be chemically modified and suitable metals coordinating groups can be effectively introduced (Dhepe & Fukuoka, 2007). Currently, biopolymers like cellulose (Koga et al., 2012), starch (Huang et al., 2002), alginate (Wei et al., 2004), gelatin (Zhang et al., 2001), and chitosan (Quignard et al., 2000) derivatives have been used as support materials for catalytic applications with an acceptable catalytic performance. Eventually, it is particularly envisaged to unfold a more general, simple and convenient catalytic process which could be applicable to various substrates of different nature under pleasant and environment-friendly reaction conditions.

Keeping on this view, in this study, palladium and copper anchored onto poly(amidoxime) functionalized corn-cob cellulose were used as efficient heterogeneous catalysts for the C-C and C-N bond formation via Mizoroki-Heck

reaction Pd(II) of aryl halide and olefin, Click reaction Cu(I) of organic azide and terminal alkyne, and chemoselective Aza-Michael Cu(0) of aliphatic amines with α , β -unsaturated compounds. The cellulose supported palladium and copper catalysts were found highly active. The catalysts were easy to recover and reuse without a significant loss of catalytic activity.

2.6 Importance of Mizoroki-Heck, Click and Aza-Michael Reactions

The Mizoroki-Heck, Click and Aza-Michael reactions are the most important reaction to C-C and C-N bond formations. These reactions have a great impact in the industry, pharmaceuticals, fine chemicals, and academic researchers for the development of new drugs and also materials. The palladium-catalyzed C-C bond forming reaction developed by Heck has a large impact on synthetic organic chemistry. Heck reaction has been used as an important C-C bond forming reactions in the synthetic organic chemistry, as well as in the synthesis of biologically active molecules such as Ozagrel, Idebenone (designed for the treatment of Alzheimer's and Parkinson's diseases) steroids, strychnine, and diterpenoid scopadulic acid B31 with cytotoxic and antitumor activities.

Ozagrel, an important antiasthmatic agent (thromboxane A_2 synthesis inhibitor), (Loo et al., 1987) was synthesized by using corn-cob cellulose supported Pd(II) complex catalyst in Mizoroki-Heck reaction. Thromboxane A_2 (TXA₂) is known to be a developmental factor in brain damage, occurring after cerebral ischemia-reperfusion because TXA₂ is a powerful vasoconstrictor (Petroni et al., 1989) and accumulates in this condition.

The Click reaction is an important cross-coupling reaction in Click chemistry which is being used increasingly in biomedical research. The Cu(I) catalyzed Click reaction afford 1,2,3-triazoles that were recently used for the preparation of functionalized resins (Löber et al., 2003). Drug discovery approaches are based on the Cu(I) catalyzed the formation of triazoles from azides and acetylenes, synthesis of neoglycoconjugates, and development of HIV protease inhibitors and fucosyltransferase inhibitors (Kolb & Sharpless, 2003). On the other hand, the Aza-Michael reaction is

also important for the synthesis of active antitubercular, cytotoxic, and antibacterial agents which can control Tuberculosis (TB) diseases and cancer.

Therefore, Mizoroki-Heck, Click, and Aza-Michael reaction have a lot of importance in the organic chemistry especially in the synthesis of drugs and valuable fine chemicals. Thus, this research focuses on Mizoroki-Heck, Click, and Aza-Michael reactions.

2.7 Summary

The purpose of this literature review was to evaluate how previous researchers carried out this chemical bond formation reactions. Along with this, it was clear that the heterogeneous catalyst would be more reliable than the homogeneous catalyst. However, from the literature survey, it was found that sometimes, heterogeneous catalysts are expensive, toxic, not sustainable under harsh reaction conditions, prone to metal leaching, and not easy to prepare the existing heterogeneous metal catalysts. Therefore, from the green technology aspects, there is still a high demand to pursue more admissible catalysts for chemical transformation reactions. Thus, researchers are amplifying their effort to investigate low-cost environmental friendly and sustainable processes using renewable resources. In this aspect, natural biopolymers (cellulose) could be considered as the most attractive material because of its numerous advantages such as large abundance in nature, low density, bio-renewability, universal availability, low-cost, and ease of surface modification.

Keeping this in view, in this report, poly(amidoxime) palladium/copper complexes were synthesized through a surface modification of waste corn-cob cellulose, and the complexes were successfully applied for C-C (Mizoroki-Heck) and C-N (Click and Aza-Michael) bond formation reactions with a regenerative catalytic activity.

CHAPTER 3

MATERIALS AND METHODS

3.1 Introduction

Chemical compounds are extensively used in many areas of research, pharmaceuticals, medicine, and industries. To overcome the limitation of the important chemicals and for a better future, industries need to have new and valuable chemicals. So, the desired chemical synthesis is the key point to achieving the targeted new compounds with different molecular structures and functional groups.

3.2 Chemicals and Instruments used

The highly pure solvents and chemicals used for the catalytic reactions, synthesis of the intermediates and the targeted compounds were purchased from Merck, Sigma-Aldrich, HmbG Chemicals, and Fisher Scientific companies.

The instrument details are as follows: ^1H NMR (500/400 MHz) and ^{13}C NMR (125/100 MHz) spectra were recorded on a Bruker-500/400 spectrometer. The ^1H NMR chemical shifts were reported relative to tetramethylsilane (TMS, 0.0 ppm). The ^{13}C NMR chemical shifts were reported relative to deuterated chloroform (77.0 ppm). Inductively coupled plasma atomic emission spectroscopy (ICP-AES) was performed on Shimadzu ICPS-8100 equipment. Fourier transform infrared spectroscopy (FTIR) spectra were measured with a Perkin Elmer 670 spectrometer equipped with an ATR device. X-ray photoelectron spectroscopy (XPS) spectra were measured with a scanning X-ray microprobe PHI Quantera II. Field emission scanning electron microscopy (FE-SEM) was measured with JSM-7800F. High-resolution transmission electron microscopy (HR-TEM) was measured with HT-7700. X-ray powder diffraction (XRD)

was measured with MINIFLEX II model. Energy-Dispersive X-Ray Spectroscopy (EDX) was measured with JSM-7800F. Thin layer chromatography (TLC) analysis was performed on Merck silica gel 60 F254. Column chromatography was carried out on silica gel (Wakogel C-200).

3.3 Research Methodology

The work flow process in this study is shown in a flowchart diagram in Figure 3.1.

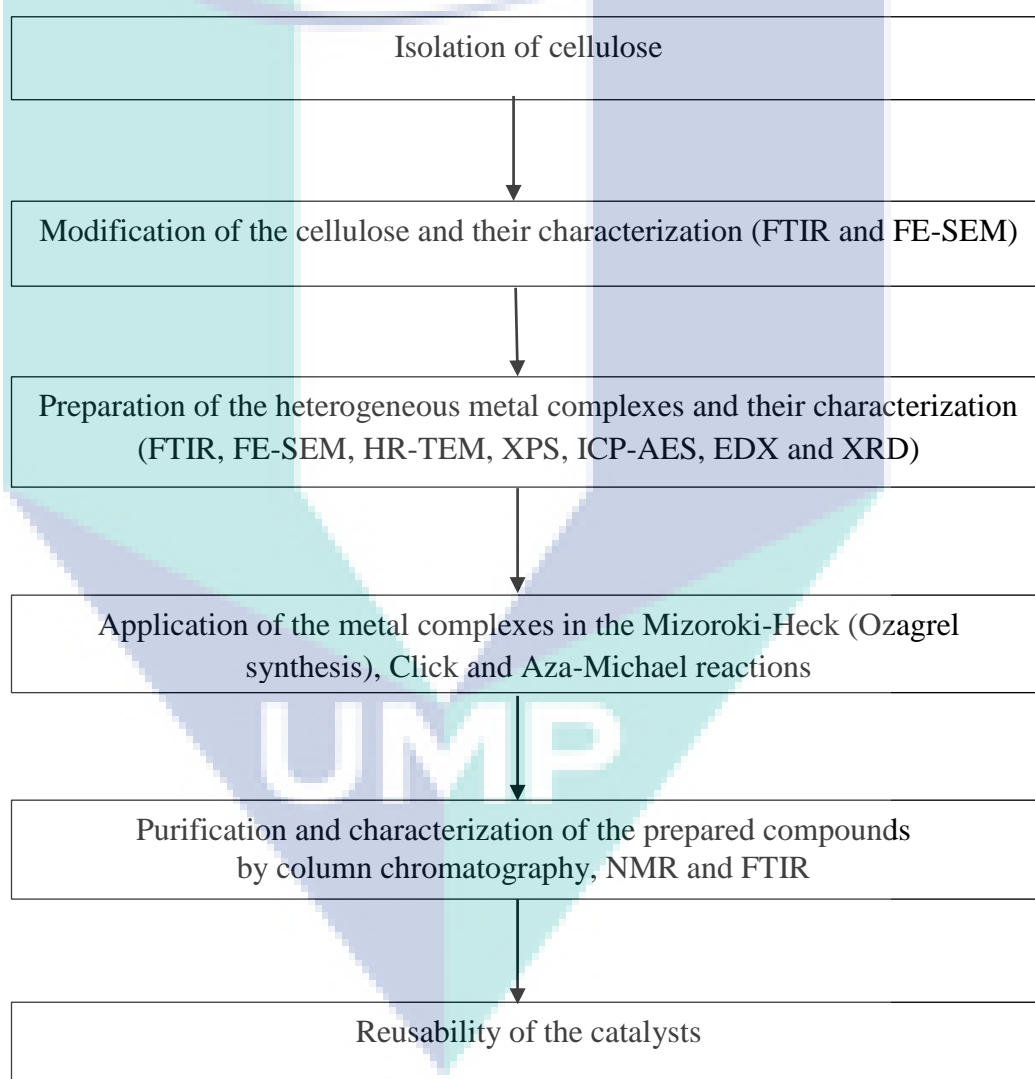


Figure 3.1 Research methodology flow chart.

3.4 Materials Collection

The waste corn-cobs materials (Figure 3.4a) were collected from Gambang, Pahang, Malaysia. The collected waste corn-cob materials were cleaned to remove dust and other contaminants.

3.5 Extraction of Cellulose from Corn-Cobs

The corn-cobs were obtained from Gambang, Pahang, Malaysia, cleaned, dried, and cut into small sizes (3 cm long average). The dried raw corn-cob (100 g) was boiled with 10% NaOH (800 mL) and glacial acetic acid (800 mL) for 4 h and 2 h respectively and later washed with distilled water. The cellulose was bleached with hydrogen peroxide (500 mL) and 5% NaOH (300 mL) and washed with distilled water (500 mL) several times. The obtained cellulose was dried at 50 °C to give whitish corn-cob cellulose with a yield of 25 wt.% (Figure 3.4b).

3.5.1 Graft Copolymerization of Corn-Cob Cellulose [Poly(acrylonitrile) 1]

The graft copolymerization reaction was performed using ceric ammonium nitrate (CAN) as an initiator. Ceric ions initiate free radical sites on the polysaccharide backbone and therefore, minimized the formation of homopolymers (Dahou et al., 2010). The mechanism by which the ceric ion reacts with cellulose materials in the presence of vinyl monomers to produce grafted copolymers has been widely studied.

The graft copolymerization reaction was carried out in one-liter three-neck round bottom flask equipped with a stirrer and condenser in a thermostat water bath. The cellulose slurry was prepared by stirring 6 g of corn-cob cellulose in 150 mL of distilled water overnight. The slurry was heated to 55 °C before the addition of 2.17 mL of diluted sulphuric acid (H₂SO₄/H₂O, 1:1). After 5 min, 2 g of ceric ammonium nitrate (in 10 mL aqueous solution) was added and the reaction mixture was stirred continuously (Siew et al., 2011). After 20 min, 14 mL of acrylonitrile monomer was added to the cellulose suspension and stirred for 4 h under nitrogen atmosphere. The reaction mixture was cooled and the resulting poly(acrylonitrile) **1** was washed (Figure 3.2) several times with aqueous methanol (methanol/water, 4:1). The poly(acrylonitrile)

1 was oven dried (Figure 3.4c) at 50 °C to a constant weight with a yield of 214 wt.% (Sultana et al., 2016; Rahman et al., 2016).

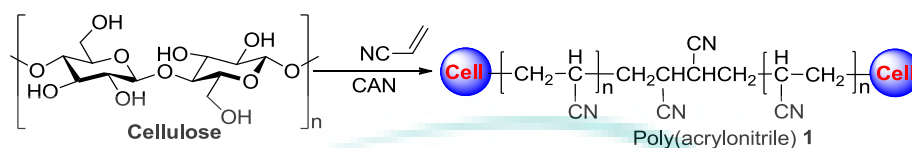


Figure 3.2 Synthesis of poly(acrylonitrile) **1**.

3.5.2 Determination of the Grafting Percentage

For the purpose of removing the homopolymer as PAN [poly(acrylonitrile)], the crude grafting product was purified with Soxhlet extraction method with dimethylformamide for 12 h. Then, the purified grafted copolymer (cellulose-graft-PAN) was dried at 50 °C to a constant weight. The percentage of grafting (G_p) was determined with the formula $G_p = W_2/W_1 \times 100$, where W_1 is the weight of the parent polymer (cellulose) and W_2 is the weight of the grafted polymer [poly(acrylonitrile)].

3.5.3 Synthesis of Poly(amidoxime) Ligand **2**

About 20 g of hydroxylamine hydrochloride ($\text{NH}_2\text{OH}\cdot\text{HCl}$) was dissolved in 500 mL of aqueous methanol (methanol/water 4:1) and neutralized with NaOH solution. The resulting NaCl precipitate was removed by filtration (Lutfor et al., 2001). The pH of the reaction was adjusted to pH 11 by the addition of NaOH solution and the ratio of methanol and water was maintained at 4:1 (v/v). The poly(acrylonitrile) grafted corn-cob cellulose **1** (10 g) was placed into a two-neck round bottom flask equipped with a stirrer and a condenser in a thermostatic water bath. The hydroxylamine solution was then, added to the flask and the reaction was stirred at 70 °C for 4 h.

After the completion of the reaction, the chelating ligand was separated from the hydroxylamine solution, filtered and washed with aqueous methanol (Rahman et al., 2016). The obtained cellulose-based amidoxime ligand (Figure 3.3) was neutralized with 100 mL of methanolic 0.1 M HCl solution. Finally, the ligand (Figure 3.4d) was filtered and washed several times with aqueous methanol and dried at 50 °C for 6 h to

obtain poly(amidoxime) ligand **2** with a yield of 220 wt.% (Lutfor et al., 2001; Siew et al., 2011; Rahman et al., 2014).

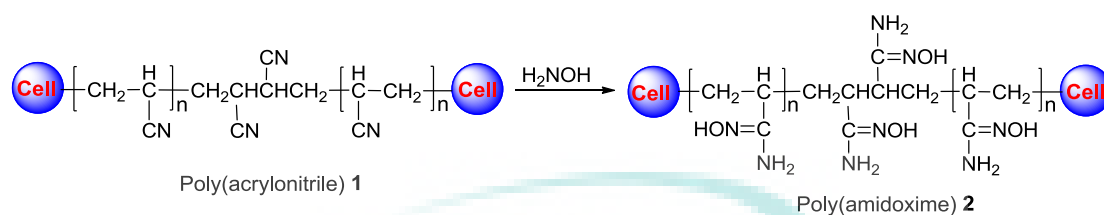


Figure 3.3 Synthesis of poly(amidoxime) ligand **2**.

The photographic images of the waste corn-cob, white color corn-cob cellulose, poly(acrylonitrile) grafted cellulose **1**, and poly(amidoxime) ligand **2** are shown in Figure 3.4.

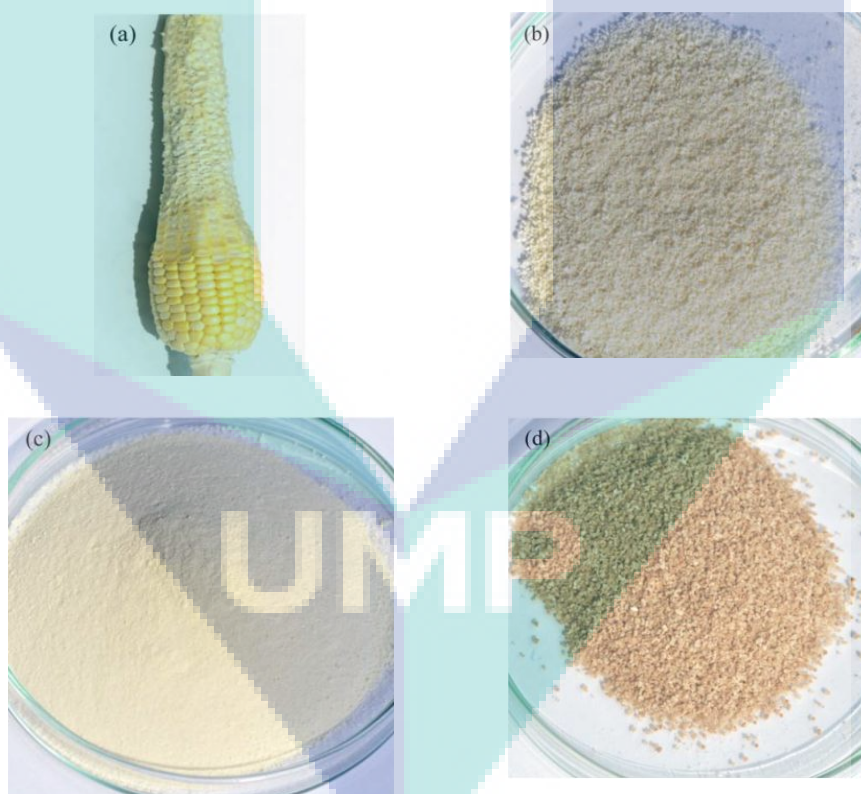


Figure 3.4 Photographic images of (a) waste corn-cob (b) corn-cob cellulose (c) poly(acrylonitrile) grafted corn-cob cellulose **1** and (d) poly(amidoxime) ligand **2**.

3.6 Preparation of the Catalysts

The waste corn-cob cellulose supported Pd(II) complex **3**, Cu(II) complex **4** and copper nanoparticles (**CuNP@PA**) were prepared using the procedures shown in Figures 3.5, 3.6 and 3.7 respectively.

3.6.1 Preparation of Poly(amidoxime) Pd(II) Complex **3**

To a stirred suspension of poly(amidoxime) ligand **2** (1 g) in 30 mL water, an aqueous solution of $(\text{NH}_4)_2\text{PdCl}_4$ (250 mg, in 30 mL water) was added. The resulting mixture was stirred for 2 h at room temperature to give light brown colored poly(amidoxime) Pd(II) complex **3**. The Pd(II) complex **3** was filtered, washed with water, MeOH, and dried at 70 °C for 2.5 h (Figure 3.5). The ICP-AES analysis revealed that 0.45 mmol/g of palladium was immobilized onto the poly(amidoxime) Pd(II) complex **3**.

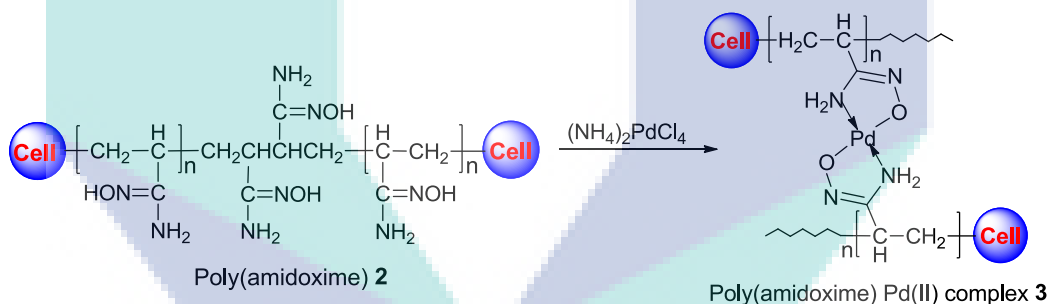


Figure 3.5 Preparation of corn-cob cellulose supported poly(amidoxime) Pd(II) complex **3**.

3.6.2 Preparation of Poly(amidoxime) Cu(II) Complex **4**

To a stirred suspension of poly(amidoxime) ligand **2** (2 g) in 50 mL water was added an aqueous solution of $\text{CuSO}_4 \cdot 5\text{H}_2\text{O}$ (492 mg, in 30 mL H_2O) at room temperature. The blue $\text{CuSO}_4 \cdot 5\text{H}_2\text{O}$ immediately turned into a green colored copper complex and the mixture was stirred for 2 h at room temperature. Then, the poly(amidoxime) Cu(II) complex was filtered and washed several times with excess amount of ammonium chloride, water, MeOH and dried at 60 °C for 2 h (Figure 3.6).

The ICP-AES analysis showed that 0.5 mmol/g of copper was immobilized onto the poly(amidoxime) Cu(II) complex **4**.

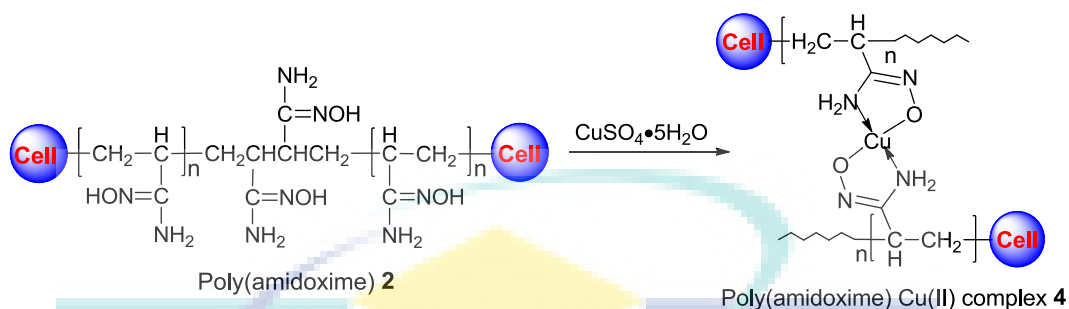


Figure 3.6 Preparation of corn-cob cellulose supported Cu(II) complex **4**.

3.6.3 Preparation of Poly (amidoxime) Copper Nanoparticles (CuNP@PA)

Poly(amidoxime) Cu(II) complex **4** (1 g) was dispersed in 100 mL of deionized water and then, 1 mL of hydrazine hydrate was added. The resulting dark brown colored **CuNP@PA** materials were collected by filtration, washed with methanol, and dried under vacuum at 100 °C for 3 h, and stored under a nitrogen atmosphere (Figure 3.7).

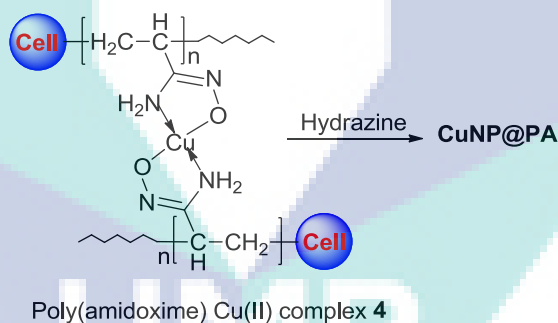


Figure 3.7 Preparation of corn-cob cellulose-supported **CuNP@PA**.

3.7 Catalytic Activity Test

The prepared waste corn-cob cellulose supported poly(amidoxime) Pd(II) complex **3**, Cu(II) complex **4**, and **CuNP@PA** were then, investigated for catalytic performance towards Mizoroki-Heck, Click, and Aza-Michael reactions as described below:

3.7.1 General Procedure for the Mizoroki-Heck Reaction of Aryl Halide and Olefins

All the reactions were carried out in a 7-mL glass vial equipped with a Teflon screw cap. The glass vial was loaded with an aryl halide (1 mmol), olefin (1.2 mmol), Et₃N (3 mmol), waste corn-cob cellulose supported poly(amidoxime) Pd(II) complex **3** (1.2 mg, 0.05 mol%) in DMF (2 mL) and stirred at 130 °C for 3-6 h (Figure 3.8). The reaction progress was monitored periodically by TLC analysis. After completion of the reaction, it was cooled at room temperature and diluted with ethyl acetate (EtOAc). The Pd(II) complex **3** was separated by filtration and washed with EtOAc. The organic layer was washed with H₂O and evaporated under reduced pressure. The residue was purified by column chromatography on silica gel eluted with (ethyl acetate/hexane) to give the corresponding cross-coupling product (**5**) in up to 96% yield. The yields of the products were calculated using the following equation (3.1).

$$\text{Yield} = \frac{\text{obtained yield (wt)}}{\text{theoretical yield (wt)}} \times 100 \dots\dots\dots(3.1)$$

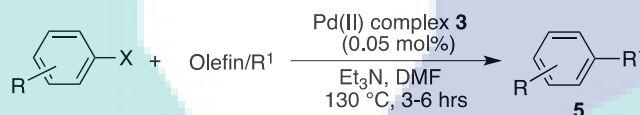


Figure 3.8 General Mizoroki-Heck reaction. Reaction conditions: aryl halide (1 mmol), olefin (1.2 mmol), 0.05 mol% of Pd(II) complex **3**, Et₃N (3 mmol), in 2 mL of DMF at 130 °C for 3-6 h.

3.7.2 General Procedure for the Heck-Matsuda Reaction of Arenediazonium Tetrafluoroborate with Olefins

In a typical experiment, a mixture of arenediazonium tetrafluoroborate salt (1 mmol), olefin (1.2 mmol), and Pd(II) complex **3** (0.05 mol%) in ethanol (2 mL) was stirred at room temperature for 6 h. The formation of coupling products was monitored by TLC analysis. After the despairing of the starting material (checked by TLC), the reaction mixture was cooled at room temperature and complex **3** was removed by filtration. The aqueous layer was extracted with ethyl acetate, dried over MgSO₄, and

concentrated under reduced pressure (Figure 3.9). The crude product was purified by silica gel column chromatography (ethyl acetate/hexane) to give the corresponding cross-coupling product (**5**) with up to 97% yield.

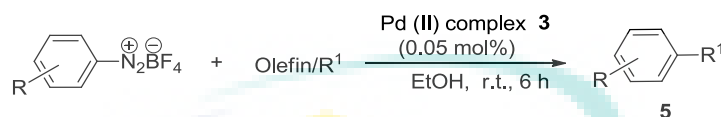


Figure 3.9 Heck-Matsuda reaction of arenediazonium tetrafluoroborate with olefins. Reactions were carried out using 1 mmol of arenediazonium tetrafluoroborate salt, 1.2 mmol of olefin, and 0.05 mol% Pd(II) complex **3** at r.t. for 6 h in ethanol (2 mL).

3.7.3 General Procedure for Click Reaction

All the reactions were carried out in a 7-mL glass vial loaded with waste corn-cob cellulose supported poly(amidoxime) Cu(II) complex **4** (1 mg, 0.05 mole%), alkyne (1 mmol), and aromatic azide (1.1 mmol) in 5 mol% aqueous solution of sodium ascorbate (3 mL). The reaction vessel was stirred at 80 °C for 3 h. The reaction mixture was diluted with water and EtOAc and the insoluble copper complex was recovered by filtration. The organic layer was separated, and the aqueous layer was extracted with EtOAc (3 × 2 mL). The combined organic layers were dried over MgSO₄ and concentrated under reduced pressure to give the corresponding crude 1,2,3-triazole (**6**) which was purified by silica gel short column chromatography (EtOAc/hexane). The yield of the final pure products was up to 96% (Figure 3.10).

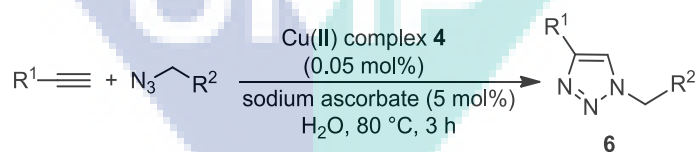


Figure 3.10 General Click reaction. Reaction condition of the Click reaction: alkyne (1 mmol), aromatic azide (1.1 mmol), 0.05 mol% of Cu(II) complex **4** in 5 mol% of aqueous sodium ascorbate at 80 °C for 3 h.

3.7.4 General Procedure for Aza-Michael Reaction

In a typical experiment, a mixture of amine (10 mmol), α , β -unsaturated Michael acceptor (11 mmol), and waste corn-cob cellulose supported poly(amidoxime) **CuNP@PA** (1 mg, 0.005 mol%) in 4.5 mL MeOH was stirred at room temperature for 8 h. The reaction progress was monitored by TLC. After the completion of the reaction, **CuNP@PA** was filtered, washed with MeOH (3 \times 5 mL), dried, and reused in the next run under the same reaction conditions. The filtrate was concentrated under reduced pressure (Figure 3.11). The crude product was purified by column chromatography (hexane/ethyl acetate) to give the corresponding Aza-Michael product (**7**) in up to 95% yield.

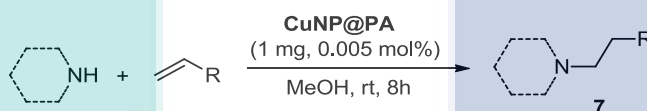


Figure 3.11 Aza-Michael reaction. Aza-Michael reaction condition: amine (10 mmol), α,β -unsaturated Michael acceptor (11 mmol) and **CuNP@PA** (1 mg, 0.005 mol%) in 4.5 mL MeOH at room temperature for 8 h.

3.8 Synthesis of Functional Molecules

The synthesis of the functional molecules such as Ozagrel is described below.

3.8.1 Preparation of (*E*)-4-(Hydroxymethyl) Cinnamic Acid Butyl Ester **5o**

To a 5-mL glass vessel, was loaded with 4-iodobenzyl alcohol (1 mmol), butyl acrylate (1.2 mmol), Et₃N (3 mmol) and 2 mL of DMF. The waste corn-cob cellulose supported Pd(II) complex **3** (1.2 mg, 0.05 mol%) was added to this reaction mixture and heated at 130 °C for 5 h with constant stirring. After cooling to 25 °C, the reaction mixture was diluted with EtOAc (30 mL) and the reaction mixture was washed with H₂O (3 \times 25 mL), dried over MgSO₄, and concentrated under reduced pressure. The residue was purified by column chromatography over silica gel, eluting with hexane/EtOAc to give (*E*)- 4-(hydroxymethyl) cinnamic acid butyl ester (**5o**) with a yield of 91% (Figure 3.12).

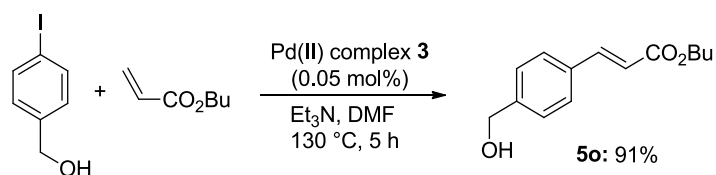


Figure 3.12 Preparation of cinnamic acid butyl ester. Reaction condition of cinnamic acid butyl ester: 4-iodobenzyl alcohol (1 mmol), butyl acrylate (1.2 mmol), Et₃N (3 mmol), 0.05 mol% of Pd(II) complex **3** and 2 mL DMF at 130 °C for 5 h.

3.8.2 Preparation of Ozagrel Butyl Ester **5p**

A mixture of (*E*)-4-(hydroxymethyl) cinnamic acid butyl ester **5o** (234.03 mg, 1 mmol), carbonyldiimidazol (324.3 mg, 2 mmol), and anhydrous NMP (7 mL) was stirred at 160 °C for 3 h (Yamada et al., 2014). After cooling to 25 °C, the reaction mixture was diluted with EtOAc (20 mL), washed with H₂O (3 × 20 mL) and brine (15 mL), dried over MgSO₄ and concentrated under reduced pressure. The residue was purified by column chromatography over silica gel, eluting with CHCl₃/MeOH (30/1) to give Ozagrel butyl ester (**5p**) in 85% yield (Figure 3.13).

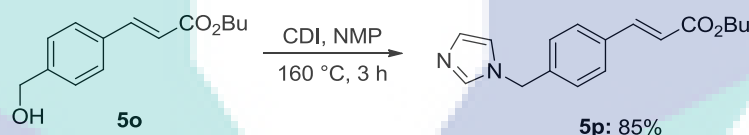


Figure 3.13 Preparation of Ozagrel butyl ester. Reaction condition of Ozagrel butyl ester: cinnamic acid butyl ester **5o** (234.03 mg, 1 mmol), carbonyldiimidazol (324.3 mg, 2 mmol) and anhydrous NMP (7 mL) at 160 °C for 3 h.

Source: Yamada et al. (2014)

3.8.3 Preparation of Ozagrel Hydrochloride **5q**

To a 10-mL glass vessel, was added Ozagrel butyl ester **5p** (100 mg, 0.352 mmol), 0.70 M aqueous sodium hydroxide (1.2 mL), methanol (0.5 mL), and the mixture was stirred at 25 °C for 3 h. The mixture was concentrated under reduced pressure and the residue was acidified with 1.5 M aqueous hydrochloric acid (6 mL). The resulting solution was concentrated under reduced pressure to remove hydrochloric acid completely (Yamada et al., 2014). The residue was dissolved in ethanol (2.5 mL) and the resulting NaCl was filtered off. The filtrate was evaporated and finally, 5 mL of

diethyl ether was added to precipitate Ozagrel hydrochloride (**5q**), (Figure 3.14) with a yield of 88%.

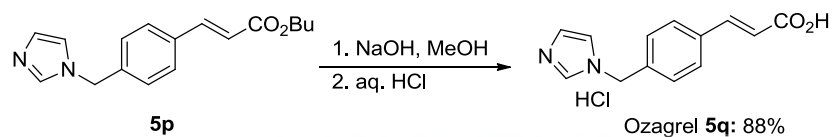


Figure 3.14 Preparation of Ozagrel hydrochloride. Reaction condition of Ozagrel hydrochloride: Ozagrel butyl ester **5p** (100 mg, 0.352 mmol), 0.70 M aqueous sodium hydroxide (1.2 mL), methanol (0.5 mL), 1.5 M aqueous hydrochloric acid (6 mL) and the mixture was stirred at 25 °C for 3 h.

Source: Yamada et al. (2014)

UMP

CHAPTER 4

RESULTS AND DISCUSSION

4.1 Introduction

Cellulose supported metal (palladium, copper, nickel, iron, and gold) complex catalysts are very important for the synthesis of organic molecules (William et al., 2008; Wan et al., 2011). The heterogeneous metal complex catalysts are usually synthesized by the surface modification of organic and inorganic solid materials (McDowall et al., 1984; Rahman et al., 2014). Currently, many economic and sustainable heterogeneous catalysts have been employed for the green processes but there is still a high demand to explore more efficient catalysts and catalyst solid supports for chemical transformations. In this recent work, chemically modified waste corn-cob cellulose supported metal (Pd, Cu) complexes have been utilized to investigate the low-cost production of fine chemicals through Mizoroki-Heck, Click, and Aza-Michael reactions.

4.2 Preparation and Characterization of Poly(amidoxime) Pd(II) Complex **3**

The waste corn-cobs were cut into small pieces and successively boiled with 10% NaOH and glacial acetic acid for 4 h and 2 h. The resulting cellulose was washed with water and bleached with hydrogen peroxide and 5% NaOH, respectively. The white colored cellulose was graft-polymerized with acrylonitrile using ceric ammonium nitrate as an initiator to give cellulose supported poly(acrylonitrile) **1** which was further reacted with hydroxylamine provide poly(amidoxime) chelating ligand **2**. The poly(amidoxime) ligand **2** was then, treated with an aqueous solution of $(\text{NH}_4)_2\text{PdCl}_4$ at room temperature to give light brown colored poly(amidoxime) Pd(II) complex **3**. The

ICP-AES analysis showed that 0.45 mmol/g of palladium was immobilized onto the poly(amidoxime) Pd(II) complex **3** (Figure 4.1).

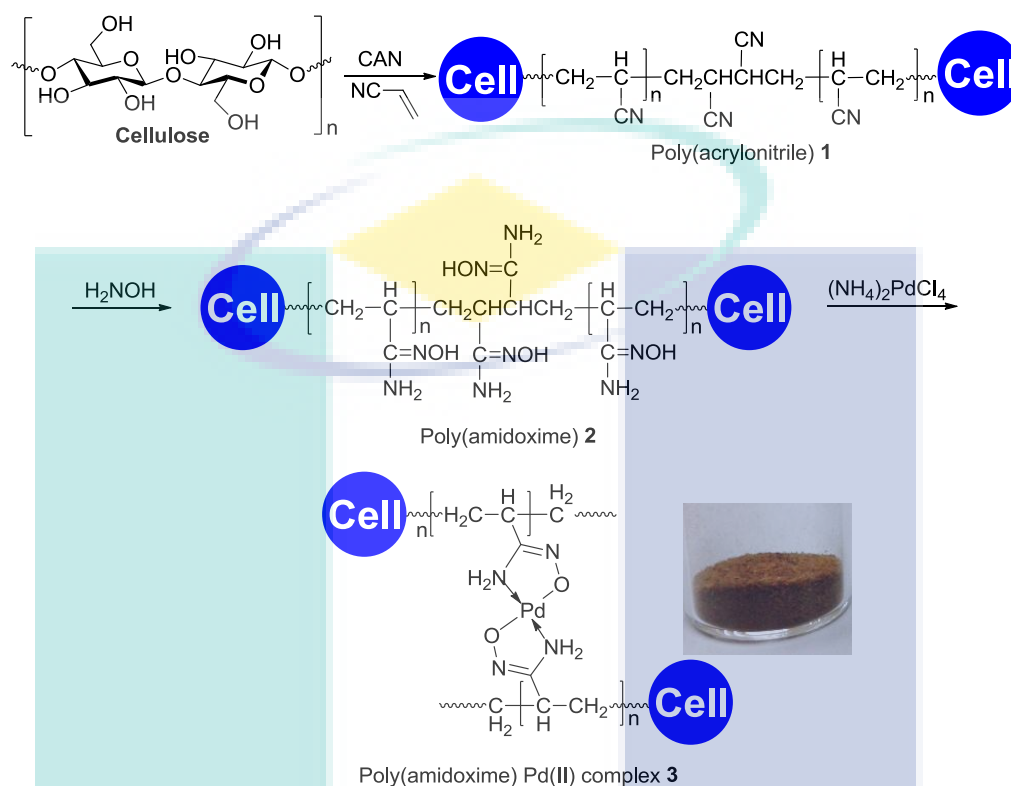


Figure 4.1 Synthesis of poly(amidoxime) Pd(II) complex **3**.

4.2.1 Fourier Transform Infrared Spectroscopy (FTIR) Analysis of Cellulose and Modified Celluloses

The waste corn-cob cellulose, modified celluloses **1** and **2**, and poly(amidoxime) Pd(II) complex **3** were characterized with an FTIR spectrometer (PerkinElmer 670) shown in Figure 4.2. The IR spectrum of fresh corn-cob cellulose showed absorption bands at 3438 and 2921 cm^{-1} for O-H and C-H stretching, respectively (Figure 4.2a). The broadband at 1638 cm^{-1} showed the bending mode of OH (Sukhov, 2016) and a smaller peak at 1426 cm^{-1} which belongs to the CH_2 symmetric bending (Liu et al., 2006). The absorbance at 1376 and 1160 cm^{-1} originated from the O-H bending and C-O stretching, respectively. The C-O-C pyranose ring skeletal vibration produced a strong band at 1065 cm^{-1} (Haron et al., 2009). A small sharp peak at 895 cm^{-1} corresponded to the glycosidic C₁-H deformation with ring vibration contributions and

OH bending which indicated the characteristic of β -glycosidic linkages between the glucose molecule units in the corn-cob cellulose (Liu et al., 2006).

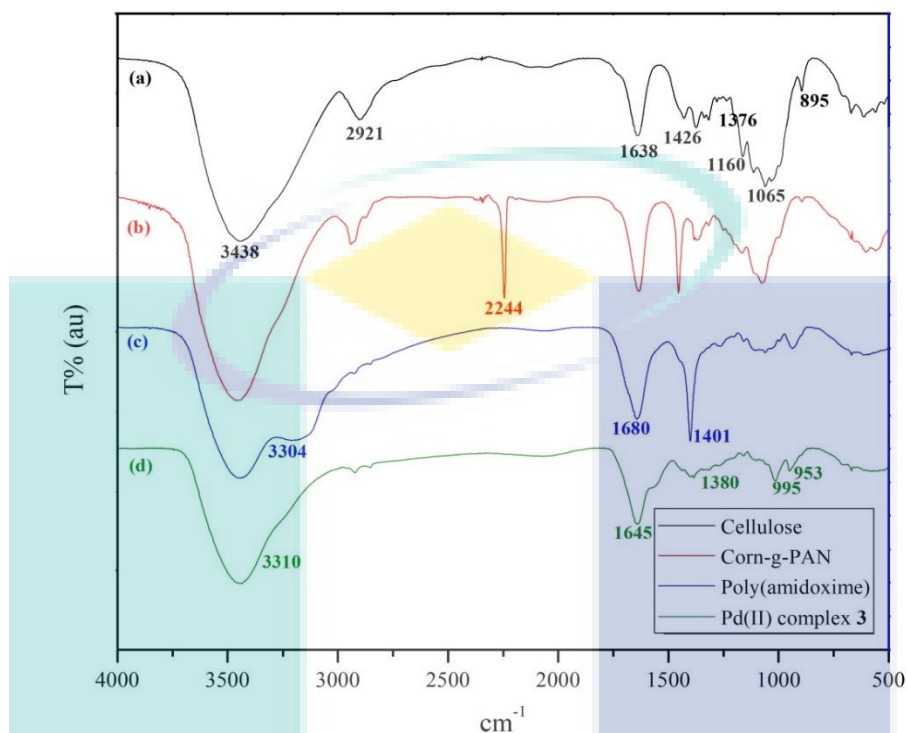


Figure 4.2 FTIR spectra of the (a) corn-cob cellulose, (b) Poly(acrylonitrile) **1** (corn-g-PAN), (c) poly(amidoxime) chelating ligand **2** and (d) poly(amidoxime) Pd(II) complex **3**.

The IR spectrum of the poly(acrylonitrile) grafted (corn-g-PAN) cellulose **1** (Figure 4.2 b) exhibited a new absorption band at 2244 cm^{-1} , which indicates the $\text{C}\equiv\text{N}$ stretching of nitrile. The other bands remain almost the same with that of the corn-cob cellulose (3438 , 2921 , 1638 , 1426 , 1376 , 1160 , 1065 , and 895 cm^{-1}). The poly(amidoxime) chelating ligand **2** which contain amidoxime functional group showed new absorption bands at 1680 which indicates $\text{C}=\text{N}$ stretching (Figure 4.2c). Additionally, a shoulder was created at 3304 cm^{-1} for N-H and OH stretching bands and another peak at 1401 cm^{-1} for OH bending. It is clearly seen that the $\text{C}\equiv\text{N}$ band at 2244 cm^{-1} fully disappeared and a new absorption band for the amidoxime group appeared at 3304 cm^{-1} , 1680 cm^{-1} stretching and 1401 cm^{-1} bending modes. This new band confirmed the successful synthesis of the amidoxime ligand onto the corn-cob cellulose backbone. The IR spectrum of corn-cob cellulose-supported poly(amidoxime) Pd(II) complex **3** showed a broad peak at 3310 cm^{-1} and other peaks at 1645 , 1380 , 995 , and

953 cm^{-1} (Figure 4.2d) which indicate a successful complexation of palladium with the poly(amidoxime) ligand **2**. The lists of FTIR data for cellulose, modified cellulose and poly(amidoxime) Pd(II) complex **3** were shown in Table 4.1.

Table 4.1 List of FTIR data for cellulose, modified cellulose and poly(amidoxime) Pd(II) complex **3**

Sample Name	Absorption band (cm^{-1})
Corn-cob cellulose	3438 (OH), 2921 (C-H), 1638 (OH), 1426 (CH ₂), 1376 (OH), 1160 (C-O), 1065 (C-O-C) and 895 (OH)
Poly(acrylonitrile) 1	2244 (C≡N), nitrile stretching
Poly(amidoxime) 2	3304 (N-H and OH), 1680 (C=N) and 1401 (OH)
Poly(amidoxime) Pd(II) complex 3	3310 (N-H), 1645 (OH bending), 1380, 995 and 953

4.2.2 Field Emission Scanning Electron Microscopy (FE-SEM) Images Analysis of Corn-Cob Cellulose, Modified Celluloses and Energy-Dispersive X-Ray Spectroscopy (EDX) of Pd(II) Complex **3**

The morphology of the cellulose synthesized celluloses, and Pd(II) complex **3** were investigated by field emission scanning electron microscopy (FE-SEM). The FE-SEM image of fresh corn-cob cellulose showed a smooth fine crystalline surface (Figure 4.3a) whereas, the FE-SEM image of poly(acrylonitrile) **1** grafted cellulose showed a less smooth surface with a small spherical like structure (Figure 4.3b) compared to the fresh cellulose.

By observing the surface morphology changes, it was assumed (Fig. 4.3 b) that graft polymerization was successfully occurred on the cellulose surface. The FE-SEM image of the poly(amidoxime) chelating ligand **2** showed (Figure 4.3 c) a grain-shaped morphology with a fine bead structure which is bigger than poly(acrylonitrile) **1**. Finally, the FE-SEM micrograph of poly(amidoxime) Pd(II) complex **3** showed bigger sized spherical shapes (Figure 4.3d) compared to the size of the poly(amidoxime) ligand

2. Thus, it clearly indicates that poly(amidoxime) ligand **2** has aggregated and coordinated with the palladium species.

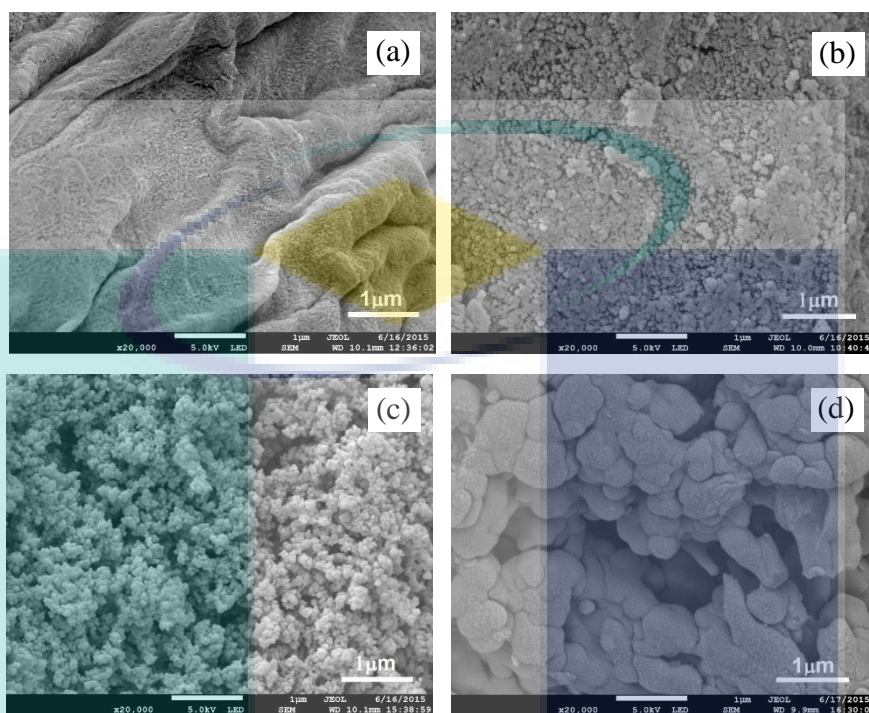


Figure 4.3 FE-SEM images of (a) corn-cob cellulose, (b) Poly(acrylonitrile) **1**, (c) poly(amidoxime) chelating ligand **2**, and (d) poly(amidoxime) Pd(II) complex **3** respectively.

Moreover, the energy dispersive X-ray spectroscopy analysis (EDX) of poly(amidoxime) Pd(II) complex **3** showed a peak around 3 eV which confirmed the presence of palladium metal in the poly(amidoxime) Pd(II) complex **3** (Figure 4.4).

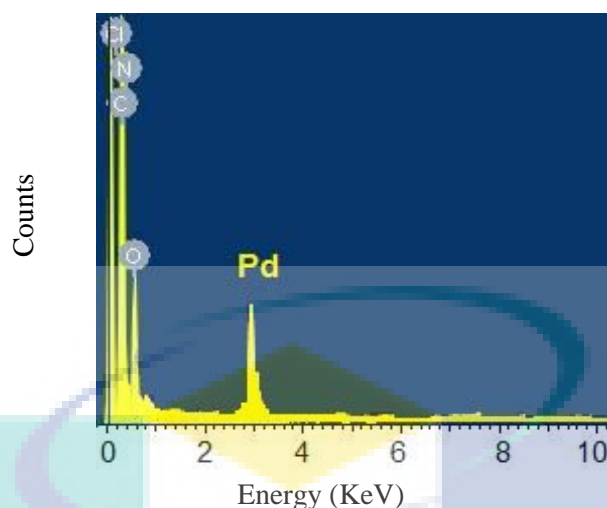


Figure 4.4 EDX spectrum of Pd(II) complex 3.

4.2.3 High-Resolution Transmission Electron Microscopy (HR-TEM) Images of Fresh and 4th Reused of Poly(amidoxime) Pd(II) Complex 3

The HR-TEM images of poly(amidoxime) Pd(II) complex 3 and 4th reused poly(amidoxime) Pd(II) complex 3 are shown in Figure 4.5. The HR-TEM images

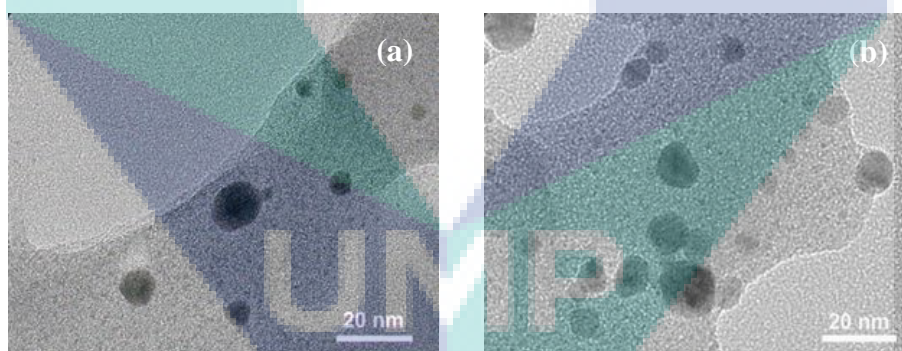


Figure 4.5 (a) HR-TEM image of poly(amidoxime) Pd(II) complex 3 and (b) HR-TEM image of 4th reused poly(amidoxime) Pd(II) complex 3.

showed a good distribution of Pd(II) complex 3 onto the modified cellulose surface with an average complex size $\phi = 7.2$ nm (Figure 4.5a). Thus, the HR-TEM micrograph confirmed the presence of palladium onto the poly(amidoxime) Pd(II) complex 3 (Shen et al., 2015; Nieman et al., 1991). The HR-TEM micrograph of the 4th recycled (Mizoroki-Heck reaction) poly(amidoxime) Pd(II) complex 3 (Figure 4.5b) also showed a similar size ($\phi = 7.2$ nm) of Pd(II) complex with well distribution. The similar complex

size and well distribution of the Pd(II) complex **3** revealed that, during the reaction progress, Pd(II) complexes were not aggregated.

4.2.4 X-Ray Powder Diffraction (XRD) of Fresh and Reused Pd(II) Complex **3**

The X-ray powder diffraction (XRD) analysis of the waste corn-cob cellulose-supported fresh and reused Pd(II) complex **3** were investigated. The powder X-ray diffraction of fresh poly(amidoxime) Pd(II) complex **3** showed Bragg's reflections at $2\theta = 40.41, 46.79, 68.15, 82.21,$ and 86.72 (Figure 4.6a) which can be indexed as (111), (200), (220), (311) and (222) planes for Pd(II), (Anan et al., 2011; Fu et al., 2015). The powder X-ray diffraction study of the reused poly(amidoxime) Pd(II) complex **3** also showed similar planes (Figure 4.6b) which confirmed that the poly(amidoxime) Pd(II) complex **3** was highly stable in the reaction media.

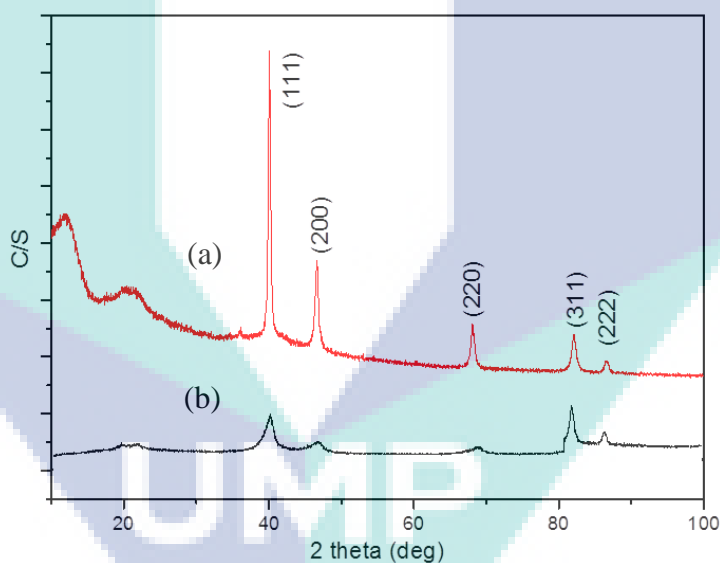


Figure 4.6 X-ray powder diffraction (XRD) of (a) fresh and (b) reused Pd(II) Complex **3**.

4.2.5 X-Ray Photoelectron Spectroscopy (XPS) of Fresh and Reused Poly(amidoxime) Pd(II) Complex **3**

The XPS analysis of the fresh and reused poly(amidoxime) Pd(II) complex **3** is shown in Figures 4.7 and 4.8, respectively. The full scan XPS spectrum of fresh poly(amidoxime) Pd(II) complex **3** showed the presence of palladium onto the cellulose surface, whereas these peaks were absent in the poly(amidoxime) ligand **2** (Figure 4.7a).

The narrow scan of Pd(II) complex **3** showed two important peaks (Figure 4.7b) at 337.8 eV and 343.3 eV which were assigned to Pd(II)3d_{5/2} and Pd(II)3d_{3/2} (Fu et al., 2015).

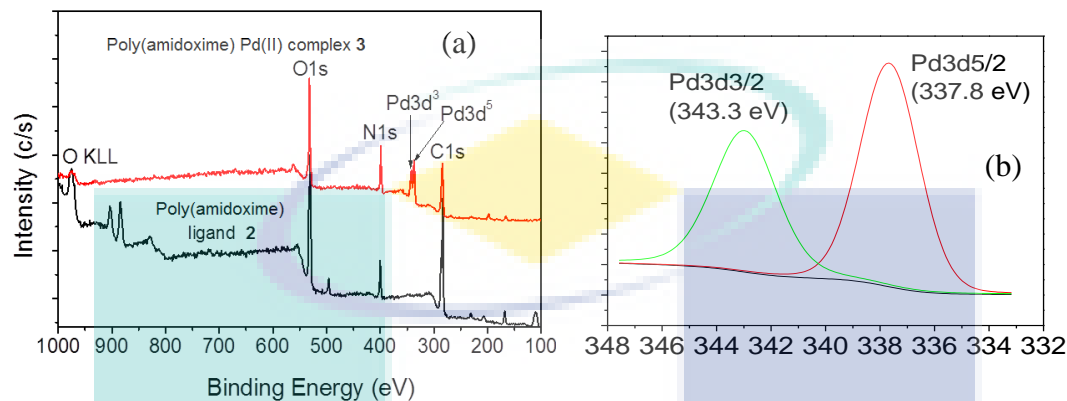


Figure 4.7 (a) Full scan XPS spectrum of fresh Pd(II) complex **3** and (b) narrow scan XPS spectrum of fresh Pd(II) complex **3**.

The XPS analysis of the reused poly(amidoxime) Pd(II) complex **3** was also carried out and the palladium peaks were still found in the XPS spectrum. The narrow XPS spectrum of reused poly(amidoxime) Pd(II) complex **3** revealed the existence of palladium species on the cellulose surface (Figure 4.8b).

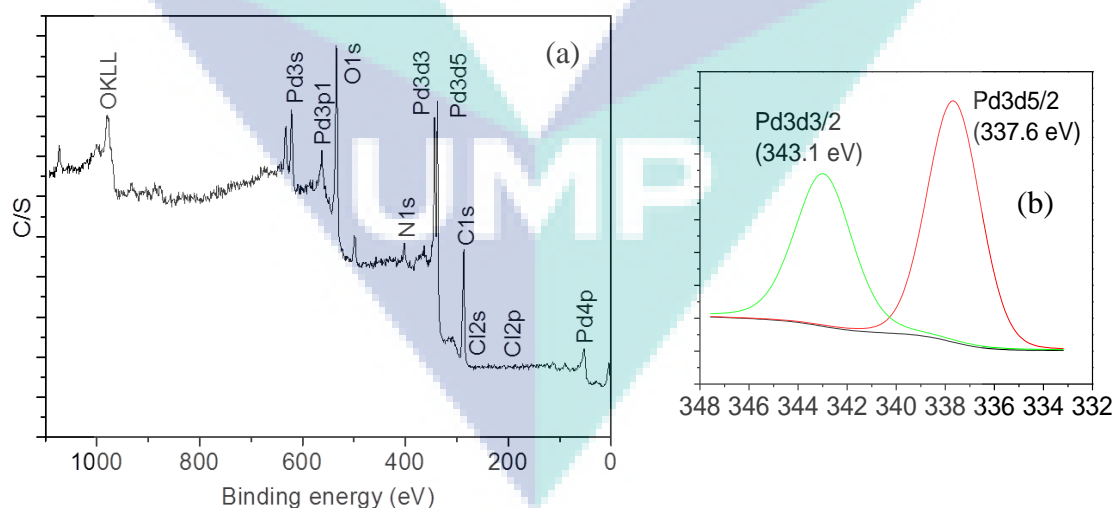


Figure 4.8 (a) Full scan XPS spectrum of reused Pd(II) complex **3** and (b) narrow scan XPS spectrum of reused Pd(II) complex **3**.

4.2.6 Inductively Coupled Plasma Atomic Emission Spectroscopy (ICP-AES)

The amount of palladium in the poly(amidoxime) Pd(II) complex **3** was quantitatively determined by ICP-AES method. The inductively coupled plasma atomic emission spectroscopy (ICP-AES) analysis revealed that 0.45 mmol/g of palladium was immobilized onto the Pd(II) complex **3**.

4.3 Characterization of the Poly(amidoxime) Cu(II) Complex **4**

The poly(amidoxime) ligand **2** was treated with an aqueous solution of copper sulfate to give the green colored cellulose-supported poly(amidoxime) Cu(II) complex **4** (Figure 4.9). The ICP-AES analysis revealed that 0.5 mmol/g of copper was immobilized onto the poly(amidoxime) Cu(II) complex **4**.

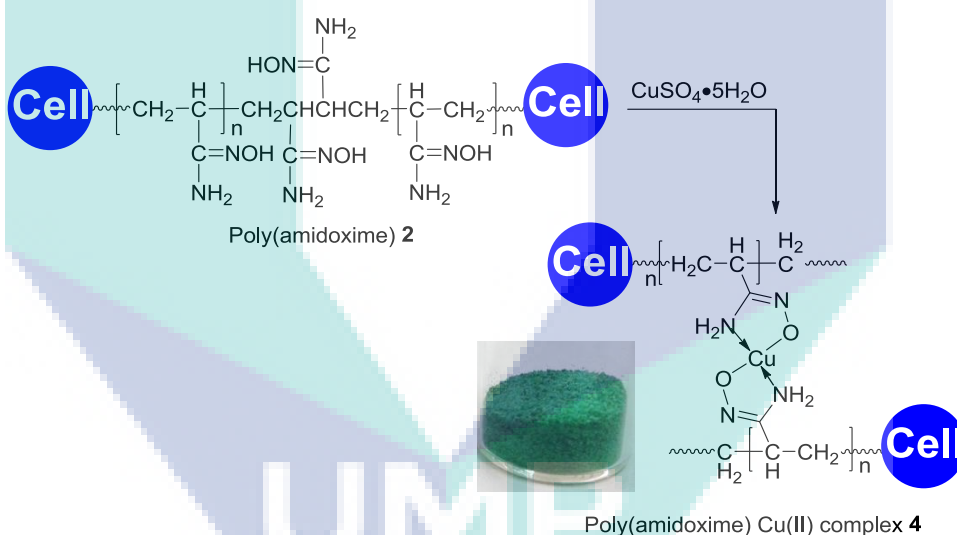


Figure 4.9 Synthesis of poly(amidoxime) Cu(II) complex **4**.

4.3.1 Fourier Transform Infrared Spectroscopy (FTIR) of Poly(amidoxime) Cu(II) Complex **4**

The amidoxime functional groups contained in the poly(amidoxime) chelating ligand **2** showed absorption bands at 1680 and 1648 cm^{-1} corresponding to the C=N stretching and N-H bending modes, respectively (Figure 4.10 c). A shoulder peak at 3304 cm^{-1} was observed for N-H and OH stretching bands and another peak at 1401 cm^{-1} for OH bending (Figure 4.10 c). The IR spectrum of the corn-cob cellulose-supported

poly(amidoxime) Cu(II) complex **4** showed a broad peak at 3306 cm^{-1} and another peak at 1125 cm^{-1} (Figure 4.10 d) which indicate the successful complexation of copper with the poly(amidoxime) ligand **2** (Prenesti & Berto, 2002).

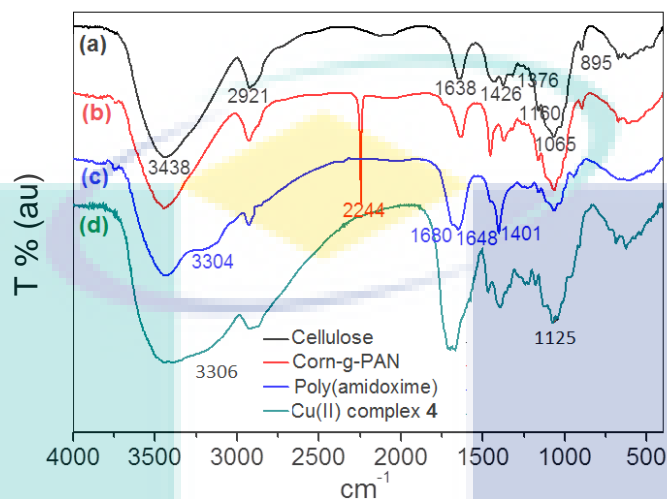


Figure 4.10 FTIR spectrum of (a) corn-cob cellulose, (b) (corn-g-PAN), (c) poly(amidoxime) **2** and (d) poly(amidoxime) Cu(II) complex **4**.

The lists of FTIR data for cellulose, modified cellulose and poly(amidoxime) Cu(II) complex **4** were shown in Table 4.2.

Table 4.2 List of FTIR data for cellulose, modified cellulose and poly(amidoxime) Cu(II) complex **4**

Sample Name	Absorption band (cm^{-1})
Corn-cob cellulose	3438 (OH), 2921 (C-H), 1638 (OH), 1426 (CH_2), 1376 (OH), 1160 (C-O), 1065 (C-O-C) and 895 (OH)
Poly(acrylonitrile) 1	2244 ($\text{C}\equiv\text{N}$), nitrile stretching
Poly(amidoxime) 2	3304 (N-H and OH), 1680 (C=N), 1648 (N-H) and 1401 (OH)
Poly(amidoxime) Cu(II) complex 4	3306 (N-H) and 1125

4.3.2 Field Emission Scanning Electron Microscopy (FE-SEM) Images of Ligand 2, Cu(II) Complex 4 and Energy-Dispersive X-Ray Spectroscopy (EDX) of Cu(II) Complex 4

The FE-SEM image of the corn-cob cellulose-supported poly(amidoxime) chelating ligand **2** showed a small grain-shaped morphology (Figure 4.11 a). However, the FE-SEM image of the poly(amidoxime) Cu(II) complex **4** showed compact aggregated morphology. The poly(amidoxime) chelating ligand **2** was coordinated with copper species by nitrogen and oxygen atoms thus the poly(amidoxime) chelating ligands were aggregated and provided bigger spherical shape (Figure 4.11 b). By observing the significant changes of surface morphology, it can be assumed that copper species were strongly bonded with the poly(amidoxime) chelating ligand **2**.

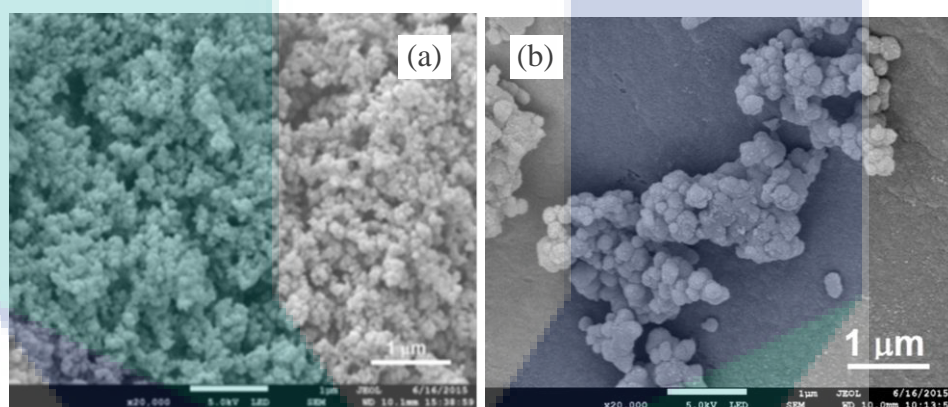


Figure 4.11 FE-SEM images of (a) poly(amidoxime) chelating ligand **2**, (b) poly(amidoxime) Cu(II) complex **4**.

Additionally, the EDX analysis of poly(amidoxime) Cu(II) complex **4** further confirmed the presence of copper species in the cellulose-supported poly (amidoxime) Cu(II) complex **4** (Figure 4.12).

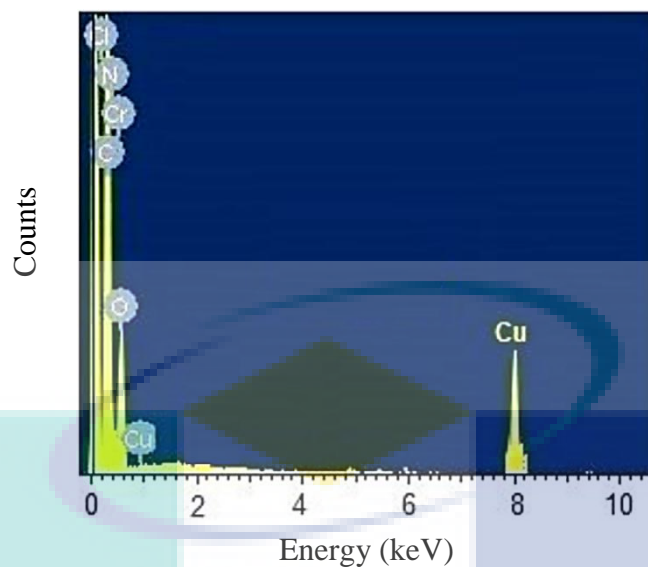


Figure 4.12 EDX spectrum of corn-cob cellulose supported poly(amidoxime) Cu(II) complex **4**.

4.3.3 High-Resolution Transmission Electron Microscopy (HR-TEM) Images of Cu(II) Complex **4** and CuNP@PA

The HR-TEM image of waste corn-cob cellulose-supported poly(amidoxime) Cu(II) complex **4** showed the good dispersion of Cu(II) complex **4** (Figure 4.13) onto the cellulose surface. The Cu(II) complex **4** particle size of average hundred particles were measured and it was found that, the average Cu(II) complex **4** particle size was $\varnothing = 17.5 \pm 2$ nm.

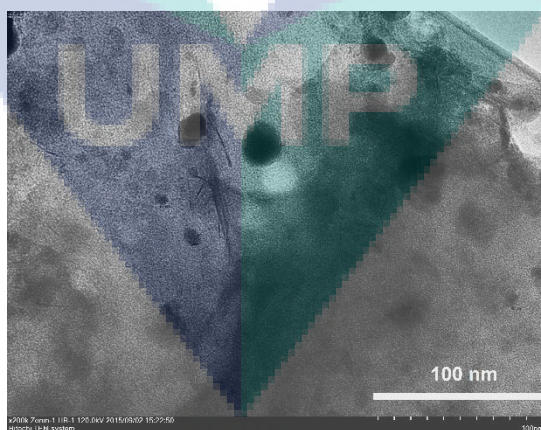


Figure 4.13 HR-TEM image of Cu(II) complex **4**.

The poly(amidoxime) Cu(II) complex **4** was then dispersed in deionized water and hydrazine hydrate was added. The resulting dark brown colored copper

nanoparticles (**CuNP@PA**) materials ($\varnothing = 6.8 \pm 2$ nm) were collected by filtration, washed with methanol, dried under vacuum, and stored under a nitrogen atmosphere (Figure 4.14).

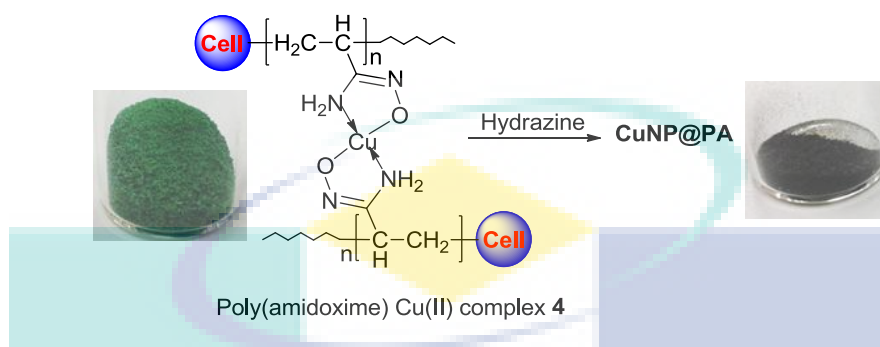


Figure 4.14 Synthesis of **CuNP@PA**.

The HR-TEM image of the **CuNP@PA** demonstrated that it was well dispersed on the cellulose backbone (Figure 4.16) and the nanoparticles were stabilized by the amidoxime functional group as well as the cellulose backbone itself and size distribution were shown in Figure 4.15.

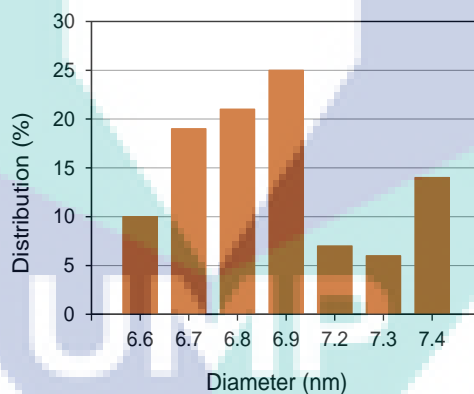


Figure 4.15 Size distribution of the **CuNP@PA** (the sizes were determined for 100 nanoparticles selected randomly).

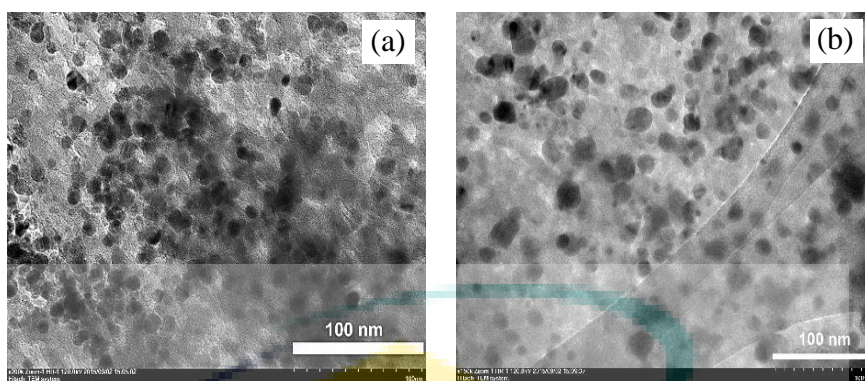


Figure 4.16 (a) HR-TEM image of **CuNP@PA**, (b) HR-TEM image of 3rd reuse **CuNP@PA**.

4.3.4 X-Ray Powder Diffraction (XRD) of Cu(II) Complex **4**, Fresh and Reused **CuNP@PA**

The powder X-ray diffraction study (XRD), (Figure 4.17) of Cu(II) complex **4** showed three peaks at 2θ values of 17.4° , 22.1° and 23.6° corresponding to the Bragg's planes (101), (101) and (002) from cellulose (Baruah et al., 2015). The Bragg's reflections at $2\theta = 26.0, 37.0, 42.1,$ and 56.02 can be indexed as Cu(110), Cu(111), Cu(200) and Cu(220) phases and attributed to Cu(II), (Anan et al., 2011).

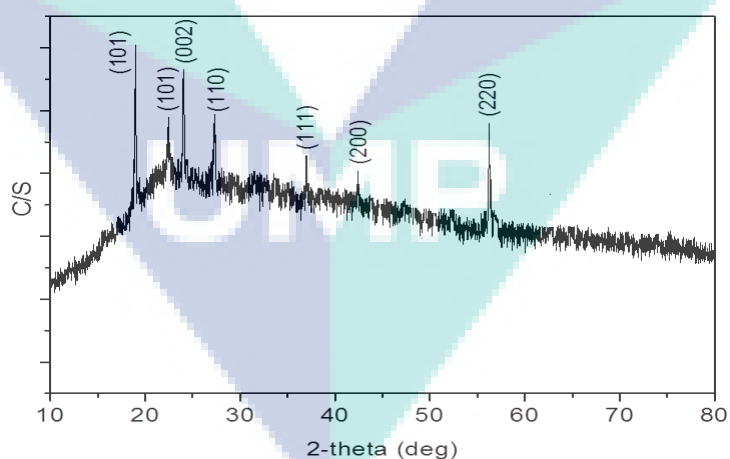


Figure 4.17 XRD pattern of Cu(II) complex **4**.

The powder X-ray diffraction study of cellulose-supported poly(amidoxime) fresh copper nanoparticles (**CuNP@PA**) showed Bragg's reflections at $2\theta = 43.6, 50.5,$ and 74.5 which can be indexed as Cu(111), Cu(200), and Cu(220) phases were

attributable to Cu(0), (Gholinejad & Jeddi, 2014). After Aza-Michael reaction, the X-ray diffraction study of the reused **CuNP@PA** was also carried out and from the XRD pattern of reused **CuNP@PA**, similar Bragg's reflections planes with fresh **CuNP@PA** were obtained (Figure 4.18).

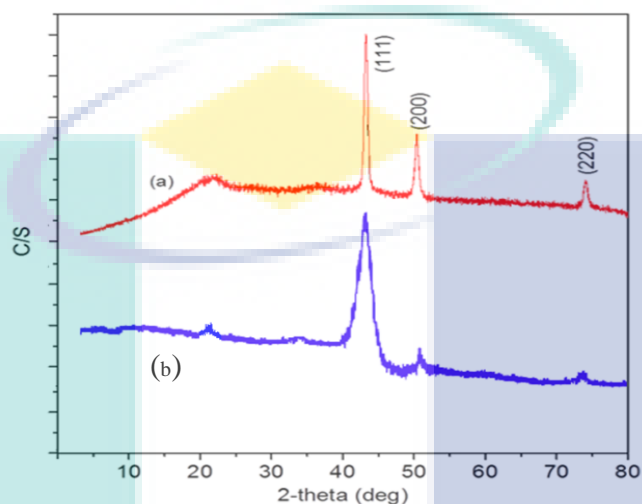


Figure 4.18 XRD pattern of (a) fresh **CuNP@PA** and (b) reused **CuNP@PA**.

4.3.5 X-Ray Photoelectron Spectroscopy (XPS) of Poly(amidoxime) Cu(II) Complex 4, Cu(I), Fresh and Reused **CuNP@PA**

The oxidation state of copper [Cu(II), Cu(I) and Cu(0)] in the waste corn-cob cellulose-supported poly(amidoxime) Cu(II) complex **4**, Cu(I), and **CuNP@PA** were confirmed by XPS analysis. The full XPS spectrum of Cu(II) complex **4** was shown in Figure 4.19a and the new peaks confirmed the presence of copper species on the cellulose. The narrow scan of poly(amidoxime) Cu(II) complex **4** showed two single peaks (Figure 4.19b) at 953.3 and 934.2 eV which were assigned to Cu2p_{1/2} and Cu2p_{3/2}, respectively (Hope et al., 2010).

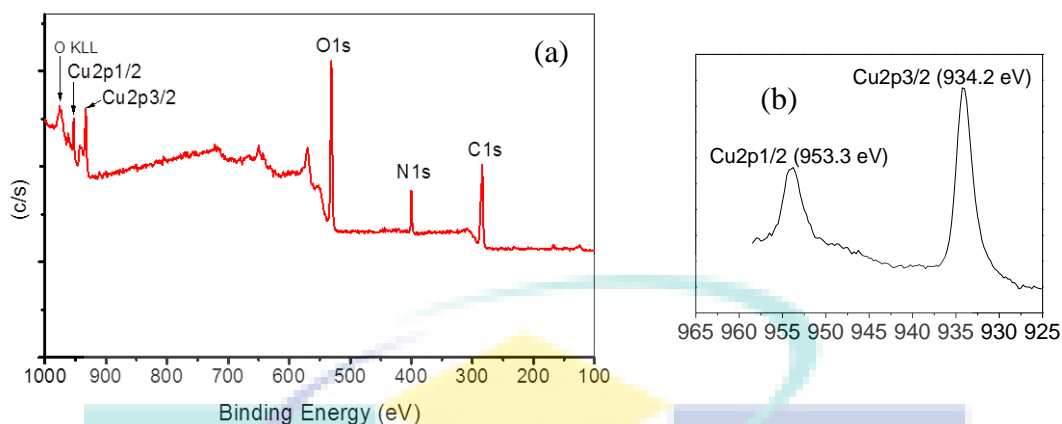


Figure 4.19 (a) Full scan XPS of Cu(II) complex **4** and (b) narrow scan XPS of Cu(II) complex **4**.

It should be noted that, during Click reaction, the Cu(II) complex **4** was reduced by sodium ascorbate to give Cu(I) species during the catalytic cycle. The green colored Cu(II) complex **4** turned to yellow which confirmed the formation of Cu(I) species. To further the study, the full and narrow scan XPS spectra of Cu(I) complex were analysed (Figure 4.20). The narrow scan XPS of Cu(I) showed two single peaks (Figure 4.20b) at 952.5 and 932.1 eV which were assigned to Cu2p1/2 and Cu2p3/2, respectively (Hope et al., 2010; Swadźba-Kwaśny et al., 2012). However, in the Cu(II) complex **4**, these peaks were observed at 953.3 and 934.2 eV.

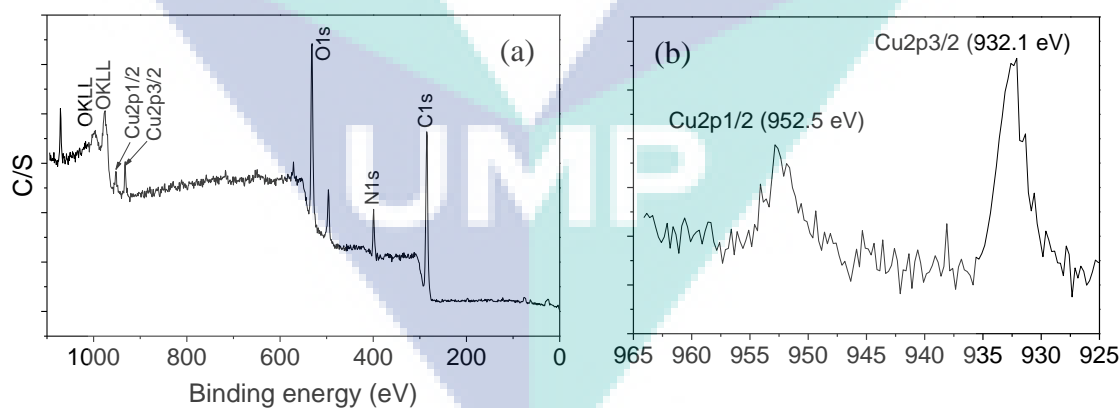


Figure 4.20 (a) Full scan XPS of Cu(I) and (b) narrow scan XPS of Cu(I).

To study Aza-Michael reaction, the Cu(II) complex **4** was treated with hydrazine to give a black colored **CuNP@PA**. The narrow scan XPS spectrum of **CuNP@PA** showed two single peaks at 951.2 and 931.4 eV which were assigned to Cu2p1/2 and

Cu2p3/2, respectively (Figure 4.21b). It is worth to note that, these peaks were perfectly different to the Cu(II) peaks at 953.3 and 934.2 eV.

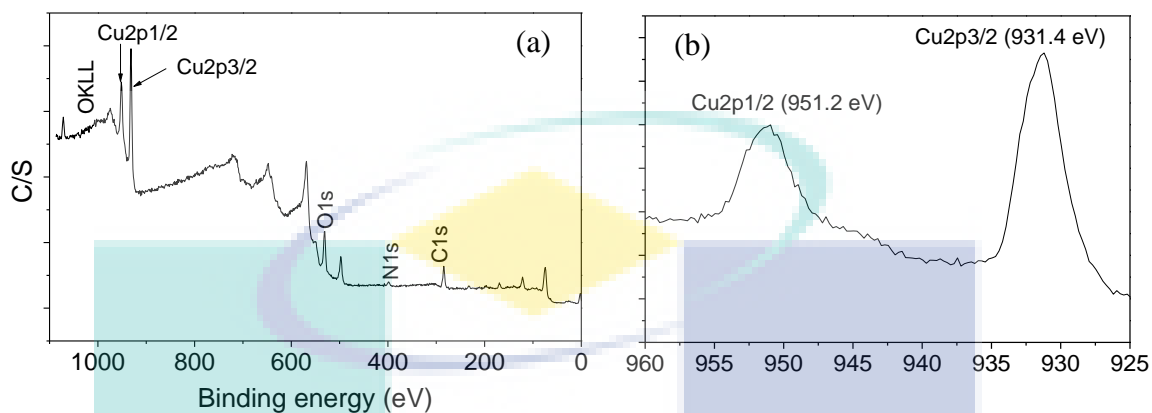


Figure 4.21 (a) Full scan XPS of fresh **CuNP@PA** and (b) narrow scan XPS of fresh **CuNP@PA**.

The XPS spectra of reused **CuNP@PA** was also analysed and its narrow scan XPS spectrum showed two single peaks (Figure 4.22b) at 951.3 and 931.6 eV which were assigned to Cu2p1/2 and Cu2p3/2, respectively (Huang et al., 2011; Yamada et al., 2012; Wu et al., 2014; Yoshida et al., 2010; Barot et al., 2016; Rossy et al., 2014). This XPS result suggests that during the Aza-Michael reaction, **CuNP@PA** was not decomposed.

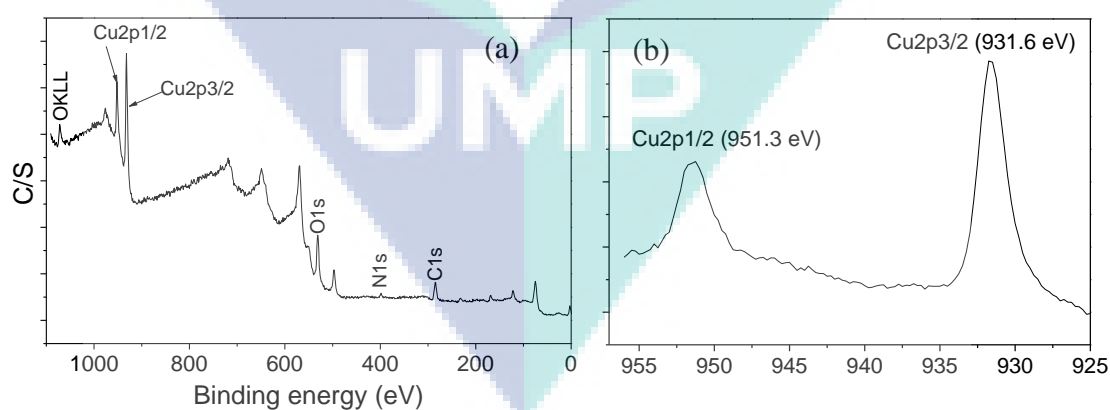


Figure 4.22 (a) Full scan XPS of reused **CuNP@PA** and (b) narrow scan XPS of reused **CuNP@PA**.

4.4 Application of the Catalysts in Cross-Coupling Reaction

The application of the prepared poly(amidoxime) Pd(II) complex **3**, poly(amidoxime) Cu(II) complex **4**, and **CuNP@PA** are described below.

4.4.1 Poly(amidoxime) Pd(II) Complex Catalyzed Mizoroki-Heck Reaction

The catalytic efficiency of the heterogeneous Pd(II) complex **3** was evaluated in the Mizoroki-Heck cross-coupling reaction as a versatile method for the formation of C-C bond in organic synthesis. Firstly, the coupling reaction of iodobenzene with butyl acrylate was chosen as a model reaction. The reaction was conducted using different amounts of Pd(II) complex **3** loading, bases, and also varying solvent compositions and temperatures (Table 4.3). The initial reaction was carried out using 0.1 mol% of Pd(II) complex **3** for the reaction between iodobenzene and butyl acrylate in the presence of sodium carbonate (3 mmol) in an aqueous solution of DMF at 130 °C to give the corresponding coupling product **5a** in 74% yield with TOF value 148 within 5 h reaction time (Table 4.3, entry 1). When the reaction was carried out under the same reaction condition with K₂CO₃ instead of the Na₂CO₃, 73% yield was obtained (entry 2). The TON and TOF values were calculated using equations 4.1 and 4.2.

$$\text{TON} = \frac{\text{yield}}{100 \times \text{mmol of catalyst}} \dots \dots \dots (4.1)$$

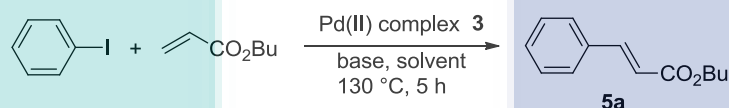
$$\text{TOF} = \frac{\text{TON}}{\text{Reaction time (h)}} \dots \dots \dots (4.2)$$

Although changing the base and solvent had no significant influence on the yields (entries 3-5), when the reaction was carried out in the presence of an organic base (*N,N*-diisopropylethyl amine) in DMF, the reaction proceeded smoothly with 90% yield (entry 6) and the TOF values were not significantly changed. When the base was replaced with triethylamine, the reaction proceeded efficiently to give the coupling product with 98% yield (entry 7). Interestingly, when the amount of catalyst loading was decreased from 0.1 mol% to 0.05 mol%, the catalyst still efficiently forwarded the coupling reaction with 96% yield (entry 8) which provided TOF value 384. However,

when using different solvents like *n*-methyl-2-pyrrolidone and dimethylacetamide, the effect of solvents was not significant to improve the yield of the final products (Table 4.3, entries 9 and 10).

Thus, in conclusion, according to the experimental results, 0.05 mol% of Pd(II) complex **3**, triethylamine (3 mmol) in DMF solvent would be the best combination in this cross-coupling reaction (Table 4.3, entry 8). It is very important to note that the loading of Pd(II) complex **3** could be further reduced to 0.001 mol%, which also efficiently forwarded the Mizoroki-Heck reaction to give 86% yield of the corresponding coupling product (Table 4.3, entry 11).

Table 4.3 Optimization of the Mizoroki-Heck reaction



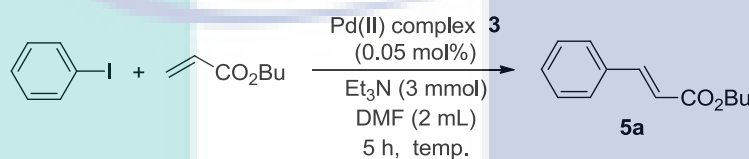
Entry	Solvent (1:1)	Base	3 (mol%)	Yield (%)	TOF (h ⁻¹)
1	DMF:H ₂ O	Na ₂ CO ₃	0.1	74	148
2	DMF:H ₂ O	K ₂ CO ₃	0.1	73	146
3	DMF:H ₂ O	NaOMe	0.1	74	148
4	DMF:H ₂ O	Na ₃ PO ₄	0.1	76	152
5	DMA:H ₂ O	K ₂ CO ₃	0.1	71	142
6	DMF	DIPEA	0.1	90	180
7	DMF	Et ₃ N	0.1	98	196
8	DMF	Et ₃ N	0.05	96	384
9	NMP	Et ₃ N	0.05	88	352
10	DMA	Et ₃ N	0.05	90	360
11	DMF	Et ₃ N	0.001	86	17200

All reactions were carried out using iodobenzene (1 mmol), butyl acrylate (1.2 mmol), a catalytic amount of Pd(II) complex **3** and 3 mmol of the base in 2 mL of solvent for 5 h.

After obtained the suitable combination (Table 4.3, entry 8, DMF, Et₃N, Pd(II) complex **3**) for the Mizoroki-Heck reaction, then the study was further forwarded to find effect of temperature in this catalytic system. The initial reaction was carried out without the presence of cellulose supported Pd(II) complex **3** at 130 °C which provided only 7% yield of the product (Table 4.4, entry 1). This result indicated that the Heck

reaction proceeded under catalytic condition. Next, the reaction temperature was gradually increased (90-150 °C) and found high conversion rate (97% yield) at 150 °C (entry 8) which provided highest TOF value 388. However, 96% yield was obtained when the reactions were carried out at 130 °C and 140 °C respectively (entries 6 & 7). After screening the reaction temperature, it should be noted that 130 °C found to be the suitable temperature to promote Mizoroki-Heck reaction efficiently.

Table 4.4 Effect of temperature on the Mizoroki-Heck reaction

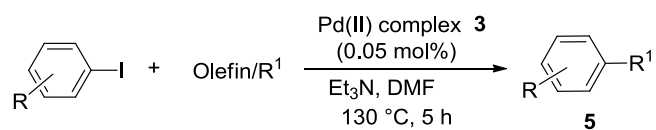


Entry	Temp. (°C)	Yield (%)	TOF (h ⁻¹)
1	130	7 ^[a]	-
2	90	74	296
3	100	86	344
4	110	90	360
5	120	91	364
6	130	96	384
7	140	96	384
8	150	97	388

All reactions were carried out using iodobenzene (1 mmol), butyl acrylate (1.2 mmol), Pd(II) complex **3** (0.05 mol%), Et₃N (3 mmol) and DMF 2 mL. ^[a]Reaction was carried out without using Pd(II) complex **3**.

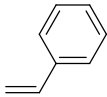
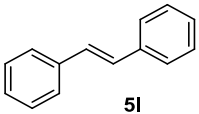
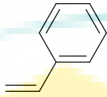
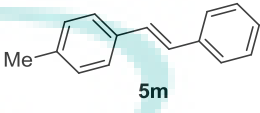
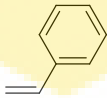
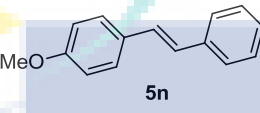
After the optimization of the coupling reaction between iodobenzene and butyl acrylate, the application of the heterogeneous Pd(II) complex **3** was extended using a variety of aryl iodides and olefins (Table 4.5). The reactions between aryl iodides and different olefins like methyl and butyl acrylate, isopropyl acrylamide, and styrene, gave

Table 4.5 Mizoroki- Heck reaction of aryl iodides with olefins



Entry	R	Olefin	Product	Yield (%)
1	H			94
2	OMe			92
3	Me			90
4	Me			91
5	OMe			91
6	NO ₂			96
7	MeCO			95
8	H			94
9	Me			93
10	OMe			90

Table 4.5 Continued

Entry	R	Olefin	Product	Yield (%)
11	H		 5l	93
12	Me		 5m	91
13	OMe		 5n	87

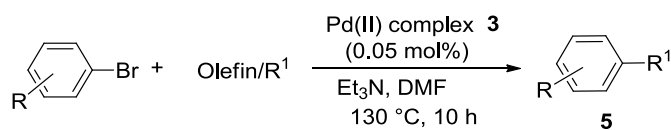
Reactions were carried using aryl iodide (1 mmol), olefin (1.2 mmol), 0.05 mol% of Pd(II) complex **3**, Et₃N (3 mmol), in 2 mL of DMF at 130 °C for 5 h.

the corresponding coupling products with excellent yields. The less reactive aryl halides e.g. iodobenzene, 4-iodoanisole, 3-iodotoluene, 4-iodotoluene showed high catalytic activity in the cross-coupling reaction (**5b-f**, entries 1-5). The activated aryl halides e.g. 4-nitroiodobenzene and 4-iodoacetophenone with butyl acrylates provided excellent yields of the corresponding products (**5g** and **5h**, entries 6 and 7). The aryl iodides which contain electron-donating groups showed slightly less reactivity compared to the other aryl iodides which contain electron-withdrawing groups.

It is very interesting that the coupling reaction between aryl iodides and *N*-isopropylacrylamide was also effectively promoted to give the desired products (**5i**, **5j**, and **5k**) in up to 94 % yield (entries 8-10). Moreover, the less reactive and sterically-hindered styrene also smoothly afforded the corresponding coupling products (**5l-5n**) with high yields (entries 11-13).

The reaction between aryl bromide and olefin of Mizoroki-Heck reaction is very important because aryl bromide is one of the most fascinating and low-cost substrates for industrial applications. So, the catalytic activity of Pd(II) complex **3** is very excellent for aryl iodides which prompted the investigation of its catalytic activity in the coupling reaction of aryl bromides with a variety of olefins (Table 4.6). The heterogeneous Pd(II) complex **3** (0.05 mol%) showed an outstanding catalytic performance in the coupling of a variety of aryl bromides with methyl and butyl acrylates (**5b**, **5c**, **5e**, **5f**, **5g** and **5h** entries 1-6) at 130 °C for 10 h.

Table 4.6 Mizoroki-Heck reaction of aryl bromides with olefins



Entry	R	Olefin	Product	Yield (%)
1	H			92
2	OMe			91
3	Me			89
4	OMe			90
5	NO ₂			96
6	MeCO			93
7	Me			90
8	H			89
9	Me			87
10	OMe			82

Reactions were carried using aryl bromide (1 mmol), olefin (1.2 mmol), 0.05 mol% of Pd(II) complex **3**, Et₃N (3 mmol), in 2 mL of DMF at 130 °C for 10 h.

The coupling reaction of aryl bromides with *N*-isopropylacrylamide and styrene was also carried out and smoothly afforded the corresponding desired products in up to 90% yield (**5j**, **5l**, **5m** and **5n** entries 7-10).

Recently, Fernández-García et al. (2016) carried out a graphene-anchored palladium complex catalyzed (0.3 mol%) Heck reaction of aryl bromide in DMF at 140 °C and obtained almost similar results. However, in this research, the Heck reaction was carried out in an aqueous solution of DMF at 130 °C using 0.05 mol% of Pd(II) complex **3** which has a six times lower palladium loading compared to their report.

To elaborate the application of Pd(II) complex **3**, it was further employed to the Heck-Matsuda coupling reaction of arenediazonium tetrafluoroborate salts (Andrus et al., 2002) which is an excellent aryl electrophilic component (Selvakumar et al., 2002). The arenediazonium tetrafluoroborate salt underwent easy oxidative addition with the metal catalyst during the catalytic cycle to generate active cationic aryl Pd(II) species (Peñafiel et al., 2012) and quickly increased the rate of the cross-coupling reaction with a variety of olefins (Felpin et al., 2008). The Heck-Matsuda cross-coupling reaction was carried out with a variety of olefins and arenediazonium tetrafluoroborate salts by using 0.05 mol% of Pd(II) complex **3** in the presence of ethanol at room temperature for 6 h without adding any base.

The arenediazonium tetrafluoroborate salts which contain electron-pushing or electron-withdrawing functional groups were readily coupled with methyl and butyl acrylates to give the desired coupling products (**5b-c**, **5e-g**) with 93-97% yields at room temperature (Table 4.7, entries 1-5). Moreover, *N*-isopropylacrylamide also underwent the coupling reaction very smoothly to give the corresponding coupling products (**5i** and **5j**) in up to 95% yield (entries 6 and 7). The coupling reaction between the less reactive styrene and arenediazonium tetrafluoroborate salts was smooth and gave the desired products (**5l-n**) in up to 92% yield (entries 8-10).

Recently, the polystyrene-supported Pd(II)-NHC complex catalyst (0.9 mol%) was used in the Heck-Matsuda cross-coupling reaction (Mohammadi & Movassagh, 2016), but in this research, only 0.05 mol% of the Pd(II) complex **3** catalysts was used which is eighteen times lower catalyst loading compare to their report. Thus, the

catalytic activity of the waste corn-cob cellulose-supported poly(amidoxime) Pd(II) complex **3** showed better activity compare to the previous report.

Table 4.7 Heck-Matsuda reaction of arenediazonium tetrafluoroborate with olefins

Entry	R	Olefin	Product	Yield (%)
1	H			96
2	OMe			93
3	Me			95
4	OMe			94
5	NO ₂			97
6	H			94
7	Me			95
8	H			91
9	Me			92
10	OMe			90

Reactions were carried out using 1 mmol of arenediazonium tetrafluoroborate salts, 1.2 mmol of olefin, and 0.05 mol% Pd(II) complex **3** at r.t. for 6 h in ethanol (2 mL).

4.4.2 Synthetic Application of Pd(II) Complex 3 (Synthesis of Ozagrel)

Ozagrel **5q** was synthesized using waste corn-cob cellulose-supported Pd(II) complex **3** through the Mizoroki-Heck reaction (Figure 4.23). Thus, the Heck reaction between 4-iodobenzylalcohol and butyl acrylate was carried out with 0.05 mol% of Pd(II) complex **3** under the same reaction conditions to give the corresponding coupling product (**5o**) in 91% yield. The installation of an imidazole unit was introduced by the reaction of (**5o**) and carbonyldiimidazole (CDI) in *N*-methylpyrrolidone (NMP) at 160 °C for 3 h to provide **5p** in 85% yield. The ester group in **5p** was then, hydrolysed by sodium hydroxide, followed by acidification with HCl to give Ozagrel hydrochloride (**5q**) in 88% yield (Loo et al., 1987).

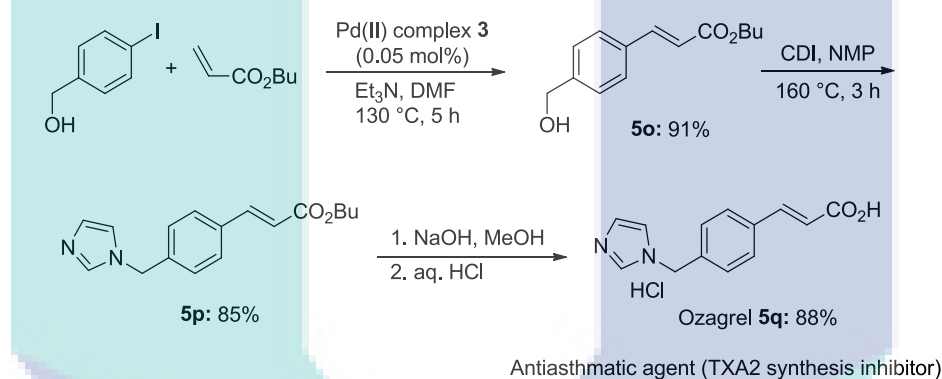
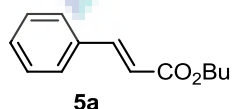


Figure 4.23 Synthesis of Ozagrel hydrochloride.

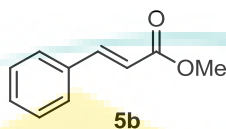
4.4.3 Characterization of Mizoroki-Heck Reaction Products

The prepared products of the Mizoroki-Heck reaction were characterized by using proton nuclear magnetic resonance (^1H NMR), carbon nuclear magnetic resonance (^{13}C NMR), and fourier transform infrared spectroscopy (FTIR) were described below.

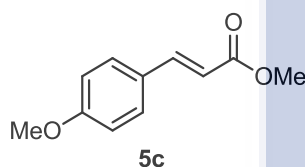


(*E*)-3-Phenylacrylic acid *n*-butyl ester **5a**: ^1H NMR (500 MHz, CDCl_3): δ 7.69 (d, $J = 16.0$ Hz, 1 H), 7.53-7.51 (m, 2 H), 7.39-7.36 (m, 3 H), 6.45 (d, $J = 16.0$ Hz, 1 H), 4.21

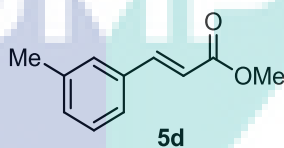
(t, $J = 6.75$ Hz, 2 H), 1.72-1.66 (m, 2 H), 1.43-1.40 (m, 2 H), 0.97 (t, $J = 7.40$ Hz, 3 H). ^{13}C NMR (125 MHz, CDCl_3): δ 167.08, 144.52, 134.46, 130.17, 128.84, 128.02, 118.28, 64.40, 30.76, 19.18, 13.72. FTIR (cm^{-1}): 2959, 1710, 1637, 1578, 1496, 1450, 1384, 1309, 1279, 1201, 1167, 1064, 978, 863, 766, 710.



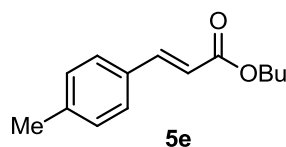
(*E*)-Methyl cinnamate **5b**: ^1H NMR (CDCl_3 , 500 MHz): δ 7.70 (d, $J = 16.0$ Hz, 1 H), 7.52-7.50 (m, 2 H), 7.38-7.37 (m, 3 H), 6.44 (d, $J = 16.0$ Hz, 1 H), 3.86 (s, 3 H). ^{13}C NMR (125 MHz, CDCl_3): δ 167.41, 144.85, 134.34, 130.26, 128.85, 128.04, 51.67. FTIR (cm^{-1}): 2958, 1722, 1637, 1578, 1450, 1345, 1313, 1280, 1172, 1109, 994, 847, 824, 759, 718, 674.



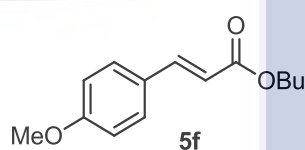
(*E*)-Methyl 3-(4-methoxyphenyl) acrylate **5c**: ^1H NMR (CDCl_3 , 500 MHz): δ 7.65 (d, $J = 15.95$ Hz, 1 H), 7.64 (d, $J = 8.65$ Hz, 2 H), 6.90 (d, $J = 8.80$ Hz, 2 H), 6.31 (d, $J = 15.95$ Hz, 1 H), 3.83 (s, 3 H), 3.79 (s, 3 H). ^{13}C NMR (125 MHz, CDCl_3): δ 167.76, 161.36, 144.51, 129.69, 127.08, 115.22, 114.29, 55.34, 51.55. FTIR (cm^{-1}): 2948, 2844, 1717, 1638, 1604, 1513, 1433, 1331, 1288, 1256, 1206, 1176, 1026, 984, 823, 768, 552.



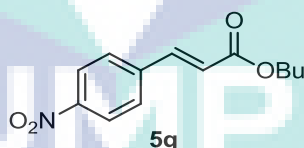
(*E*)-Methyl 3-(*m*-tolyl) acrylate **5d**: ^1H NMR (CDCl_3 , 500 MHz): δ 7.67 (d, $J = 16.0$ Hz, 1 H), 7.33 (d, $J = 6.60$ Hz, 2 H), 7.27 (t, $J = 8.15$ Hz, 1 H), 7.19 (d, $J = 7.20$ Hz, 1 H), 6.43 (d, $J = 16.0$ Hz, 1 H), 3.80 (s, 3 H), 2.36 (s, 3 H). ^{13}C NMR (125 MHz, CDCl_3): δ 167.47, 145.02, 138.50, 134.28, 128.69, 125.22, 117.50, 51.63, 21.27. FTIR (cm^{-1}): 2949, 1716, 1637, 1485, 1435, 1313, 1270, 1236, 1160, 1038, 1016, 981, 909, 859, 786, 727, 712.



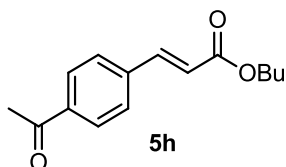
(*E*)-3-(4'-Tolyl) acrylic acid *n*-butyl ester **5e**: ^1H NMR (500 MHz, CDCl_3): δ 7.66 (d, $J = 16.0$ Hz, 1 H), 7.41 (d, $J = 8.10$ Hz, 2 H), 7.18 (d, $J = 8.0$ Hz, 2 H), 6.40 (d, $J = 16.0$ Hz, 1 H), 4.20 (t, $J = 6.55$ Hz, 2 H), 2.37 (s, 3 H), 1.69-1.62 (m, 2 H), 1.44-1.41 (m, 2 H), 0.96 (t, $J = 7.45$ Hz, 3 H). ^{13}C NMR (125 MHz, CDCl_3): δ 167.27, 144.52, 140.58, 131.72, 129.57, 128.02, 117.18, 64.32, 30.77, 21.42, 19.18, 13.73. FTIR (cm^{-1}): 2958, 1710, 1637, 1585, 1463, 1382, 1309, 1260, 1234, 1160, 1091, 1063, 1026, 785, 726.



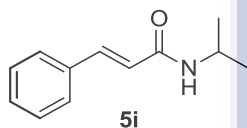
(*E*)-3-(4'-Methoxyphenyl) acrylic acid *n*-butyl ester **5f**: ^1H NMR (500 MHz, CDCl_3): δ 7.64 (d, $J = 16.0$ Hz, 1 H), 7.47 (d, $J = 8.50$ Hz, 2 H), 6.90 (d, $J = 8.80$ Hz, 2 H), 6.31 (d, $J = 16.0$ Hz, 1 H), 4.20 (t, $J = 6.55$ Hz, 2 H), 3.84 (s, 3 H), 1.71-1.63 (m, 2 H), 1.43-1.40 (m, 2 H), 0.96 (t, $J = 7.40$ Hz, 3 H). ^{13}C NMR (125 MHz, CDCl_3): δ 167.37, 161.25, 144.13, 129.61, 127.15, 115.71, 114.23, 64.19, 55.29, 30.75, 19.14, 13.68. FTIR (cm^{-1}): 2958, 1706, 1634, 1602, 1462, 1422, 1384, 1287, 1248, 1180, 1028, 981, 828, 773, 738.



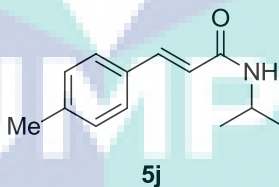
(*E*)-3-(4'-Nitrophenyl) acrylic acid *n*-butyl ester **5g**: ^1H NMR (500 MHz, CDCl_3): δ 8.25 (d, $J = 8.70$ Hz, 2 H), 7.72-7.66 (m, 3 H), 6.57 (d, $J = 15.95$ Hz, 1 H), 4.24 (t, $J = 6.60$ Hz, 2 H), 1.74-1.66 (m, 2 H), 1.49-1.42 (m, 2 H), 0.97 (t, $J = 7.40$ Hz, 3 H). ^{13}C NMR (125 MHz, CDCl_3): δ 166.10, 148.46, 141.56, 140.59, 128.59, 124.15, 122.61, 64.90, 30.68, 19.14, 13.70. FTIR (cm^{-1}): 2958, 2875, 1709, 1642, 1602, 1518, 1459, 1412, 1343, 1308, 1176, 1109, 982, 845, 759, 717, 673.



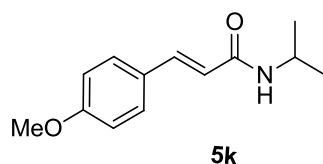
(*E*)-3-(4-Acetylphenyl) acrylic acid *n*-butyl ester **5h**: ^1H NMR (500 MHz, CDCl_3): δ 7.97 (d, $J = 8.25$ Hz, 2 H), 7.69 (d, $J = 16.05$ Hz, 1 H), 7.61 (d, $J = 8.25$ Hz, 2 H), 6.53 (d, $J = 16.0$ Hz, 1 H), 4.22 (t, $J = 6.80$ Hz, 2 H), 2.61 (s, 3 H), 1.71-1.67 (m, 2 H), 1.44-1.40 (m, 2 H), 0.97 (t, $J = 7.20$ Hz, 3 H). ^{13}C NMR (125 MHz, CDCl_3): δ 197.28, 166.55, 142.93, 138.80, 137.94, 128.81, 128.08, 120.82, 64.65, 30.70, 26.64, 19.15, 13.70. FTIR (cm^{-1}): 2960, 1711, 1683, 1637, 1604, 1562, 1465, 1409, 1358, 1310, 1262, 1204, 1170, 1116, 1063, 1014, 981, 826, 738.



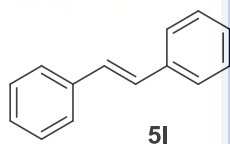
(*E*)-*N*-Isopropyl-cinnamamide **5i**: ^1H NMR (500 MHz, CDCl_3): δ 7.61 (d, $J = 15.65$ Hz, 1 H), 7.48-7.47 (m, 2 H), 7.34-7.33 (m, 3 H), 6.38 (d, $J = 15.50$ Hz, 1 H), 5.63 (br.s, 1 H), 4.25-4.19 (m, 1 H), 1.22 (d, $J = 6.35$ Hz, 6 H). ^{13}C NMR (125 MHz, CDCl_3): δ 164.97, 140.62, 134.91, 129.49, 128.74, 127.68, 121.06, 41.54, 22.81. FTIR (cm^{-1}): 3061, 2971, 2927, 2873, 2359, 1951, 1880, 1653, 1616, 1558, 1446, 1331, 1225, 1167, 976, 862, 767, 666, 523.



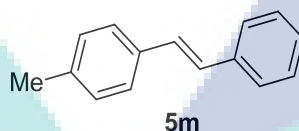
(*E*)-*N*-Isopropyl-3-(*p*-tolyl) acrylamide **5j**: ^1H NMR (500 MHz, CDCl_3): δ 7.58 (d, $J = 15.55$ Hz, 1 H), 7.39 (d, $J = 8.0$ Hz, 2 H), 7.16 (d, $J = 7.85$ Hz, 2 H), 6.31 (d, $J = 15.55$ Hz, 1 H), 5.46 (br. s, 1 H), 4.25-4.19 (m, 1 H), 2.35 (s, 3 H), 1.21 (d, $J = 6.50$ Hz, 6 H). ^{13}C NMR (125 MHz, CDCl_3): δ 165.18, 140.66, 139.80, 132.18, 129.52, 127.70, 120.01, 41.53, 22.88, 21.39. FTIR (cm^{-1}): 3067, 2969, 2873, 1652, 1616, 1545, 1456, 1384, 1245, 1170, 1010, 975, 863, 783, 676, 555.



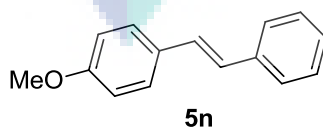
(*E*)-*N*-Isopropyl-3-(4-methoxyphenyl) acrylamide **5k**: ^1H NMR (500 MHz, CDCl_3): δ 7.56 (d, $J = 15.55$ Hz, 1 H), 7.43 (d, $J = 8.75$ Hz, 2 H), 6.87 (d, $J = 8.70$ Hz, 2 H), 6.25 (d, $J = 15.65$ Hz, 1 H), 5.56 (br. s, 1 H), 4.22-4.16 (m, 1 H), 3.81 (s, 3 H), 1.21 (d, $J = 6.75$ Hz, 6 H). ^{13}C NMR (125 MHz, CDCl_3): δ 165.31, 160.72, 140.22, 129.20, 127.63, 118.70, 114.17, 55.30, 41.45, 22.84. FTIR (cm^{-1}): 3293, 3062, 2974, 2837, 2049, 1890, 1651, 1604, 1539, 1459, 1361, 1179, 1029, 973, 826, 711, 659, 551.



(*E*)-Stilbene **5l**: ^1H NMR (500 MHz, CDCl_3): δ 7.53-7.52 (m, 4 H), 7.38-7.35 (m, 4 H), 7.28-7.23 (m, 2 H), 7.12 (d, $J = 3.45$ Hz, 2 H). ^{13}C NMR (125 MHz, CDCl_3): δ 137.31, 128.66, 127.60, 126.50. FTIR (cm^{-1}): 3078, 3059, 3020, 1637, 1577, 1495, 1451, 1072, 962, 764, 692, 540, 525, 468.

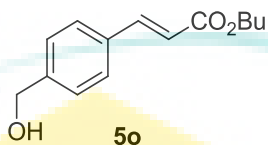


(*E*)-4-Methylstilbene **5m**: ^1H NMR (500 MHz, CDCl_3): δ 7.43 (d, $J = 8.10$ Hz, 2 H), 7.35 (d, $J = 7.50$ Hz, 2 H), 7.34 (t, $J = 8.0$ Hz, 2 H), 7.27-7.23 (m, 1 H), 7.17 (d, $J = 8.50$ Hz, 2 H), 6.99 (d, $J = 8.05$ Hz, 2 H), 2.28 (s, 3 H). ^{13}C NMR (125 MHz, CDCl_3): δ 137.51, 134.54, 129.38, 128.64, 127.69, 127.39, 126.38, 21.24. FTIR (cm^{-1}): 3080, 3054, 3022, 2920, 2363, 1949, 1817, 1600, 1495, 1448, 1090, 965, 903, 783, 748, 694, 520.

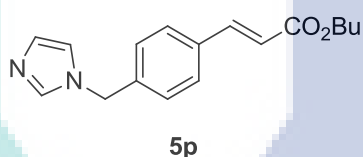


(*E*)-4-Methoxystilbene **5n**: ^1H NMR (500 MHz, CDCl_3): δ 7.50-7.43 (m, 4 H), 7.35 (t, $J = 7.50$ Hz, 2 H), 7.27-7.22 (m, 1 H), 7.07 (d, $J = 16.05$ Hz, 1 H), 6.70 (d, $J = 16.05$ Hz,

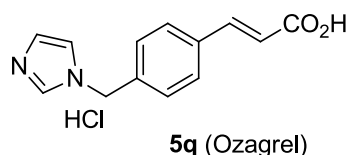
1 H), 6.90 (d, $J = 7.50$ Hz, 2 H), 3.82 (s, 3 H). ^{13}C NMR (125 MHz, CDCl_3): δ 159.33, 137.67, 128.66, 128.23, 127.73, 127.23, 126.64, 126.26, 114.16, 55.34. FTIR (cm^{-1}): 3002, 2963, 2934, 1892, 1660, 1509, 1487, 1302, 1247, 1179, 1110, 1030, 967, 812, 751, 688, 538, 502.



(*E*)-4-(Hydroxymethyl) cinnamic acid butyl ester **5o**: ^1H NMR (400 MHz, CDCl_3): δ 7.63 (d, $J = 16.0$ Hz, 1H), 7.47 (d, $J = 8.20$ Hz, 2H), 7.35 (d, $J = 8.16$ Hz, 2H), 6.39 (d, $J = 16.0$ Hz, 1H), 4.66 (s, 2H), 4.19 (t, $J = 6.68$ Hz, 2H), 2.03 (s, 1H), 1.72-1.64 (m, 2H), 1.47-1.42 (m, 2H), 0.97 (t, $J = 7.36$ Hz, 3H). ^{13}C NMR (100 MHz, CDCl_3): δ 167.35, 144.35, 143.47, 133.52, 128.21, 127.21, 117.93, 64.53, 30.74, 19.19, 13.75. FTIR (cm^{-1}): 3399, 2958, 2872, 1702, 1634, 1459, 1415, 1385, 1313, 1278, 1171, 1022, 983, 819.



(*E*)-Butyl 3-(4-((1*H*-imidazol-1-yl)methyl)phenyl) acrylate **5p**: ^1H NMR (500 MHz, CDCl_3): δ 7.66 (d, $J = 16.05$ Hz, 1H), 7.55 (s, 1H), 7.51 (d, $J = 8.20$ Hz, 2H), 7.16 (d, $J = 8.20$ Hz, 2H), 7.10 (s, 1H), 6.90 (s, 1H), 6.44 (d, $J = 16.0$ Hz, 1H), 5.14 (s, 2H), 4.21 (t, $J = 6.65$ Hz, 2H), 1.71-1.67 (m, 2H), 1.46-1.42 (m, 2H), 0.96 (t, $J = 7.40$ Hz, 3H). ^{13}C NMR (125 MHz, CDCl_3): δ 166.89, 143.50, 138.23, 137.46, 134.52, 129.97, 128.59, 127.67, 119.28, 119.0, 64.54, 50.41, 30.74, 19.18, 13.74. FTIR (cm^{-1}): 3416, 2958, 2872, 1704, 1634, 1611, 1459, 1417, 1384, 1313, 1276, 1170, 1119, 1021, 983, 819.



(*E*)-Butyl 3-(4-((1*H*-imidazol-1-yl) methyl) phenyl) acrylate hydrochloride **5q** (Ozagrel): ^1H NMR (400 MHz, DMSO- d_6): δ 12.62 (br. s, 1H), 9.44 (s, 1H), 7.85 (s, 1H), 7.75 (m, 3H), 7.60 (d, $J = 16.20$ Hz, 1H), 7.56-7.46 (m, 2H), 6.60 (d, $J = 16.04$ Hz, 1H), 5.51 (s, 2H). ^{13}C NMR (100 MHz, DMSO- d_6): δ 167.36, 143.0, 137.0, 135.37, 134.49, 128.68, 121.97, 120.09, 51.09. FTIR (cm^{-1}): 3158, 3074, 1696, 1677, 1630, 1427, 1316, 1285, 1093, 950, 819, 697, 620, 542, 493.

4.4.4 Recycling of Pd(II) Complex **3**

The recycling and reusability of catalysts are significantly important from the economic and environmental perspectives. Thus, this study focused on the recovery and reusability of the bio-waste corn-cob cellulose-supported Pd(II) complex **3** (Table 4.5, entry 7), using 4-iodoacetophenone with butyl acrylate (Figure 4.24). After completing the reactions, the bio-waste corn-cob cellulose-supported Pd(II) complex **3** was separated from the reaction mixture using a filter paper and washed with ethyl acetate. The corn-cob cellulose-supported solid Pd(II) complex **3** was dried under reduced pressure and reused in the next run under the same reaction conditions.

The corn-cob cellulose-supported Pd(II) complex **3** was consecutively used for seven cycles without a significant reduction of catalytic activity. A slight loss of catalytic activity of Pd(II) complex **3** was observed after five cycles due to the loss of Pd(II) complex during the separation process. The (HR-TEM) image of recovered Pd(II) complex **3** was also investigated and presented in Figure 4.5(b). The HR-TEM micrograph showed that the Pd(II) complex **3** was still well distributed in the recovered Pd(II) complex **3** and did not aggregate during the reaction progress. Therefore, it is realistic that the corn-cob cellulose-supported Pd(II) complex **3** can be used several times for large-scale production in the Mizoroki-Heck coupling reaction and still keep its full catalytic performance.

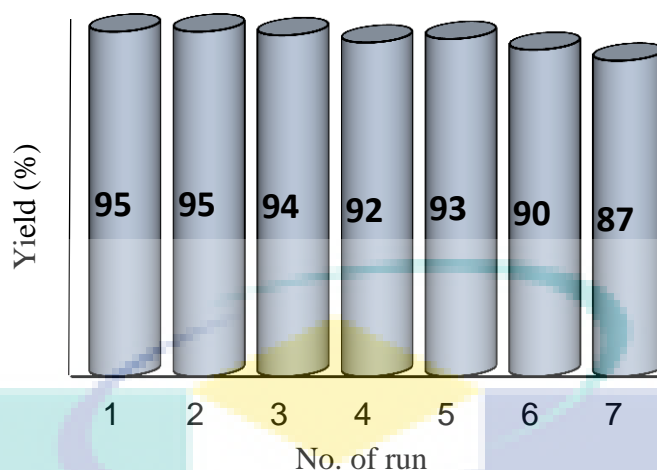


Figure 4.24 Mizoroki- Heck reaction using recycled Pd(II) complex **3**.

4.4.5 Hot Filtration or Heterogeneity Test of Pd(II) Complex **3**

During the reaction progress, the heterogeneity of catalyst is another important issue. To investigate the heterogeneity of the Pd(II) complex **3**, hot filtration experiment was performed (Figure 4.25). To realize the heterogeneity of Pd(II) complex **3**, the Mizoroki-Heck reaction of 4-iodotoluene with methyl acrylate was investigated. After 1 h of the reaction progress, the reaction mixture was filtrated on a glass filter at hot condition and the filtrate was reheated under the same reaction conditions for another 5 h and monitored the product yield. However, it was observed that no reaction was further preceded at all and 4-iodotoluene remained almost unreacted in the reaction mixture.

The ICP-AES analysis of the filtrate also revealed that no palladium species were leached out into the filtrate. Thus, it is clear to demand that the Mizoroki-Heck cross-coupling reactions were forwarded under heterogeneous conditions.

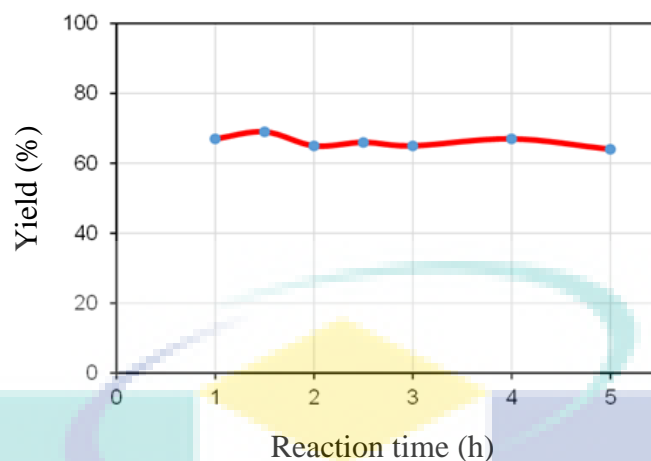


Figure 4.25 Hot filtration or heterogeneity test (according to Table 4.5, entry 3).

4.4.6 Corn-Cob Cellulose Supported Poly(amidoxime) Cu(II) Complex **4** Catalyzed Click Reaction

The reactivity of the bio-waste corn-cob cellulose-supported poly(amidoxime) Cu(II) complex **4** was investigated in Click reaction of alkynes and aryl azides. Initially, the reaction between phenyl acetylene and benzyl azide was taken as a model reaction to optimize the reaction conditions. Here, water was used as a reaction medium and in this experiment, showed that it is the most available, safe and economical solvent. To get an optimized reaction conditions, the reactions were carried out using different mol% of poly(amidoxime) Cu(II) complex **4**, reaction time, and temperature. The results of the optimization reactions were represented in Table 4.8. The initial reaction was carried out with phenyl acetylene and benzyl azide at 80 °C for 3 h in the presence of 5 mol% of aqueous solution of sodium ascorbate without adding of Cu(II) complex **4** which, provided **6a** with 4.42% yield (entry 1). The second reaction was carried using 1 mol% of Cu(II) complex **4** with phenyl acetylene and benzyl azide at 50 °C for 2 h in the presence of 5 mol% aqueous solution of sodium ascorbate to give the desired triazole (**6a**) in 92% yield with TOF value 46 (entry 2). The triazole **6a** was obtained with 94% and 90% yields when the catalytic loading of Cu(II) complex **4** reduced from 0.5 mol% to 0.1 mol%, respectively and the TOF values were also increased (entries 3 and 4). After observing the high catalytic performance, the model reaction was carried using 0.05 mol% of Cu(II) complex **4** at 60 °C-100 °C (entries 5-9). From this optimization table, it can be seen that, the yield was not significantly improved when

the reaction was carried out at 80 °C to 100 °C using 0.05 mol% of Cu(II) complex **4** for 3 h. Thus, it would be assumed that the suitable temperature for this reaction would be 80 °C which provided 96% yield of the product (entry 7).

Table 4.8 Optimization of the Click reaction using phenyl acetylene and benzyl azide

Ph-C≡CH + Ph-CH₂-N₃ $\xrightarrow[\text{sodium ascorbate (5 mol\%)}]{\text{Cu(II) complex 4}}$ Ph-1,2,3-triazole-4-yl-CH₂-Ph (**6a**)

Entry	Cu(II) complex 4 (mol%)	Temp.(°C)	Time (h)	Yield (%)	TOF(h ⁻¹)
1	-	80	3	4.42 ^[a]	-
2	1	50	2	92	46
3	0.5	50	4.5	94	41
4	0.1	50	7	90	128
5	0.05	60	6	95	316
6	0.05	70	4.5	94	417
7	0.05	80	3	96	640
8	0.05	90	3	97	646
9	0.05	100	3	95	633

Reactions were carried out using 1 mmol of phenyl acetylene, 1.1 mmol of benzyl azide, catalytic amount Cu(II) complex **4** in 5 mol% of aqueous sodium ascorbate.

^[a]Reaction was carried out without using Cu(II) complex **4**.

Using the above optimized reaction conditions, the scope and the broad applicability of the Cu(II) complex **4** was investigated and the results are summarized in Table 4.9. When the reaction was carried out between phenyl acetylene and 4-methylbenzyl azide in the presence of 5 mol% of sodium ascorbate at 80 °C for 3 h, it produced triazole **6b** at 95% yield (entry 1). It should be noted that during the reaction time, sodium ascorbate reduced Cu(II) to Cu(I) and the color of the waste corn-cob cellulose-supported Cu(II) complex **4** was changed from green to yellow (Figure. 4.26).

Substituted alkyne such as 4-tolylacetylene reacted with benzyl azide and 1-azido-2-phenylethane smoothly to give the corresponding 1,4-disubstituted 1,2,3-triazoles **6c** and **6d** (entries 2 and 3) at 93% and 91% yields, respectively. Moreover, an aliphatic alkynol hex-5-yn-1-ol, smoothly reacted with naphthyl and benzyl azides to

give the corresponding 1,4-disubstituted 1,2,3-triazoles **6e**, **6f** and **6g** (entries 4, 5 and 6) at 88–90% yields. The cellulose-supported Cu(II) complex **4** also smoothly promoted the reaction of alkynes containing tertiary alcohol, amine, and acetal moieties with benzyl azide to give the corresponding products **6h**, **6i** and **6j** (entries 7, 8 and 9) at 89 – 91% yields.

Interestingly, the Cu(II) complex **4** did not affect the acetal, alcohol, and amine groups; as a result, they remained intact during the cyclization steps. Therefore, waste corn-cob cellulose-supported Cu(II) complex **4** is a functional group-tolerant catalyst which can be widely used in the Click reaction.

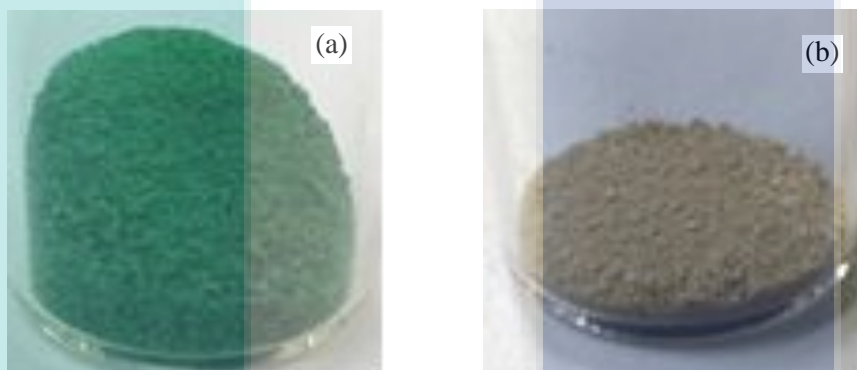
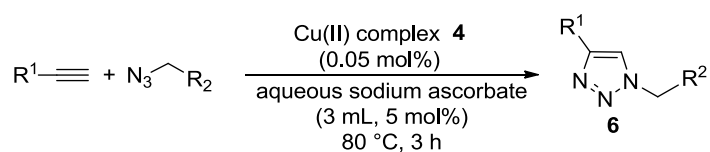
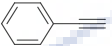
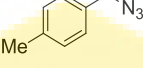
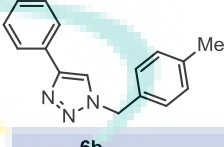

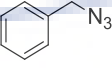
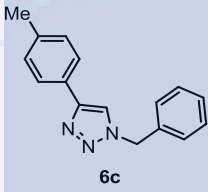

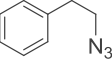
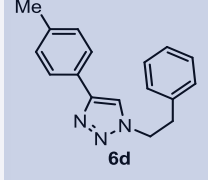
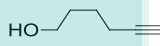
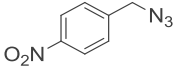
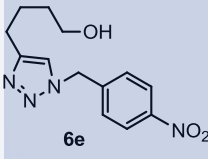
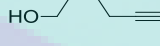
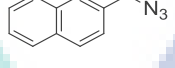
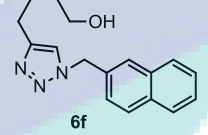

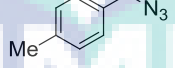
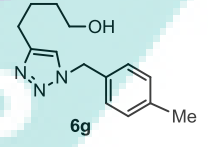
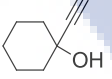
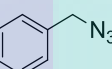
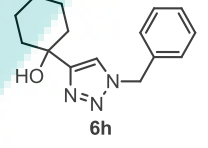
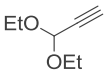
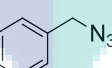
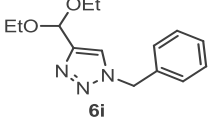
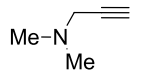
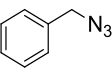
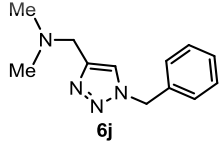


Figure 4.26 Photo images of (a) Cu(II) complex **4**, (b) after reduction of Cu(II) complex **4** using sodium ascorbate.

UMP

Table 4.9 Click reaction of organic azides and alkynes

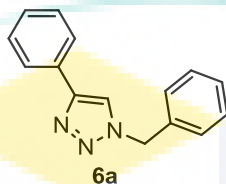


Entry	Alkyne	Organic azide	Product	Yield (%)
1				95
2				93
3				91
4				90
5				88
6				90
7				89
8				90
9				91

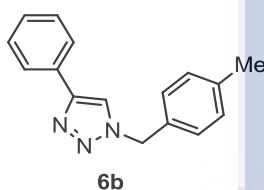
Reactions were carried out using 1 mmol of alkyne, 1.1 mmol of organic azide, 0.05 mol% of Cu(II) complex **4** in 5 mol% of aqueous sodium ascorbate (3 mL) at 80 °C for 3 h.

4.4.7 Characterization of Click Reaction Products

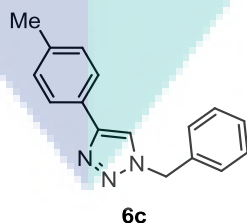
The Click reaction-prepared products were characterized using proton nuclear magnetic resonance (^1H NMR), carbon nuclear magnetic resonance (^{13}C NMR) and fourier transform infrared spectroscopy (FTIR) were described below:



1-Benzyl-4-phenyl-1*H*-1,2,3-triazole **6a**: ^1H NMR (500 MHz, CDCl_3): δ 5.59 (s, 2 H), 7.26-7.37 (m, 3 H), 7.38-7.42 (m, 5 H), 7.66 (s, 1 H), 7.81 (d, $J = 7.70$ Hz, 2 H). ^{13}C NMR (125 MHz, CDCl_3): δ 148.37, 134.82, 129.30, 128.20, 125.84, 119.60, 54.40. FTIR (cm^{-1}): 3122, 3053, 2925, 2858, 1481, 1457, 1434, 1336, 1226, 1196, 1077, 1053, 979, 913, 812, 769, 713, 708.

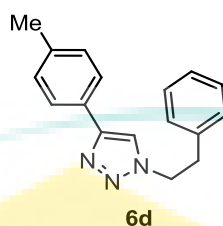


1-(4-Methylbenzyl)-4-phenyl-1*H*-1,2,3-triazole **6b**: ^1H NMR (500 MHz, CDCl_3): δ 2.35 (s, 3 H), 5.52 (s, 2 H), 7.18-7.22 (m, 4 H), 7.30-7.31 (m, 1 H), 7.38 (dd, $J = 1.85, 8.05$ Hz, 2 H), 7.63 (s, 1 H), 7.79 (d, $J = 7.0$ Hz, 2 H). ^{13}C NMR (125 MHz, CDCl_3): δ 148.12, 138.71, 131.61, 129.78, 128.75, 128.10, 125.65, 119.34, 54.01, 21.13. FTIR (cm^{-1}): 3080, 2922, 2857, 1624, 1534, 1450, 1354, 1228, 1072, 1045, 976, 928, 836, 752, 687.

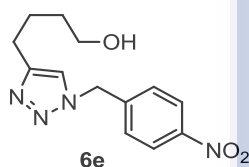


1-Benzyl-4-*p*-tolyl-1*H*-1,2,3-triazole **6c**: ^1H NMR (500 MHz, CDCl_3): δ 2.36 (s, 3 H), 5.56 (s, 2 H), 7.19 (d, $J = 7.90$ Hz, 2 H), 7.29-7.30 (m, 2 H), 7.36-7.41 (m, 3 H), 7.61 (s, 1 H), 7.69 (d, $J = 8.10$ Hz, 2 H). ^{13}C NMR (125 MHz, CDCl_3): δ 148.27, 137.97,

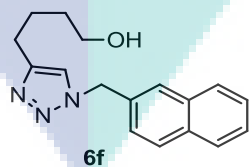
134.72, 129.42, 128.71, 128.02, 127.69, 125.57, 119.10, 54.16, 21.24. FTIR (cm⁻¹): 3145, 3027, 2928, 2853, 1745, 1499, 1452, 1356, 1211, 1136, 1057, 978, 828, 799, 726.



1-Phenethyl-4-*p*-tolyl-1*H*-1,2,3-triazole **6d**: ¹H NMR (500 MHz, CDCl₃): δ 2.36 (s, 3 H), 3.24 (t, *J* = 7.25 Hz, 2 H), 4.62 (t, *J* = 7.35 Hz, 2 H), 7.12 (d, *J* = 6.80 Hz, 2 H), 7.22 (d, *J* = 7.45 Hz, 2 H), 7.28-7.31 (m, 3 H), 7.42 (s, 1 H), 7.65 (d, *J* = 8.15 Hz, 2 H). ¹³C NMR (125 MHz, CDCl₃): δ 147.54, 137.90, 128.82, 128.71, 127.80, 127.10, 125.58, 119.54, 51.70, 36.80, 21.25. FTIR (cm⁻¹): 3110, 3025, 2932, 2860, 1644, 1492, 1459, 1363, 1219, 1085, 1043, 977, 912, 825, 726, 705.

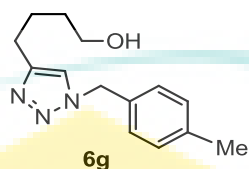


4-(1-(4-*p*-Nitrobenzyl)-1*H*-1,2,3-triazol-4-yl)butane-1-ol **6e**: ¹H NMR (500 MHz, CDCl₃): δ 1.61-1.71 (m, 2 H), 1.74-1.78 (m, 3 H), 2.76 (t, *J* = 7.45 Hz, 2 H), 3.67 (t, *J* = 6.30 Hz, 2 H), 5.61 (s, 2 H), 7.29 (s, 1 H), 7.38 (d, *J* = 8.60 Hz, 2 H), 8.23 (d, *J* = 8.55 Hz, 2 H). ¹³C NMR (125 MHz, CDCl₃): δ 149.0, 147.9, 141.9, 128.4, 124.2, 120.8, 62.3, 52.9, 32.0, 25.4, 25.2. FTIR (cm⁻¹): 3368, 3134, 3071, 2930, 2857, 1607, 1522, 1455, 1348, 1218, 1053, 852, 801, 727.

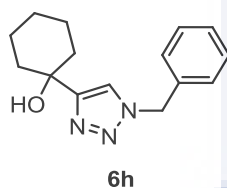


4-(1-((Naphthalen-3-yl)methyl)-1*H*-1,2,3-triazol-4-yl)butan-1-ol **6f**: ¹H NMR (500 MHz, CDCl₃): δ 1.58-1.64 (m, 3 H), 1.70-1.76 (m, 2 H), 2.72 (t, *J* = 7.45 Hz, 2 H), 3.65 (t, *J* = 6.35 Hz, 2 H), 5.64 (s, 2 H), 7.22 (d, *J* = 8.50 Hz, 1 H), 7.33 (d, *J* = 8.50 Hz, 1 H), 7.50 (d, *J* = 8.50 Hz, 2 H), 7.73 (dd, *J* = 3.40, 6.45 Hz, 1 H), 7.81-7.85 (m, 3 H). ¹³C

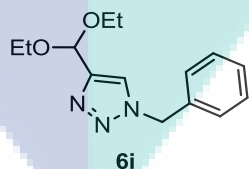
NMR (125 MHz, CDCl₃): δ 148.54, 133.20, 132.22, 127.77, 125.33, 120.65, 62.45, 54.22, 32.13, 25.46, 25.31. FTIR (cm⁻¹): 3446, 3395, 3116, 3053, 2935, 2853, 1645, 1546, 1516, 1467, 1339, 1213, 1136, 1058, 999, 864, 825, 784, 756.



4-(1-(4-Methylbenzyl)-1*H*-1,2,3-triazol-4-yl) butan-1-ol **6g**: ¹H NMR (500 MHz, CDCl₃): δ 1.58-1.70 (m, 2 H), 1.71-1.76 (m, 2 H), 2.02 (br. s, 1 H), 2.34 (s, 3 H), 2.71 (t, J = 7.45 Hz, 2 H), 3.65 (t, J = 7.0 Hz, 2 H), 5.43 (s, 2 H), 7.14-7.27 (m, 5 H). ¹³C NMR (125 MHz, CDCl₃): δ 148.37, 138.52, 131.80, 129.68, 128.01, 120.44, 62.31, 53.78, 32.11, 25.47, 21.10. FTIR (cm⁻¹): 3445, 3406, 3107, 3063, 2925, 2869, 1646, 1558, 1519, 1431, 1335, 1213, 1122, 1045, 990, 865, 778, 674.

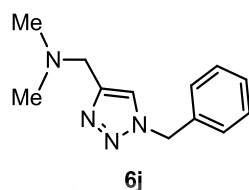


1-(1-Benzyl-1*H*-1,2,3-triazol-4-yl) cyclohexanol **6h**: ¹H NMR (500 MHz, CDCl₃): δ 1.24-1.33 (m, 1 H), 1.53-2.04 (m, 9 H), 2.24 (br. s, 1 H), 5.50 (d, J = 7.85 Hz, 2 H), 7.24 (d, J = 7.95 Hz, 2 H), 7.32-7.36 (m, 4 H). ¹³C NMR (125 MHz, CDCl₃): δ 156.03, 134.64, 129.07, 128.08, 119.35, 69.54, 54.10, 38.07, 25.31, 21.91. FTIR (cm⁻¹): 3393, 3136, 2931, 2855, 1643, 1492, 1456, 1347, 1251, 1216, 1157, 1054, 973, 907, 805, 728.



1-Benzyl-4-(diethoxymethyl)-1*H*-1,2,3-triazole **6i**: ¹H NMR (500 MHz, CDCl₃): δ 1.22 (t, J = 7.15 Hz, 6 H), 3.59 (q, J = 7.50 Hz, 2 H), 3.65 (q, J = 7.50 Hz, 2 H), 5.51 (s, 2 H), 5.69 (s, 1 H), 7.26 (dd, J = 7.40, 2.25 Hz, 2 H), 7.30-7.37 (m, 3 H), 7.50 (s, 1 H). ¹³C NMR (125 MHz, CDCl₃): δ 147.55, 134.46, 129.08, 128.72, 128.13, 121.77, 96.82, 61.64, 54.15, 15.10. FTIR (cm⁻¹): 3136, 2973, 2883, 1695, 1533, 1456, 1387, 1223,

1153, 1125, 1056, 912, 798, 766, 728.



(1-Benzyl-1*H*-1, 2, 3-triazol-4-yl)-*N*, *N*-dimethylmethanamine **6j**: ¹H NMR (500 MHz, CDCl₃): δ 2.25 (s, 6 H), 3.57 (s, 2 H), 5.51 (s, 2 H), 7.26 (d, *J* = 7.40 Hz, 2 H), 7.34-7.37 (m, 3 H), 7.38 (s, 1 H). ¹³C NMR (125 MHz, CDCl₃): δ 145.77, 134.67, 129.06, 128.67, 128.06, 122.20, 54.47, 54.10, 45.17. FTIR (cm⁻¹): 3138, 3077, 2949, 2864, 2827, 2773, 1647, 1453, 1329, 1256, 1217, 1177, 1122, 1046, 1213, 1176, 1124, 1042, 845, 801, 726.

4.4.8 Recycling Test of Cu(II) Complex **4**

The recyclability, reusability, and selectivity of the cellulose-supported Cu(II) complex catalyst are important issues from the environmental and economical points of view. Therefore, this research focused on the recovery and reusability of the bio-waste corn-cob cellulose-supported Cu(II) complex **4** using phenyl acetylene with benzyl azide under optimized reaction conditions (Figure 4.27). After completing the reactions, it was cooled to room temperature and Cu(II) complex **4** was separated from the reaction mixture (yellow color) using filter paper; washed with ethyl acetate, water, and methanol; dried at 80 °C and reused for the next run without changing the reaction conditions. The corn-cob cellulose-supported Cu(II) complex **4** was consecutively used six cycles without a significant reduction in its catalytic activity. The catalytic activity of the Cu(II) complex **4** was slightly decreased after the fourth cycles due to the loss of Cu(II) complex **4** during the separation process.

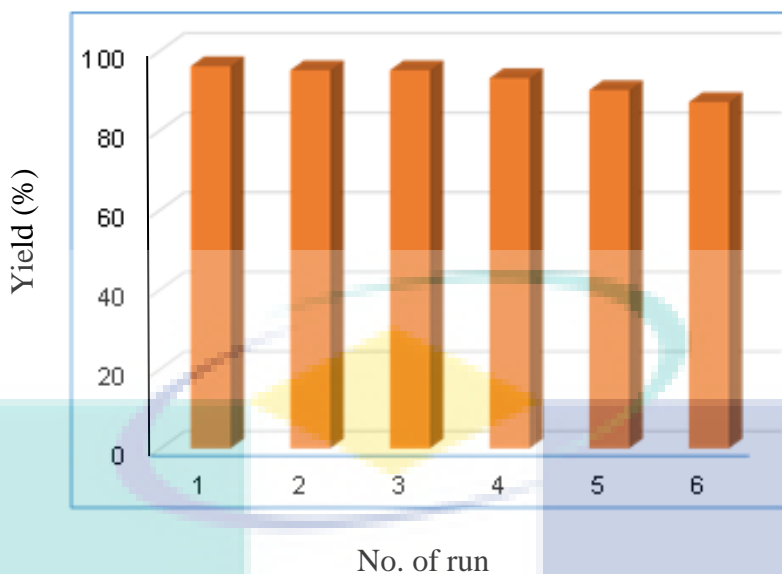


Figure 4.15 Recycling of the Cu(II) complex **4**.

4.4.9 Hot Filtration or Heterogeneity Test of Cu(II) Complex **4**

Checking for the leaching of copper species from the supported Cu(II) complex **4** into the aqueous solution is another important task. To investigate the heterogeneity of the Cu(II) complex **4**, hot filtration experiment was performed (Figure 4.28). To figure out whether the reaction proceeds under a heterogeneous condition or not, the Click reaction between phenyl acetylene and benzyl azide in the presence of Cu(II) complex **4** under the optimized reaction conditions was performed. After 1 h, the reaction mixture was filtered and the solid catalyst was separated using filter paper at hot condition. The filtrate was again, heated under the same reaction conditions for another 4 h. It was observed that no reaction proceeded and the phenyl acetylene remained almost unreacted in the reaction mixture, suggesting that the supported catalyst showed a heterogeneous character. The ICP-AES analysis of the filtrate also showed that no copper species leached out into the aqueous solution.

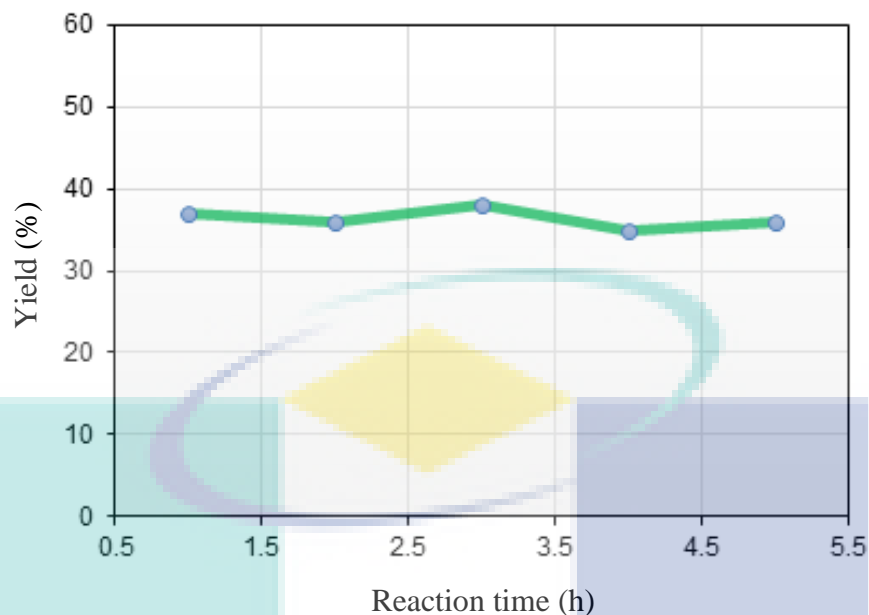


Figure 4.28 Hot filtration of Cu(II) complex **4**.

4.4.10 Copper Nanoparticles (CuNP@PA) Catalyzed Aza-Michael Reaction

The *N*-alkylation or Aza-Michael reaction is a very important reaction in synthetic organic chemistry for the C-N bond formation. The copper nanoparticles (CuNP@PA) was utilized for a C-N bond formation which is readily prepared by the reduction of Cu(II) complex **4** in the presence of hydrazine. The Aza-Michael reaction of amines with α , β -unsaturated compounds was considered for the investigation of the catalytic performance of the CuNP@PA. The CuNP@PA was found to work well and the optimum reaction condition was determined. For the optimization, the addition reaction between piperidine and butyl acrylate was chosen as a model reaction to evaluate the catalytic activity of CuNP@PA. Table 4.10 presents the results of the effect of catalyst concentration and reaction time. The initial reaction was carried out using 0.1 mol% of CuNP@PA in methanol at room temperature.

The CuNP@PA efficiently forwarded the reaction to give the corresponding addition product **7a** with 95% yield within 1.5 h (entry 1). The reaction completion time was found to be increased to 3 h when 0.05 mol% of CuNP@PA was used (entry 2). When the loading of CuNP@PA was further decreased (0.02 - 0.01 mol%), it took a longer time to complete the reaction (entries 3 and 4). The CuNP@PA loading can be reduced to 0.005 mol%, which also efficiently promoted this addition reaction. For each

entry, the TOF of the **CuNP@PA** was calculated and the highest value was obtained when 0.005 mol% **CuNP@PA** was used (entry 5). It should be noted that the *N*-alkylation reaction was also carried out using **2** and **4** which gave only 12% and 19% yield of **7a**, respectively (entries 6 and 7).

Table 4.10 Optimization of the Aza-Michael reaction

C1CCNCC1 + CH2=CHCO2Bu $\xrightarrow[\text{MeOH, r.t.}]{\text{CuNP@PA}}$ C1CCN(CC(=O)OCC)CC1

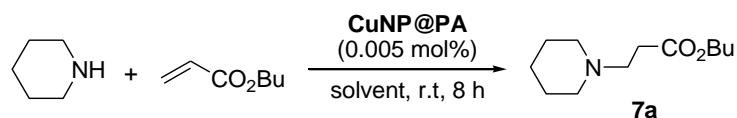
7a

Entry	Catalyst	Time (h)	Yield (%)	TOF (h ⁻¹)
1	0.1 mol% (20 mg) CuNP@PA	1.5	95	633
2	0.05 mol% (10 mg) CuNP@PA	3	93	620
3	0.02 mol% (4 mg) CuNP@PA	4.5	92	1022
4	0.01 mol% (2 mg) CuNP@PA	5.5	93	1690
5	0.005 mol% (1 mg) CuNP@PA	8	90	2250
6	Poly(amidoxime) 2 (1 mg)	8	12	-
7	Cu(II) complex 4 (1 mg)	8	19	-

Reactions were carried out using 10 mmol of piperidine, 11 mmol of butyl acrylate, and catalytic amount of **CuNP@PA** in 4.5 mL MeOH at room temperature.

Furthermore, after getting the suitable conditions (0.005 mol% **CuNP@PA**, 8 h, and room temperature), the solvent effect was determined in this catalytic system. At first, the blank experiment (without **CuNP@PA**) was carried in MeOH at room temperature which provided only 23% yield of the product (Table 4.11, entry 1). When the reactions were carried out in polar aprotic solvent i.e. ethyl acetate and dimethylformamide (DMF), the reaction was forwarded with 27-32% yield of the product entries (2 & 3). However, the yield was not significantly increased when the reactions were carried in hexane, diethyl ether, and tetrahydrofuran (THF), (entries 4-6).

Table 4.11 Effect of solvent on the Aza-Michael reaction



Entry	Solvent	Yield (%)	TOF (h ⁻¹)
1	MeOH	23 ^[a]	-
2	ethyl acetate	27	675
3	DMF	32	800
4	hexane	18	450
5	diethyl ether	22	550
6	THF	25	625

Reactions were carried out using 10 mmol of piperidine, 11 mmol of butyl acrylate, and 1 mg of **CuNP@PA** in different solvent at room temperature. ^[a]Reaction was carried out without using **CuNP@PA**.

4.4.11 Aza-Michael Reaction of Aliphatic Amines with Olefins

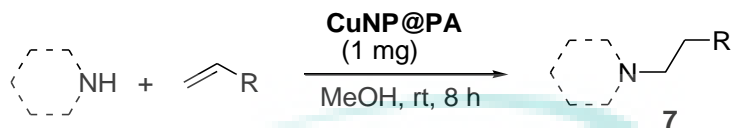
After establishing the optimized condition, the scope of the Aza-Michael reaction was explored. The acceptability of the cellulose-supported copper nanoparticles catalyst depends on the large scale of its application. Thus, we concentrated our attention on using 0.005 mol% (1 mg) of **CuNP@PA** at room temperature for 8 h.

The α, β -unsaturated carbonyl compound methyl acrylate, was found to smoothly forward the Aza-Michael reaction with a secondary aliphatic amine such as dibutylamine, piperidine, morpholine, cyclohexyl amine, and even sterically hindered secondary dibenzylamine to give the corresponding products **7b-f** in up to 95% yields (Table 4.12, entries 1-5). In addition, the Michael acceptor butyl acrylate also strongly combined with different types of amines to give alkylated products **7g-k** at 88-95% yields (entries 6-10).

Moreover, it was noticed that the cellulose-supported **CuNP@PA** efficiently promoted the addition reaction of α, β -unsaturated acrylonitrile with a variety of

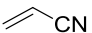
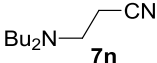
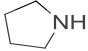
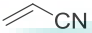
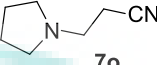

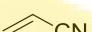
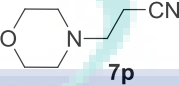

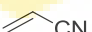
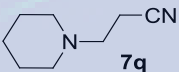
aliphatic amines to give the corresponding products **7l-q** at up to 92% yield (entries 11-16).

Table 4.12 Aza-Michael reaction with olefins^[a]



Entry	Amin	Olefin	Product	Yield (%)
1	Bu ₂ NH		 7b	93
2			 7c	95
3			 7d	93
4 ^[b]			 7e	88
5			 7f	94
6			 7g	95
7 ^[c]	H ₂ NCH ₂ CH ₂ NH ₂		 7h	88
8			 7i	92
9			 7j	93
10	Bu ₂ NH		 7k	93
11			 7l	92
12 ^[c]	H ₂ NCH ₂ CH ₂ NH ₂		 7m	87

Table 4.12 Continued

Entry	Amin	Olefin	Product	Yield (%)
13	Bu ₂ NH		 7n	90
14			 7o	88
15			 7p	92
16			 7q	90

^[a]Reactions were carried out using 10 mmol of amine, 11 mmol of α , β -unsaturated compounds, and **CuNP@PA** (1 mg) in 4.5 mL MeOH at room temperature for 8 h. ^[a] 2.2 mmol of α , β -unsaturated compound was used. ^[b] 2.2 mmol of α , β -unsaturated compound was used. ^[c] 4.4 mmol of α , β -unsaturated compound was used.

Recently, Reddy & Kumar (2006) carried out Aza-Michael reaction of aliphatic amine using microcrystalline cellulose-supported copper nanoparticles. According to their report, the amount of catalyst loading was 3.6 mol% and obtained almost similar results. However, in this study, only 0.005 mol% of the cellulose-supported poly(amidoxime) copper nanoparticles **CuNP@PA** was used, which is seven hundred twenty times lower catalyst loading. Therefore, the waste corn-cob cellulose-supported poly(amidoxime) copper nanoparticles catalyst exhibited a better performance than the reported catalyst.

The chemoselectivity of catalysts plays an important role in transformation reactions. To investigate the chemoselectivity of **CuNP@PA**, a mixture of aniline and dibenzylamine were subjected to butyl acrylate (4 mmol) using 0.01 mol% of **CuNP@PA**. It was fascinating that aniline did not undergo this reaction rather, only the *N*-alkylation adduct of dibenzylamine was obtained exclusively (Figure 4.29). It definitely demonstrated the chemoselectivity of aliphatic amines versus aromatic amines towards **CuNP@PA**. The less reactivity of aromatic amines is the cause of this selectivity and therefore, this selectivity could be functional to differentiate between the two types of amines for synthetic applications.

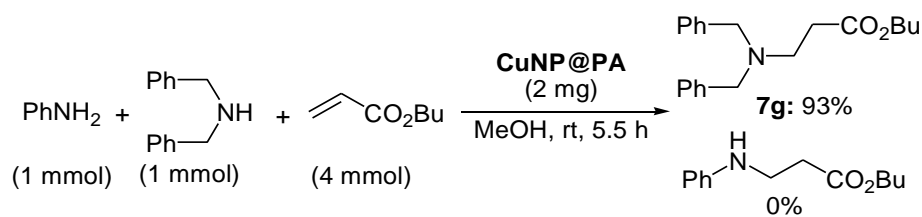
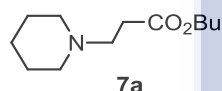


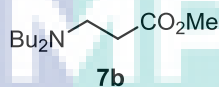
Figure 4.29 Chemoselective Aza-Michael reaction.

4.4.12 Characterization of Aza-Michael Reaction Products

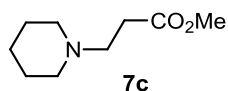
The Aza-Michael reaction-prepared products were characterized using proton nuclear magnetic resonance (^1H NMR), carbon nuclear magnetic resonance (^{13}C NMR) and Fourier transform infrared spectroscopy (FTIR) were described below.



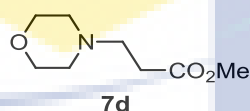
Butyl 3-(piperidin-1-yl) propanoate **7a**: ^1H NMR (500 MHz, CDCl_3): δ 4.02 (t, $J = 6.65$ Hz, 2H), 2.60 (t, $J = 7.65$ Hz, 2H), 2.44 (t, $J = 7.80$ Hz, 2H), 2.43-2.34 (m, 4H), 1.55-1.49 (m, 6H), 1.34-1.30 (m, 4H), 0.89 (t, $J = 7.35$ Hz, 3H). ^{13}C NMR (125 MHz, CDCl_3): δ 171.73, 63.18, 53.31, 53.25, 31.31, 29.70, 23.30, 18.13, 12.67. FTIR (cm^{-1}): 3368, 2953, 2871, 2685, 2557, 1735, 1580, 1449, 1382, 1216, 1152, 1078, 962, 855, 798.



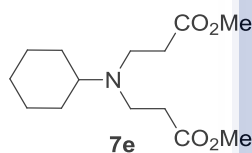
Methyl 3-(dibutylamino) propanoate **7b**: ^1H NMR (500 MHz, CDCl_3): δ 3.63 (s, 3H), 2.75-2.70 (m, 2H), 2.41-2.32 (m, 6H), 1.37-1.21 (m, 8H), 0.88 (t, $J = 7.30$ Hz, 6H). ^{13}C NMR (125 MHz, CDCl_3): δ 172.94, 53.39, 51.07, 49.14, 32.03, 29.04, 20.32, 13.73. FTIR (cm^{-1}): 3777, 3398, 2955, 2873, 2814, 2369, 1738, 1578, 1465, 1379, 1202, 1068, 935, 884, 787, 738.



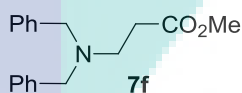
Methyl 3-(piperidin-1-yl) propanoate **7c**: ^1H NMR (500 MHz, CDCl_3): δ 3.63 (s, 3H), 2.62 (t, $J = 6.65$ Hz, 2H), 2.48 (t, $J = 7.80$ Hz, 2H), 2.37-2.35 (m, 4H), 1.56-1.51 (m, 4H), 1.41-1.37 (m, 2H). ^{13}C NMR (125 MHz, CDCl_3): δ 173.05, 54.11, 53.07, 51.47, 31.84, 25.74, 24.11. FTIR (cm^{-1}): 2956, 2871, 2561, 2365, 1736, 1581, 1520, 1452, 1384, 1216, 1154, 1084, 963, 855.



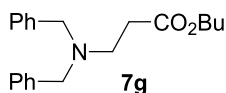
Methyl 3-morpholinopropanoate **7d**: ^1H NMR (500 MHz, CDCl_3): δ 3.69 (t, $J = 5.95$ Hz, 7H), 2.69-2.66 (m, 2H), 2.52-2.45 (m, 6H). ^{13}C NMR (125 MHz, CDCl_3): δ 172.27, 66.38, 53.50, 52.96, 51.12, 31.40. FTIR (cm^{-1}): 3383, 2960, 2873, 2819, 2366, 1826, 1736, 1577, 1454, 1378, 1305, 1267, 1203, 983, 915, 864, 782.



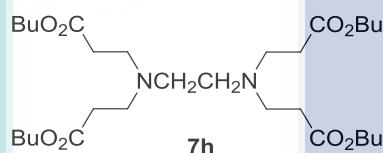
Dimethyl 3,3'-(cyclohexylazanediyl) dipropanoate **7e**: ^1H NMR (500 MHz, CDCl_3): δ 3.50 (s, 6H), 2.63 (t, $J = 7.15$ Hz, 3H), 2.27 (t, $J = 7.15$ Hz, 4H), 1.62-1.44 (m, 6H), 1.07-0.91 (m, 6H). ^{13}C NMR (125 MHz, CDCl_3): δ 173.05, 172.94, 68.77, 53.40, 53.39, 52.25, 51.08, 51.07, 49.85, 49.15, 32.03, 29.04, 20.32, 13.73. FTIR (cm^{-1}): 2927, 2853, 1734, 1435, 1321, 1251, 1194, 1171, 1127, 1046, 993, 891, 840, 705, 602.



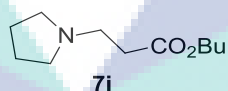
Methyl 3-(dibenzylamino) propanoate **7f**: ^1H NMR (500 MHz, CDCl_3): δ 7.41-7.28 (m, 10H), 3.67 (dd, $J = 4.45$ Hz, 7H), 2.89-2.84 (m, 2H), 2.58-2.55 (m, 2H). ^{13}C NMR (125 MHz, CDCl_3): δ 172.25, 138.91, 128.39, 127.81, 126.58, 57.67, 50.87, 48.76, 32.24. FTIR (cm^{-1}): 3030, 2804, 2366, 1955, 1717, 1569, 1503, 1451, 1380, 1193, 1126, 1074, 1025, 978, 917, 865.



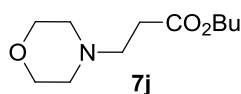
Butyl 3-(dibenzylamino) propanoate **7g**: ^1H NMR (500 MHz, CDCl_3): δ 7.45-7.38 (m, 8H), 7.32 (t, $J = 7.20$, Hz, 2H), 4.15 (t, $J = 6.75$ Hz, 2H), 3.67 (s, 4H), 2.93 (t, $J = 7.15$ Hz, 2H), 2.61 (t, $J = 7.15$ Hz, 2H), 1.66-1.62 (m, 2H), 1.45-1.42 (m, 2H), 1.03 (t, $J = 7.40$ Hz, 3H). ^{13}C NMR (125 MHz, CDCl_3): δ 172.30, 139.20, 128.68, 128.08, 126.83, 64.01, 57.04, 49.17, 32.71, 30.52, 19.03, 13.63. FTIR (cm^{-1}): 3032, 2963, 2880, 2802, 2369, 1955, 1730, 1494, 1453, 1369, 1243, 1182, 1125, 1070, 1027, 975, 912, 889, 740.



Tetrabutyl 3,3',3'',3'''-(ethane-1,2-diylbis(azanetriyl)) tetrapropanoate **7h**: ^1H NMR (500 MHz, CDCl_3): δ 3.97 (t, $J = 6.75$ Hz, 8H), 2.69 (t, $J = 7.20$ Hz, 8H), 2.43 (t, $J = 8.90$ Hz, 4H), 2.35 (t, $J = 7.20$ Hz, 8H), 1.52-1.48 (m, 8H), 1.31-1.25 (m, 8H), 0.85 (t, $J = 7.40$ Hz, 12H). ^{13}C NMR (125 MHz, CDCl_3): δ 171.80, 63.49, 51.73, 49.28, 32.20, 30.14, 18.57, 13.08. FTIR (cm^{-1}): 2958, 2873, 2832, 2366, 1728, 1637, 1457, 1381, 1308, 1186, 1064, 1032, 991, 963, 842.

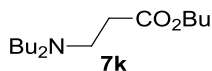


Butyl 3-(pyrrolidin-1-yl) propanoate **7i**: ^1H NMR (500 MHz, CDCl_3): δ 4.05 (t, $J = 6.70$ Hz, 2H), 2.74 (t, $J = 7.30$ Hz, 2H), 2.48-2.46 (m, 6H), 1.74-1.72 (m, 4H), 1.53-1.51 (m, 2H), 1.34-1.31 (m, 2H), 0.90 (t, $J = 7.40$ Hz, 3H). ^{13}C NMR (125 MHz, CDCl_3): δ 172.18, 63.89, 53.64, 51.08, 51.06, 33.86, 33.84, 30.33, 23.13, 18.79, 13.36. FTIR (cm^{-1}): 2959, 2876, 2792, 1733, 1688, 1611, 1460, 1390, 1350, 1243, 1182, 1063, 955, 852, 736.

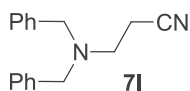


Butyl 3-morpholinopropanoate **7j**: ^1H NMR (500 MHz, CDCl_3): δ 4.03 (t, $J = 6.65$ Hz, 2H), 3.63 (t, $J = 4.70$ Hz, 4H), 2.63 (t, $J = 7.20$ Hz, 2H), 2.44-2.39 (m, 6H), 1.55-1.51

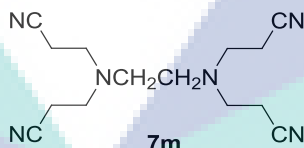
(m, 2H), 1.34-1.29 (m, 2H), 0.88 (t, $J = 7.40$ Hz, 3H). ^{13}C NMR (125 MHz, CDCl_3): δ 171.73, 66.29, 63.63, 53.50, 52.88, 31.62, 30.17, 18.58, 13.14. FTIR (cm^{-1}): 2957, 2867, 2812, 1732, 1457, 1382, 1299, 1252, 1187, 1118, 1065, 1011, 935, 863, 776.



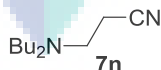
Butyl 3-(dibutylamino) propanoate **7k**: ^1H NMR (500 MHz, CDCl_3): δ 4.03 (t, $J = 6.70$ Hz, 2H), 2.74 (t, $J = 7.15$ Hz, 2H), 2.38-2.33 (m, 6H), 1.56-1.53 (m, 2H), 1.33-1.22 (m, 6H), 0.91-0.90 (m, 4H), 0.88 (s, 9H). ^{13}C NMR (125 MHz, CDCl_3): δ 172.66, 63.88, 53.42, 49.26, 32.25, 30.48, 29.11, 20.37, 20.24, 18.91, 13.76, 13.42. FTIR (cm^{-1}): 2962, 2875, 2810, 2366, 1803, 1745, 1632, 1580, 1519, 1468, 1383, 1200, 1074, 935, 739.



3-(Dibenzylamino) propanenitrile **7l**: ^1H NMR (500 MHz, CDCl_3): δ 7.33 (d, $J = 7.55$ Hz, 4H), 7.24 (t, $J = 7.40$ Hz, 4H), 7.17 (t, $J = 7.35$ Hz, 2H), 3.45 (s, 4H), 2.56 (t, $J = 6.85$ Hz, 2H), 2.17 (t, $J = 6.75$ Hz, 2H). ^{13}C NMR (125 MHz, CDCl_3): δ 138.48, 128.60, 128.30, 127.15, 118.75, 57.00, 48.56, 16.11. FTIR (cm^{-1}): 3061, 3029, 2809, 2334, 2247, 1494, 1451, 1370, 1328, 1249, 1128, 1074, 1024, 973, 911, 739.

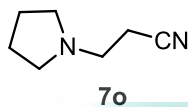


3,3',3'',3'''-(Ethane-1,2-diylbis(azanetriyl)) tetrapropanenitrile **7m**: ^1H NMR (500 MHz, CDCl_3): δ 2.80-2.75 (m, 4H), 2.71 (t, $J = 6.70$ Hz, 4H), 2.55-2.52 (m, 4H), 2.42-2.39 (m, 8H). ^{13}C NMR (125 MHz, CDCl_3): δ 118.61, 52.69, 49.03, 47.76, 46.15, 44.61, 44.38, 18.23, 18.06, 16.58. FTIR (cm^{-1}): 3532, 3309, 2950, 2837, 2336, 2248, 1658, 1463, 1421, 1366, 1281, 1244, 1131, 1035, 984, 761.

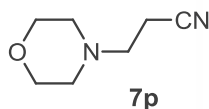


3-(Dibutylamino) propanenitrile **7n**: ^1H NMR (500 MHz, CDCl_3): δ 2.77 (t, $J = 7.0$ Hz, 2H), 2.43-2.39 (m, 6H), 1.39-1.32 (m, 4H), 1.30-1.28 (m, 4H), 0.89 (t, $J = 7.30$ Hz, 6H). ^{13}C NMR (125 MHz, CDCl_3): δ 118.78, 53.18, 49.20, 29.17, 20.11, 15.85, 13.63. FTIR

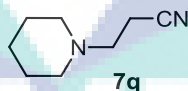
(cm^{-1}): 2955, 2868, 2814, 2359, 2335, 2248, 1463, 1373, 1308, 1274, 1245, 1180, 1158, 1089, 948.



3-(Pyrrolidin-1-yl) propanenitrile **7o**: ^1H NMR (500 MHz, CDCl_3): δ 2.78 (t, $J = 7.0$ Hz, 2 H), 2.58-2.52 (m, 6 H), 1.80-1.77 (m, 4 H). ^{13}C NMR (125 MHz, CDCl_3): δ 119.02, 53.97, 51.45, 23.69, 17.74. FTIR (cm^{-1}): 3028, 2930, 2868, 2335, 2250, 1728, 1677, 1538, 1457, 1375, 1273, 1227, 1074, 1037, 796, 741.



3-Morpholinopropanenitrile **7p**: ^1H NMR (500 MHz, CDCl_3): δ 3.67 (t, $J = 4.55$ Hz, 4H), 2.64 (t, $J = 6.95$ Hz, 2H), 2.50-2.46 (m, 6H). ^{13}C NMR (125 MHz, CDCl_3): δ 118.37, 66.29, 53.19, 52.63, 15.24. FTIR (cm^{-1}): 3509, 2954, 2822, 2335, 2250, 1654, 1455, 1361, 1283, 1114, 1069, 1009, 913, 859, 764.



3-(Piperidin-1-yl) propanenitrile **7q**: ^1H NMR (500 MHz, CDCl_3): δ 2.69 (t, $J = 7.20$ Hz, 2H), 2.49 (t, $J = 7.21$ Hz, 2H), 2.46-2.43 (m, 4H), 1.59-1.57 (m, 4H), 1.47-1.42 (m, 2H). ^{13}C NMR (125 MHz, CDCl_3): δ 118.78, 53.73, 51.22, 23.46, 17.50. FTIR (cm^{-1}): 2937, 2850, 2806, 2697, 2249, 1446, 1354, 1308, 1275, 1158, 1119, 1038, 914, 865, 734.

4.4.13 Recycling Test of Cellulose Supported CuNP@PA

According to the green chemistry protocol, the ease of separation, deactivation, and reusability of the catalyst are important issues when using heterogeneous catalysts for organic synthesis. The catalyst is best suited when it can be recovered easily and reused several times before it finally gets deactivated. Thus, **CuNP@PA** catalyst was considered for recyclability and reusability for *N*-alkylation reactions over seven successive runs through repeated separation of **CuNP@PA** from the reaction mixture, washing, and reusing. After the initial reaction, the reaction mixture was diluted with EtOAc and filtered. The solid dark brown colored **CuNP@PA** was washed with MeOH and dried at 80 °C under vacuum and then, applied to the next cycle without changing the reaction conditions. Seven cycles were performed and **CuNP@PA** was found to retain its catalytic activity to a remarkable extent (Figure 4.30). Only a slight loss of catalytic activity was observed under the same reaction conditions as for initial run which may be due to the loss of **CuNP@PA** during the filtration process.

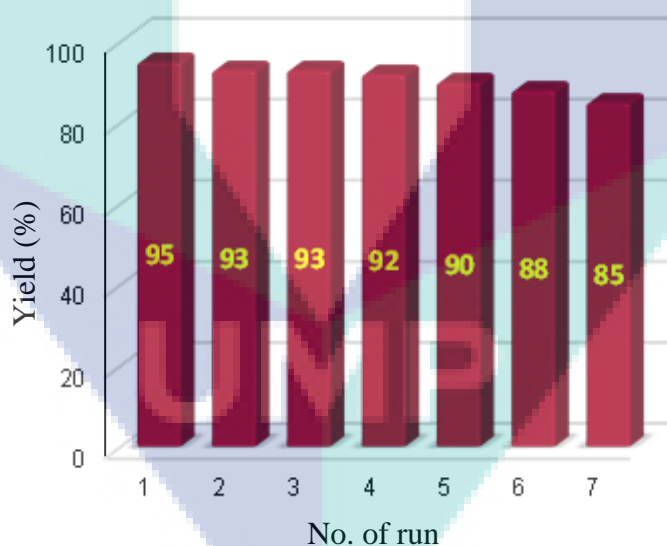
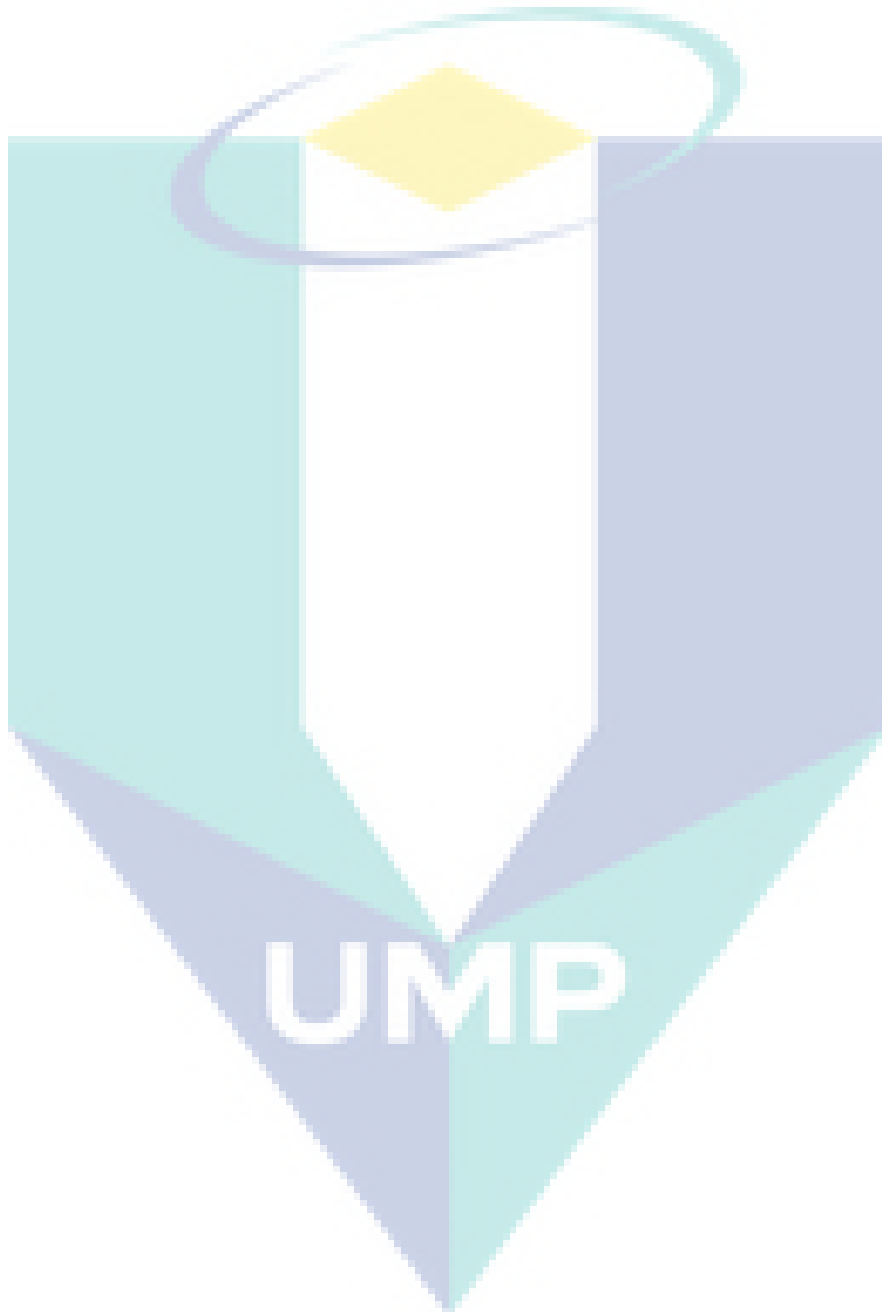


Figure 4.30 Recycling test of **CuNP@PA** in Aza-Michael reaction.

The ICP-AES analysis also indicated that no copper species was leached out into the reaction mixture. Thus, it clearly showed that the corn-cob cellulose-supported **CuNP@PA** could be used repeatedly for large-scale production with no notable loss of its catalytic activity. The TEM image (Figure 4.16b) of the reused **CuNP@PA**

exhibited similar nanoparticles size ($\varnothing = 6.8 \pm 2$ nm) with the original **CuNP@PA** (Figure 4.16a).



CHAPTER 5

CONCLUSION AND RECOMMENDATION

5.1 Conclusion

Chemical bond formation is very important in the synthesis of organic molecules. The use of transition metal catalysts has proven to be one of the most diverse tools for the mild and selective bond formation (C-C, C-N, C-O, C-S etc.). In particular, copper and palladium catalysts have been widely used for a variety of bond formation reactions. Homogeneous metal catalyzed-reactions have several limitations; thus, heterogeneous metal catalysts are emerging as an alternative pathway. The solid support of a metal catalyst plays a crucial role in obtaining a reliable and sustainable heterogeneous catalyst. However, many economic and sustainable protocols have been employed to prepare suitable solid supports but there is still a high demand to explore more efficient solid support for metal-catalyzed chemical transformation reactions.

In view of environmentally-friendly renewable resources and sustainable processes, cellulose would be the most compatible material. Moreover, the backbone of cellulose can be chemically modified and effective chelating ligands can be incorporated. Thus, the main focus of this research was directed towards the utilization of bio-waste material as a valuable material for the construction of C-C and C-N bonds through the cross-coupling reactions. Herein, prepared and characterized waste corn-cob cellulose-supported poly(amidoxime) palladium and copper catalysts were successfully employed as an efficient catalyst for chemical transformations. The cellulose-supported poly(amidoxime) Pd(II) complex **3** was found stabilized and showed a high catalytic activity towards the Mizoroki-Heck reaction. The Pd(II) complex **3** efficiently (0.1 to 0.05 mol%) promoted the Mizoroki-Heck reaction of activated and inactivated aryl

halides and arenediazonium tetrafluoroborate salts with a variety of olefins in aqueous DMF with good yields. The bio-waste corn-cob cellulose-supported Pd(II) complex **3** was easy to recycle and showed magnificent reusability for seven successive cycles with no remarkable degradation of its catalytic activity. In addition, the complex was also used for the synthesis of antiasthmatic agent Ozagrel hydrochloride.

On the other hand, poly(amidoxime) Cu(II) complex **4** smoothly (1 to 0.05 mol%) promoted the Click reaction of organo azide and terminal alkyne in the presence of aqueous sodium ascorbate to give the corresponding triazole with excellent yields. Moreover, this complex was reused six times without a significant loss of its catalytic activity. Furthermore, the poly(amidoxime) Cu(II) complex **4** was reduced by hydrazine to give copper nanoparticles (**CuNP@PA**). The **CuNP@PA** was also successfully applied (0.1 to 0.005 mol%) to the chemoselective Aza-Michael reaction of cyclic or alicyclic amines with a variety of olefins to give the corresponding addition products in up to 95% yield with reusability of the **CuNP@PA**. The cellulose solid support demonstrated an additional role in allowing the reusability of these complexes under air moisture sensitive reaction conditions.

5.2 Recommendation

The bio-waste corn-cob cellulose supported poly(amidoxime) metal complexes were prepared and successfully applied to the C-C and C-N bond formation reactions through Mizoroki-Heck, Click and Aza-Michael reactions. However, from this research, it was realized that the isolation of corn-cob cellulose process followed several steps and provided only 25-30% yields of the cellulose. Additionally, it was difficult to determine the monomer unit in the amidoxime polymer chain as well as the molecular weight of the polymer. Gel Permeation Chromatography (GPC) may be useful to determine the molecular weight of the polymer. These obstacles should be addressed in the future study.

REFERENCES

- Aiken, J. D., & Finke, R. G. (1999). A review of modern transition-metal nanoclusters: their synthesis, characterization, and applications in catalysis. *Journal of Molecular Catalysis A: Chemical*, 145(1-2), 1–44.
- Amara, Z., Caron, J., & Joseph, D. (2013). Recent contributions from the asymmetric Aza-Michael reaction to alkaloids total synthesis. *Natural Product Reports*, 30(9), 1211–1225.
- Amatore, C., & Jutand, A. (2000). Anionic Pd(0) and Pd(II) Intermediates in Palladium-Catalyzed Heck and Cross-Coupling Reactions, *Accounts of Chemical Research*, 33(5), 314–321.
- Anan, N. A., Hassan, S. M., Saad, E. M., Butler, I. S., & Mostafa, S. I. (2011). Preparation, characterization and pH-metric measurements of 4-hydroxysalicylidenechitosan Schiff-base complexes of Fe(III), Co(II), Ni(II), Cu(II), Zn(II), Ru(III), Rh(III), Pd(II) and Au(III). *Carbohydrate Research*, 346(6), 775–793.
- Anastas, P., & Eghbali, N. (2010). Green Chemistry: Principles and Practice. *Chemical Society Reviews*, 39(1), 301–312.
- Anastas, P. T., & Kirchhoff, M. M. (2002). Origins, current status, and future challenges of green chemistry. *Accounts of Chemical Research*, 35(9), 686–694.
- Andrus, M. B., Song, C., & Zhang, J. (2002). Palladium–Imidazolium Carbene Catalyzed Mizoroki–Heck Coupling with Aryl Diazonium Ions. *Organic Letters*, 4(12), 2079–2082.
- Anil Kumar, B. S. P., Harsha Vardhan Reddy, K., Karnakar, K., Satish, G., & Nageswar, Y. V. D. (2015). Copper on chitosan: An efficient and easily recoverable heterogeneous catalyst for one pot synthesis of 1,2,3-triazoles from aryl boronic acids in water at room temperature. *Tetrahedron Letters*, 56(15), 1968–1972.
- Appukkuttan, P., Dehaen, W., Fokin, V. V., & Eycken, E. Van Der. (2004). A Microwave-Assisted Click Chemistry Synthesis of 1, 4-Disubstituted 1, 2, 3 Triazoles via a copper(I)-Catalyzed Three-Component Reaction. *Organic Letters*, 6(23), 4223–4225.
- Aragão-Leoneti, V., Campo, V. L., Gomes, A. S., Field, R. A., & Carvalho, I. (2010). Application of copper(I)-catalysed azide/alkyne cycloaddition (CuAAC) “Click chemistry” in carbohydrate drug and neoglycopolymer synthesis. *Tetrahedron*, 66(49), 9475–9492.

- Azizi, N., Baghi, R., Ghafari, H., Bolourtchian, M., & Hashemi, M. (2010). Silicon tetrachloride catalyzed Aza-Michael addition of amines to conjugated alkenes under solvent-free conditions. *Synlett*, (3), 379–382.
- Bagherzadeh, M., Ashouri, F., Hashemi, L., & Morsali, A. (2014). Supported Pd nanoparticles on Mn-based metal-organic coordination polymer: Efficient and recyclable heterogeneous catalyst for Mizoroki-Heck cross coupling reaction of terminal alkenes. *Inorganic Chemistry Communications*, 44, 10–14.
- Bakherad, M., Keivanloo, A., Bahramian, B., & Jajarmi, S. (2013). Suzuki, Heck, and copper-free Sonogashira reactions catalyzed by 4-amino-5-methyl-3-thio-1,2,4-triazole-functionalized polystyrene resin-supported Pd(II) under aerobic conditions in water. *Journal of Organometallic Chemistry*, 724, 206–212.
- Bakherad, M., Keivanloo, A., & Samangoeei, S. (2012). Solvent-free Heck and copper-free Sonogashira cross-coupling reactions catalyzed by a polystyrene-anchored Pd(II) phenyldithiocarbamate complex. *Tetrahedron Letters*, 53(43), 5773–5776.
- Bakherad, M., Keivanloo, A., & Samangoeei, S. (2014). Poly(vinyl chloride)-supported Pd(II) complex as an efficient catalyst for Heck and Cu-free Sonogashira reactions under aerobic conditions. *Chinese Journal of Catalysis*, 35, 324–328.
- Barot, N., Patel, S. B., & Kaur, H. (2016). Nitro resin supported copper nanoparticles: An effective heterogeneous catalyst for C-N cross coupling and oxidative C-C homocoupling. *Journal of Molecular Catalysis A: Chemical*, 423, 77–84.
- Baruah, D., Das, R. N., Hazarika, S., & Konwar, D. (2015). Biogenic synthesis of cellulose supported Pd(0) nanoparticles using hearth wood extract of *Artocarpus lakoocha* Roxb-A green, efficient and versatile catalyst for Suzuki and Heck coupling in water under microwave heating. *Catalysis Communications*, 72, 73–80.
- Bauer, J. E., Ocelli, M. L., Williams, P. M., & McCaslin, P. C. (1993). Heterogeneous catalyst structure and function: review and implications for the analysis of dissolved organic carbon and nitrogen in natural waters. *Marine Chemistry*, 41(1-3), 75–89.
- Beletskaya, I. P., & Kustov, L. M. (2010). Catalysis as an important tool of green chemistry. *Russian Chemical Reviews*, 79(6), 441–461.
- Bo, K. L., Wu, Q., Xue, Q. Q., De, S. L., & Xian, F. L. (2007). *N*-Methylimidazole as a promising catalyst for the Aza-Michael addition reaction of *N*-heterocycles. *Synthesis*, (17), 2653–2659.
- Bolton, A. J. (1994). Natural Fibers for Plastic Reinforcement. *Materials Technology*, 9(1-2), 12–20.
- Brown, R. M. (2004). Cellulose Structure and Biosynthesis: What is in Store for the 21st Century? *Journal of Polymer Science, Part A: Polymer Chemistry*, 42(3), 487–495.

- Casares, J. A., Espinet, P., Fuentes, B., & Salas, G. (2007). Insights into the mechanism of the Negishi reaction: ZnRX versus ZnR₂ reagents. *Journal of the American Chemical Society*, 129(12), 3508–3509.
- Chao-Jun, L., & Anastas, P. (2012). Green Chemistry: present and future. *Chemical Society Reviews*, (41), 1413–1414.
- Chaudhuri, M. K., Hussain, S., Kantam, M. L., & Neelima, B. (2005). Boric acid: A novel and safe catalyst for Aza-Michael reactions in water. *Tetrahedron Letters*, 46(48), 8329–8331.
- Chavan, P. V, Pandit, K. S., Desai, U. V, Kulkarni, M. A, & Wadgaonkar, P. P. (2014). Cellulose supported cuprous iodide nanoparticles (Cell-CuI NPs): a new heterogeneous and recyclable catalyst for the one pot synthesis of 1,4-disubstituted -1,2,3-triazoles in water. *RSC Advances*, 4(79), 42137–42146.
- Cole-Hamilton, D. J. (2003). Homogeneous Catalysis-New Approaches to Catalyst Separation, Recovery, and Recycling. *Science*, 299(5613), 1702–1706.
- Cordovilla, C., Bartolomé, C., Martínez-Ilarduya, J. M., & Espinet, P. (2015). The stille reaction, 38 years later. *ACS Catalysis*, 5(5), 3040–3053.
- Corma, A, Garcia, H., & Llabres, I. X. F. X. (2010). Engineering metal organic frameworks for heterogeneous catalysis. *Chemical Reviews*, 110(8), 4606–4655.
- Dahou, W., Ghemati, D., Oudia, A., & Aliouche, D. (2010). Preparation and biological characterization of cellulose graft copolymers. *Biochemical Engineering Journal*, 48, 187–194.
- Dai, L., Zhang, Y., Dou, Q., Wang, X., & Chen, Y. (2013). Chemo/regioselective Aza-Michael additions of amines to conjugate alkenes catalyzed by polystyrene-supported AlCl₃. *Tetrahedron*, 69(6), 1712–1716.
- Dai, Q., Gao, W., Liu, D., Kapes, L. M., & Zhang, X. (2006). Triazole-based monophosphine ligands for palladium-catalyzed cross-coupling reactions of aryl chlorides. *The Journal of Organic Chemistry*, 71, 3928–3934.
- Das, B., & Chowdhury, N. (2007). Amberlyst-15: An efficient reusable heterogeneous catalyst for Aza-Michael reactions under solvent-free conditions. *Journal of Molecular Catalysis A: Chemical*, 263(1-2), 212–215.
- Datta, A., Adhikary, J., Chatterjee, S., Ghosh, D., Khamarui, S., & Chattopadhyay, T. (2016). Synthesis and characterization of a magnetically separable novel Fe₃O₄@L-DOPA@Cu(II) nanocatalyst (L-DOPA = L-3,4-dihydroxyphenylalanine): Asymmetric Aza-Michael addition reaction. *Inorganica Chimica Acta*, 444, 209–216.
- Dhepe, P. L., & Fukuoka, A. (2007). Cracking of cellulose over supported metal catalysts. *Catalysis Surveys from Asia*, 11(4), 186–191.

- Di Lena, F., & Matyjaszewski, K. (2010). Transition metal catalysts for controlled radical polymerization. *Progress in Polymer Science*, 35(8), 959–1021.
- Dijkstra, H. P., Van Klink, G. P. M., & Van Koten, G. (2002). The use of ultra- and nanofiltration techniques in homogeneous catalyst recycling. *Accounts of Chemical Research*, 35(9), 798–810.
- Du, Q., Zhang, W., Ma, H., Zheng, J., Zhou, B., & Li, Y. (2012). Immobilized palladium on surface-modified Fe₃O₄/SiO₂ nanoparticles: As a magnetically separable and stable recyclable high-performance catalyst for Suzuki and Heck cross-coupling reactions. *Tetrahedron*, 68(18), 3577–3584.
- Dunn, P. J. (2012). The importance of Green Chemistry in Process Research and Development. *Chemical Society Reviews*, 41(4), 1452–1461.
- Echeandia, S., Pawelec, B., Barrio, V. L., Arias, P. L., Cambra, J. F., Loricera, C. V., & Fierro, J. L. G. (2014). Enhancement of phenol hydrodeoxygenation over Pd catalysts supported on mixed HY zeolite and Al₂O₃. An approach to O-removal from bio-oils. *Fuel*, 117, 1061–1073.
- Ehrentraut, A, Zapf, A, & Beller, M. (2000). A New Efficient Palladium Catalyst for Heck Reactions of Deactivated Aryl Chlorides. *Synlett: Accounts and Rapid Communications in Synthetic Organic Chemistry*, (11), 1589–1592.
- Elazab, H. A., Siamaki, A. R., Moussa, S., Gupton, B. F., & El-Shall, M. S. (2015). Highly efficient and magnetically recyclable graphene-supported Pd/Fe₃O₄ nanoparticle catalysts for Suzuki and Heck cross-coupling reactions. *Applied Catalysis A: General*, 491, 58–69.
- Espinet, P., & Echavarren, A. M. (2004). The mechanisms of the Stille reaction. *Angewandte Chemie International Edition*, 43(36), 4704–4734.
- Favier, I., Madec, D., Teuma, E., & Gomez, M. (2011). Palladium Nanoparticles Applied in Organic Synthesis as Catalytic Precursors. *Current Organic Chemistry*, 15(18), 3127–3174.
- Felpin, F. X., Fouquet, E., & Zakri, C. (2008). Heck cross-coupling of aryldiazonium tetrafluoroborate with acrylates catalyzed by palladium on charcoal. *Advanced Synthesis and Catalysis*, 350(16), 2559–2565.
- Fernández-García, L., Blanco, M., Blanco, C., Álvarez, P., Granda, M., Santamaría, R., & Menéndez, R. (2016). Graphene anchored palladium complex as efficient and recyclable catalyst in the Heck cross-coupling reaction. *Journal of Molecular Catalysis A: Chemical*, 416, 140–146.
- Fu, G. T., Wu, R., Liu, C., Lin, J., Sun, D. M., & Tang, Y. W. (2015). Arginine-assisted synthesis of palladium nanochain networks and their enhanced electrocatalytic activity for borohydride oxidation. *RSC Advances*, 5(23), 18111–18115.

- Fustero, S., Pina, B., Salavert, E., Navarro, A., Ramírez de Arellano, M. C., & Fuentes, A. S. (2002). New strategy for the stereoselective synthesis of fluorinated beta-amino acids. *The Journal of Organic Chemistry*, 67(14), 4667–4679.
- García, A., Gandini, A., Labidi, J., Belgacem, N., & Bras, J. (2016). Industrial and crop wastes: A new source for nanocellulose biorefinery. *Industrial Crops and Products*, 93, 26–38.
- Gholinejad, M., & Jeddi, N. (2014). Copper nanoparticles supported on agarose as a bioorganic and degradable polymer for multicomponent Click synthesis of 1,2,3-triazoles under low copper loading in water. *ACS Sustainable Chemistry and Engineering*, 2(12), 2658–2665.
- Girard, S. A., Knauber, T., & Li, C. J. (2014). The cross-dehydrogenative coupling of C_{sp3}-H bonds: A versatile strategy for C-C bond formations. *Angewandte Chemie International Edition*, 53(1), 74–100.
- Gladysz, J. A. (2001). Recoverable catalysts. Ultimate goals, criteria of evaluation, and the green chemistry interface. *Pure and Applied Chemistry*, 73(8), 1319–1324.
- Gøgsig, T. M., Nielsen, D. U., Lindhardt, A. T., & Skrydstrup, T. (2012). Palladium catalyzed carbonylative Heck reaction affording monoprotected 1,3-ketoaldehydes. *Organic Letters*, 14(10), 2536–2539.
- Gong, H. P., Quan, Z. J., & Wang, X. C. (2016). Palladium catalyzed Mizoroki–Heck reaction of pyrimidin-2-yl tosylates with aromatic and aliphatic olefins. *Tetrahedron*, 72(16), 2018–2025.
- Guibal, E. (2005). Heterogeneous catalysis on chitosan-based materials: A review. *Progress in Polymer Science (Oxford)*, 30(1), 71–109.
- Haas, D., Hammann, J. M., Greiner, R., & Knochel, P. (2016). Recent Developments in Negishi Cross-Coupling Reactions. *ACS Catalysis*, 6(3), 1540–1552.
- Hajipour, A. R., Tadayoni, N. S., & Khorsandi, Z. (2016). Magnetic iron oxide nanoparticles-N-heterocyclic carbene-palladium(II): a new, efficient and robust recyclable catalyst for Mizoroki-Heck and Suzuki-Miyaura coupling reactions. *Applied Organometallic Chemistry*, 30(7), 590–595.
- Haron, M. J., Tiansih, M., Ibrahim, N. A., Kassim, A., & Wan Yunus, W. M. Z. (2009). Sorption of Cu(II) by poly(hydroxamic acid) chelating exchanger prepared from poly(methyl acrylate) grafted oil palm empty fruit bunch (OPEFB). *BioResources*, 4(4), 1305–1318.
- Hartmann, M., & Kevan, L. (1999). Transition-Metal Ions in Aluminophosphate and Silicoaluminophosphate Molecular Sieves: Location, Interaction with Adsorbates and Catalytic Properties. *Chemical Reviews*, 99(3), 635–664.
- Hattori, H. (2001). Solid base catalysts: Generation of basic sites and application to organic synthesis. *Applied Catalysis A: General*, 222(1-2), 247–259.

- Heck, R. F. (1979). Palladium-catalyzed reactions of organic halides with olefins. *Accounts of Chemical Research*, 12(1968), 146-151.
- Heck, R. F., & Nolley, J. P. (1972). Palladium-catalyzed vinylic hydrogen substitution reactions with aryl, benzyl, and styryl halides. *The Journal of Organic Chemistry*, 37(14), 2320–2322.
- Himaja, M., Poppy, D., & Asif, K. (2011). Green Technique-Solvent Free Synthesis and Its Advantages. *International Journal of Research in Ayurveda & Pharmacy*, 2(24), 1079–1086.
- Himo, F., Lovell, T., Hilgraf, R., Rostovtsev, V. V., Noodleman, L., Sharpless, K. B., & Fokin, V. V. (2005). Copper(I)-catalyzed synthesis of azoles. DFT study predicts unprecedented reactivity and intermediates. *Journal of the American Chemical Society*, 127(1), 210–216.
- Hope, G. A., Woods, R., Parker, G. K., Buckley, A. N., & McLean, J. (2010). A vibrational spectroscopy and XPS investigation of the interaction of hydroxamate reagents on copper oxide minerals. *Minerals Engineering*, 23(11-13), 952–959.
- Hosseini, S. G., & Abazari, R. (2015). A facile one-step route for production of CuO, NiO, and CuO–NiO nanoparticles and comparison of their catalytic activity for ammonium perchlorate decomposition. *RSC Advances*, 5(117), 96777–96784.
- Huang, K., Xue, L., Hu, Y. C., Huang, M. Y., & Jiang, Y. Y. (2002). Catalytic behaviors of silica-supported starch-polysulfosiloxane-Pt complexes in asymmetric hydrogenation of 4-methyl-2-pentanone. *Reactive and Functional Polymers*, 50(3), 199–203.
- Huang, Z., Li, F., Chen, B., Xue, F., Chen, G., & Yuan, G. (2011). Nitrogen-rich copolymeric microsheets supporting copper nanoparticles for catalyzing arylation of N-heterocycles. *Applied Catalysis A: General*, 403(1-2), 104–111.
- Huisgen, R. (1963). 1,3-Dipolar Cycloadditions. Past and Future. *Angewandte Chemie International Edition*, 2(10), 565–598.
- Iranpoor, N., Firouzabadi, H., Motevalli, S., & Talebi, M. (2012). Palladium nanoparticles supported on silicadiphenyl phosphinite (SDPP) as efficient catalyst for Mizoroki-Heck and Suzuki-Miyaura coupling reactions. *Journal of Organometallic Chemistry*, 708-709, 118–124.
- Jadhav, S., Jagdale, A., Kamble, S., Kumbhar, A., & Salunkhe, R. (2016). Palladium nanoparticles supported on a titanium dioxide cellulose composite (PdNPs@TiO₂ – Cell) for ligand-free carbon–carbon cross coupling reactions. *RSC Advances*, 6(5), 3406–3420.
- Janssen, M., Müller, C., & Vogt, D. (2011). Recent advances in the recycling of homogeneous catalysts using membrane separation. *Green Chemistry*, 13(9), 2247–2257.

- Jun, C. (2004). Transition metal-catalyzed carbon–carbon bond activation. *Chemical Society Reviews*, 33, 610–618.
- Kalidindi, S. B., & Jagirdar, B. R. (2012). Nanocatalysis and prospects of green chemistry. *ChemSusChem*, 5(1), 65–75.
- Kang, S., Choi, S., Ryu, H., & Yamaguchi T. (1998). Palladium-Catalyzed Coupling of Organolead Compounds with Olefins. *Journal of Organic Chemistry*, 63(8), 5748–5749.
- Karthikeyan, P., Muskawar, P. N., Aswar, S. A., Bhagat, P. R., & Sythana, S. K. (2012). Development of an efficient solvent free one-pot Heck reaction catalyzed by novel palladium(II) complex-via green approach. *Journal of Molecular Catalysis A: Chemical*, 358, 112–120.
- Keipour, H., Khalilzadeh, M. A., Hosseini, A., Pilevar, A., & Zareyee, D. (2012). An active and selective heterogeneous catalytic system for Michael addition. *Chinese Chemical Letters*, 23(5), 537–540.
- Khalafi-Nezhad, A., & Panahi, F. (2014). Size-Controlled Synthesis of Palladium Nanoparticles on a Silica–Cyclodextrin Substrate: A Novel Palladium Catalyst System for the Heck Reaction in Water. *ACS Sustainable Chemistry & Engineering*, 2(5), 1177–1186.
- Khazaei, A., Khazaei, M., & Rahmati, S. (2015). A green method for the synthesis of gelatin/pectin stabilized palladium nano-particles as efficient heterogeneous catalyst for solvent-free Mizoroki-Heck reaction. *Journal of Molecular Catalysis A: Chemical*, 398, 241–247.
- Khazaei, A., Rahmati, S., Hekmatian, Z., & Saeednia, S. (2013). A green approach for the synthesis of palladium nanoparticles supported on pectin: Application as a catalyst for solvent-free Mizoroki-Heck reaction. *Journal of Molecular Catalysis A: Chemical*, 372, 160–166.
- Kobayashi, S., Kakumoto, K., & Sugiura, M. (2002). Transition Metal Salts-Catalyzed Aza-Michael Reactions of Enones with Carbamates. *Organic Letters*, 4(8), 1319–1322.
- Koga, H., Azetsu, A., Tokunaga, E., Saito, T., Isogai, A., & Kitaoka, T. (2012). Topological loading of Cu(I) catalysts onto crystalline cellulose nanofibrils for the Huisgen Click reaction. *Journal of Materials Chemistry*, 22(12), 5538–5542.
- Kolb, H. C., & Sharpless, K. B. (2003). The growing impact of Click chemistry on drug discovery. *Drug Discovery Today*, 8(24), 1128–1137.
- Lasch, R., Fehler, S. K., & Heinrich, M. R. (2016). Hydrogen Peroxide Promoted Mizoroki-Heck Reactions of Phenyl diazenes with Acrylates, Acrylamides, and Styrenes. *Organic Letters*, 18(7), 1586–1589.

- Leclerc, J. P., & Fagnou, K. (2006). Palladium-Catalyzed Cross-Coupling Reactions of Diazine *N*-Oxides with Aryl Chlorides, Bromides, and Iodides. *Angewandte Chemie International Edition*, 45(46), 7781–7786.
- Lee, D., Taher, A., Hossain, S., & Jin, M. (2011). An Efficient and General Method for the Heck and Buchwald À Hartwig Coupling Reactions of Aryl Chlorides. *Organic Letters*, 13(7), 5540–5543.
- Lee, J., Farha, O. K., Roberts, J., Scheidt, K. A., Nguyen, S. T., & Hupp, J. T. (2009). Metal-organic framework materials as catalysts. *Chemical Society Reviews*, 38(5), 1450–1459.
- Liu, C. F., Ren, J. L., Xu, F., Liu, J. J., Sun, J. X., & Sun, R. C. (2006). Isolation and characterization of cellulose obtained from ultrasonic irradiated sugarcane bagasse. *Journal of Agricultural and Food Chemistry*, 54(16), 5742–5748.
- Liu, C., Zhang, H., Shi, W., & Lei, A. (2011). Bond formations between two nucleophiles: Transition metal catalyzed oxidative cross-coupling reactions. *Chemical Reviews*, 111(3), 1780–1824.
- Löber, S., Rodriguez-Loaiza, P., & Gmeiner, P. (2003). Supporting Information Available Click Linker : Efficient and High Yielding Synthesis of a New Family of SPOS Resins by 1,3-Dipolar Cycloaddition Experimental details : *Organic Letters*, 5(10), 1753–1755.
- Loo, M. H., Egan, D., Vaughan, E. D., Marion, D., Felsen, D., & Weisman, S. (1987). The Effect of the Thromboxane A₂ Synthesis Inhibitor Oky-046 on Renal Function in Rabbits Following Release of Unilateral Ureteral Obstruction. *The Journal of Urology*, 137(3), 571–576.
- Lutfor, M. R., Sidik, S., Wan Yunus, W. M. Z., Ab Rahman, M. Z., Mansoor, A., & Jelas, H. (2001). Preparation and swelling of polymeric absorbent containing hydroxamic acid group from polymer grafted sago starch. *Carbohydrate Polymers*, 45(1), 95–100.
- Lutfor, M. R., Sidik, S., Yunus, W. M. Z. W. A. N., Rahman, M. Z. A., Mansor, A., & Haron, M. J. (2001). Synthesis and Characterization of Poly(hydroxamic acid) Chelating Resin from Poly(methyl acrylate)-Grafted Sago Starch. *Journal of Applied Polymer Science*, 79, 1256–1264.
- Lv, X., Wang, Z., & Bao, W. (2006). CuI catalyzed C-N bond forming reactions between aryl/heteroaryl bromides and imidazoles in [Bmim]BF₄. *Tetrahedron*, 62(20), 4756–4761.
- Mahdavi, H., & Sahraei, R. (2016). Synthesis and Application of Hyperbranched Polyester-Grafted Polyethylene (HBPE-g-PE) Containing Palladium Nanoparticles as Efficient Nanocatalyst. *Catalysis Letters*, 146(5), 977–990.
- Maluenda, I., & Navarro, O. (2015). Recent developments in the Suzuki-Miyaura reaction: 2010-2014. *Molecules*, 20(5), 7528–7557.

- Mandal, B. H., Rahman, M. L., Rahim, M. H. A., & Sarkar, S. M. (2016). Highly Active Kenaf Bio-Cellulose Based Poly(hydroxamic acid) Copper Catalyst for Aza-Michael Addition and Click Reactions. *ChemistrySelect*, 1(11), 2750–2756.
- Marion, N., Ecarnot, E. C., Navarro, O., Amoroso, D., Bell, A., & Nolan, S. P. (2006). (IPr)Pd(acac)Cl: An Easily Synthesized, Efficient, and Versatile Precatalyst for C-N and C-C Bond Formation. *Journal of Organic Chemistry*, 71, 3816–3821.
- Marion, N., Navarro, O., Mei, J., Stevens, E. D., Scott, N. M., & Nolan, S. P. (2006). Modified (NHC)Pd(allyl)Cl (NHC=N-Heterocyclic Carbene) Complexes for Room-Temperature Suzuki - Miyaura and Buchwald - Hartwig Reactions. *Journal of the American Chemical Society*, 128(11), 4101–4111.
- Marques, C. A., & Machado, A. A. S. C. (2014). Environmental Sustainability: Implications and limitations to Green Chemistry. *Foundations of Chemistry*, 16(2), 125–147.
- Marulasiddeshwara, M. B., & Kumar, P. R. (2016). Synthesis of Pd(0) nanocatalyst using lignin in water for the Mizoroki–Heck reaction under solvent-free conditions. *International Journal of Biological Macromolecules*, 83, 326–334.
- McDowall, D. J., Gupta, B. S., & Stannett, V. T. (1984). Grafting of vinyl monomers to cellulose by ceric ion initiation. *Progress in Polymer Science*, 10(1), 1–50.
- McGlacken, G. P., & Bateman, L. M. (2009). Recent advances in aryl–aryl bond formation by direct arylation. *Chemical Society Reviews*, 38(8), 2447–2464.
- Mekhzoum, M. E. M., Benzeid, H., Qaiss, A. E. K., Essassi, E. M., & Bouhfid, R. (2016). Copper(I) Confined in Interlayer Space of Montmorillonite: A Highly Efficient and Recyclable Catalyst for Click Reaction. *Catalysis Letters*, 146(1), 136–143.
- Meldal, M. (2008). Polymer “Clicking” by CuAAC reactions. *Macromolecular Rapid Communications*, 29(12-13), 1016–1051.
- Mino, T., Suzuki, S., Hirai, K., Sakamoto, M., & Fujita, T. (2011). Hydrazone-promoted Sonogashira coupling reaction with aryl bromides at low palladium loadings. *Synlett*, (9), 1277–1280.
- Miyaura, N., Yanagi, T., & Suzuki, A. (1981). The Palladium-Catalyzed Cross-Coupling reaction of Phenylboronic Acid with Haloarenes in the Presence of Bases. *Synthetic Communications*, 11(7), 513–519.
- Mirsafaei, R., Heravi, M. M., Ahmadi, S., Moslemin, M. H., & Hosseinejad, T. (2015). In situ prepared copper nanoparticles on modified KIT-5 as an efficient recyclable catalyst and its applications in Click reactions in water. *Journal of Molecular Catalysis A: Chemical*, 402, 100–108.
- Mizoroki, T., Mori, K., & Ozaki, A. (1971). Arylation of Olefin with Aryl Iodide Catalyzed by Palladium. *Bulletin of the Chemical Society of Japan*, 44, 581–581

- Mohammadi, E., & Movassagh, B. (2016). Synthesis of polystyrene-supported Pd(II)-NHC complex derived from theophylline as an efficient and reusable heterogeneous catalyst for the Heck-Matsuda cross-coupling reaction. *Journal of Molecular Catalysis A: Chemical*, 418-419, 158–167.
- Molnár, Á. (2011). Efficient, selective, and recyclable palladium catalysts in carbon-carbon coupling reactions. *Chemical Reviews*, 111(3), 2251–2320.
- Mondal, M. I. H., Yeasmin, M. S., & Rahman, M. S. (2015). Preparation of food grade carboxymethyl cellulose from corn husk agrowaste. *International Journal of Biological Macromolecules*, 79, 144–150.
- Morán, J. I., Alvarez, V. A., Cyras, V. P., & Vázquez, A. (2008). Extraction of cellulose and preparation of nanocellulose from sisal fibers. *Cellulose*, 15(1), 149–159.
- Mori, K., Mizoroki, T., & Ozaki, A. (1973). Arylation of Olefin with Iodobenzene Catalyzed by Palladium. *Bulletin of the Chemical Society of Japan*, 46, 1505-1508.
- Movassagh, B., Tahershamsi, L., & Mobaraki, A. (2015). A magnetic solid sulfonic acid modified with hydrophobic regulators: An efficient recyclable heterogeneous catalyst for one-pot Aza-Michael-type and Mannich-type reactions of aldehydes, ketones, and amines. *Tetrahedron Letters*, 56(14), 1851–1854.
- Naeimi, H., & Shaabani, R. (2017). Ultrasound promoted facile one pot synthesis of triazole derivatives catalyzed by functionalized graphene oxide Cu(I) complex under mild conditions. *Ultrasonics Sonochemistry*, 34, 246–254.
- Naghipour, A., & Fakhri, A. (2016). Heterogeneous Fe₃O₄@chitosan-Schiff base Pd nanocatalyst: Fabrication, characterization and application as highly efficient and magnetically-recoverable catalyst for Suzuki-Miyaura and Heck-Mizoroki C-C coupling reactions. *Catalysis Communications*, 73, 39–45.
- Negishi, E. I., King, A. O., & Okukado, N. (1977). Selective carbon-carbon bond formation via transition metal catalysis. 3. A highly selective synthesis of unsymmetrical biaryls and diarylmethanes by the nickel or palladium-catalyzed reaction of aryl and benzylzinc derivatives with aryl halides. *The Journal of Organic Chemistry*, 42(10), 1821–1823.
- Nguyen, L. T. L., Nguyen, T. T., Nguyen, K. D., & Phan, N. T. S. (2012). Metal-organic framework MOF-199 as an efficient heterogeneous catalyst for the Aza-Michael reaction. *Applied Catalysis A: General*, 425-426, 44–52.
- Nicolaou, K. C., Bulger, P. G., & Sarlah, D. (2005). Palladium-catalyzed cross-coupling reactions in total synthesis. *Angewandte Chemie International Edition*, 44(29), 4442–4489.
- Nieman, G. W., Weertman, J. R., & Siegel, R. W. (1991). Mechanical behavior of nanocrystalline Cu and Pd. *Journal of Materials Research*, 6(05), 1012–1027.

- Oger, N., Le Grogne, E., & Felpin, F. X. (2014). Continuous-flow Heck-Matsuda reaction: Homogeneous versus heterogeneous palladium catalysts. *Journal of Organic Chemistry*, 79(17), 8255-8262.
- Ozawa, F., Kubo, A., Matsumoto, Y., Hayashi, T., Nishioka, E., Yanagi, K., & Moriguchi, K. I. (1993). Palladium-Catalyzed Asymmetric Arylation of 2,3-Dihydrofuran with Phenyl Triflate. A Novel Asymmetric Catalysis Involving a Kinetic Resolution Process. *Organometallics*, 12(10), 4188-4196.
- Pagliaro, M., Pandarus, V., Béland, F., Ciriminna, R., Palmisano, G., & Carà, P. D. (2011). A new class of heterogeneous Pd catalysts for synthetic organic chemistry. *Catalysis Science & Technology*, 1(5), 736-739.
- Paul, S., Islam, M. M., & Islam, S. M. (2015). Suzuki-Miyaura reaction by heterogeneously supported Pd in water: recent studies. *RSC Advances*, 5(53), 42193-42221.
- Peñafiel, I., Pastor, I. M., & Yus, M. (2012). Heck-Matsuda reactions catalyzed by a hydroxyalkyl-functionalized NHC and palladium acetate. *European Journal of Organic Chemistry*, (16), 3151-3156.
- Petroni, A., Bertazzo, A., Sarti, S., & Galli, C. (1989). Accumulation of Arachidonic Acid Cyclo and Lipoxygenase Products in Rat Brain During Ischemia and Reperfusion: Effects of Treatment with GM1-Lactone. *Journal of Neurochemistry*, 53(3), 747-752.
- Phapale, V. B., & Cárdenas, D. J. (2009). Nickel-catalysed Negishi cross-coupling reactions: scope and mechanisms. *Chemical Society Reviews*, 38(6), 1598-1607.
- Pontes da Costa, A., Rosa Nunes, D., Tharaud, M., Oble, J., Poli, G., & Rieger, J. (2017). Pd(0)-Nanoparticles Embedded in Core-Shell Nanogels as Recoverable Catalysts for the Mizoroki-Heck Reaction. *ChemCatChem*, 9(12), 2167-2175.
- Prenesti, E., & Berto, S. (2002). Interaction of copper(II) with imidazole pyridine nitrogen-containing ligands in aqueous medium: A spectroscopic study. *Journal of Inorganic Biochemistry*, 88(1), 37-43.
- Pryjomska-Ray, I., Gniewek, A., Trzeciak, A. M., Ziółkowski, J. J., & Tylus, W. (2006). Homogeneous/heterogeneous palladium based catalytic system for Heck reaction. The reversible transfer of palladium between solution and support. *Topics in Catalysis*, 40(1-4), 173-184.
- Quignard, F., Choplin, A., & Domard, A. (2000). Chitosan: A natural polymeric support of catalysts for the synthesis of fine chemicals. *Langmuir*, 16(24), 9106-9108.
- Rahman, L., Rohani, N., Mustapa, N., & Yusoff, M. M. (2014). Synthesis of Polyamidoxime Chelating Ligand from Polymer-Grafted Corn-Cob Cellulose for Metal Extraction, *Journal of Applied Polymer Science*, 40833, 1-8.

- Rahman, M. L., Sarkar, S. M., Yusoff, M. M., & Abdullah, M. H. (2016). Efficient removal of transition metal ions using poly(amidoxime) ligand from polymer grafted kenaf cellulose. *RSC Advances*, 6(1), 745–757.
- Rai, R. K., Tyagi, D., Gupta, K., & Singh, S. K. (2016). Activated nanostructured bimetallic catalysts for C–C coupling reactions: recent progress. *Catalysis Science and Technology*, 6(10), 3341–3361.
- Rangel Rangel, E., Maya, E. M., Sánchez, F., de la Campa, J. G., & Iglesias, M. (2015). Palladium-heterogenized porous polyimide materials as effective and recyclable catalysts for reactions in water. *Green Chemistry*, 17(1), 466–473.
- Reddy, K. R., & Kumar, N. S. (2006). Cellulose-supported copper(0) catalyst for Aza-Michael addition. *Synlett*, (14), 2246–2250.
- Reddy, K. R., Kumar, N. S., Sreedhar, B., & Kantam, M. L. (2006). *N*-Arylation of nitrogen heterocycles with aryl halides and arylboronic acids catalyzed by cellulose supported copper(0). *Journal of Molecular Catalysis A: Chemical*, 252(1–2), 136–141.
- Rossy, C., Majimel, J., Tréguer, M., Fouquet, E., & Felpin, F. (2014). Palladium and copper-supported on charcoal : A heterogeneous multi-task catalyst for sequential Sonogashira-Click and Click-Heck reactions. *Journal of Organometallic Chemistry*, 755, 78–85.
- Roy, S., Chatterjee, T., Pramanik, M., Roy, A. S., Bhaumik, A., & Islam, S. M. (2014). Cu(II)-anchored functionalized mesoporous SBA-15: An efficient and recyclable catalyst for the one-pot Click reaction in water. *Journal of Molecular Catalysis A: Chemical*, 386, 78–85.
- Sanchez-Rosello, M., Acena, J. L., Simon-Fuentes, A., & del Pozo, C. (2014). A general overview of the organocatalytic intramolecular Aza-Michael reaction. *Chemical Society Reviews*, 43(21), 7430–7453.
- Sarkar, S. M., Rahman, M. L., Chong, K. F., & Yusoff, M. M. (2017). Poly(hydroxamic acid) palladium catalyst for heck reactions and its application in the synthesis of Ozagrel. *Journal of Catalysis*, 350, 103–110.
- Sarkar, S. M., Rahman, M. L., & Yusoff, M. M. (2015). Pyridinyl functionalized MCM-48 supported highly active heterogeneous palladium catalyst for cross-coupling reactions. *RSC Advances*, 5(25), 19630–19637.
- Sarkar, S. M., Sultana, T., Biswas, T. K., Rahman, M. L., & Yusoff, M. M. (2016). Waste corn-cob cellulose supported bio-heterogeneous copper nanoparticles for Aza-Michael reactions. *New Journal of Chemistry*, 40(1), 497–502.
- Schatz, A., Reiser, O., & Stark, W. J. (2010). Nanoparticles as semi-heterogeneous catalyst supports. *Chemistry-A European Journal*, 16(30), 8950–8967.

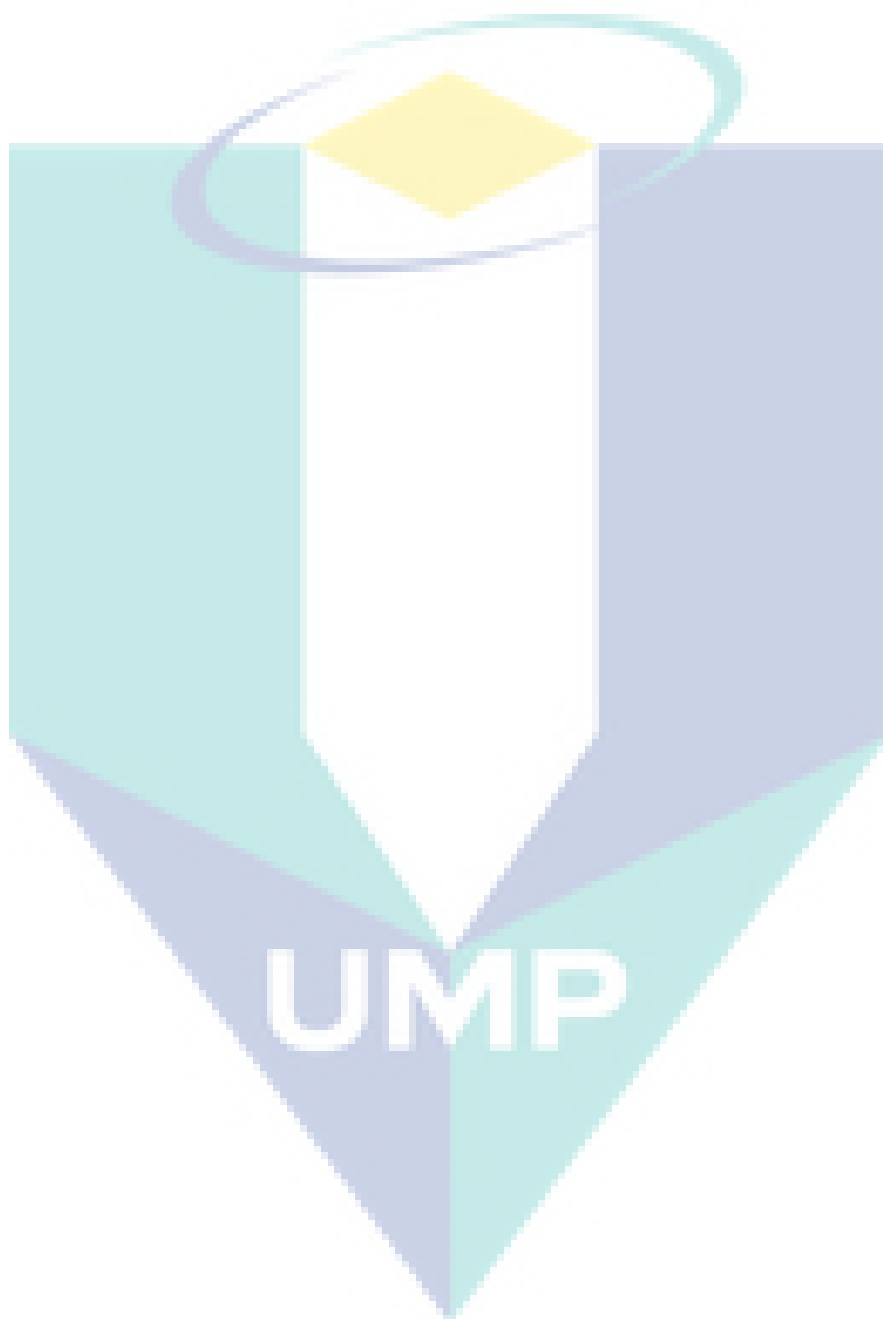
- Schmidt, B., & Wolf, F. (2017). Synthesis of Phenylpropanoids via Matsuda–Heck Coupling of Arene Diazonium Salts. *Journal of Organic Chemistry*, 82, 4386–4395.
- Selvakumar, K., Zapf, A., Spannenberg, A., & Beller, M. (2002). Synthesis of monocarbenepalladium(0) complexes and their catalytic behavior in cross-coupling reactions of aryldiazonium salts. *Chemistry-A European Journal*, 8(17), 3901–3906.
- Shang, N., Gao, S., Zhou, X., Feng, C., Wang, Z., & Wang, C. (2014). Palladium nanoparticles encapsulated inside the pores of a metal–organic framework as a highly active catalyst for carbon–carbon cross-coupling. *RSC Advances*, 4(97), 54487–54493.
- Sharpless, K. B., & Manetsch, R. (2006). Click Chemistry: A Powerful Means for Lead Discovery. *Expert Opinion on Drug Discovery*, 1(6), 525–538.
- Sheldon, R. A. (2012). Fundamentals of green chemistry: efficiency in reaction design. *Chemical Society Reviews*, 41(4), 1437–1451.
- Sheldon, R. A. (2014). Green and sustainable manufacture of chemicals from biomass: state of the art. *Green Chemistry*, 16(3), 950–963.
- Shen, C., Shen, H., Yang, M., Xia, C., & Zhang, P. (2015). A novel D-glucosamine-derived pyridyl-triazole@palladium catalyst for solvent-free Mizoroki–Heck reactions and its application in the synthesis of Axitinib. *Green Chemistry*, 17, 225–230.
- Shi, W., Liu, C., & Lei, A. (2011). Transition-metal catalyzed oxidative cross-coupling reactions to form C–C bonds involving organometallic reagents as nucleophiles. *Chemical Society Reviews*, 40(5), 2761–2776.
- Shibasaki, M., & Vogl, E. M. (1999). The palladium-catalysed arylation and vinylation of alkenes-enantioselective fashion. *Journal of Organometallic Chemistry*, 576, 1–15.
- Shirakawa, E., Yoshida, H., Nakao, Y., & Hiyama, T. (1999). Palladium-catalyzed dimerization-carbostannylation of alkynes: Synthesis of highly conjugated alkenylstannanes. *Journal of the American Chemical Society*, 121(17), 4290–4291.
- Siew, S., Wen, Y., Rahman, L., Arshad, S. E., Surugau, N. L., & Musta, B. (2011). Synthesis and characterization of poly(hydroxamic acid)–poly(amidoxime) chelating ligands from polymer-grafted acacia cellulose. *Journal of Applied Polymer Science*, 124(6), 4443–4451.
- Smith, A. K., & Basset, J. M. (1977). Transition metal cluster complexes as catalysts. A review. *Journal of Molecular Catalysis*, 2(4), 229–241.

- Sobhani, S., & Pakdin-Parizi, Z. (2014). Palladium-DABCO complex supported on γ - Fe_2O_3 magnetic nanoparticles: A new catalyst for C-C bond formation via Mizoroki-Heck cross-coupling reaction. *Applied Catalysis A: General*, 479, 112–120.
- Sodhi, R. K., Paul, S., Gupta, V. K., & Kant, R. (2015). Conversion of α , β -unsaturated ketones to 1,5-diones via tandem retro-Aldol and Michael addition using $\text{Co}(\text{acac})_2$ covalently anchored onto amine functionalized silica. *Tetrahedron Letters*, 56(15), 1944–1948.
- Sonogashira, K., Tohda, Y., & Hagihara, N. (1975). A convenient synthesis of acetylenes: catalytic substitutions of acetylenic hydrogen with bromoalkenes, iodoarenes and bromopyridines. *Tetrahedron Letters*, 16(50), 4467–4470.
- Srivastava, N., & Banik, B. K. (2003). Bismuth nitrate-catalyzed versatile Michael reactions. *Journal of Organic Chemistry*, 68(6), 2109–2114.
- Su, D. S., Zhang, J., Frank, B., Thomas, A., Wang, X., Paraknowitsch, J., & Schlögl, R. (2010). Metal-free heterogeneous catalysis for sustainable chemistry. *Chem. Sustainable Chemistry*, 3(2), 169–180.
- Sukhov, D. (2016). Quick non-destructive analysis of lignin condensation and precipitation by FTIR. *Cellulose Chemistry and Technology* 50(2), 213–217.
- Sultana, T., Mandal, B. H., Rahman, M. L., & Sarkar, S. M. (2016). Bio-Waste Corn-cob Cellulose Supported Poly(amidoxime) Palladium Nanoparticles for Suzuki-Miyaura Cross-Coupling Reactions. *ChemistrySelect*, 1(13), 4108–4112.
- Sunaba, H., Kamata, K., & Mizuno, N. (2014). Selective N-alkylation of indoles with α,β -unsaturated compounds catalyzed by a monomeric phosphate. *ChemCatChem*, 6(8), 2333–2338.
- Suzuki, A. (1999). Recent advances in the cross-coupling reactions of organoboron derivatives with organic electrophiles, 1995–1998. *Journal of Organometallic Chemistry*, 576(1-2), 147–168.
- Swadźba-Kwaśny, M., Chancelier, L., Ng, S., Manyar, H. G., Hardacre, C., & Nockemann, P. (2012). Facile in situ synthesis of nanofluids based on ionic liquids and copper oxide clusters and nanoparticles. *Dalton Transactions*, 41(1), 219–227.
- Tasker, S. Z., Gutierrez, A. C., & Jamison, T. F. (2014). Nickel-catalyzed Mizoroki-Heck reaction of aryl sulfonates and chlorides with electronically unbiased terminal olefins: High selectivity for branched products. *Angewandte Chemie - International Edition*, 53(7), 1858–1861.
- Tavassoli, M., Landarani-Isfahani, A., Moghadam, M., Tangestaninejad, S., Mirkhani, V., & Mohammadpoor-Baltork, I. (2015). Polystyrene-supported ionic liquid copper complex: A reusable catalyst for one-pot three-component Click reaction. *Applied Catalysis A: General*, 503, 186–195.

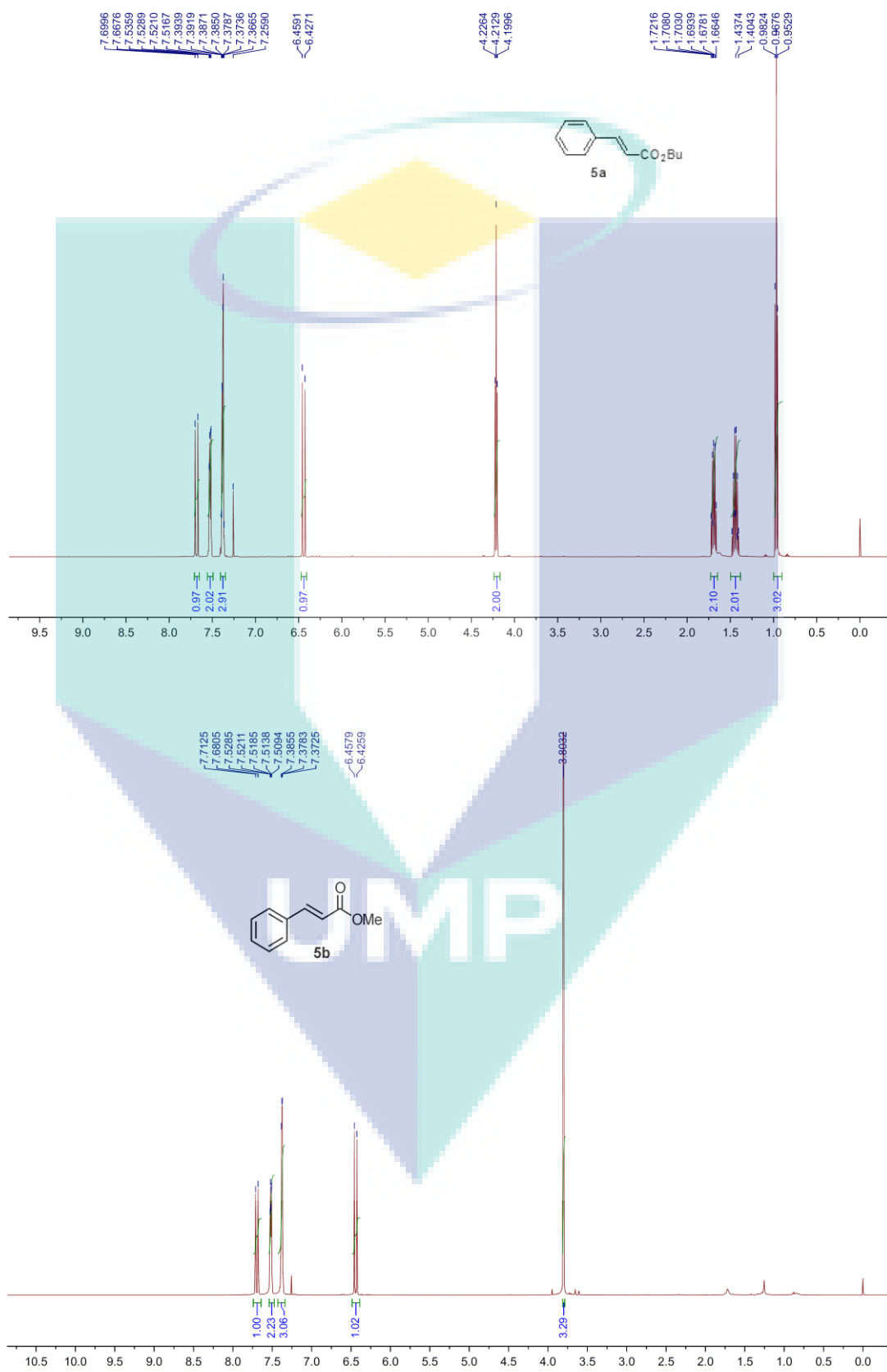
- Taylor, P., Turker, M. F., Ayaz, H., & Kaygusuz, K. (2010). Forest Biomass as a Source of Renewable Energy in Turkey. *North*, 8312, 37–41.
- Torborg, C., & Beller, M. (2009). Recent applications of palladium-catalyzed coupling reactions in the pharmaceutical, agrochemical, and fine chemical industries. *Advanced Synthesis and Catalysis*, 351(18), 3027–3043.
- Tsuji, Y., & Fujihara, T. (2007). Homogeneous nanosize palladium catalysts. *Inorganic Chemistry*, 46(6), 1895–1902.
- Urgaonkar, S., Xu, J. H., & Verkade, J. G. (2003). Application of a New Bicyclic Triaminophosphine Ligand in Pd-Catalyzed Buchwald-Hartwig Amination Reactions of Aryl Chlorides, Bromides, and Iodides. *Journal of Organic Chemistry*, 68(22), 8416–8423.
- Vadaparthi, P. R. R., Pavan Kumar, C., Kumar, K., Venkanna, A., Lakshma Nayak, V., Ramakrishna, S., & Babu, K. S. (2015). Synthesis of costunolide derivatives by Pd-catalyzed Heck arylation and evaluation of their cytotoxic activities. *Medicinal Chemistry Research*, 24(7), 2871–2878.
- Wan, Z., Xiong, Z., Ren, H., Huang, Y., & Liu, H. (2011). Graft copolymerization of methyl methacrylate onto bamboo cellulose under microwave irradiation. *Carbohydrate Polymers*, 83(1), 264–269.
- Wang, Y., Yuan, Y. Q., & Guo, S. R. (2009). Silica sulfuric acid promotes Aza-Michael addition reactions under solvent-free condition as a heterogeneous and reusable catalyst. *Molecules*, 14(11), 4779–4789.
- Wei, W., Zhu, H., Zhao, C., Huang, M., & Jiang, Y. (2004). Asymmetric hydrogenation of furfuryl alcohol catalyzed by a biopolymer–metal complex, silica-supported alginate acid–amino acid–Pt complex. *Reactive & Functional Polymers*, 59, 33–39.
- Wenda, S., Illner, S., Mell, A., & Kragl, U. (2011). Industrial biotechnology-the future of green chemistry. *Green Chemistry*, 13(11), 3007–3047.
- Wesselbaum, S., Vom Stein, T., Klankermayer, J., & Leitner, W. (2012). Hydrogenation of carbon dioxide to methanol by using a homogeneous ruthenium-phosphine catalyst. *Angewandte Chemie International Edition*, 51(30), 7499–7502.
- William, D., Connell, O., Birkinshaw, C., Francis, T., & Dwyer, O. (2008). Heavy metal adsorbents prepared from the modification of cellulose: A review. *Bioresource Technology*, 99, 6709–6724.
- Wu, H., Li, H., Kwok, R. T. K., Zhao, E., Sun, J. Z., Qin, A., & Tang, B. Z. (2014). A recyclable and reusable supported Cu(I) catalyzed azide-alkyne Click polymerization. *Scientific Reports*, 4, 1–5.
- Wu, S., Ma, H., Jia, X., Zhong, Y., & Lei, Z. (2011). Biopolymer-metal complex wool-Pd as a highly active heterogeneous catalyst for Heck reaction in aqueous media. *Tetrahedron*, 67(1), 250–256.

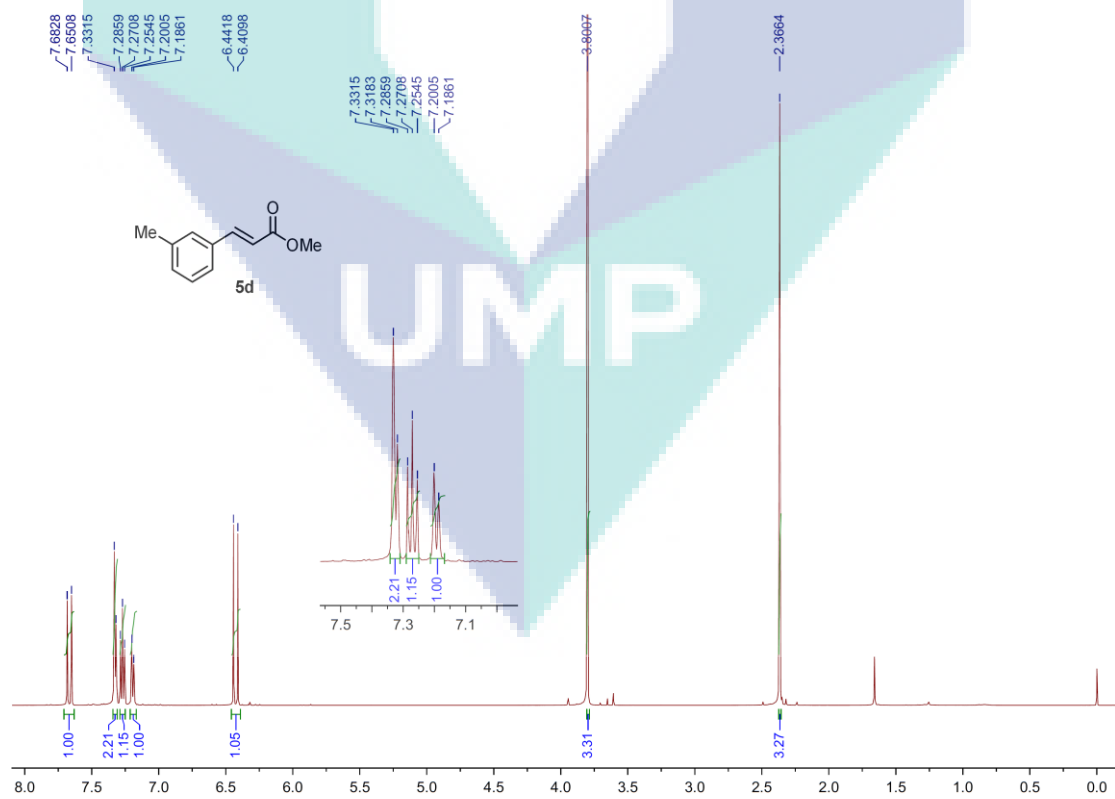
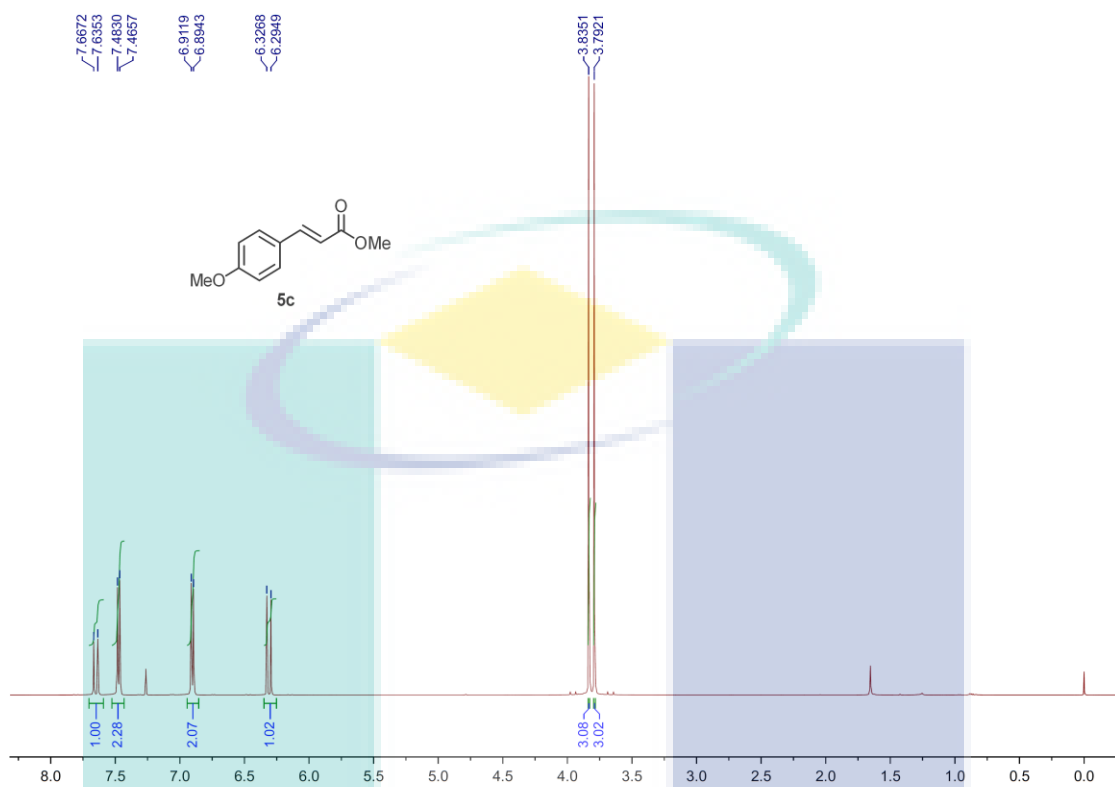
- Xie, S. L., Hui, Y. H., Long, X. J., Wang, C. C., & Xie, Z. F. (2013). Aza-Michael addition reactions between nitroolefins and benzotriazole catalyzed by MCM-41 immobilized heteropoly acids in water. *Chinese Chemical Letters*, 24(1), 28–30.
- Xu, G., Zhang, Y., Wang, K., Fu, Y., & Du, Z. (2015). Microwave-assisted Stille cross-coupling reaction catalysed by in situ formed palladium nanoparticles. *Journal of Chemical Research*, 39(7), 399–402.
- Xu, J. M., Wu, Q., Zhang, Q. Y., Zhang, F., & Lin, X. F. (2007). A basic ionic liquid as catalyst and reaction medium: A rapid and simple procedure for Aza-Michael addition reactions. *European Journal of Organic Chemistry*, (11), 1798–1802.
- Yamada, Y. M. A., Sarkar, S. M., & Uozumi, Y. (2012). Amphiphilic self-assembled polymeric copper catalyst to parts per million levels: Click chemistry. *Journal of the American Chemical Society*, 134(22), 9285–9290.
- Yamada, Y. M. A., Yuyama, Y., Sato, T., Fujikawa, S., & Uozumi, Y. (2014). A palladium-nanoparticle and silicon-nanowire-array hybrid: A platform for catalytic heterogeneous reactions. *Angewandte Chemie International Edition*, 53(1), 127–131.
- Yang, J., Tan, X., Wang, Y., & Wang, X. (2013). Ethylenediamine-functionalized activated carbon anchored palladium complex: A recyclable catalyst for Heck reaction. *Journal of Porous Materials*, 20(3), 501–506.
- Yang, L., Xu, L. W., & Xia, C. G. (2007). Efficient catalytic Aza-Michael additions of carbamates to enones: revisited dual activation of hard nucleophiles and soft electrophiles by $\text{InCl}_3/\text{TMSCl}$ catalyst system. *Tetrahedron Letters*, 48(9), 1599–1603.
- Ying, A., Zhang, Q., Li, H., Shen, G., Gong, W., & He, M. (2013). An environmentally benign protocol: Catalyst-free Michael addition of aromatic amines to α,β -unsaturated ketones in glycerol. *Research on Chemical Intermediates*, 39(2), 517–525.
- Yoshida, K., Gonzalez-Arellano, C., Luque, R., & Gai, P. L. (2010). Efficient hydrogenation of carbonyl compounds using low-loaded supported copper nanoparticles under microwave irradiation. *Applied Catalysis A: General*, 379(1–2), 38–44.
- Yu, W., Jiang, L., Shen, C., Xu, W., & Zhang, P. (2016). A highly efficient synthesis of *N*-glycosyl-1,2,3-triazoles using a recyclable cellulose-copper(0) catalyst in water. *Catalysis Communications*, 79, 11–16.
- Zhang, X., Geng, Y., Han, B., Ying, M., Huang, M., & Jiang, Y. (2001). Asymmetric Hydrogenation of Ketones Catalyzed by Zeolite-supported Gelatin-Fe Complex. *Polymers for Advanced Technologies*, 12, 642–646.

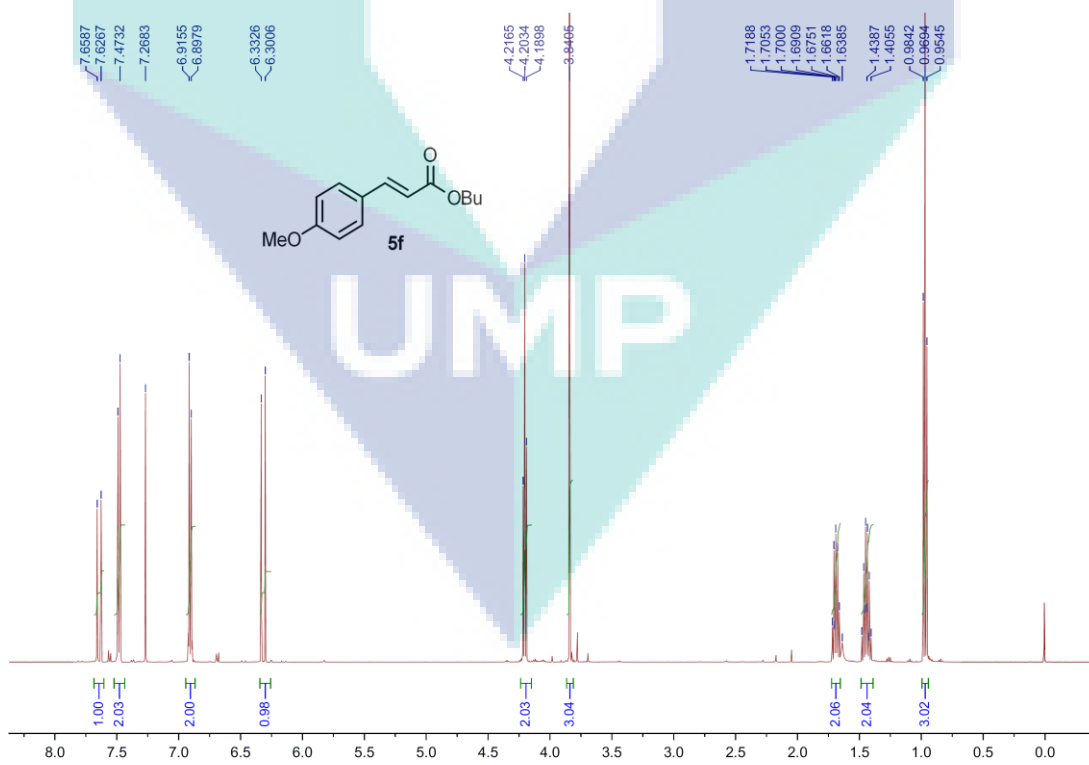
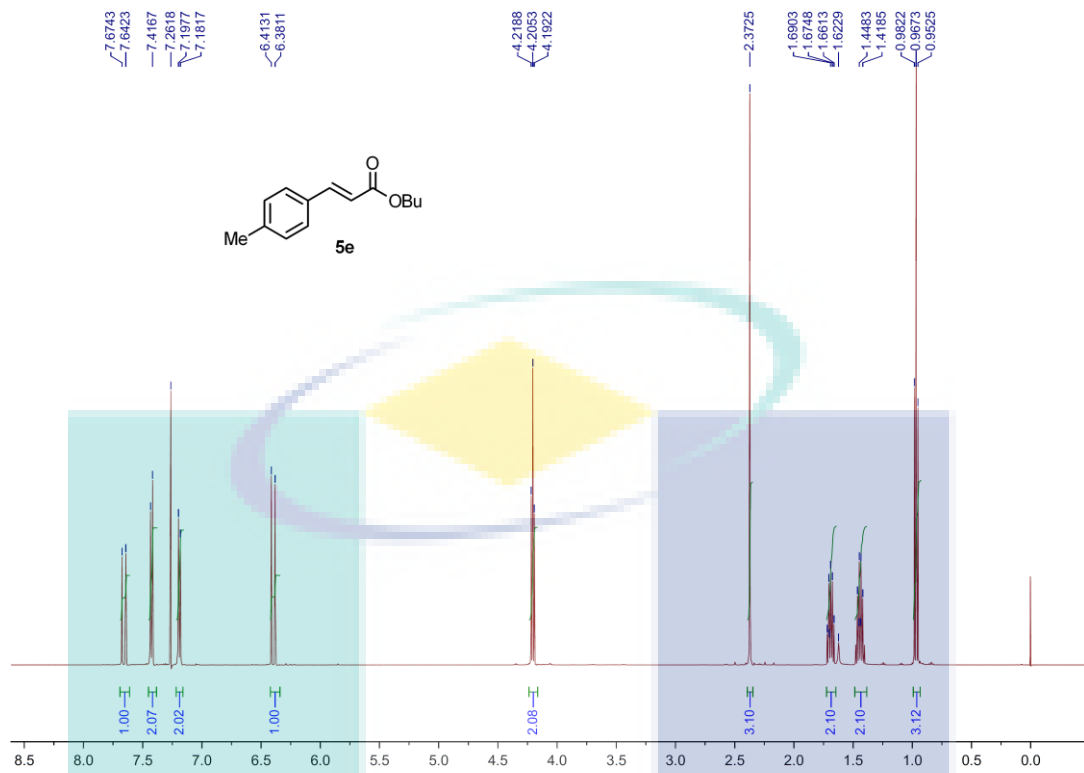
Zhou, X., Xu, W., Liu, G., Panda, D., & Chen, P. (2010). Size Dependent Catalytic Activity and Dynamics of Gold Nanoparticles at the Single-Molecule Level. *Journal of the American Chemical Society*, 132(11), 138–146.

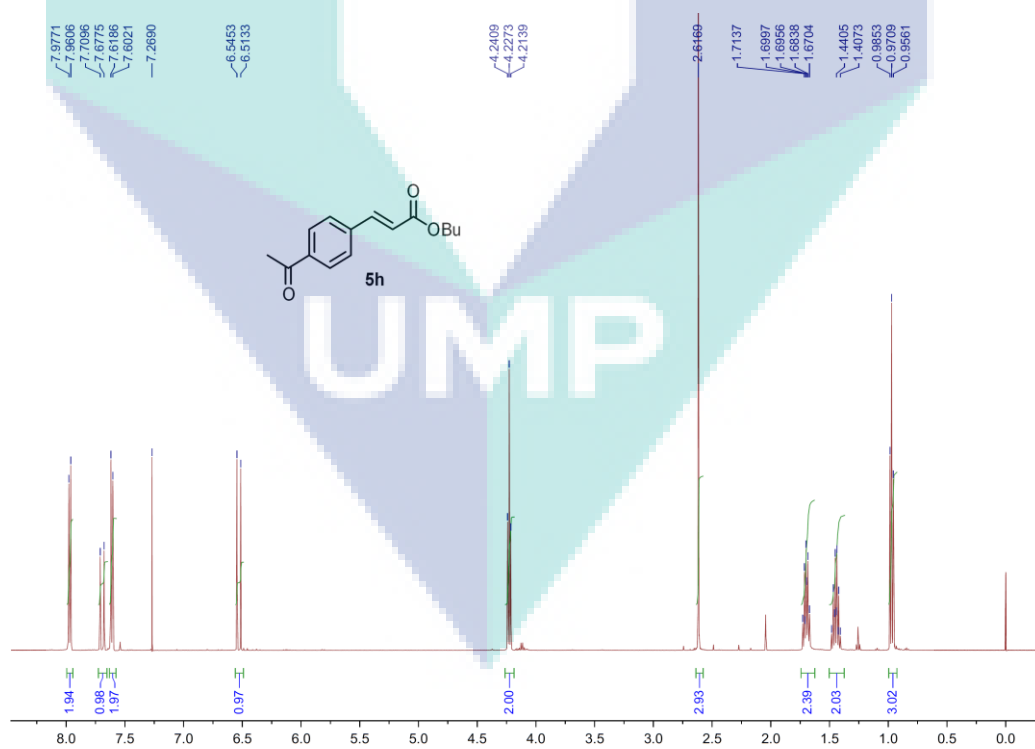
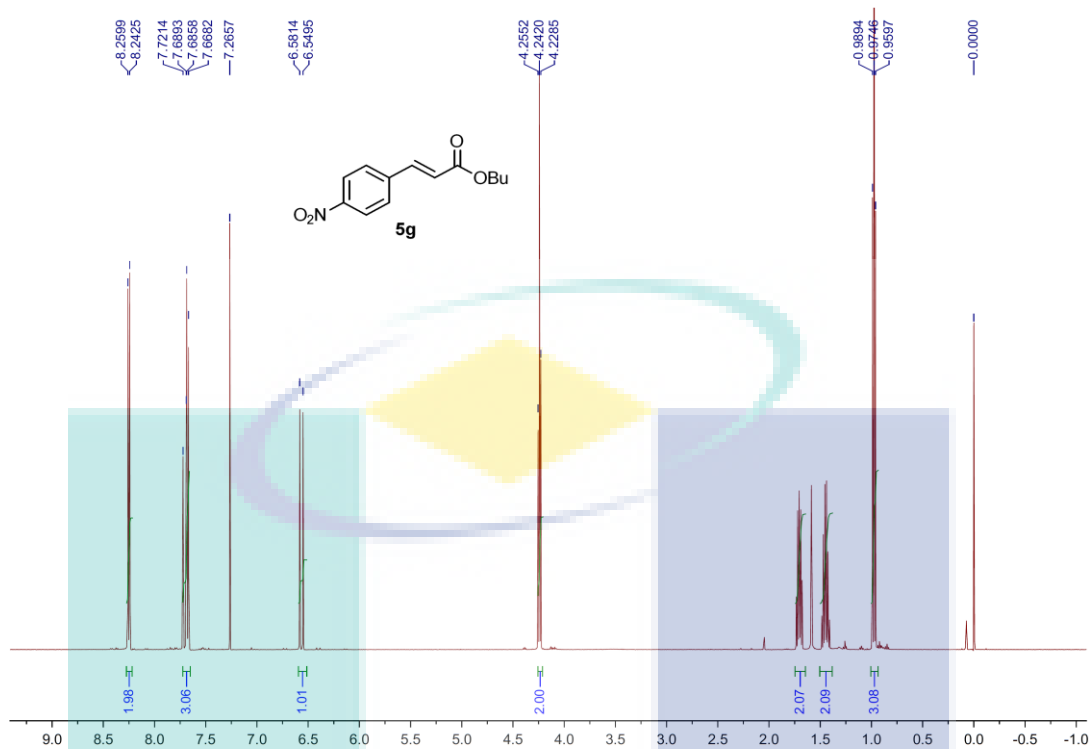


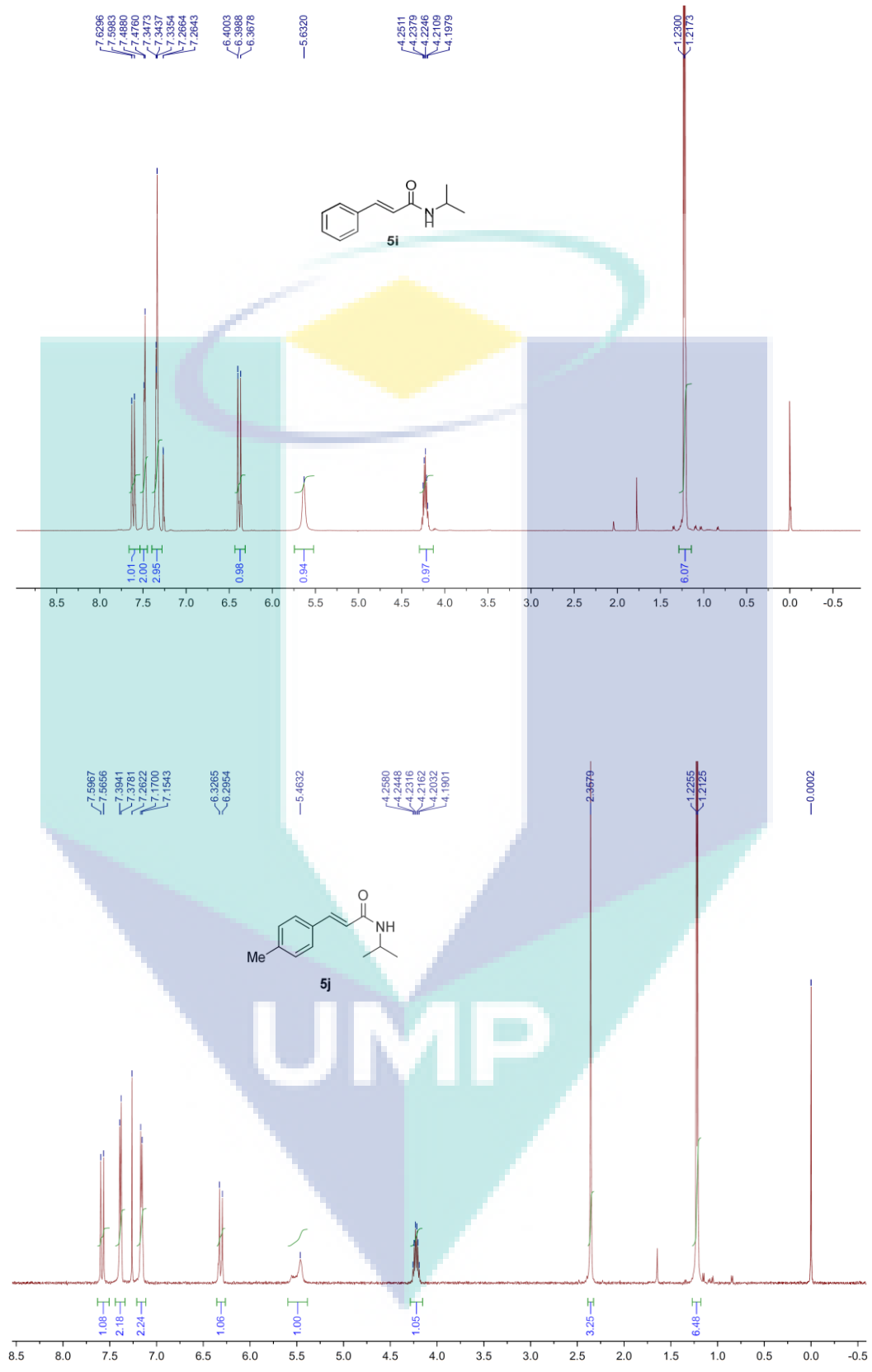
APPENDIX A (¹H NMR)

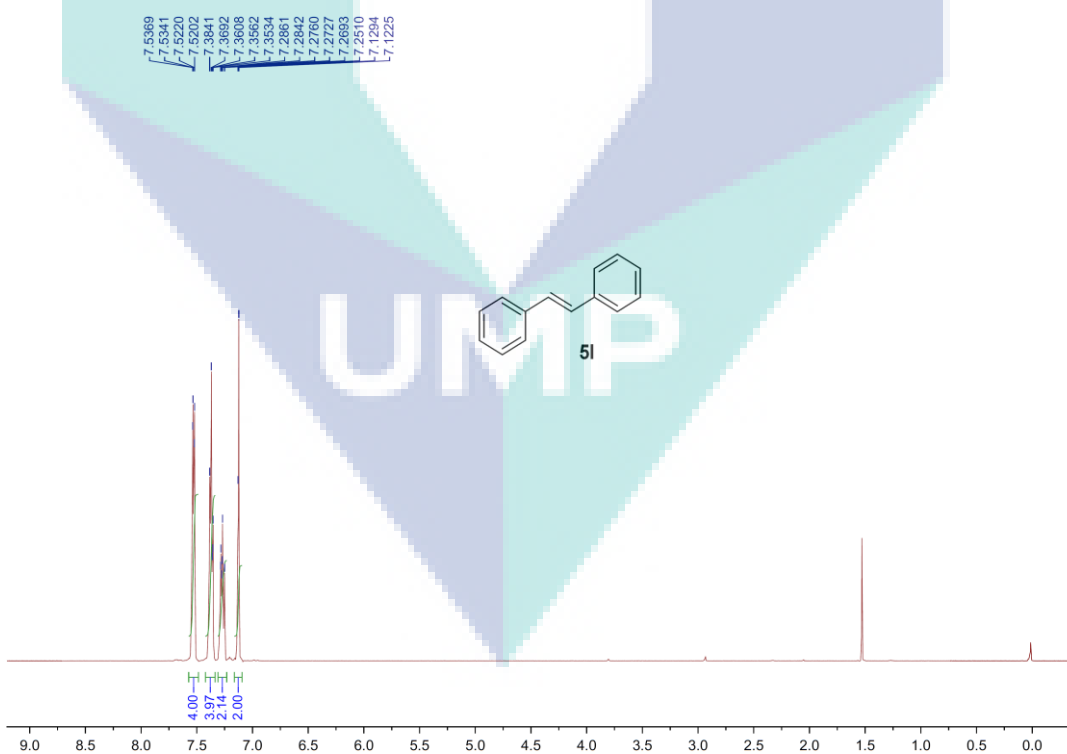
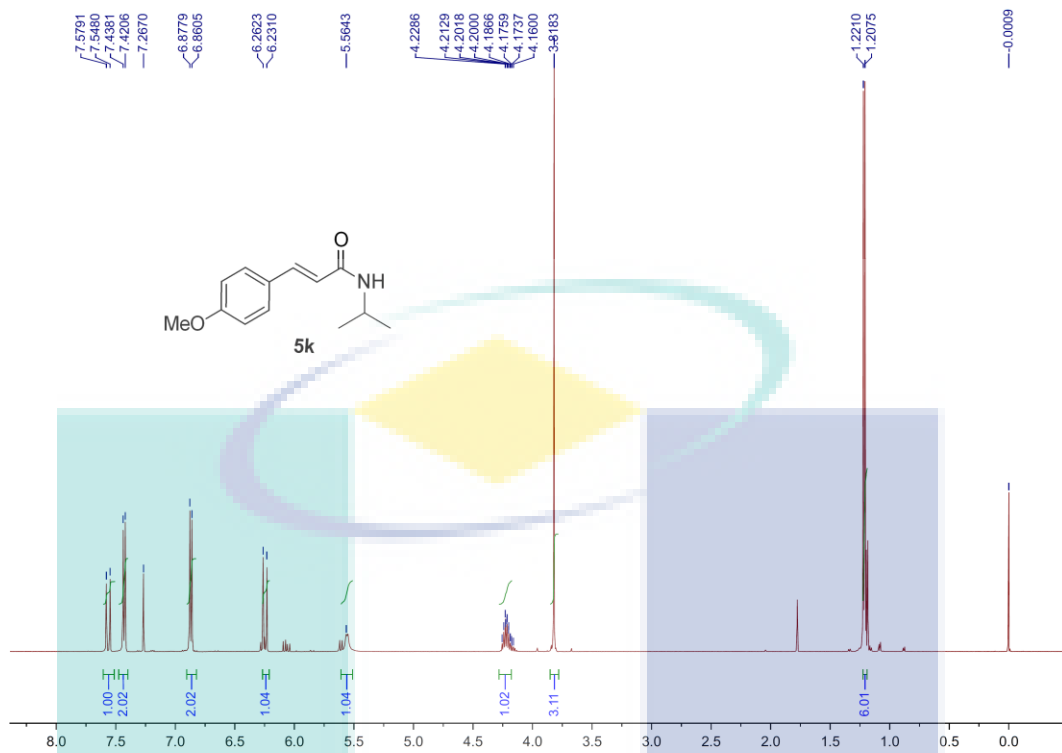


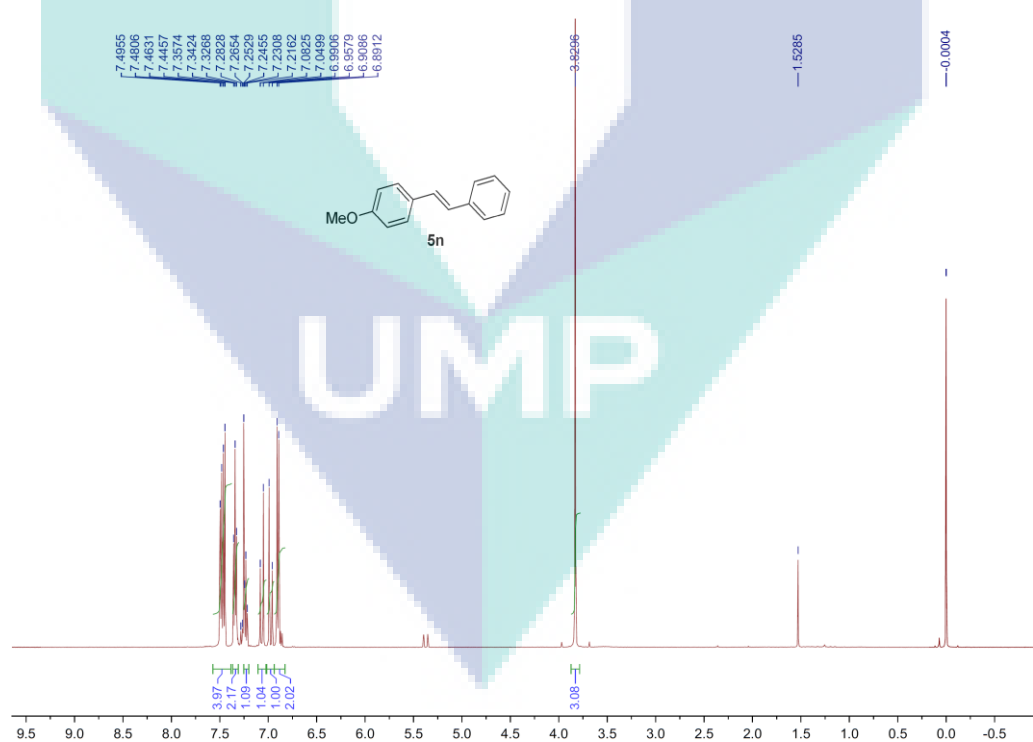
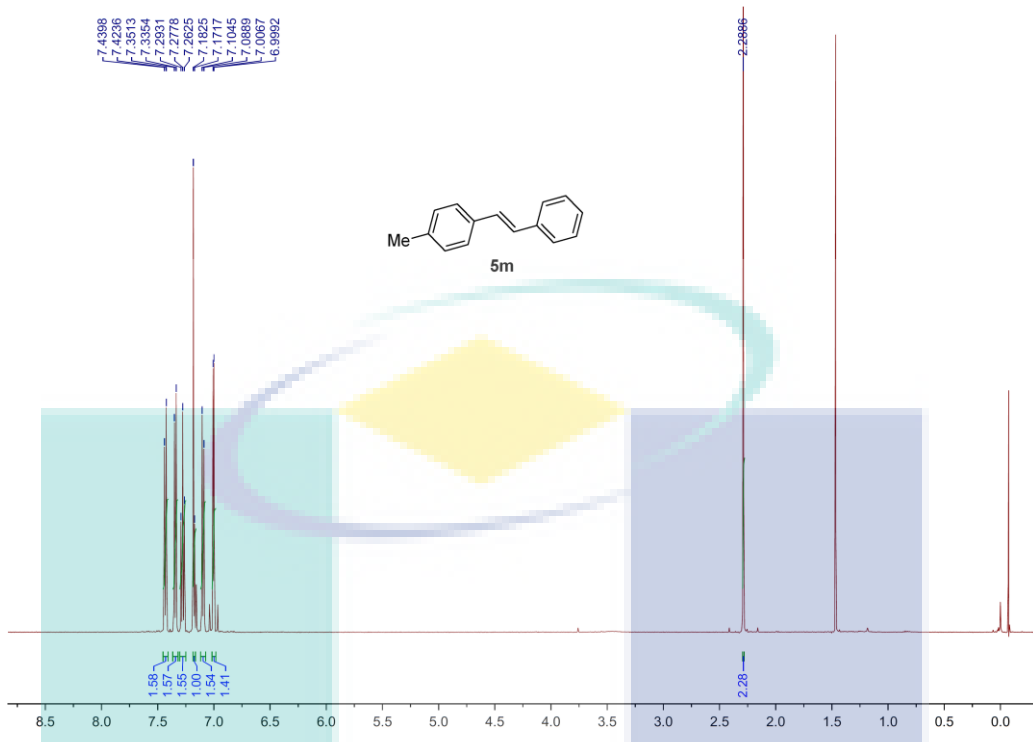


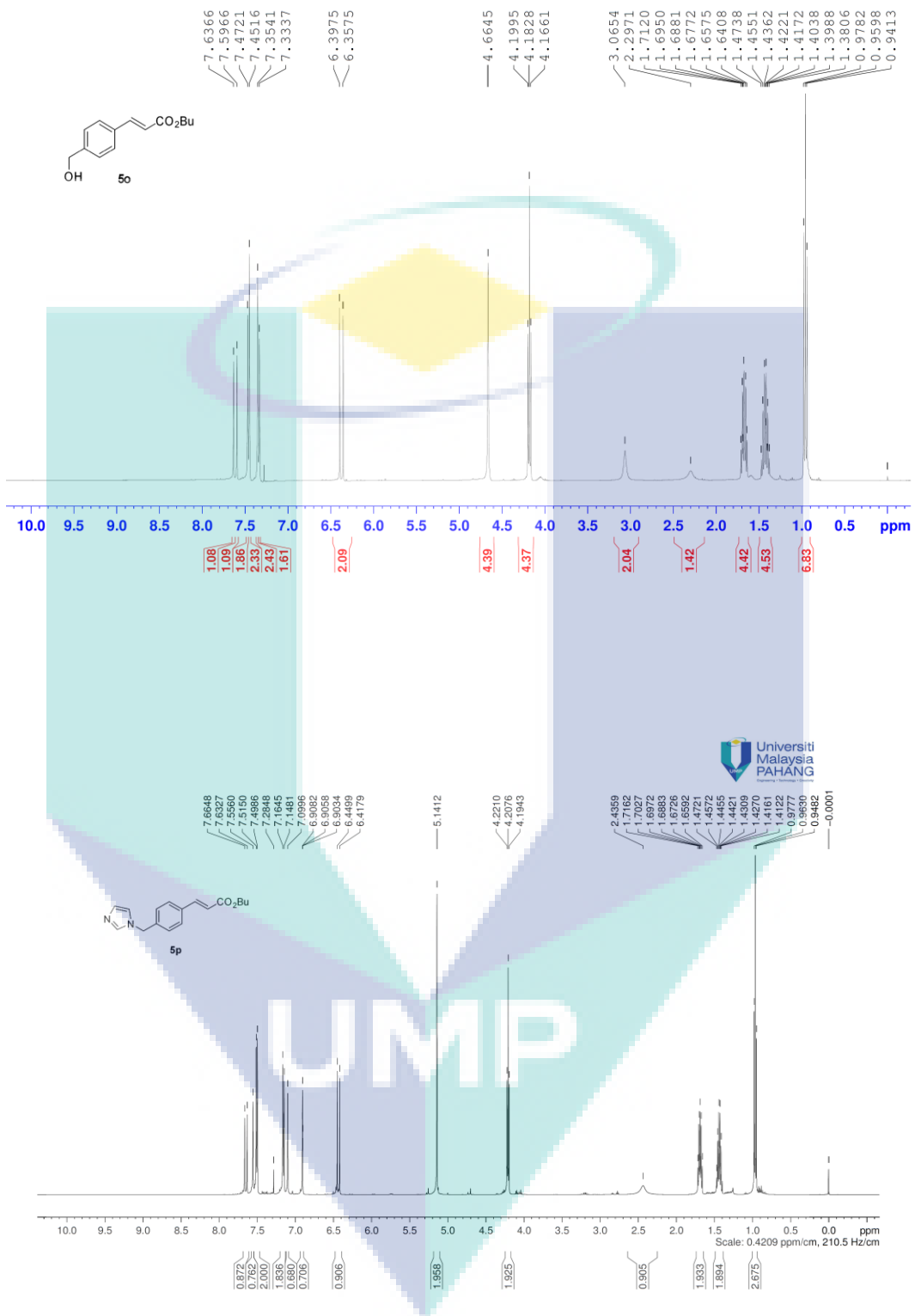


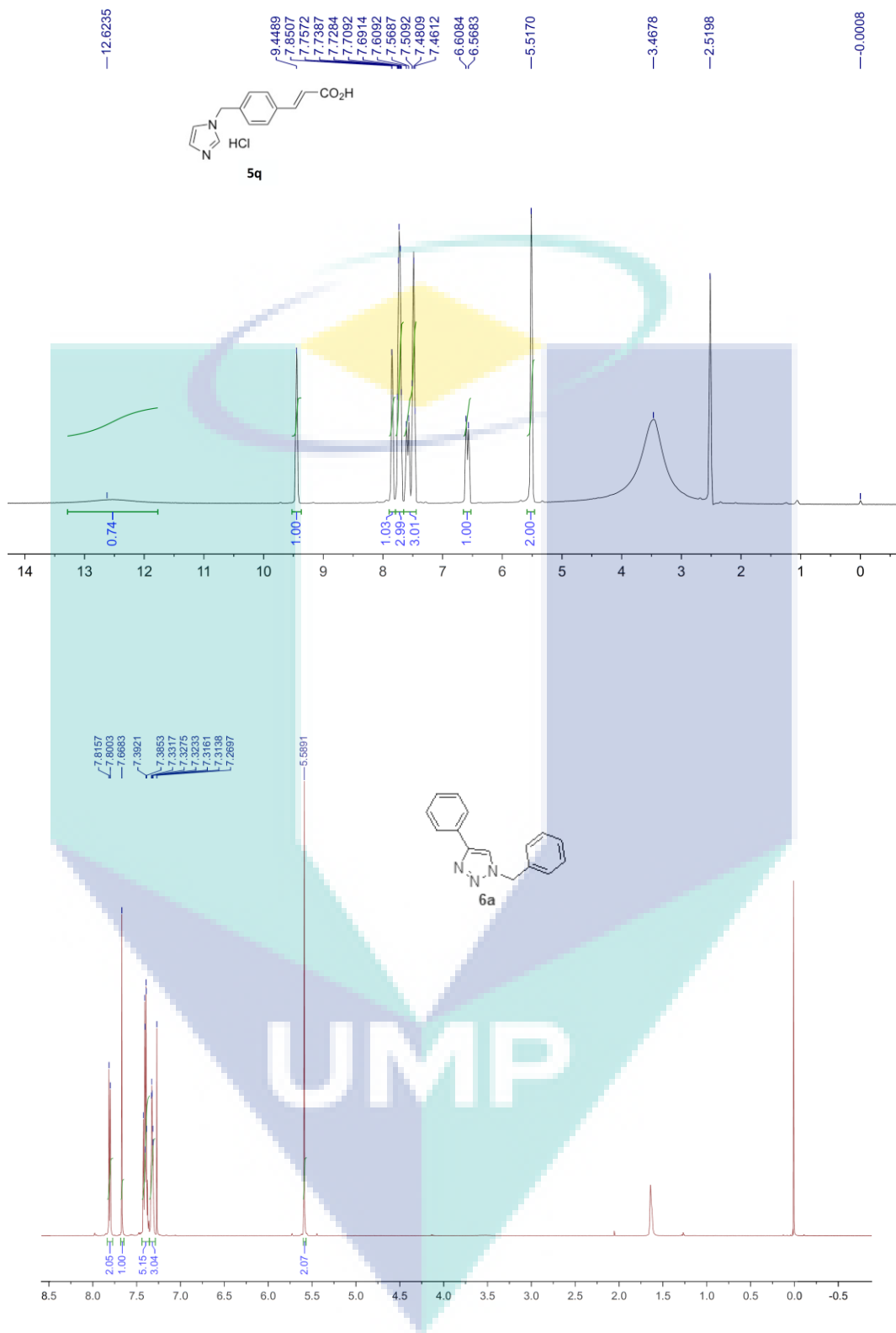


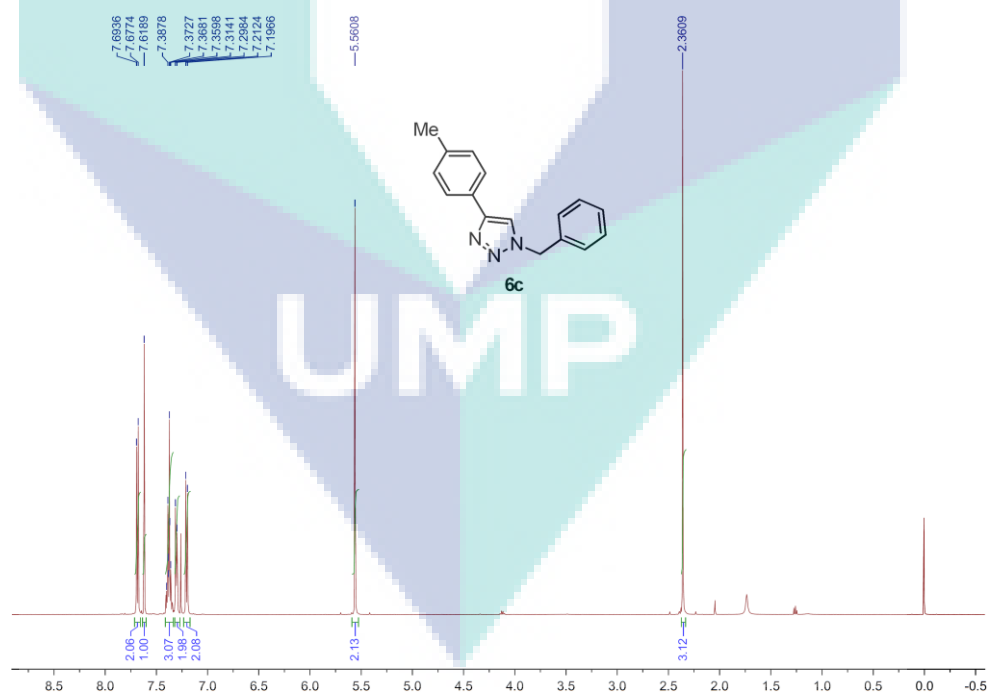
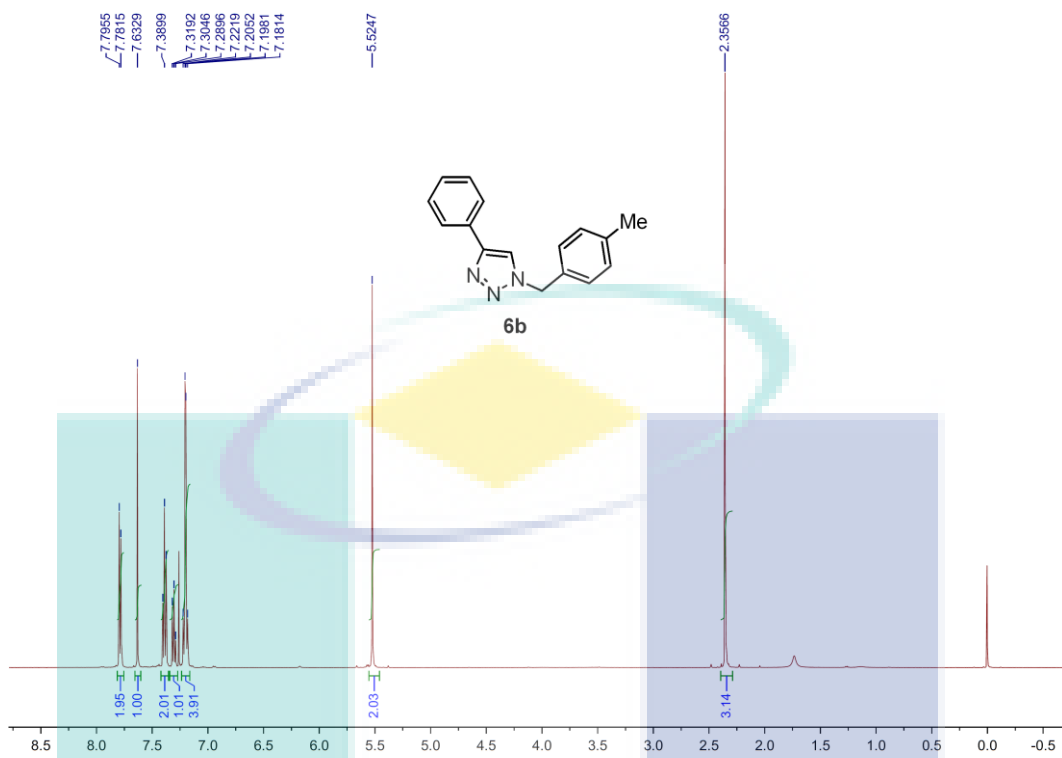


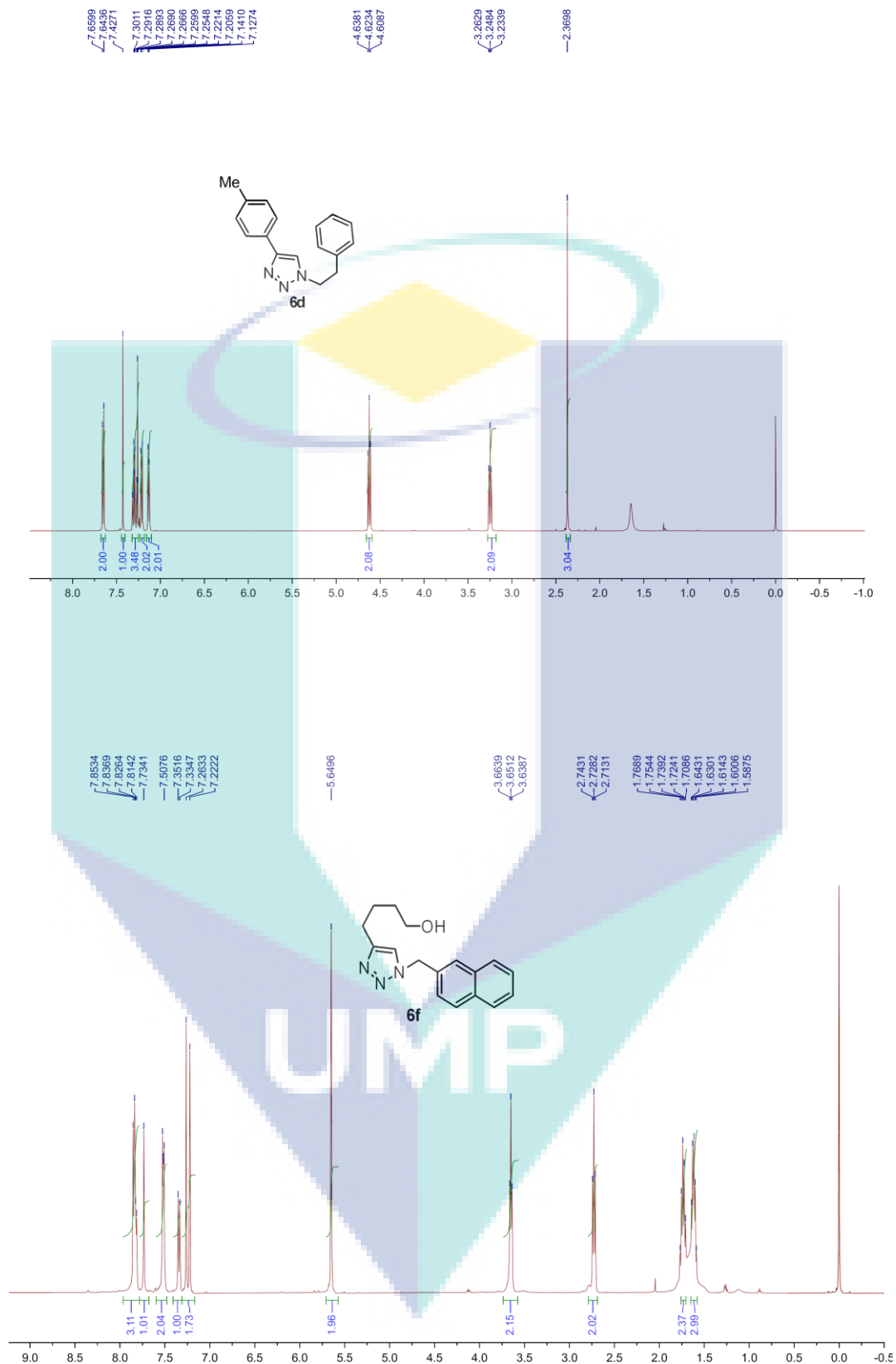


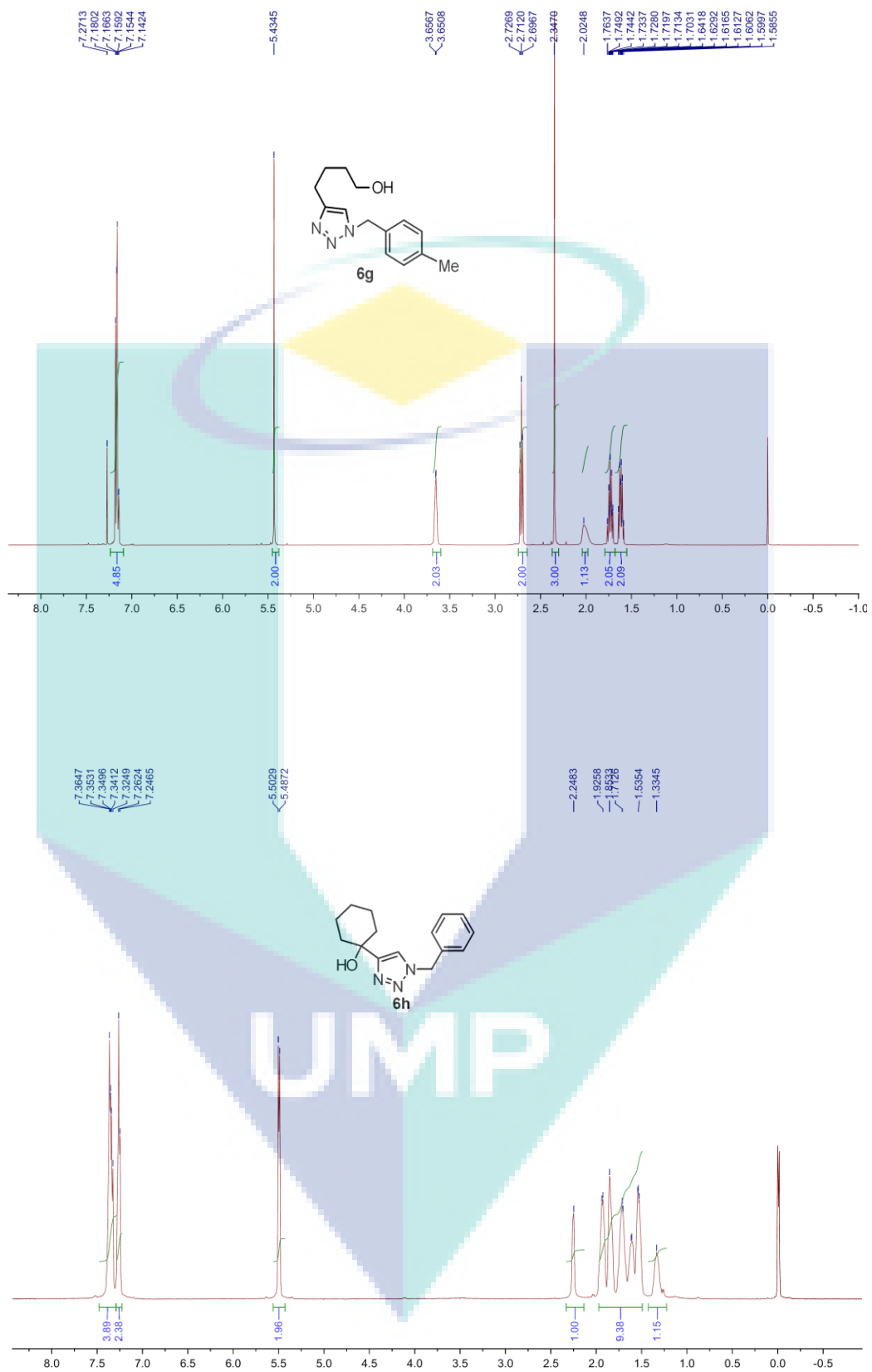


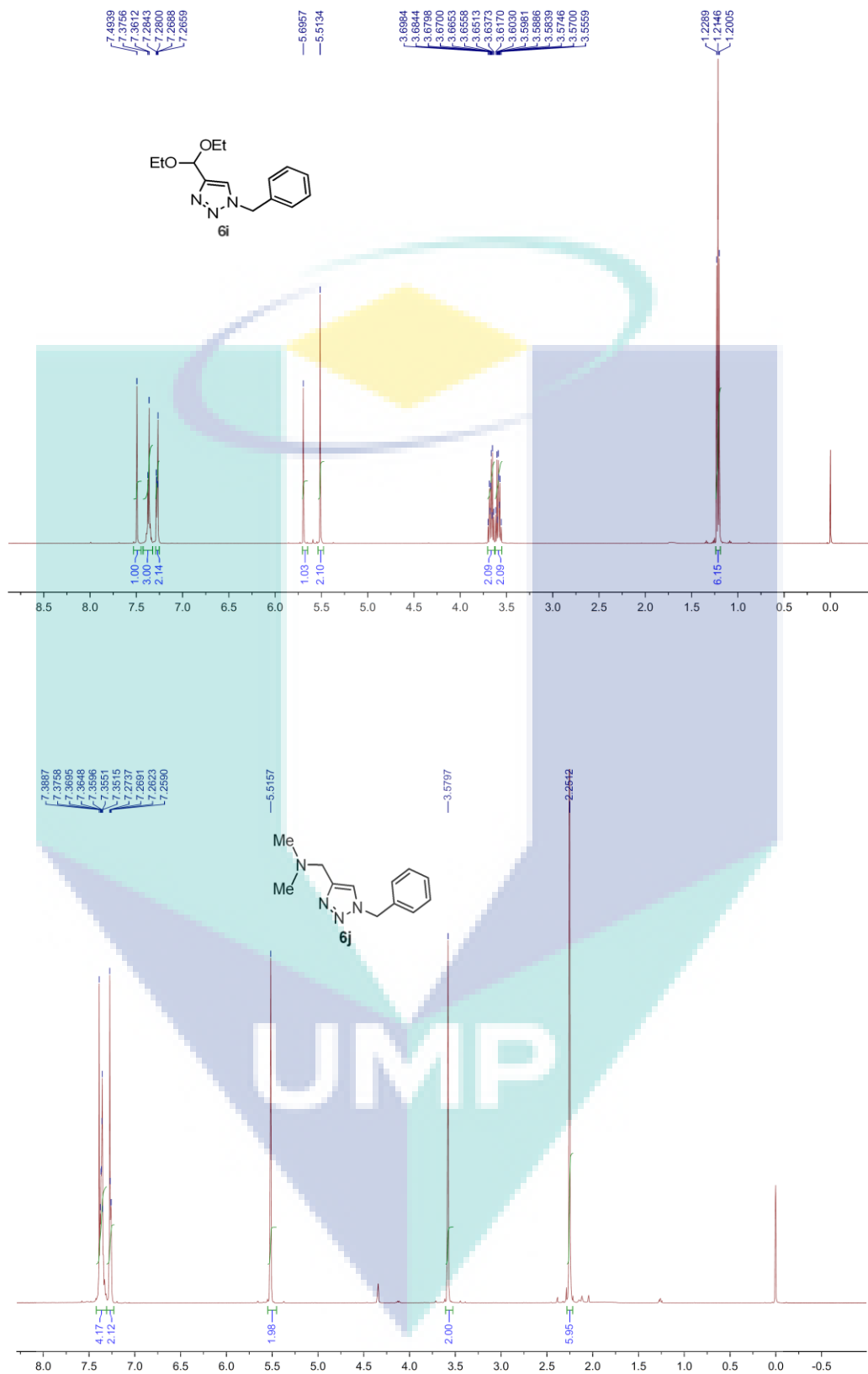


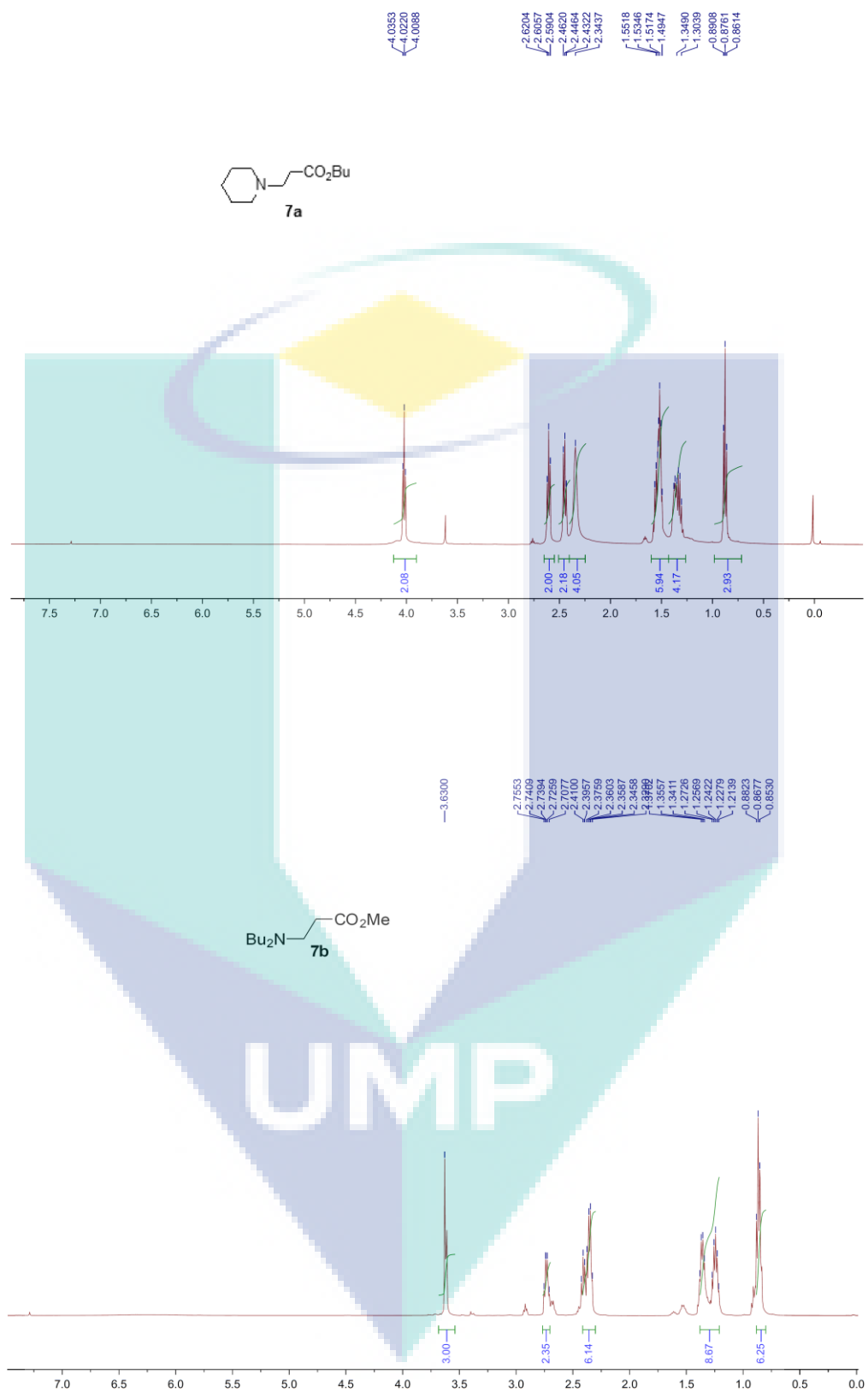


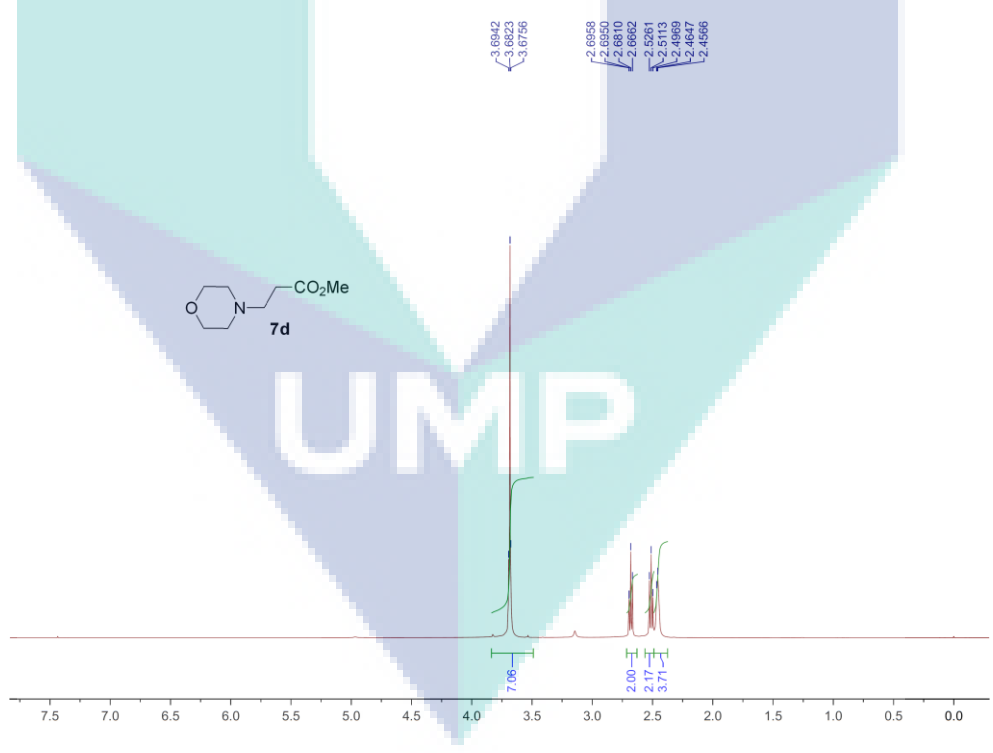
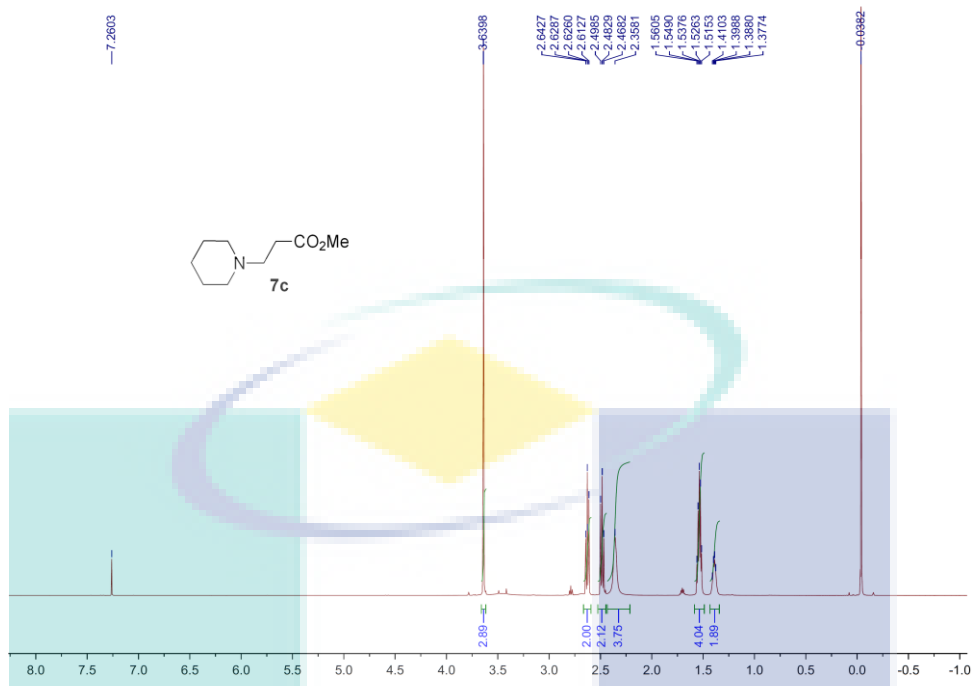


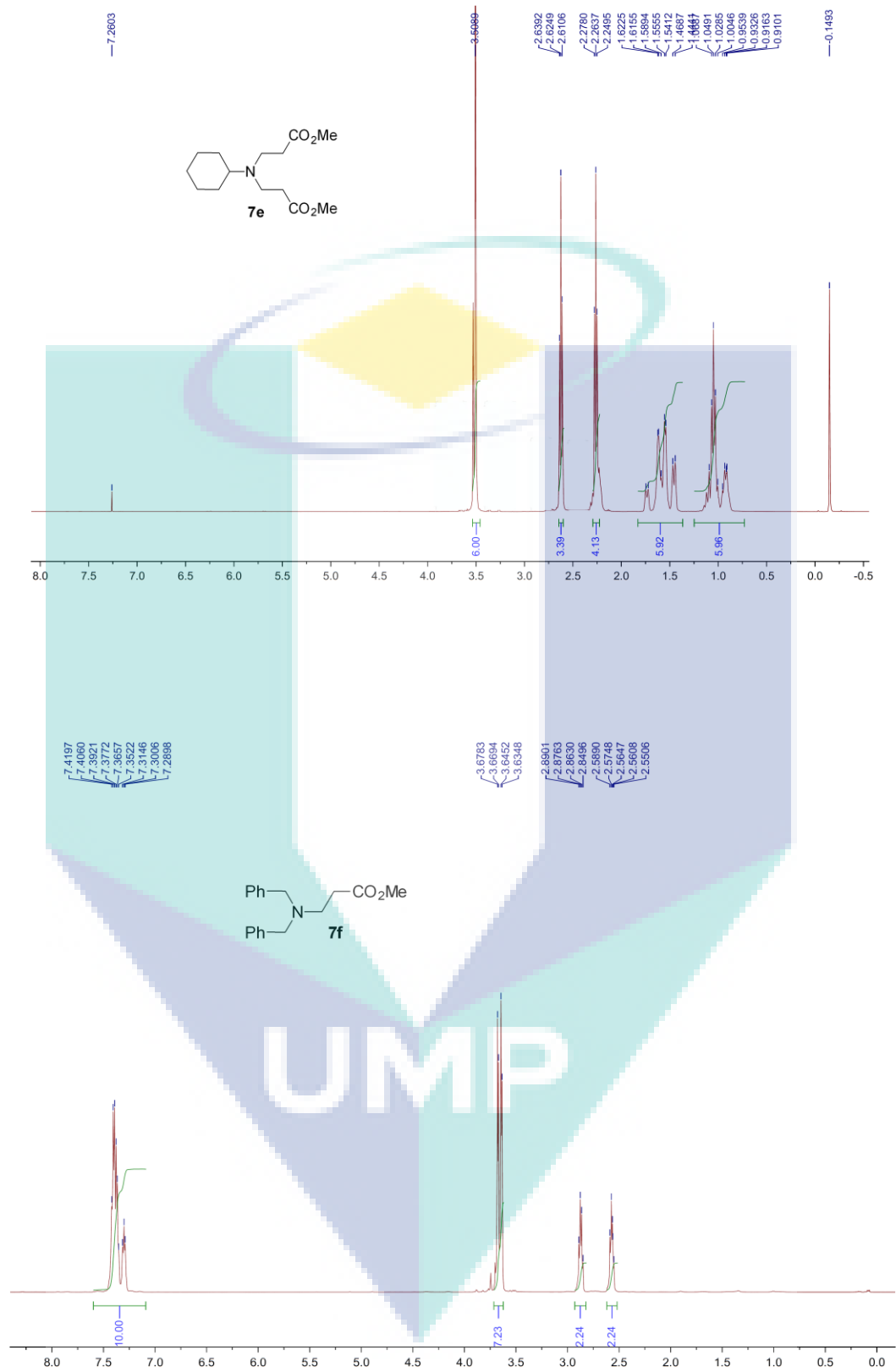


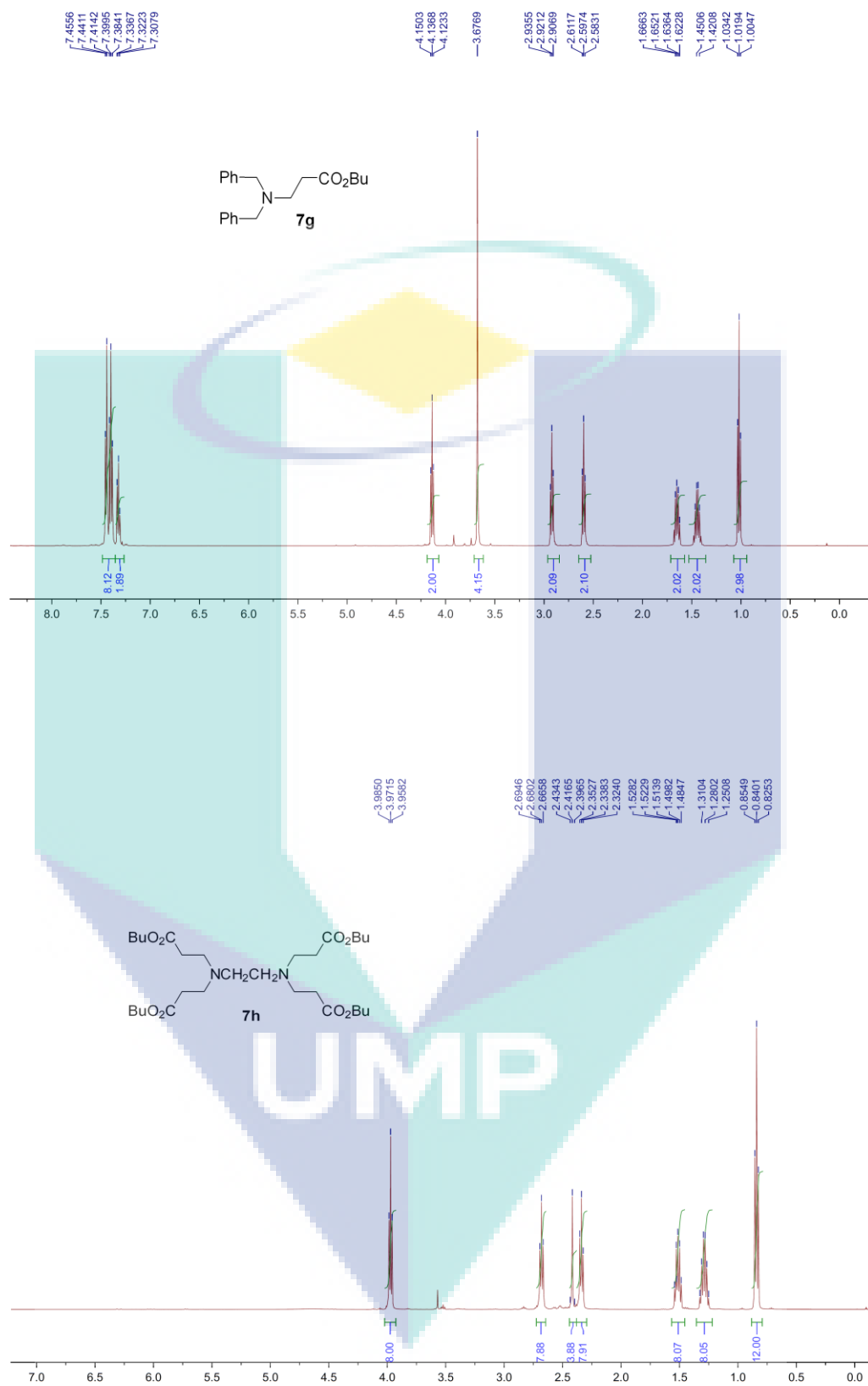


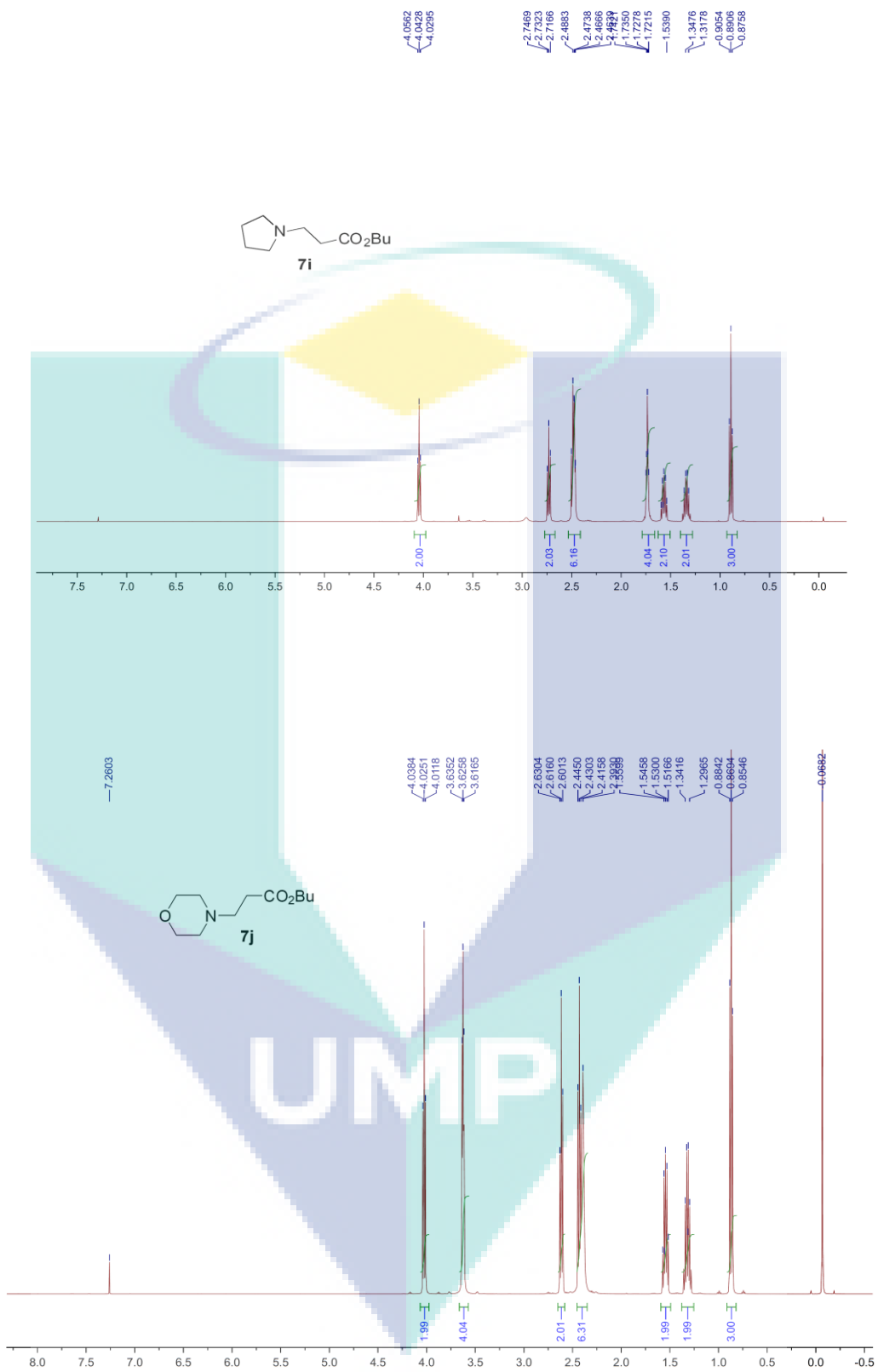


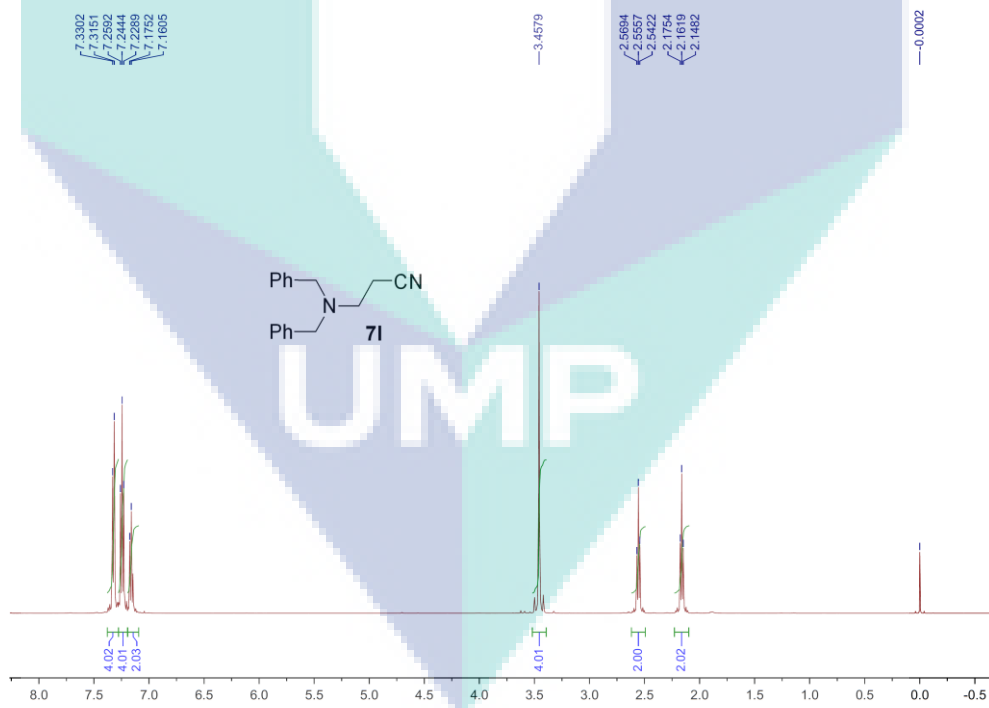
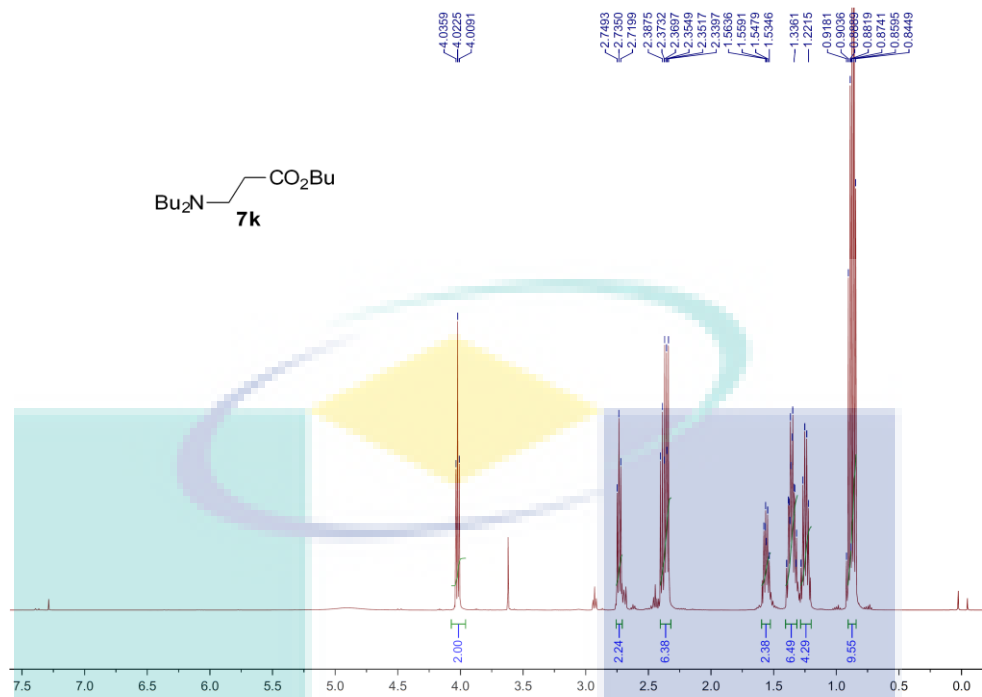


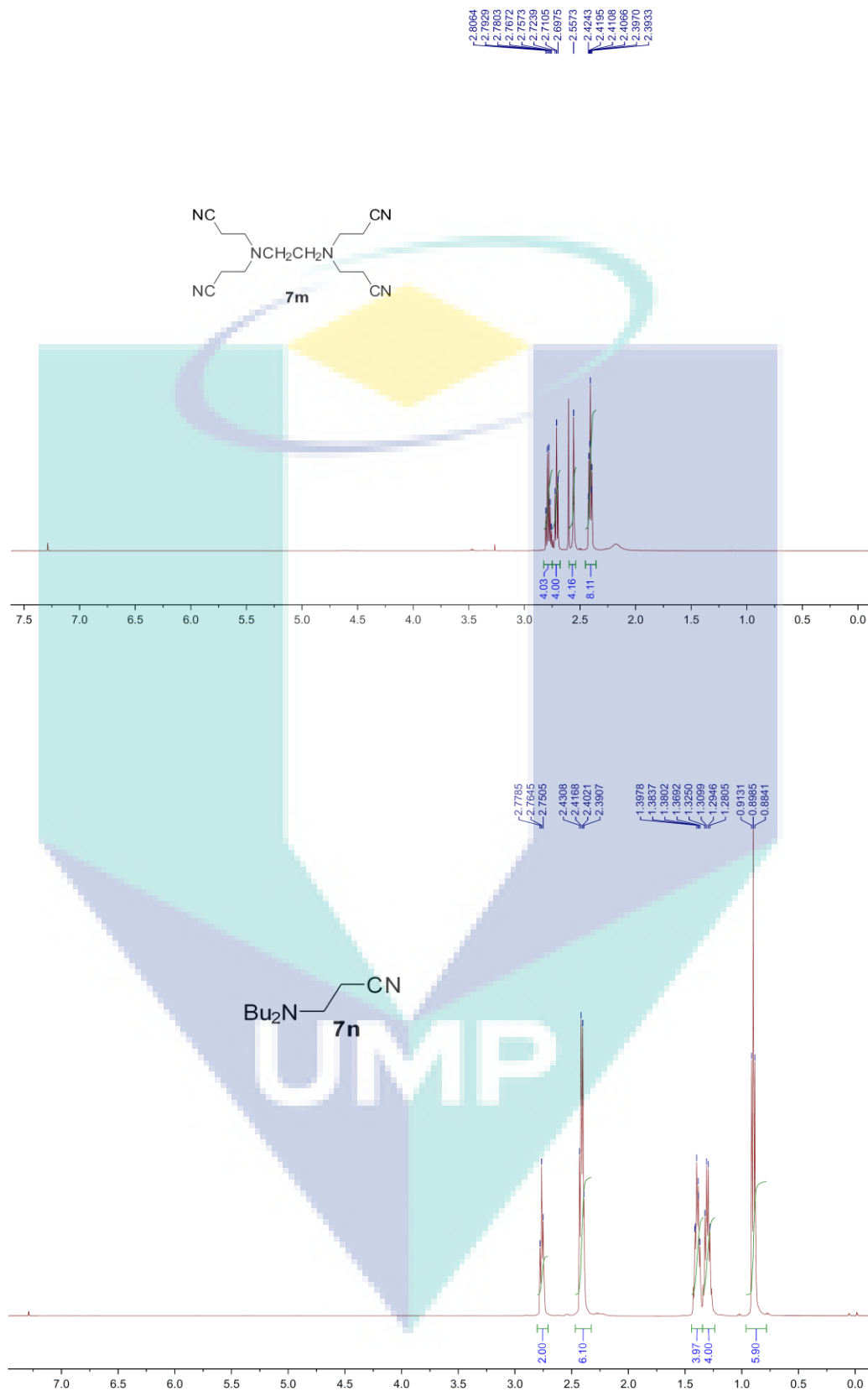




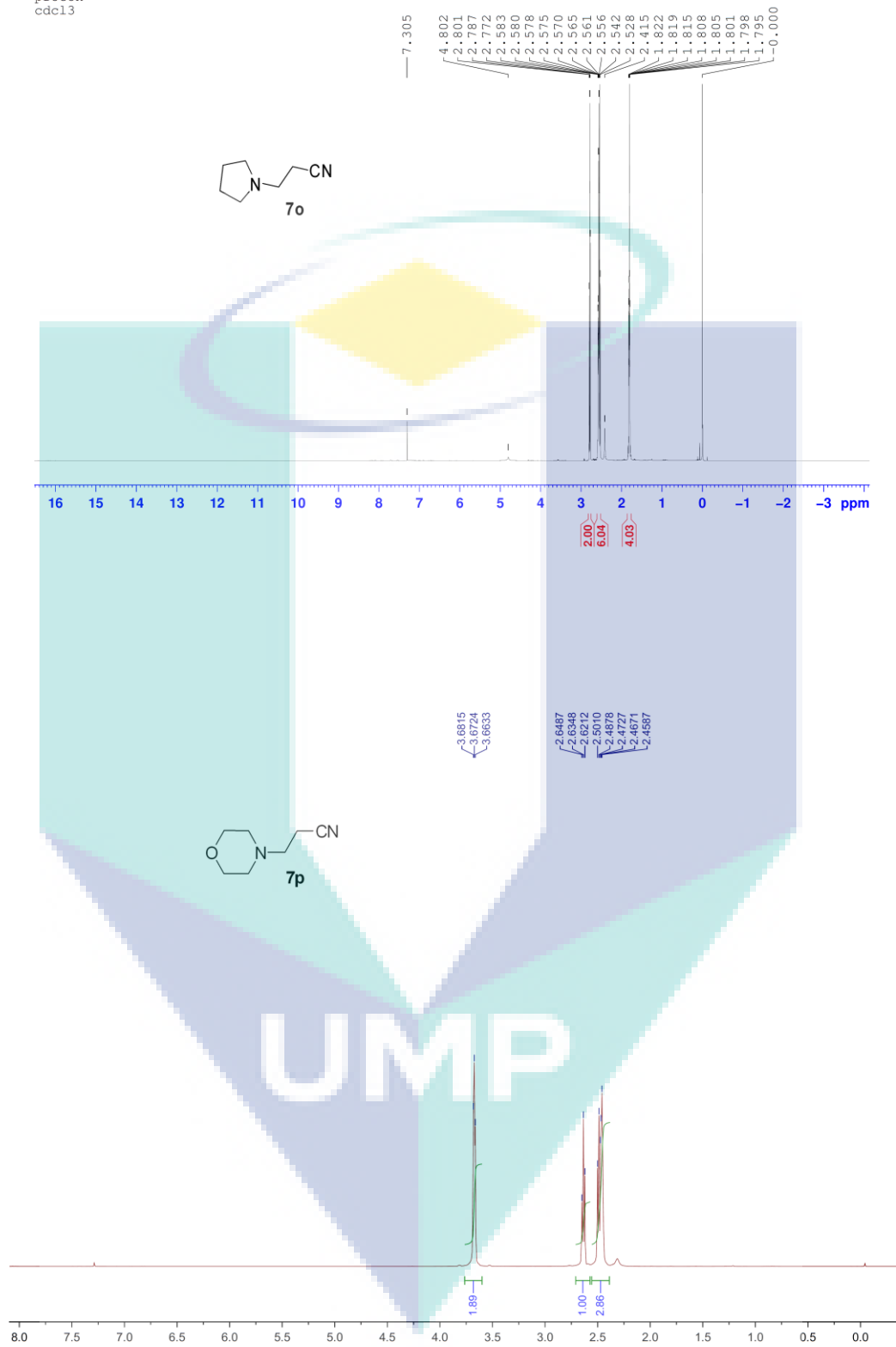


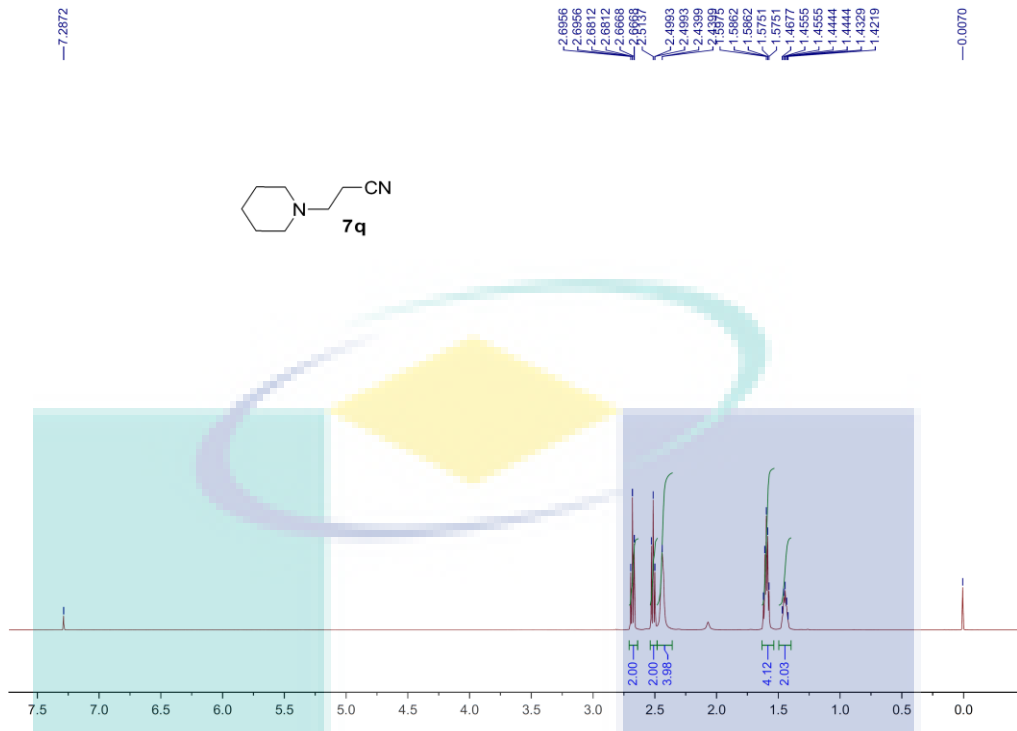






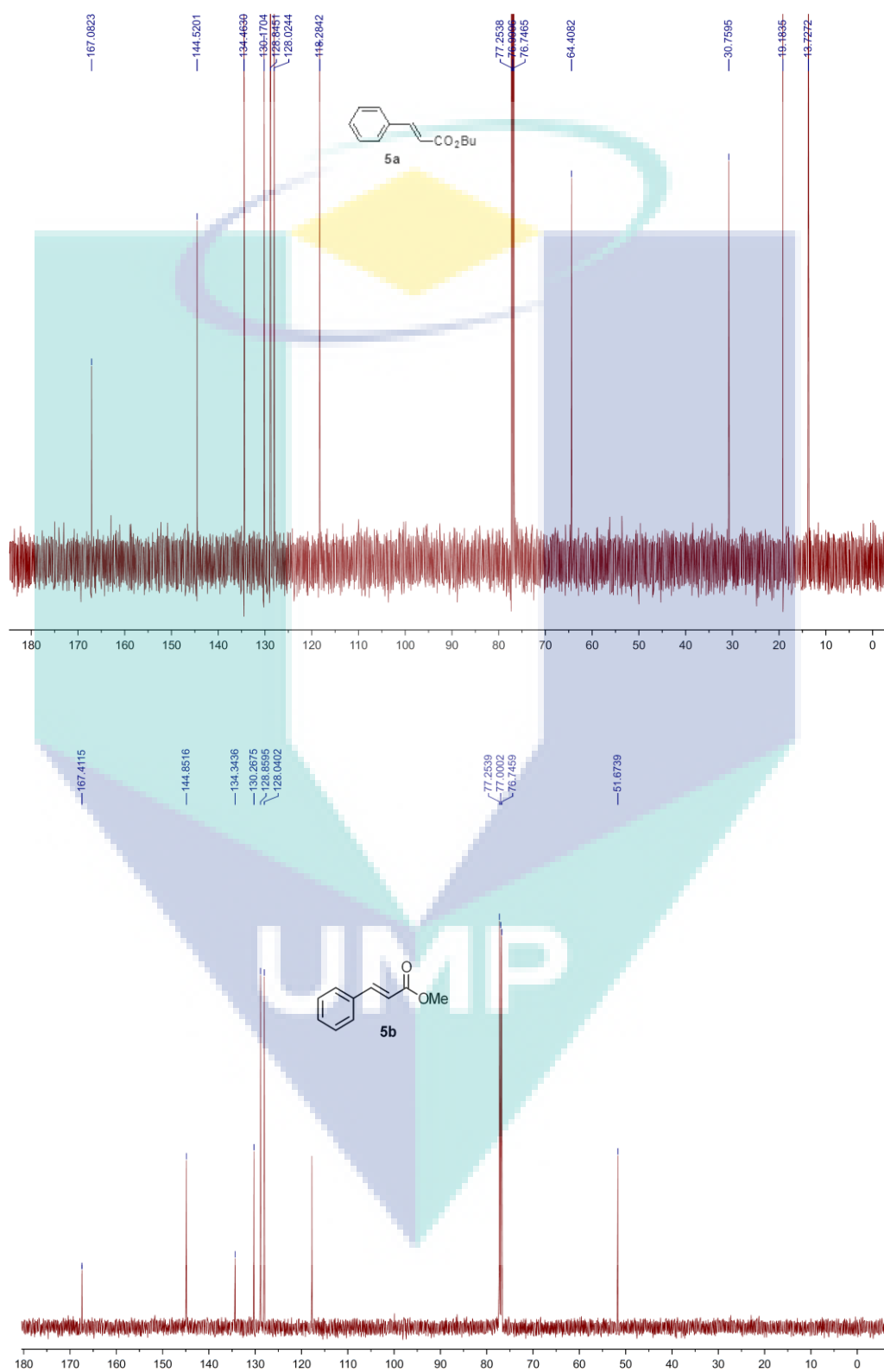
sample 20
proton
cdcl3

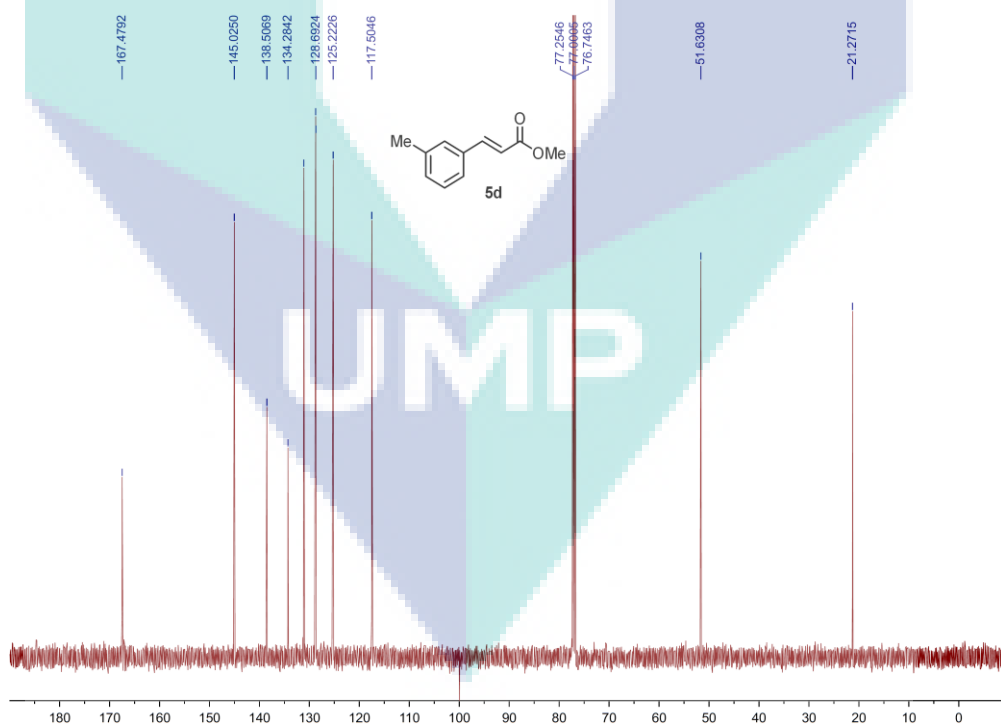
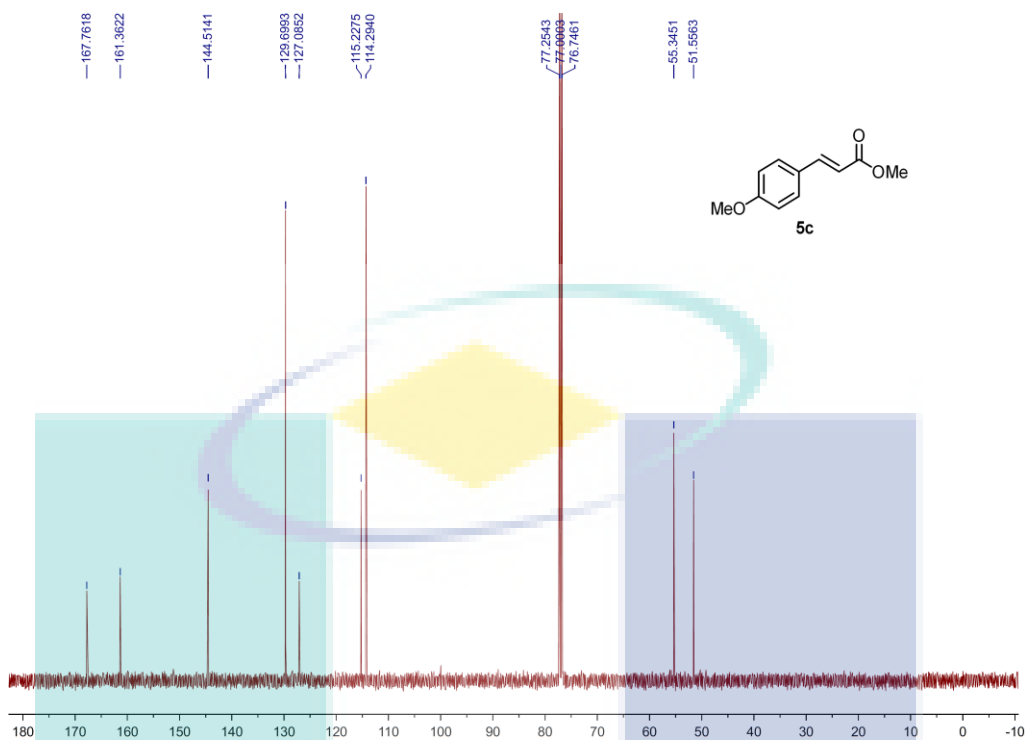


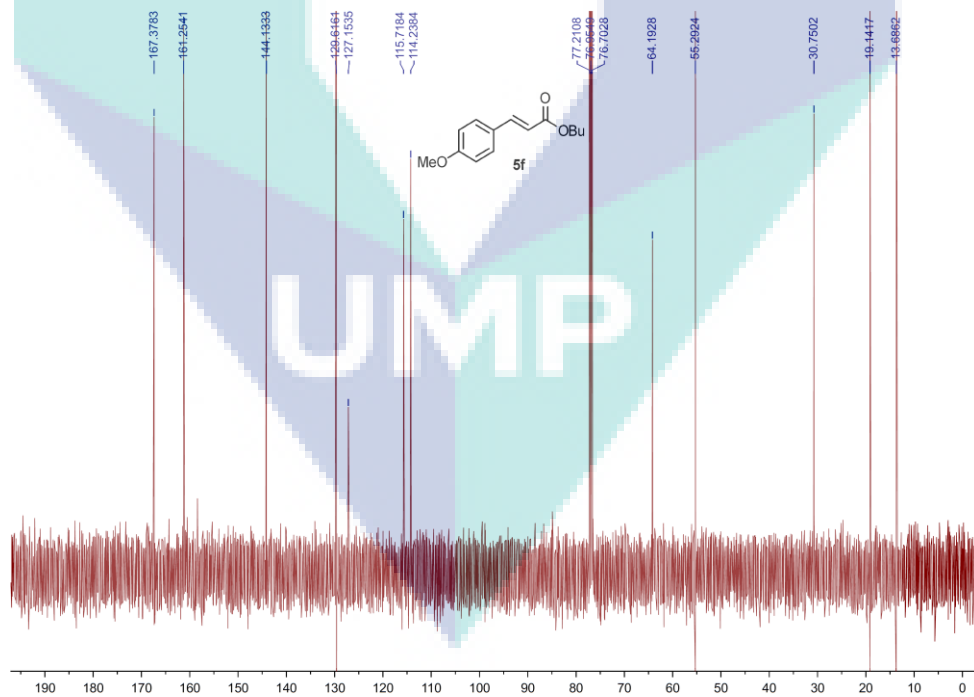
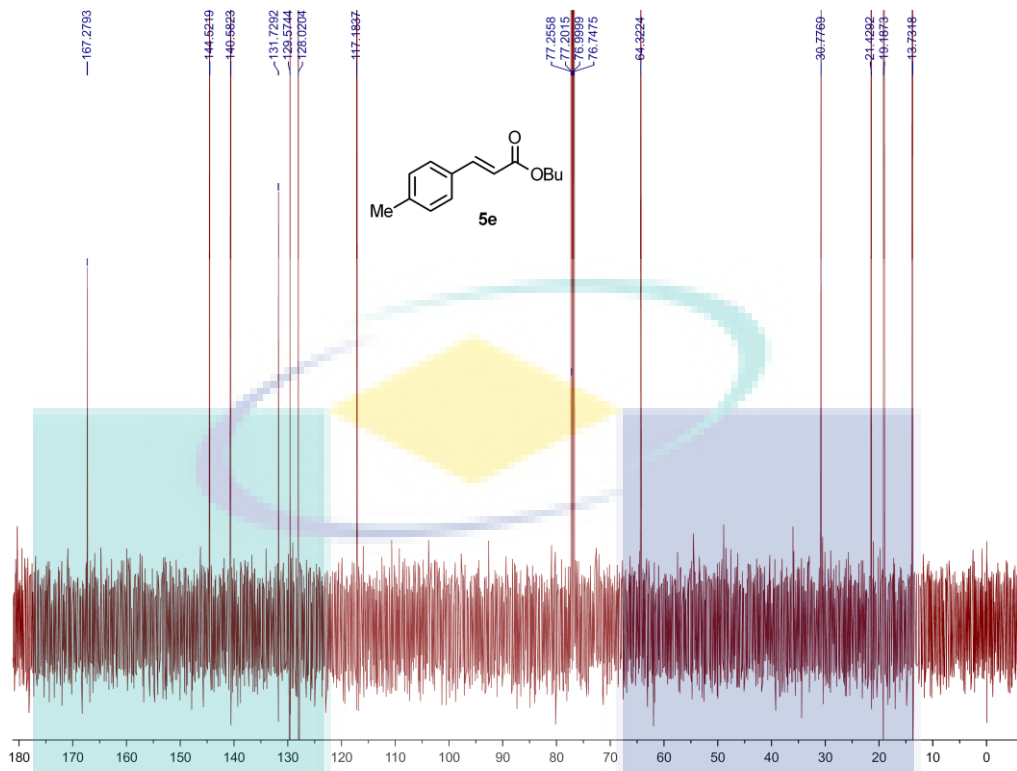


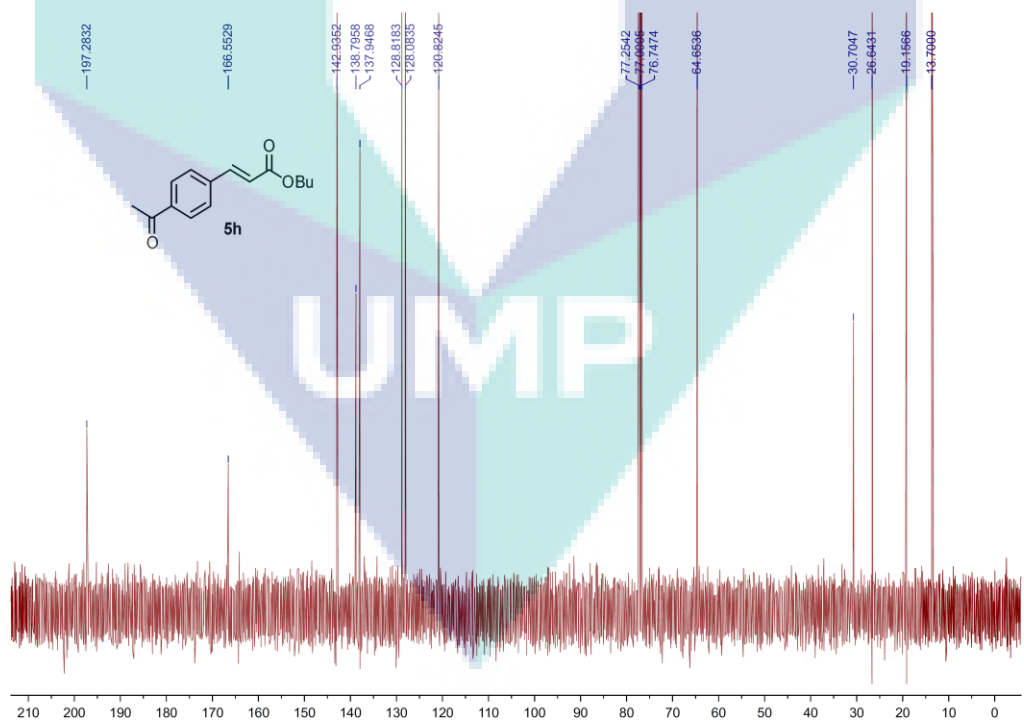
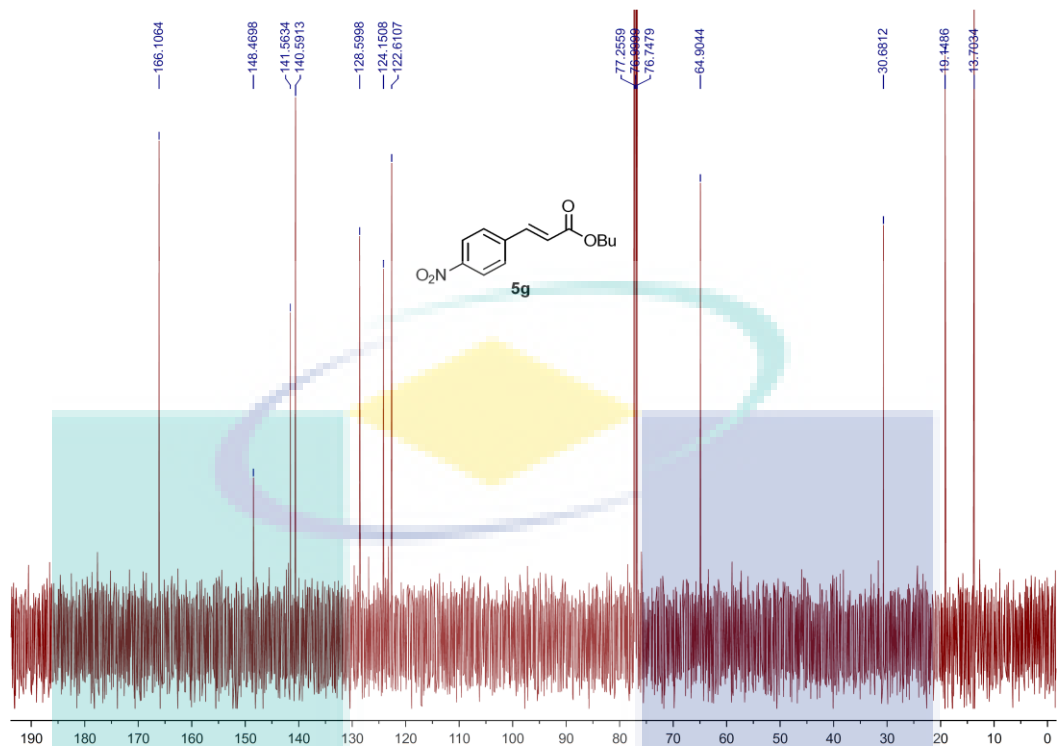
UMP

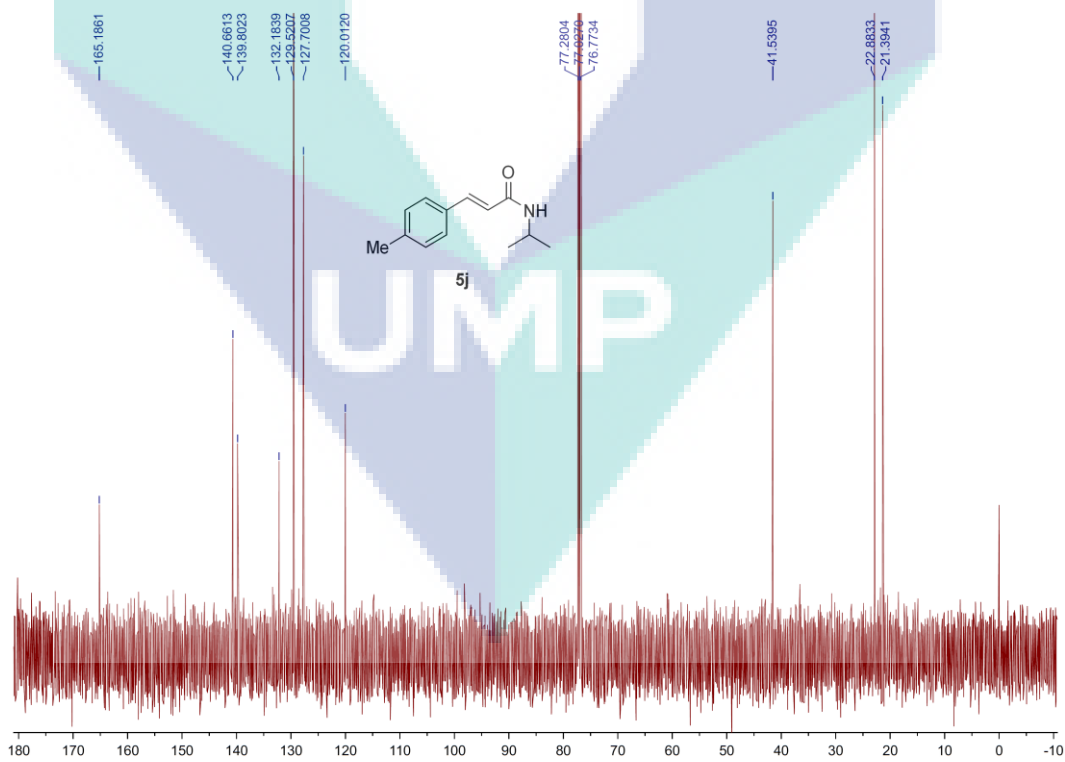
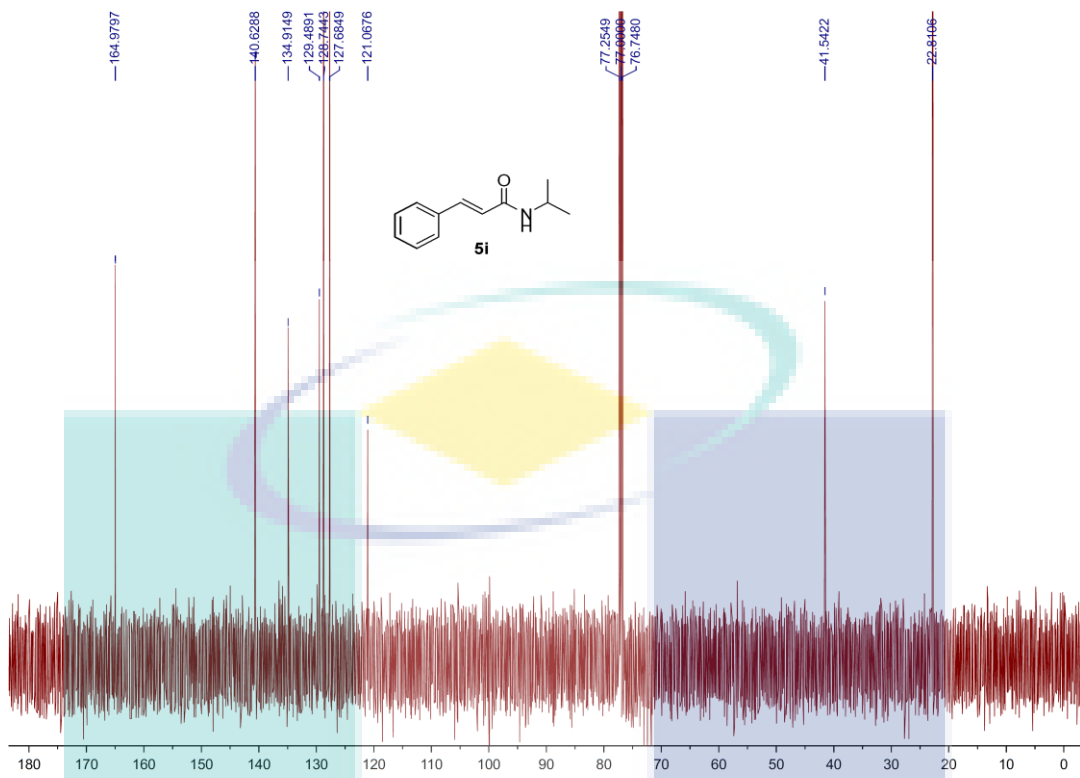
APPENDIX B (¹³C NMR)

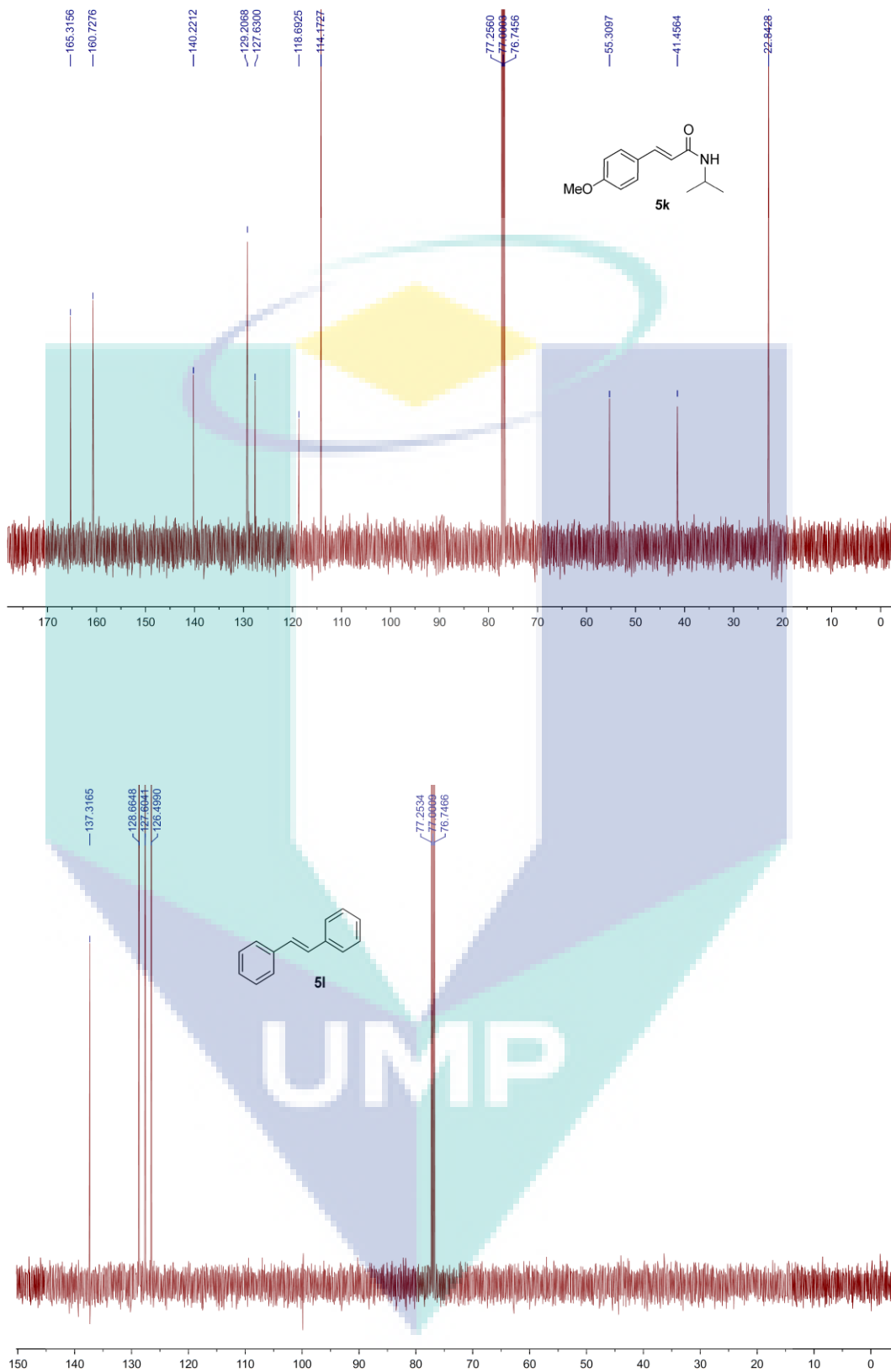


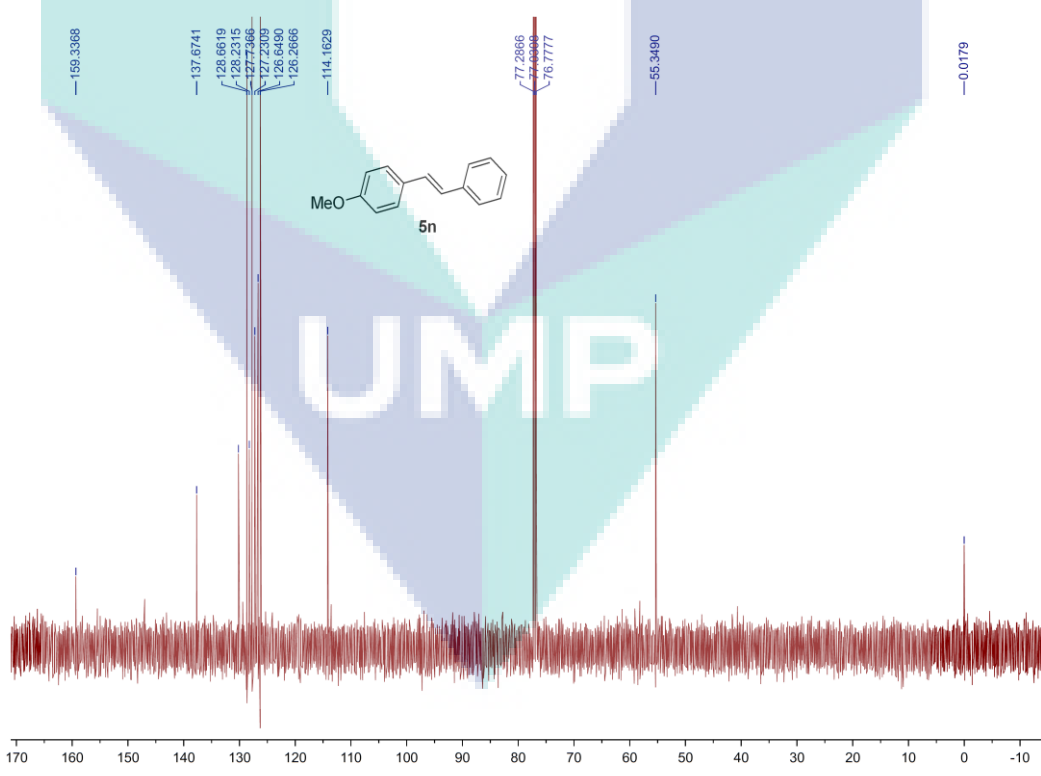
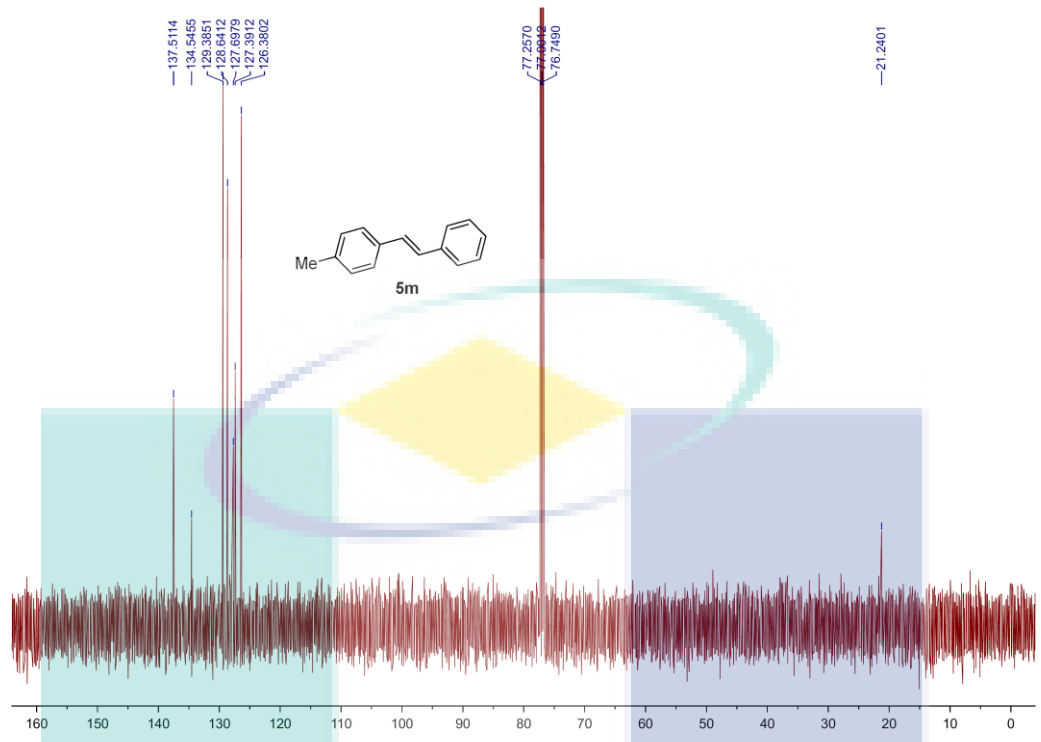


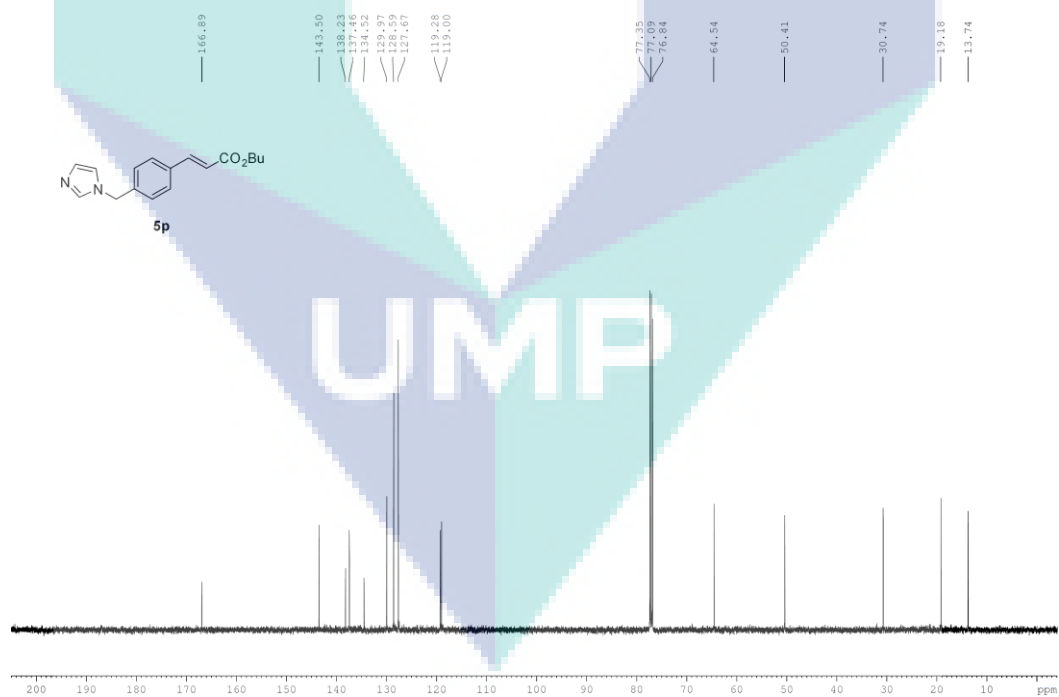
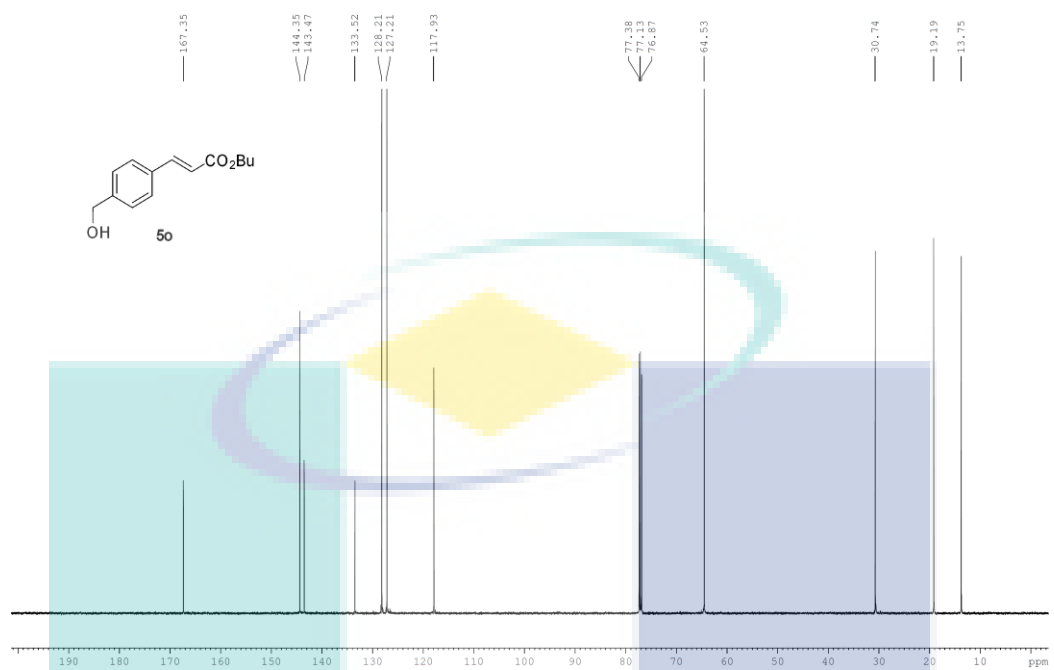


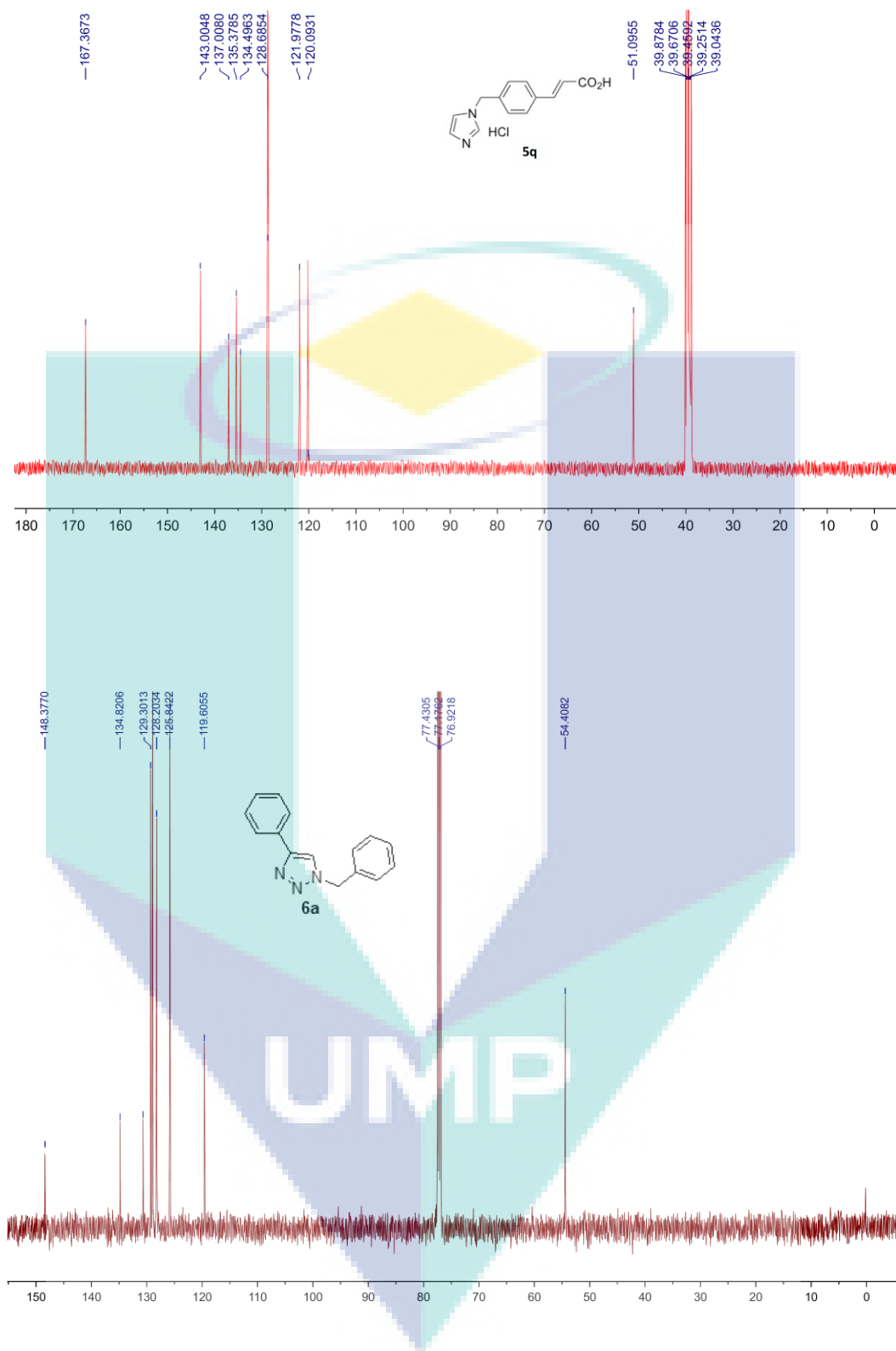


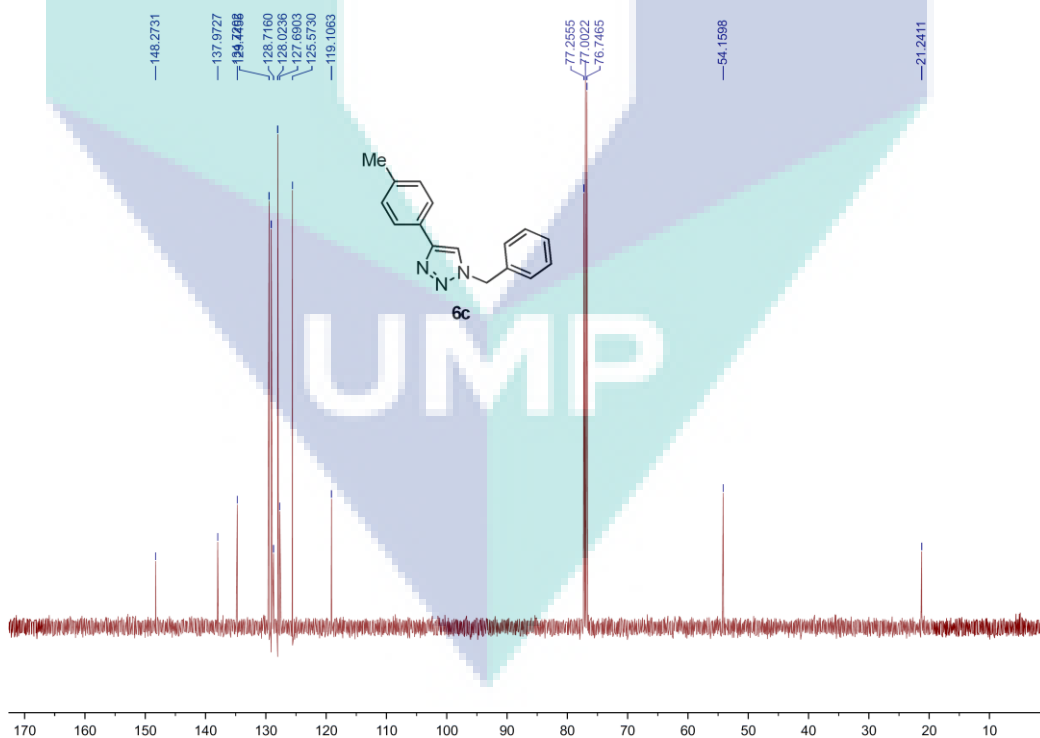
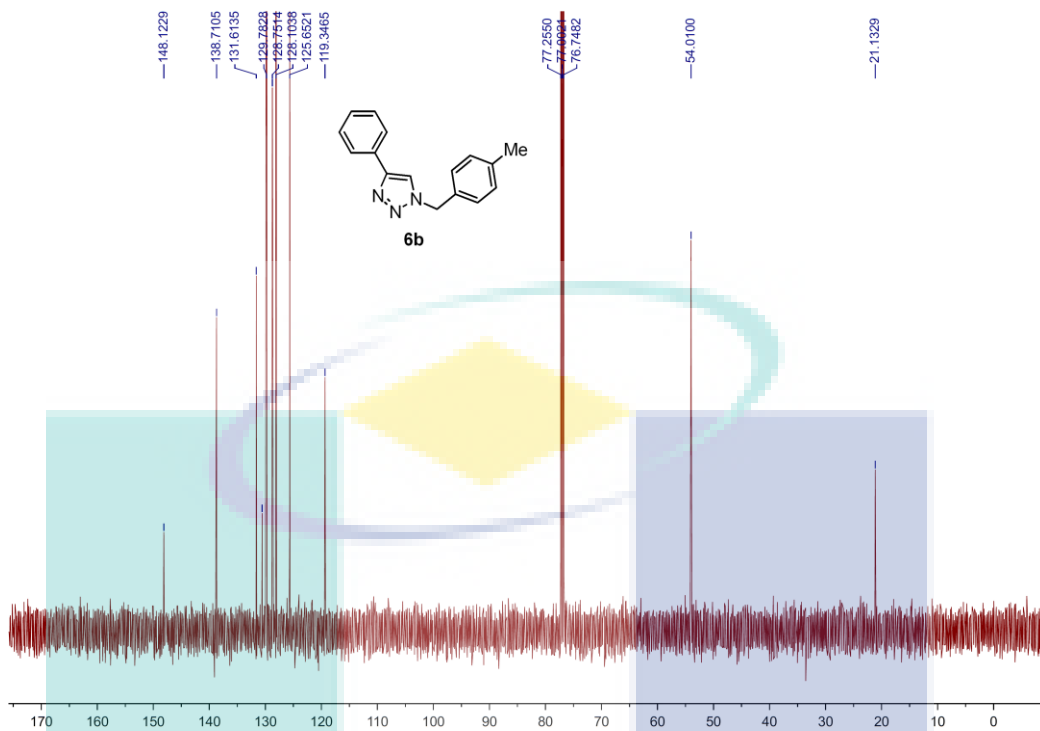


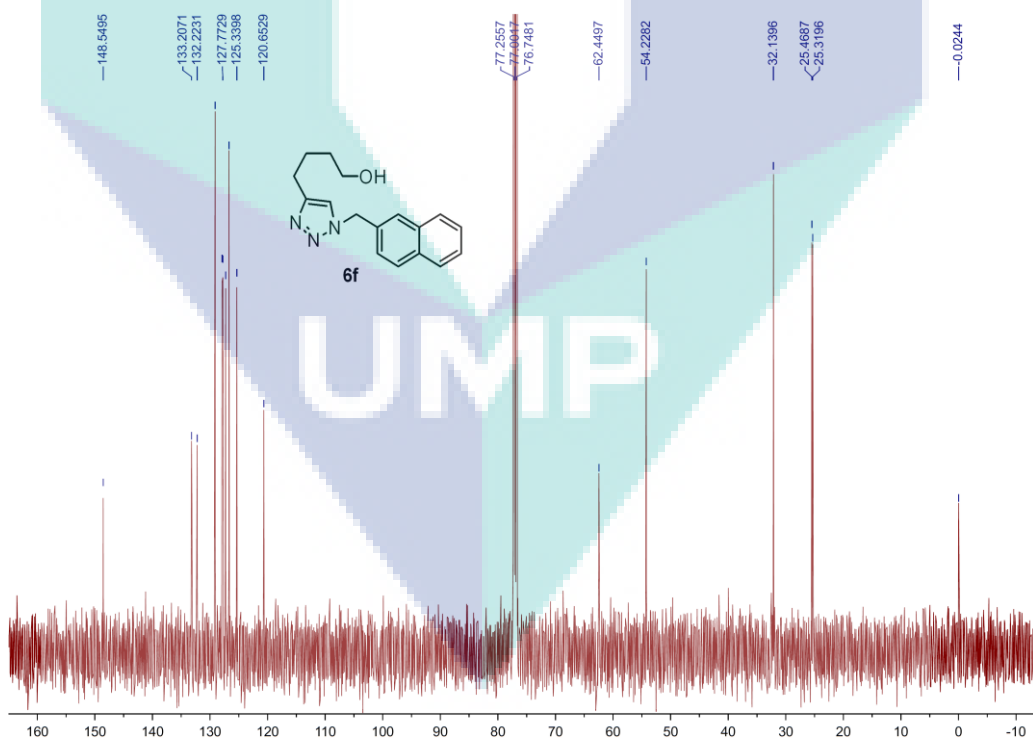
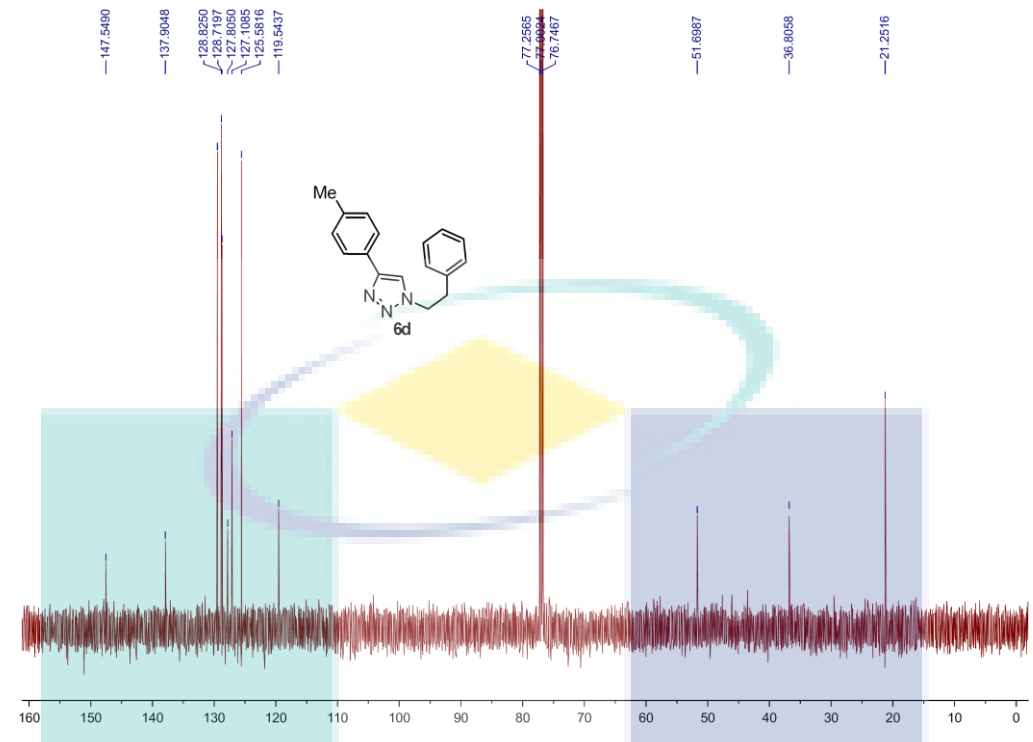


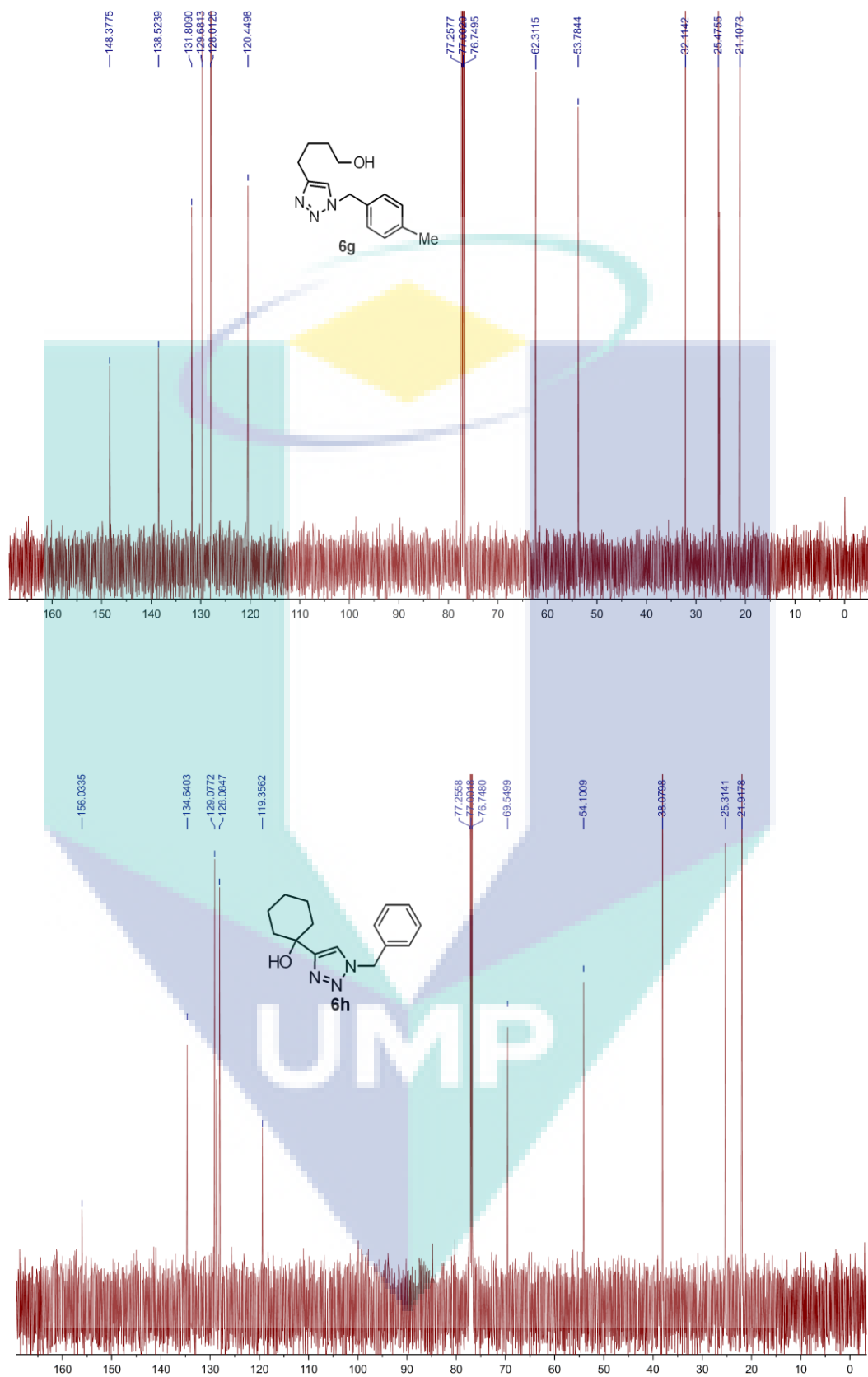


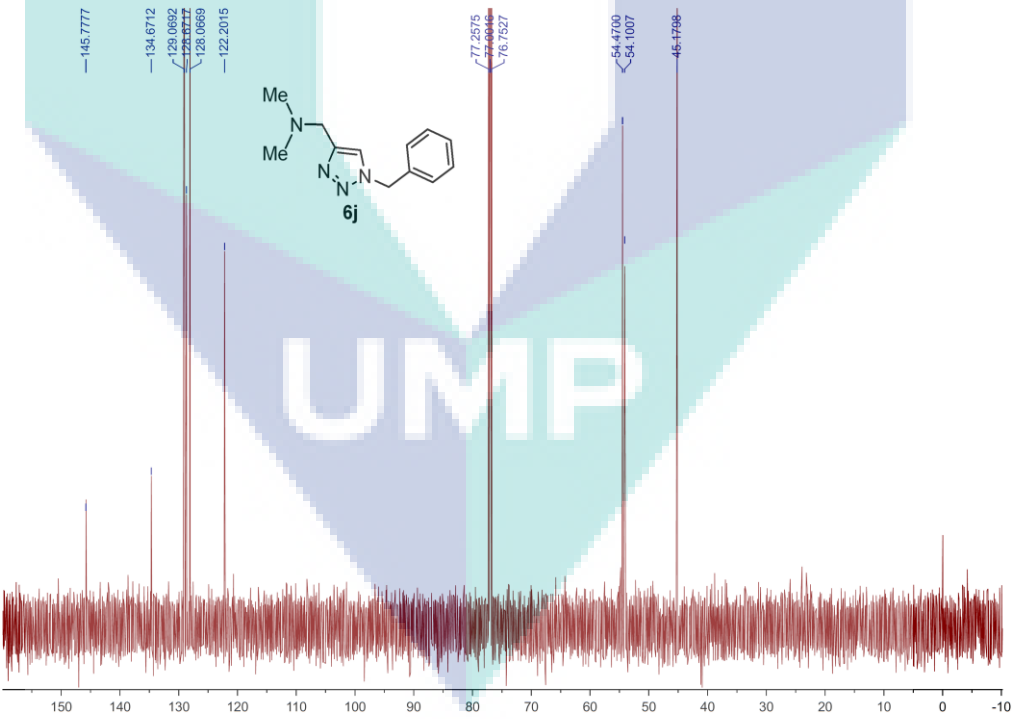
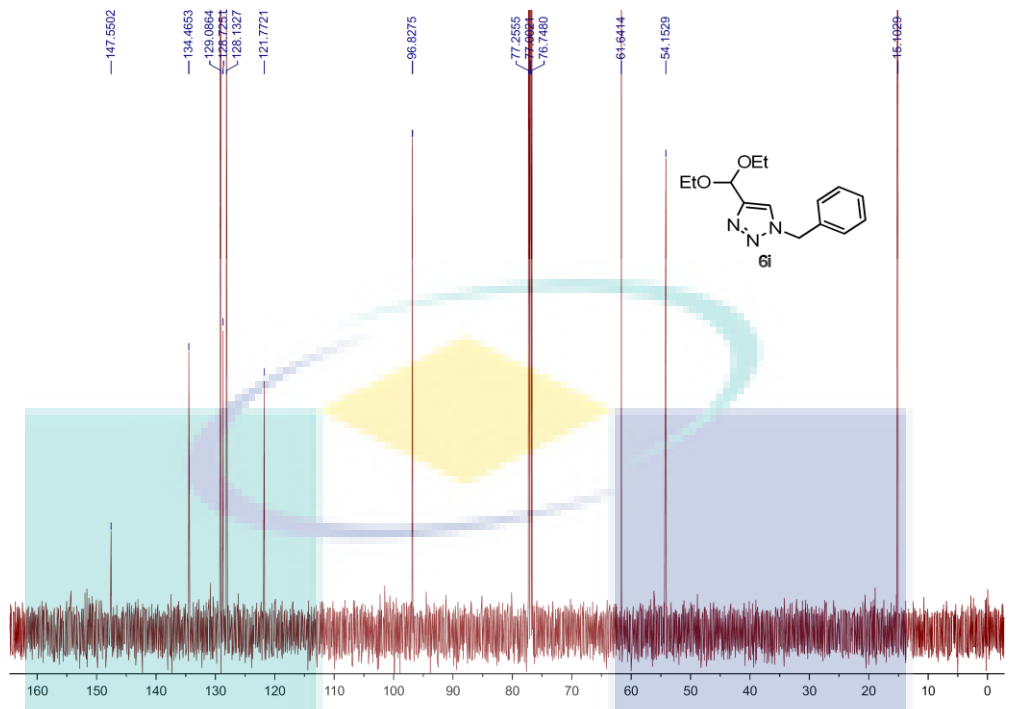


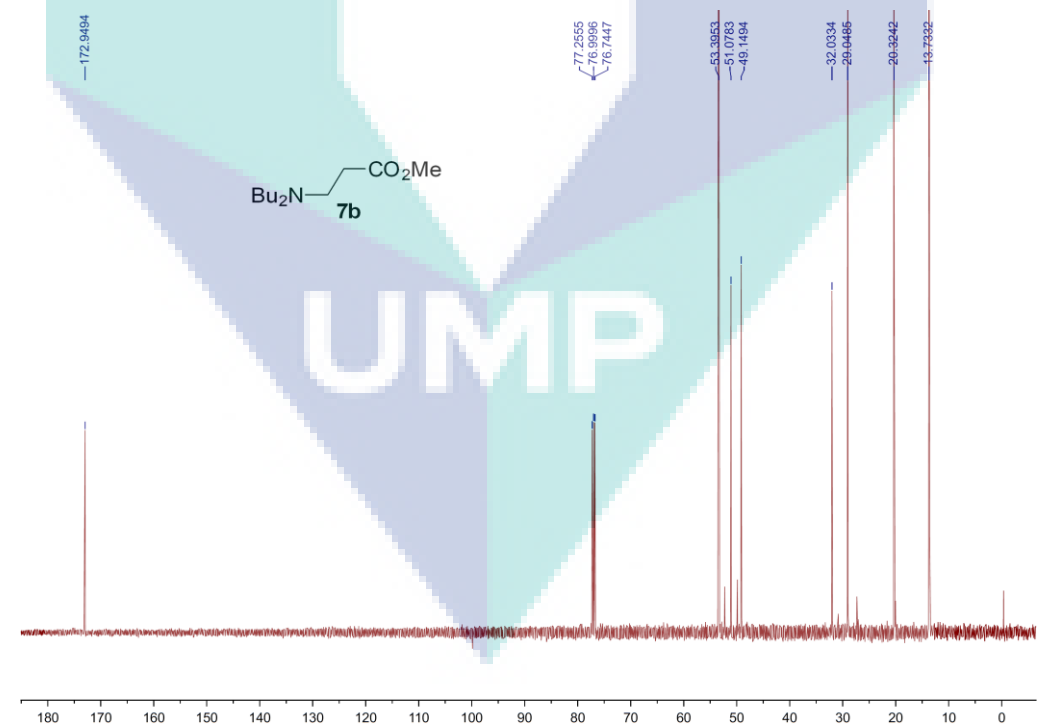
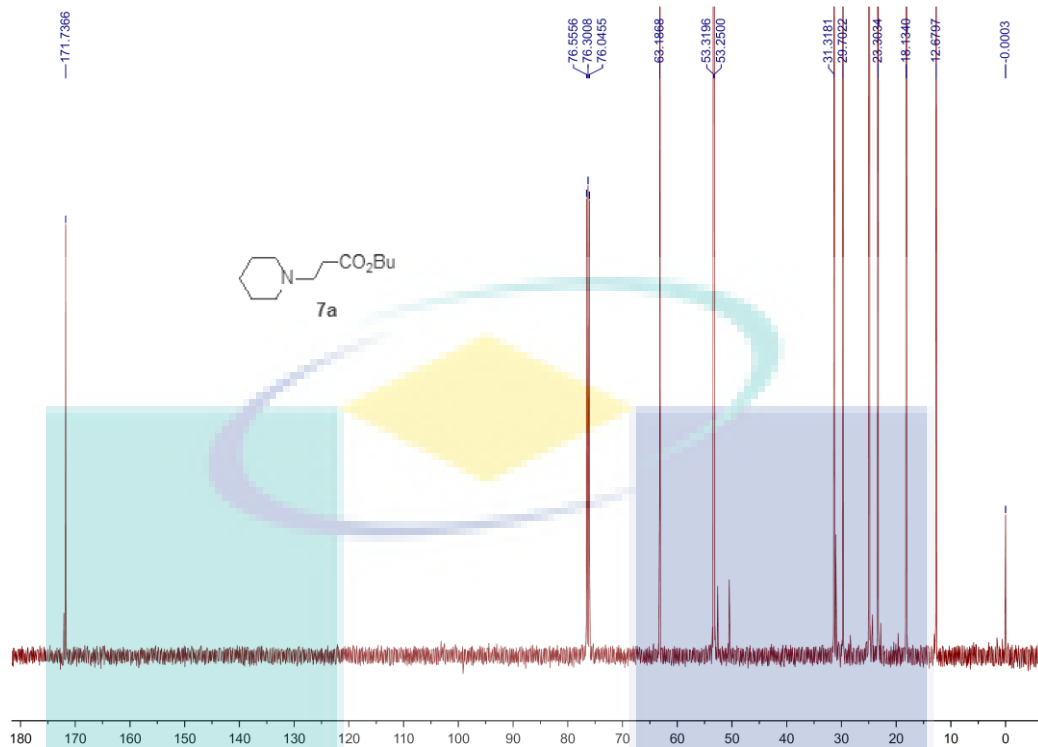


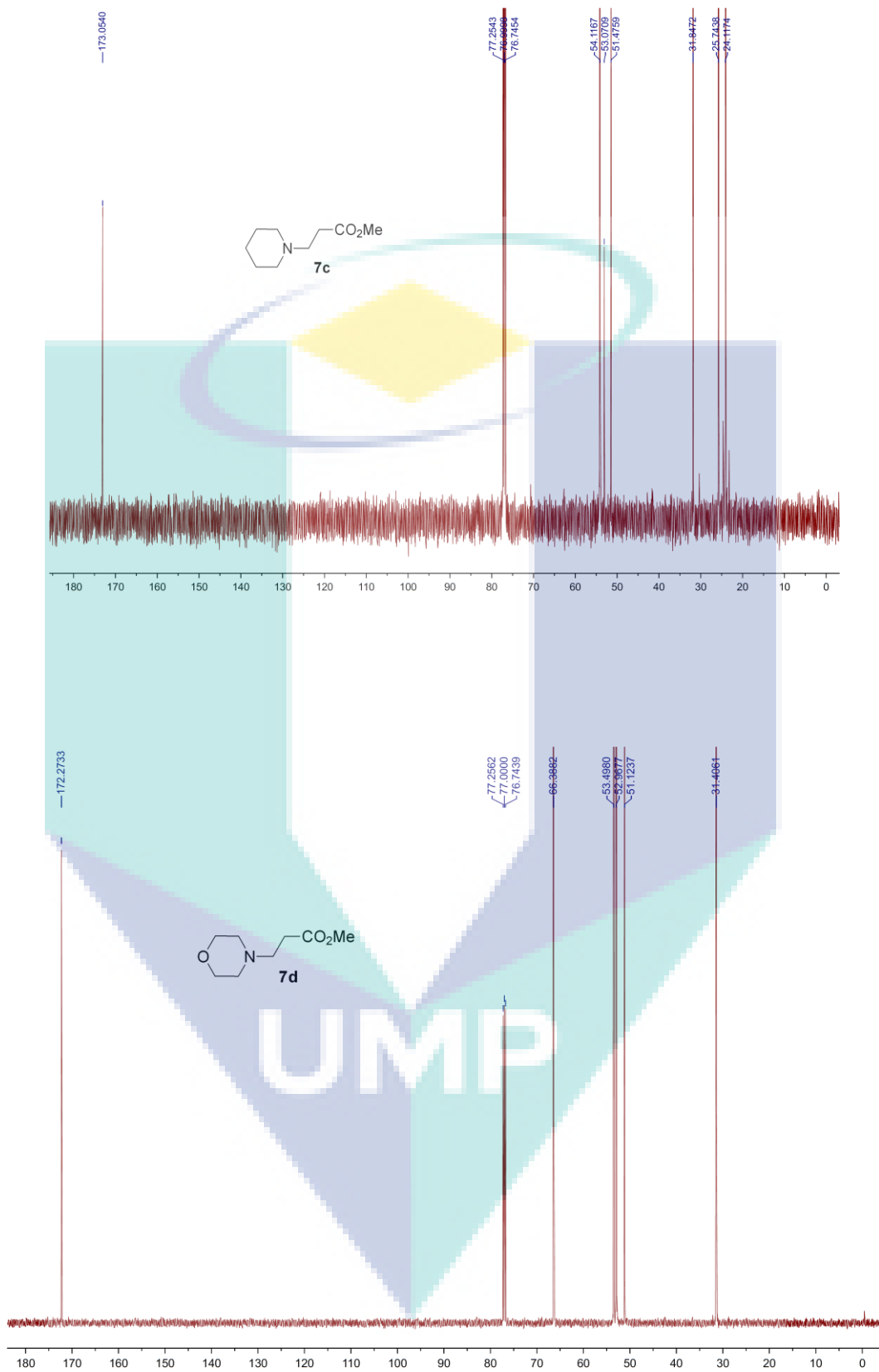


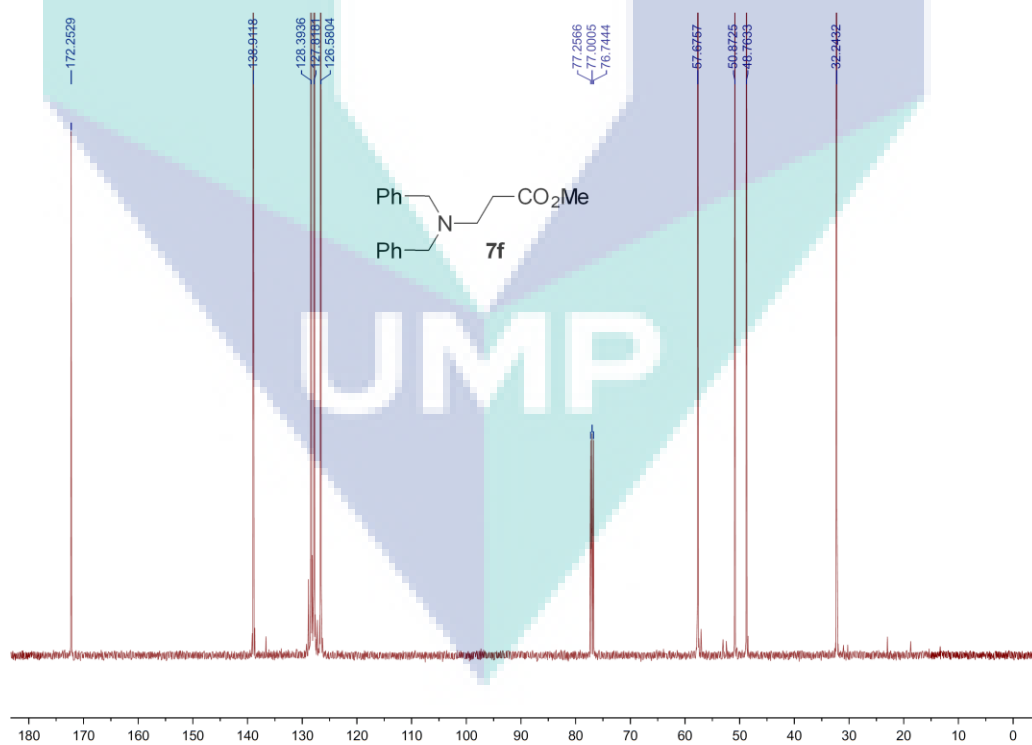
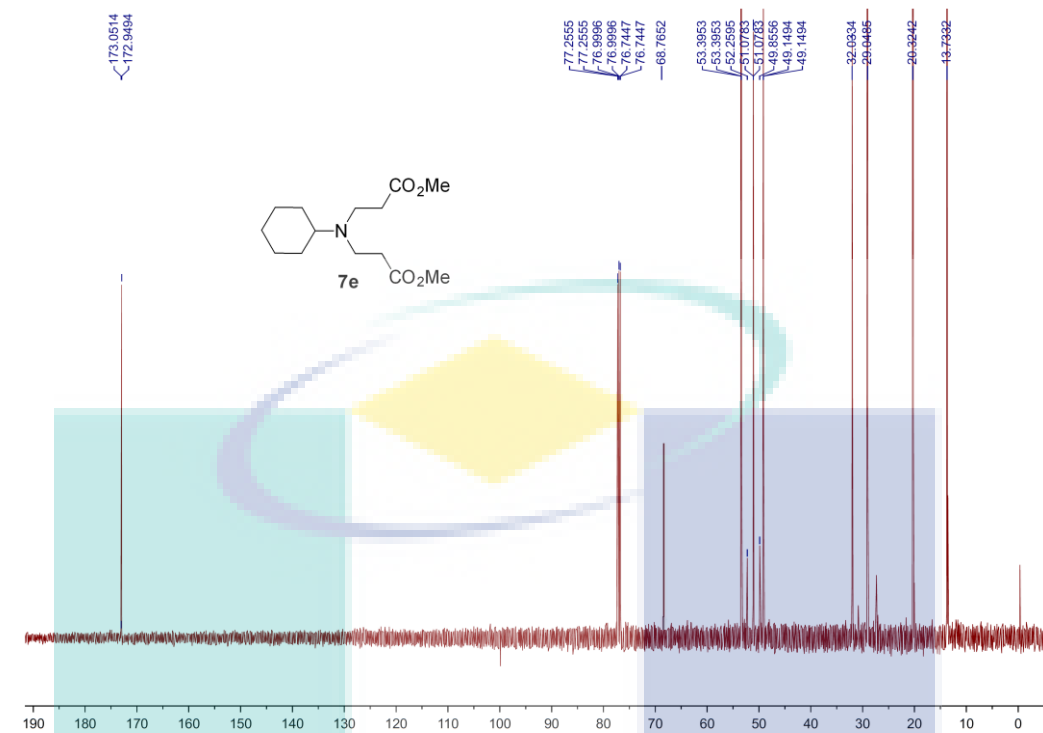


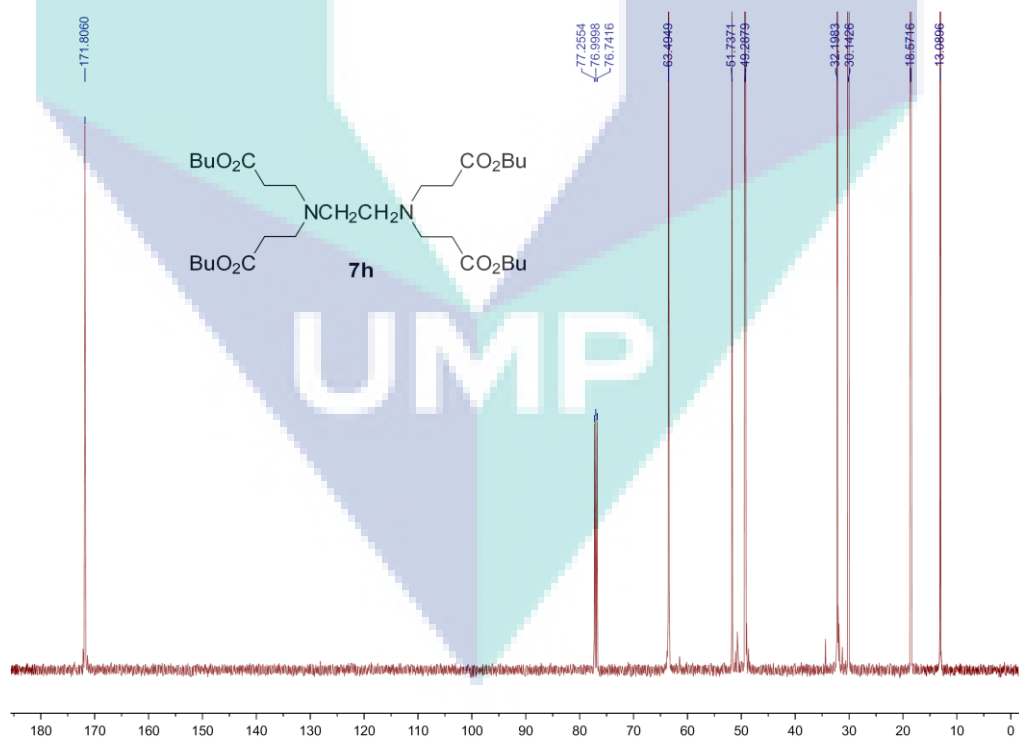
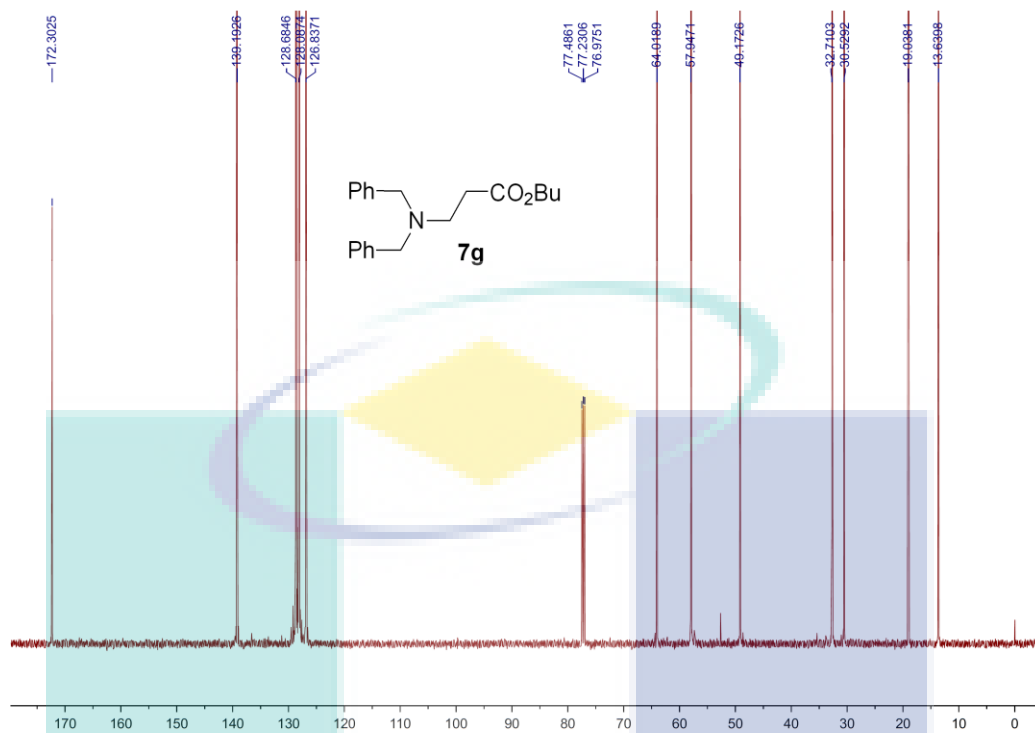


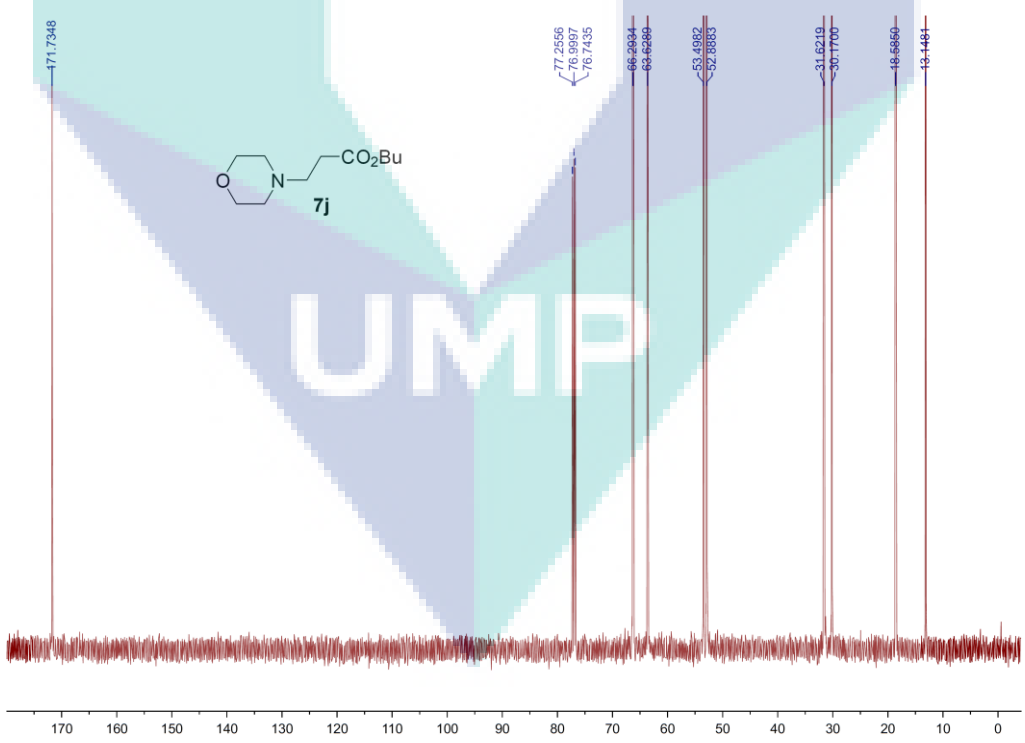
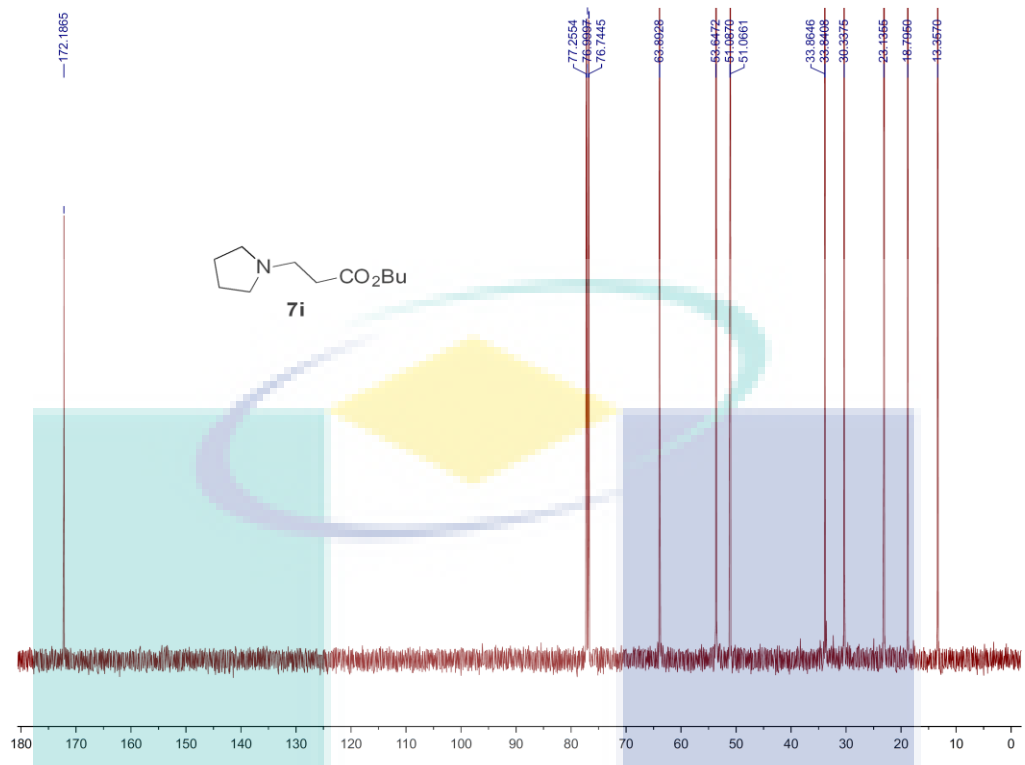


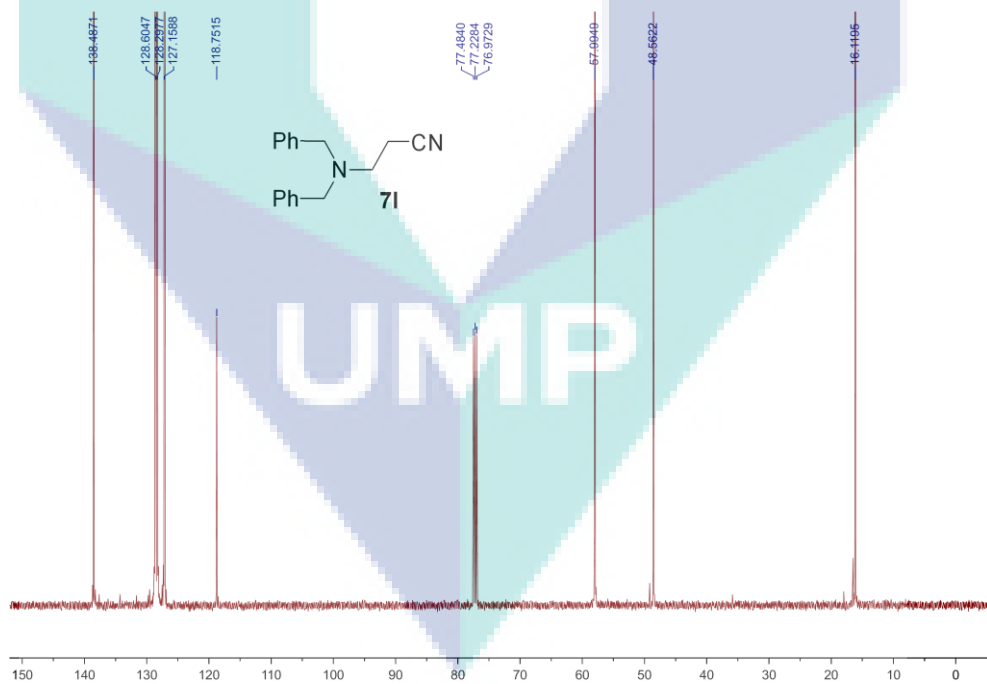
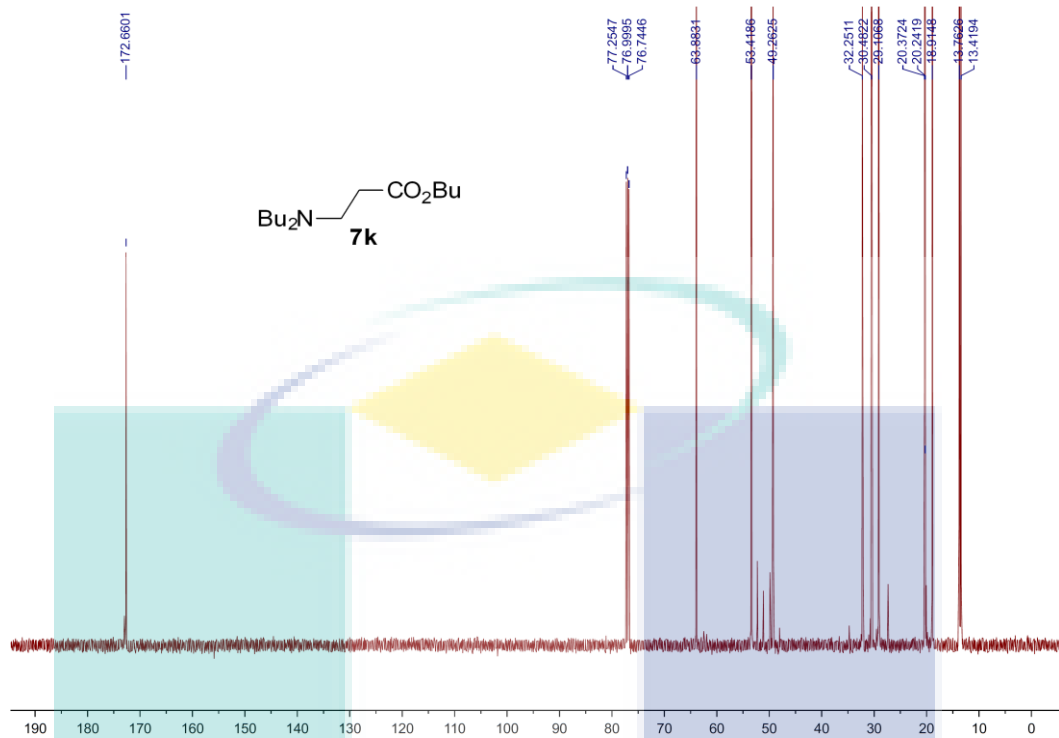


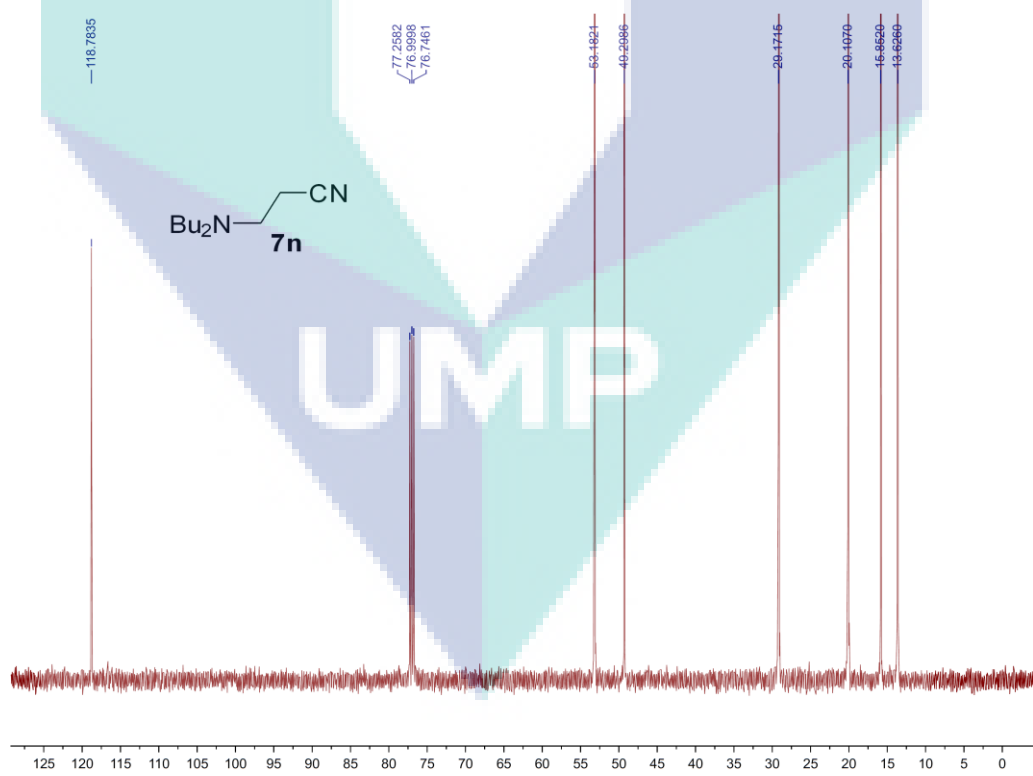
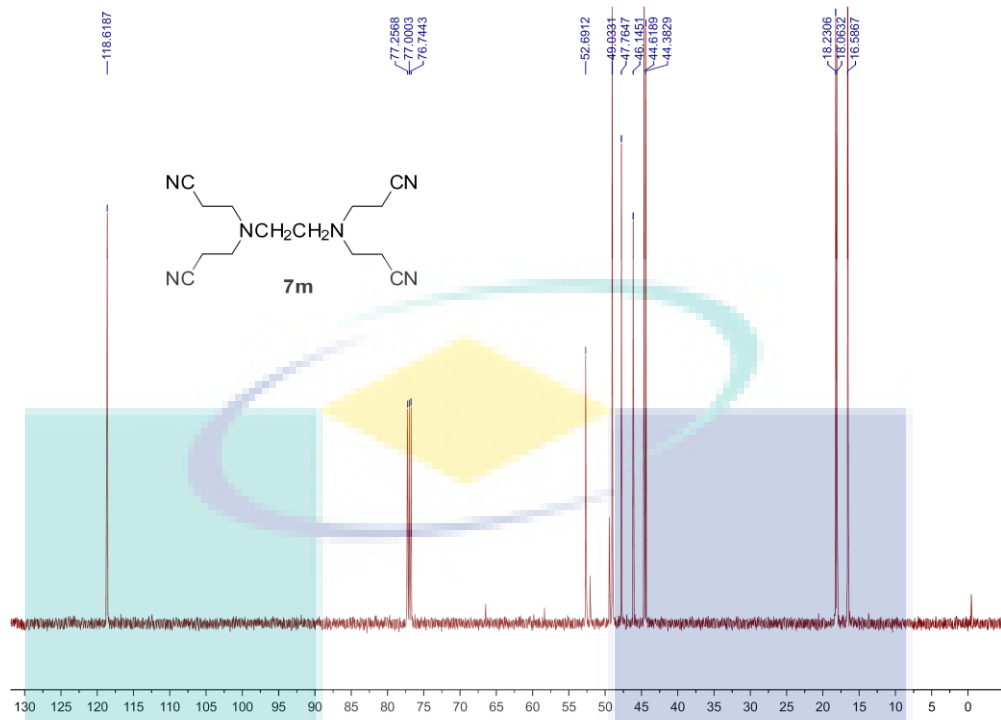




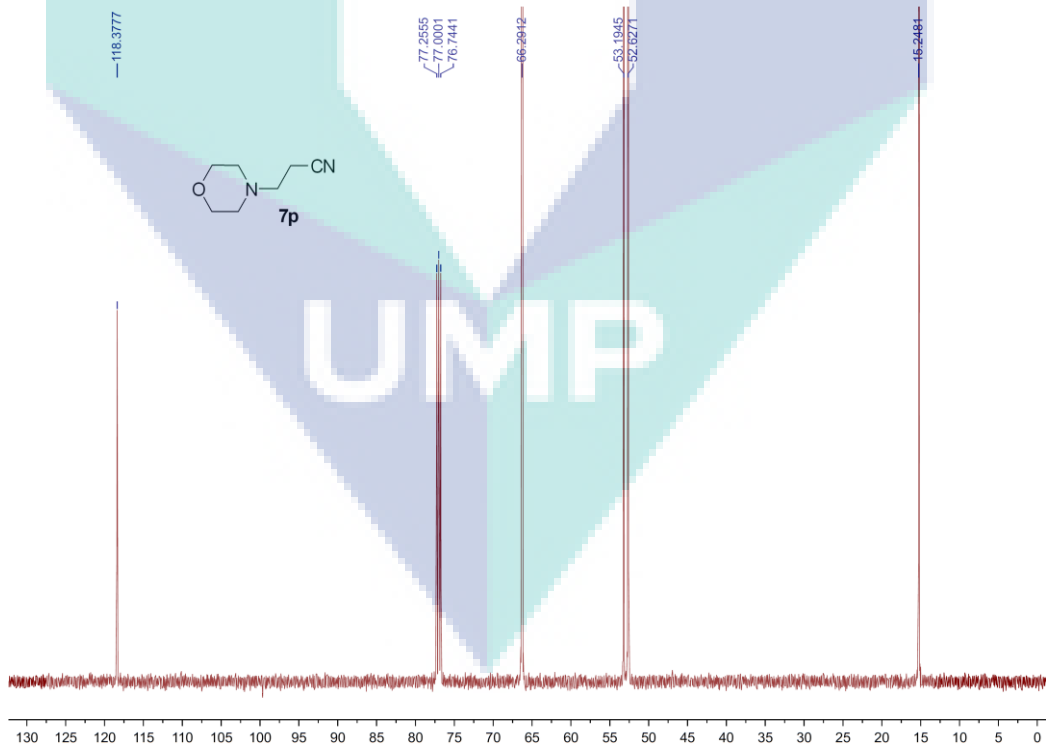
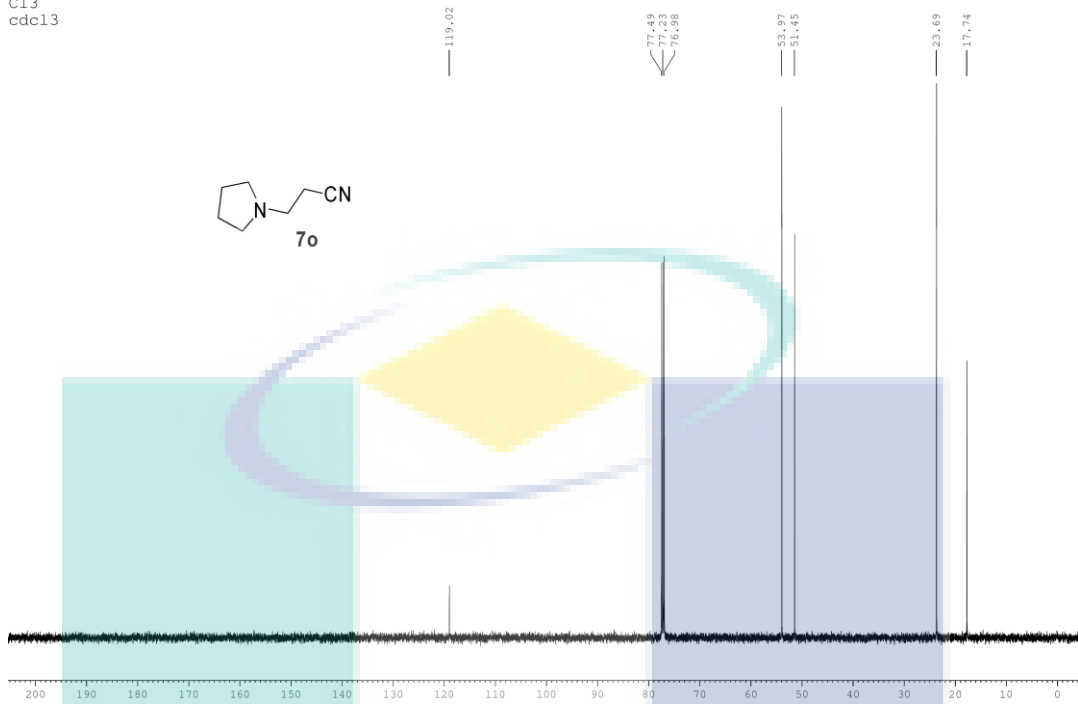


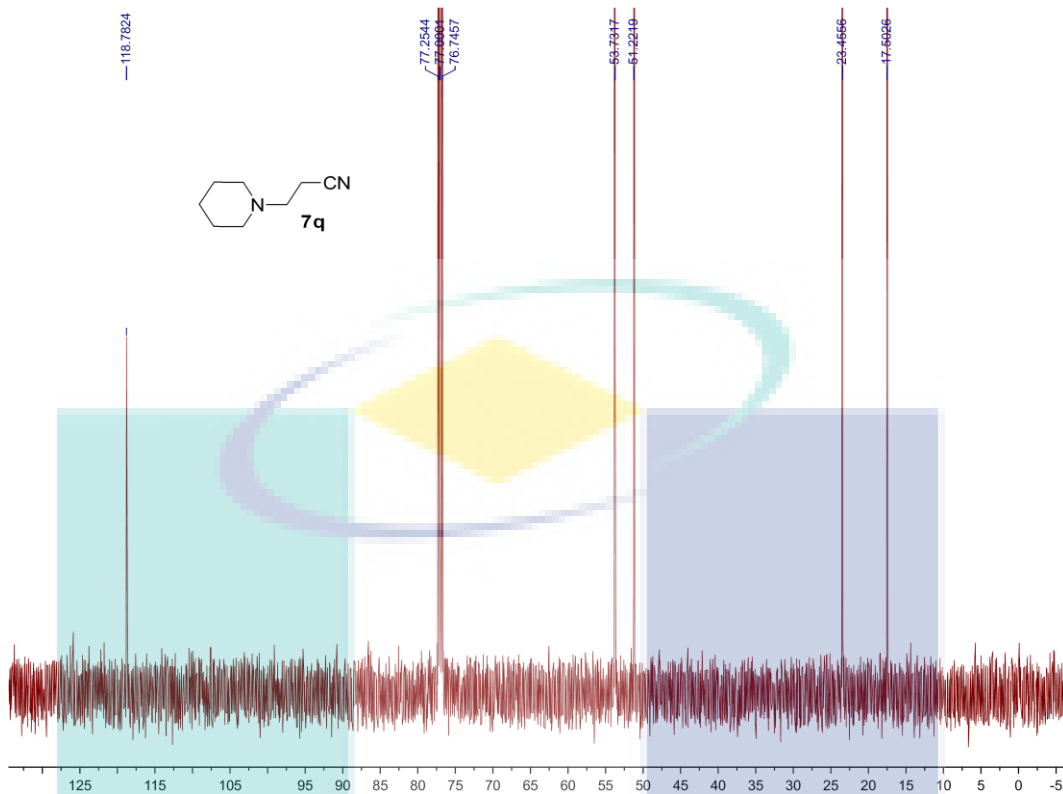






sample 20
C13
cdcl3





UMP

ACHIEVEMENTS

JOURNAL ARTICLES

- 1) Islam, M. S., Mandal, B. H., Biswas, T. K., Rahman, M. L., Rashid, S. S., Tan, S.-H., and Sarkar, S. M. (2016). Poly(hydroxamic acid) functionalized copper catalyzed C–N bond formation reactions. *RSC Advances*, **6**(61), 56450-56457.
- 2) Islam, M. S., Rahman, M. L., Yusoff, M. M., and Sarkar, S. M. (2017). Highly active bio-waste cellulose supported poly(amidoxime) palladium(II) complex for Heck reactions. *Journal of Cleaner Production*, **149**, 1045-1050.
- 3) Islam, M. S., Mandal, B. H., Biswas, T. K., Rahman, M. L., Rashid, S. S., Tan, S.-H., and Sarkar, S. M. (2016). Tapioca Cellulose Based Copper Nanoparticles for Chemoselective *N*-Alkylation. *Journal of Nanoscience and Nanotechnology*, **16**, 1-8.
- 4) Hajar, S., Islam, S., Rahman, L., Rashid, S., Zaman, Z., Ali, E., and Sarkar, S. (2017). Highly Active and Reusable Kenaf Cellulose Supported Bio-Poly(hydroxamic acid) Functionalized Copper Catalyst for C-N Bond Formation Reactions. *BioResources*, **12**(1), 882-898.
- 5) Sarkar, S. M., Ali, M. E., Islam, M. S., Rahman, M. L., Rashid, S. S., Karim, M. R., and Yusoff, M. M. (2015). Mesoporous Silica-Supported Sulfonyldiamine Ligand for Microwave-Assisted Transfer Hydrogenation. *Journal of Nanomaterials*, **2015**, 1-7.
- 6) Karim, M. R., Islam, M. S., Sarkar, S. M., Murugan, A. C., Makky, E. A., Rashid, S. S., and Yusoff, M. M. (2014). Anti-amylolytic activity of fresh and cooked okra (*Hibiscus esculentus* L.) pod extract. *Biocatalysis and Agricultural Biotechnology*, **3**(4), 373-377.

CONFERENCE PROCEEDINGS

- 1) Islam M. S., Karim, M. R., Tan S. H., Rashid, S. S. and Sarkar, S. M. Antiamyolytic activity of okra (*Abelmoschus esculentus* L.) pod glycoprotein. GNOBB Conference 2015, Bangladesh.
- 2) Islam M. S., Karim, M. R., Rashid, S. S. and Tan S. H. Comparative bioactivity study of *Glinus oppositifolius* extracted in different solvents. Institute for Research in Molecular Medicine (INFORMM), 2014. Universiti Sains Malaysia, Malaysia.
- 3) Islam M. S., Karim, M. R., Tan S. H., Rashid, S. S. and Sarkar, S. M. Okra (*Abelmoschus esculentus* L.) Pod Glycoprotein Demonstrates Antiamyolytic Activity. National Conference for Postgraduates Research 2015, Universiti Malaysia Pahang, Gambang.



UMP